Department of Precision and Microsystems Engineering

Design of a Miniature Gas Exchanger for Oxygen Control in Microfluids

M.P. van Reeuwijk

Report no	: 2021.041
Coach	: Dr. ir. M. (Matthijs) Langelaar & Dr. N.J.H. (Harold) Raat
Professor	: Prof. dr. U. (Urs) Staufer
Specialisation	: Micro- and Nano Engineering (MNE)
Type of report	: Design Report
Date	: 8th of July 2021

TU Delft Delft University of Technology

MSc Thesis Report

Design, integration, fabrication and validation of a miniature cell medium gas exchanger to control (sub)physiological oxygen concentrations on a liver chip

by

M.P. van Reeuwijk

to obtain the degree of Master of Science
at the Delft University of Technology,
to be defended publicly on Thursday July 22, 2021 at 14:00 PM.

Report number:	2021.041
Student number:	4442776
Project duration:	February, 2021 – July, 2021
Thesis committee:	Prof. dr. Urs Staufer, TU Delft
	Dr. ir. Matthijs Langelaar, TU Delft
	Dr. Harold Raat, Erasmus MC
Master Track:	Hightech Engineering as part of Mechanical Engineering
Specialisation:	Micro- and Nano Engineering (MNE)
Type of Report:	Design Report

An electronic version of this thesis is available at `http://repository.tudelft.nl/`.

TU Delft

Preface

This design report presents my master thesis project of mechanical engineering applied in the biological domain of cell research at Erasmus MC. I hope that this research contribution improves the reliability and biological relevance of human cell research outside the body, which guides biologists in studying the effect of changing cell environments. Grateful I am for the to the point questions and detailed creativity of Urs Staufer, as well as the helicopter view and comprehensive reasoning of Matthijs Langelaar. Also I owe many thanks to Harold Raat for initiating an inspiration biological design project in the first place. Especially, his willingness to discuss experimental approaches and ability to understand technical concepts was of great help. Besides, I would also like to thank Patrick van Holst for his guidance in the microscopic experiments at TU Delft, as well as Patricia Specht and Mariëlle van der Kaaij for their enthusiastic assistance in the biological lab work. Finally, I thanks my family and friends for the wonderful time together in the final year at TU Delft.

M.P. van Reeuwijk
Delft, July 2021

Summary

For cell studies outside the human body (Organs-On-Chip), this thesis presents the design, integration, fabrication and validation of a gas exchanger module to control oxygen in liquid medium for a liver cell layer on chip. Liver cells experiments at Erasmus MC require a gas exchanger module that lowers the medium oxygen concentration from saturated 0.20 mol/m^3 towards a range between 0.10-0.01 mol/m^3 within a time of 1-5 minutes. This provides a medium flow to a microfluidic chip channel for physiological (normal human liver situation) as well as hypoxia (low oxygen) conditions.

Prior to the design, for an adequate chip model experimental work resulted in the following. Imaging of a liver cell layer identified a cell layer height of 31.5 μm. The shape of the compressed elastomer chip wall was determined to derive the chip channel height of 250 μm. The elastomer oxygen permeability was tested for the elastomer diffusion coefficient (D = 1.1 $\times$ 10^{-11} m^2/s).

Next, the chip channel model including a cell layer simulated the oxygen gradient over the cell layer at 35 μL/min medium flow. This model can also predict the oxygen decrease during a medium flow stop to indicate cellular oxygen consumption. Further, a gas exchanger tubular prototype is simulated and tested based on the concept of gas exchange between medium and nitrogen flow through an oxygen permeable tubing. The test verified the desired low oxygen medium of 0.01 mol/m^3 within 5 minutes for 18 cm tubing. In addition, oxygen leakage in the microfluidic connectors did not allow the transfer of low oxygen medium to the integrated chip channel.

After that, the designed gas exchanger box (60 x 60 x 27 mm) contains 18 cm long silicone tubing for medium flow. Along the tubing, with 0.40 mm thickness, nitrogen gas can flow to decrease the medium concentration. Simulation of this design shows a 0.01 mol/m^3 medium oxygen concentration after 7.2 minutes. The fabricated gas exchanger box validation results in low oxygen concentrations of 0.01 mol/m^3 within 12.5 minutes. The extra time required compared to the modelled time is due absence of the tube guiding part in the model that alters the nitrogen flow. The gas exchanger box shows the ability to tune hypoxia oxygen concentrations with steps of 0.05 mol/m^3 by adjusting the air/nitrogen ratio in the gas flow. The gas exchanger with the integrated chip channel resulted in oxygen concentrations of 0.031 mol/m^3 within 21 minutes. The slower oxygen decay might be caused by the initial elastomer oxygen concentration and the further lowering of the concentration might be hindered by an oxygen leakage at the microfluidic connectors.

Finally, a system test of the gas exchanger box with a liver cell layer on chip demonstrated a physiological oxygen gradient over the cell layer and a steep decrease in oxygen concentration during a medium flow stop. This demonstrated that the gas exchanger can facilitate cellular oxygen measurements at physiological conditions for liver cell experiments on chip. This generic gas exchanger module can be integrated with different microfluidic chip channels for physiological or hypoxia research at lung, bone or cancer cells.

To reduce the time for achieved low oxygen concentrations, future research is recommended towards an optimal silicone tubing path and simulation of the nitrogen flow along a tube guiding part. Also, the saturation concentration of medium should be included in the model. Further, a miniature microfluidic connector design would allow a smaller tubing of 0.15 mm thickness for faster oxygen exchange. Lastly, an oxygen sensor in the chip fluidic inlet will allow feedback coupling to the gas exchanger for more reliable operation.

Table of Contents

List of Figures

List of Tables

1 Introduction

1.1. Context

Human cell behaviour is researched on the microlevel, to acquire understanding of occurring diseases or processes in the human body on the macrolevel. Especially low oxygen availability (hypoxia), such as liver injury, tumour growth [4], or human bone growth, can be researched on the microscale. Studies at patients on oxygen delivery and consumption in the human body (in vivo) are dependent on the availability of patients and are time consuming as well. Study of human cells outside the human body (in vitro) is performed relatively rapid, can be duplicated in parallel and has the opportunity to study individual types of cells. Physiological relevant studies require a controlled microenvironment for a living cell culture, which recapitulates part of the organ dynamics, functionality and physiological response.

Nowadays, Organ on Chip (OoC) technology provides a microenvironment with a microfluidic channel for flow of liquid cell medium (perfusion) which allows real-time imaging and measurements. In the human body oxygen is tightly regulated and fluctuations in oxygen concentration influences the cell functioning significantly. Control of oxygen is still required on organ chips, since molecular oxygen is one of the most important variables to control in modern cell culture systems [3] [5].

Oxygen concentrations in microfluidics are sensed with the optical luminescence detection method. In this method, after excitation by a (laser) light pulse, the fluorescence response of dyes varies with the dissolved oxygen in the fluid. The dyes can be either dissolved in the liquid, embedded in a sensor layer or incorporated in microparticles. Preferably, the fluorescence lifetime is detected that limits the interference of fluctuating light sources, interference of ambient light and differences in dye concentration [1].

Existing oxygen control methods show accurate control in the range of 0.1% for gas perfusion integrated in the microfluidic channel [6] and show compact systems using chemical scavengers [7]. On the contrary, gas perfusion methods on chip dry out the chip channel [8] and let cell medium evaporate [9] [10]. Chemical scavengers can interfere with cellular processes at higher concentrations [8]. The pre-equilibration gas control method regulates the oxygen concentration apart from the microfluidic channel. Before the medium flows over the cells, the cell medium exchanges oxygen with a gas mixture of O_2/N_2 separated by a oxygen permeable membrane. Figure 1.1 visualises the oxygen flux from the flowing cell medium towards the flowing gas. This method is designed apart from the chip channel, which requires an oxygen-tight transfer from the gas exchanger towards the chip [7]. Above all, this method allows a generic exchanger module for integration with various microfluidic chips for compatibility with a wider range of cell research.

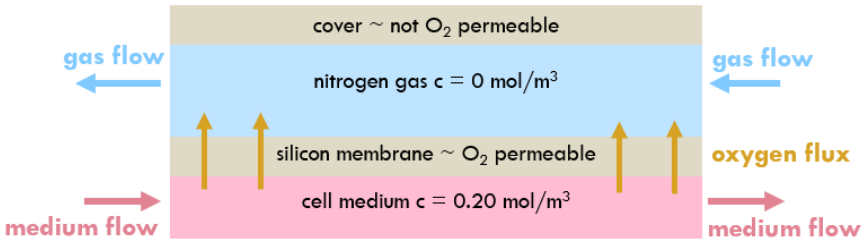

Figure 1.1: Pre-equilibration gas control method for lowering the oxygen concentration in cell medium.

1.2. Problem Statement and Research Aim

At the Erasmus MC anaesthesiology department, research on behavioural changes of hepatocytes (liver cells) at hypoxia conditions is performed by monitoring cellular oxygen consumption. It is desired to research a cell layer of 1 cm^2 consisting of 200,000 hepatocytes, which have a diameter of 20-25 μm [11]. To improve the physiological relevance, oxygen control is required in the cell medium flow over a cell layer in a chip channel. Control of the oxygen at the chip inlet provides a physiological oxygen gradient over the cell layer and low oxygen conditions (hypoxia) for varying duration. The dissolved oxygen in cell medium at 37°C is 0.20 mol/m^3 [3]. For physiological relevant experiments this oxygen concentration should be lowered towards 0.09 mol/m^3 or towards 0.01 mol/m^3 for low oxygen. The proposed system with pump and chip is presented in Chapter 2.

Recent work of an oxygen scavenging chip by Sticker *et al.* is limited to maximum flow rates of 5 μL/min and does not allow adjusting the oxygen concentration during cell experiments. Besides, the state-of-the-art pre-equilibration system of Busek *et al.* with an integrated microfluidic channel cannot be integrated by biologists with various microfluidic channels limiting the flexibility in cell research [12]. For different types of cell research in academic hospitals a gas exchanger independent of the microfluidic pump or chip channel is preferred. This gas exchanger module would allow coupling with commercial microfluidic chips, low-cost fabrication and operation by a non-technician.

This research aims to design, integrate, fabricate and validate a miniature cell medium gas exchanger to control (sub)physiological oxygen concentrations on a liver chip. First of all, the design context and requirements for cell research at low oxygen conditions are identified. Second, the chip channel and gas exchanger are modelled and simulated to determine the gas exchanger design dimensions. Third, the gas exchanger is integrated with the chip channel and the suitable material choice with appropriate manufacturing method is defined. Fourth, the system is tested for low oxygen conditions and tested with a cell layer to verify cellular oxygen consumption.

1.3. Thesis Outline

To start, Chapter 2 states the gas exchanger design requirements for the Erasmus MC liver cell research. Chapter 3 contains the experimental work to generate knowledge required for an adequate chip channel model. Next, Chapter 4 presents the simulation of the chip channel and gas exchanger to define the required gas exchanger dimensions. Chapter 5 presents the tested tubular gas exchanger prototype. Following, Chapter 6 presents the detailed design choices, integration with the chip channel, material choice and manufacturing method. The gas exchanger design is validated in Chapter 7 with a system test. Chapter 8 states the summary of design requirements and the design conclusions. Finally, Chapter 9 lists the design recommendations and Chapter 10 presents a personal reflection on the research project.

Additionally, Appendix A states the requirements, experimental work and prototype details. Appendix states B the modelling and simulations details, Appendix C the detailed design drawings, Appendix D the validation testing procedures, Appendix E the MATLAB code for data processing and Appendix F displays all the oxygen measurement data.

2

Design Requirements

This chapter presents the design requirements identified for biological research of human liver cells at the department of experimental anaesthesiology of Dr. Harold Raat. The presented design requirements, specific for research on liver cells, are used as functional description and performance criteria of an oxygen control module. In the detailed design (Chapter 6) the separate module of the gas exchanger is motivated in order to also let lung, bone and cancer cell research benefit from oxygen regulation in the future.

By measuring oxygen consumption during liver cell experiments, the cell functioning is studied. The research goal for biologist researchers of the Erasmus MC is to perform reliable and repeatable oxygen consumption measurements on liver cells (hepatocytes) in a micro physiological environment outside the human body (in vitro). The system setup of this research contains a syringe pump, a gas exchanger and a microfluidic chip channel. Figure 2.1 displays the syringe pump which provides cell medium to the gas exchanger and the Micronit system which contains the microfluidic channel. On top of the chip holder the laser-fiber is situated to measure oxygen. Currently, for chip channel experiments including flow of medium, there is no control of the oxygen concentration in cell medium. Therefore, the design scope of this research is defined as the gas exchanger module in connection with the syringe pump and the Micronit microfluidic chip.

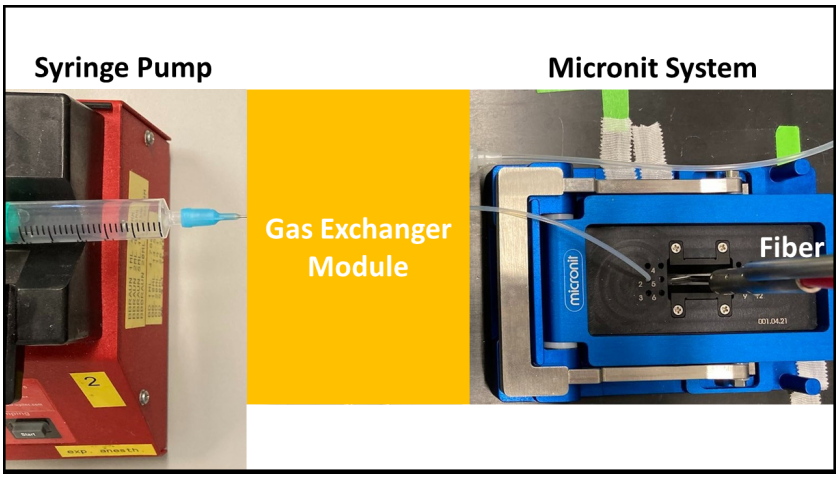

Figure 2.1: System setup with microfluidic syringe pump (left), gas exchanger module (middle) and Micronit chip holder with fiber (right).

The design requirements of the chip channel are listed in Appendix Table A.1. In short, the chip material should have low oxygen permeability (req. 2.10) to create low oxygen conditions on the chip. Glass is preferred for its low diffusion constant [13] compared to common organ chip materials such as PMMA, PLA, PC or PDMS [9]. Besides, the chip channel should provide direct access (req. 2.5) to the cells seeded on chip as well as provide transparency (req. 1.6) to perform optical oxygen measurements. The commercial Micronit resealable flow cell fulfils the chip channel requirements and is therefore chosen as microfluidic chip. The Micronit system provides a microfluidic channel, consisting of glass plates, that is leak tight for fluids through mechanical clamping in a chip holder.

For a cell layer, the minimum medium flow rate is defined by sufficient oxygen supply for the oxygen consumption of the cells. For a liver cell layer of 200,000 cells with a cellular consumption of 1 nmol O_2/(min · 2×10^5 cells) [11], an oxygen molar flow rate of $\dot{c}_{in}$ = 1.67 $\times10^{-11}$ mol/s is required at the channel inlet. At a physiological inlet concentration of c_{in} = 0.09 mol/m^3, the minimum flow rate should be $Q_{med} = \dot{c}_{in}/c_{in}$ = 1.85 $\times10^{-10}$ m^3/s (11.1 μL/min). The work of Ehrlich *et al.* states that the human liver delivers a higher oxygen flow rate of 72 nmol/(min · 10^6 cells) than the oxygen consumption of primary cells (in vitro) of 54-18 nmol/(min · 10^6 cells) [11]. Although this is a rough estimation, this indicates an oxygen supply of an order 2-4 higher than oxygen consumption. With this in mind, the flow rate of 5.83 $\times10^{-10}$ m^3/s, further noted as 35 μL/min, is chosen for medium flow. To allow variation of cell number on chip, the a medium flow rate is required between 25-45 μL/min.

The design requirements of the gas exchanger are listed in Table 2.1. Most importantly, the oxygen concentration should be lowered compared to the saturated concentration within a desired time of 1-5 minutes. Besides, the gas exchanger should allow renewal of the oxygen permeable membrane between different experiments to eliminate absorption of medium components by the membrane.

Functional Requirements	**Performance Requirements**
1.1 Oxygen Concentration - Set the oxygen concentration from the saturated inflowing medium to a lower oxygen concentration suitable for physiological or low oxygen cell experiments.	Reduce the oxygen concentration from saturated 0.20 mol/m^3 at 37 °C [3] to a range between physiological 0.10 to 0.01 mol/m^3 low oxygen concentration. It is desired that the exchanger reaches the desired oxygen level within 1-5 minutes time.
1.2 Sterile - The gas exchanger should be cleaned to avoid contamination of cell medium.	Ability to clean exchanger with ethanol/iso-propanol and renew the oxygen permeable membrane of the gas exchanger.
1.3 Medium Flow Rate - Gas exchanger function independent from flow rate since the flow rate is adjusted to the amount of cells present in the chip channel.	Medium flow rate in the range of 25-45 μL/min.
1.4 Temperature - The exchanger should prevent increase of cell medium temperature, since at higher temperatures less oxygen will dissolve in the medium causing gas bubbles.	The gas exchanger shall operate at 37 °C.
1.5 User - The exchanger shall be operated by a non-technician in the biological lab. This implicates ease-of-use in the exchanger setup and no required specialised tools or procedures.	

Table 2.1: Cell medium gas exchanger requirements.

3

Experimental Work

This chapter presents the experimental work prior to the gas exchanger design to obtain knowledge for the modelling and simulation in Chapter 4. First, Section 3.1 describes the cell layer height estimation with the confocal microscope. Second, Section 3.2 describes the width of the chip channel elastomer to estimate the chip channel height. Third, Section 3.3 presents the oxygen permeability test of the chip elastomer to obtain the elastomer diffusion constant. Lastly, a summary of the experimental results is provided in Section 3.4.

3.1. Cell Layer Height

Variation of the cell layer height in the chip channel influences the medium flow speed over the cells relating to the shear stress on the cells. The HepaRG is a bipotent cell line consisting of flat (epithelial like) cholangiocytes (bile cells) as well as hepatocytes (functional liver cells) that form higher islands on top of the flat cholangiocytes. Literature states a 20-25 μm diameter of the hepatocytes [11]. Regarding the shape of the cells, the cultured hepatocytes at Erasmus MC do not form round spheres. Instead, they form stretched elliptical shapes.

To define the height of the cell layer, the cultured cell layer on a glass slide was imaged with an upright confocal microscope with APO water dipping lens. This Leica SP5 Intravital microscope (Figure 3.1), with a 20 x magnfication lens, NA = 1 and working distance of 1.95 mm, images cells covered with cell medium. Further information about the microscope is available on the Erasmus Optical Imaging Centre website: wwww.erasmusoic.nl/facility/equipment/leica-sp5-intravital-ee-880 . The procedure of cell culture and fluorescent staining of the cells with calcein AM is described in Appendix Section A.2.

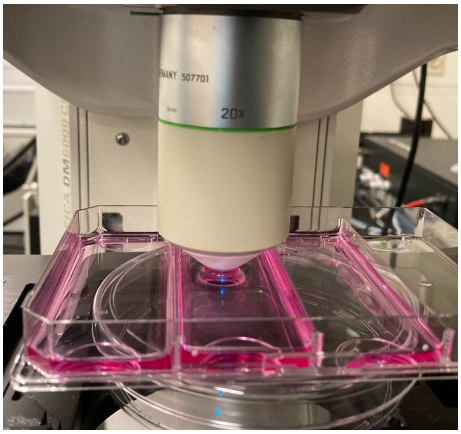

Figure 3.1: Setup of cell layer height measurement at the Leica SP5 Intravital microscope with water dipping lens.

The confocal microscope laser was excited with blue light (488 nm). With the expected green emission of 517 nm of the fluorescent calcein AM, the emission was recorded in the range of 500-550 nm. With a field of view of 738 x 738 μm, the lens was vertically moved down (along z-axis) with steps of 1 μm to obtain a stack of 80 fluorescence images along and beyond the cell layer.

To start, the middle of the cell layer was imaged with four fields of view (1476 x 1476 μm) resulting in the height profile (z-profile) displayed in Figure 3.2. This profile shows variation in height of the cell layer. The maximum heights relate to the clusters of hepatocytes cells. According to the interpretation of Dr. Harold Raat the obtained fluorescent images show both hepatocytes (liver cells) and cholangiocytes (bile cells). An enlarged imaged is presented in Appendix A.2. Besides, it is important to note that the cell layer is an uneven surface with possible stacking of cells on top of each other.

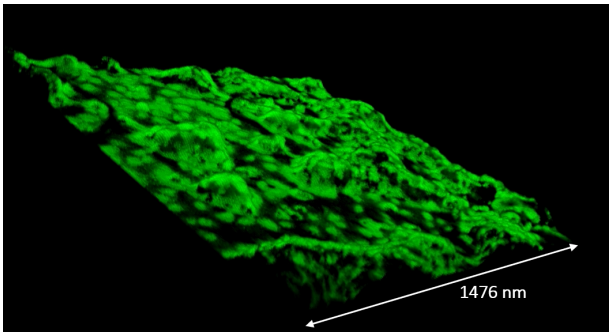

Figure 3.2: Cell layer 3D projection of the height profile of a 1476 x 1476 μm cell area. Image created with Fiji software.

Similarly, a second larger area with 22 fields of view (8118 x 1476 μm) along the length of the cell layer (Figure 3.3) was imaged. To determine the cell layer height, the fluorescence signal amplitude of the microscopic images was analysed. In these images, a relative high fluorescence signal amplitude indicates the presence of cells.

The images were processed with the Fiji software to plot the mean fluorescence signal per image for the sequence of 80 images along the cell height per field of view (738 x 738 μm). Figure 3.4 shows the mean fluorescence signals the field of view series along the cell layer length. In this figure, the fluorescence peak indicates the presence of cells along the z-axis. For all plots, the z-axis interval

for the mean signal above 10 was determined, resulting in 18 estimations of the cell layer height of which the full peak above 10 could be read. These averages cell layer height per field of view are noted in Table 3.1. There is a shift in mean fluorescence peak along the field of views, because the glass plate is not in perfect horizontal position. Overall, the average of the 18 cell height estimations presented in Table 3.1, results in an average cell layer height of 31.5 ± 3.17 μm.

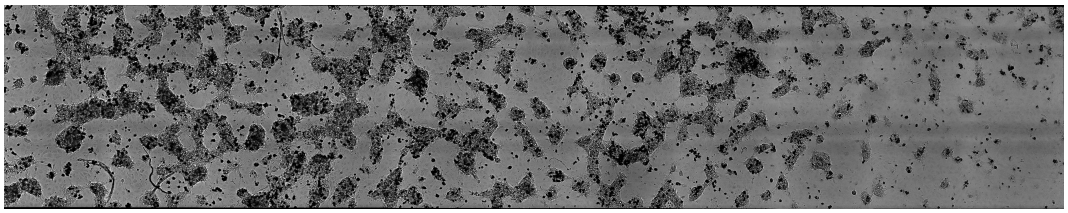

Figure 3.3: Brightfield image of a 8118 x 1476 μm area at the centre of the cell layer.

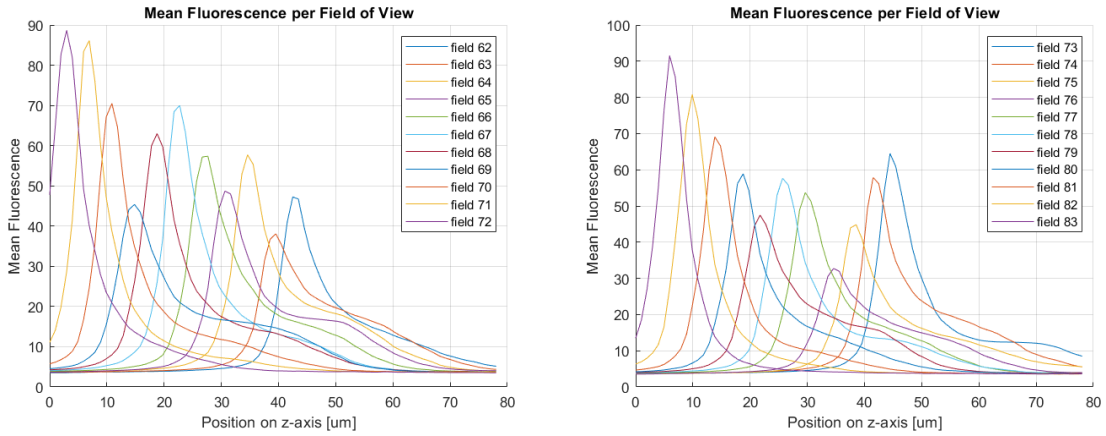

(a) Mean fluorescence signal of first field of view line along the length, from upper right to upper left of cell layer in Figure 3.3.

(b) Mean fluorescence signal of second field of view line along the length, from lower right to lower left of cell layer in Figure 3.3.

Figure 3.4: Mean fluorescence signal of 22 fields of views at two scans along the cell layer length.

	Cell height along length cell layer [μm]								
Cell Height along width cell layer [μm]	30.7	38.5	32.6	31.6	33.6	32.6	31.6	30.6	28.7
	23.7	28.6	31.6	32.6	29.6	29.6	30.6	32.6	36.6

Table 3.1: Height estimation of cell layer (Figure 3.3), determined by fluorescence peak width of each field of view visualised in Figure 3.4.

3.2. Chip Channel Height

The commercial Micronit resealable flow cell (Figure 3.5) forms a microfluidic channel consisting of two glass slides. The top 1100 μm thick glass slide contains microfluidic connections holes and an attached elastomer gasket as the channel wall. This top slide is placed on the bottom 700 μm thick glass slide closing the channel. The glass slides are inserted in the Micronit chip holder (Figure 3.6) and lightly compressed to create a leak tight channel for fluid flow.

The dimensions of the microfluidic channel are 40 mm in length, 4 mm in width and 300 μm in height before compression of the glass slides. Figure 3.8 shows a microscopic view of half of the

chip channel with the elastomer in white and several holes in the glass for fluidic inlets. From the microscopic image the inner width was estimated to be 3.9 mm. The resealable chip is symmetric along the vertical axis.

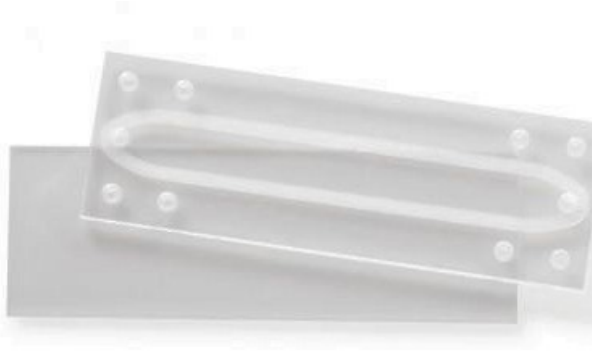

Figure 3.5: Micronit resealable flow cell chip channel

Figure 3.6: Micronit fluidic connect chip holder.

The height of the channel will decrease due to compression of the elastomer in the chip holder as visualised in Figure 3.7. The elastomer material contains similar mechanical characteristics as FKM or FVMQ elastomers according to information provided by Micronit. For the simulations of oxygen concentrations in the chip channel the channel height should be defined, which determines the medium flow speed over the cell layer. The flow speed determines the time to establish a stationary oxygen gradient, therefore the channel height is of interest. Besides, the known elastomer shape allows modelling of oxygen diffusion through the elastomer.

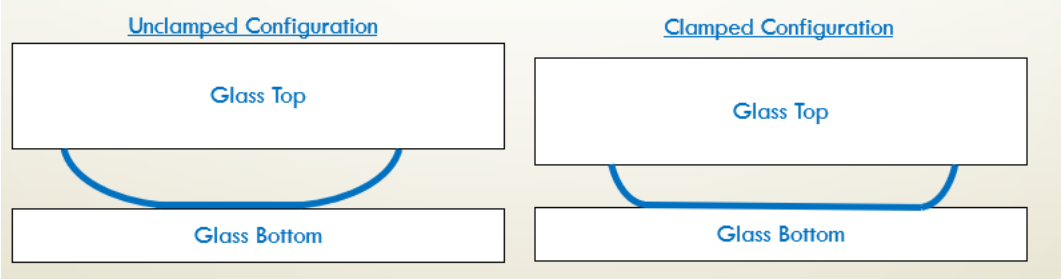

Figure 3.7: Schematic of the predicted Micronit elastomer chip wall shape (in blue) between glass slides without and with compression of the chip holder.

Assuming a reduction in channel height by the compressed elastomer, the velocity profile of the chip model presented in Section 4.2.1 was simulated for different channel heights including a 50 μm cell layer. The flow velocity on the cell layer, due no-slip conditions, remains the same. The maximum flow velocities in the middle of the channel for channel heights 200, 225, 250, 275 μm are 1.5, 1.2, 1.1 and 1 mm/s respectively. The velocity profiles are visualised in Figure B.6.

The oxygen concentration along the 25 mm long x 4 mm wide cell layer was investigated for varying channel heights. For channel heights from 200 to 275 μm, the longitudinal oxygen gradient along the cell layer centre surface was not changed as displayed in figure B.8. There exists a small variation in the lateral oxygen gradient, which is best noticeable at the end of the cell layer. Figure 3.9 displays the oxygen concentrations along half the width of the chip channel. The 200 μm and 225 μm have a similar gradients, however the 250 μm and 275 μm height show a deviations of 0.0005 mol/m^3 and 0.001 mol/m^3 respectively. These results show that a stationary oxygen gradients after 300 seconds is not significantly affected by the channel height between 200 μm and 275 μm.

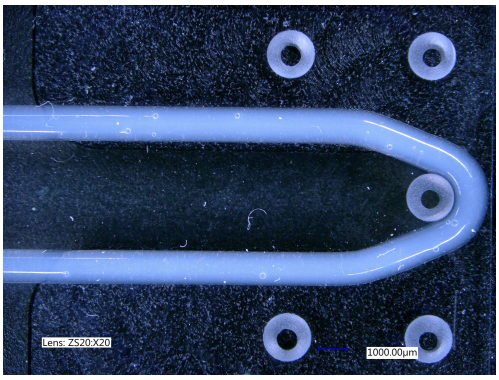

Figure 3.8: Micronit flow cell top glass slide of 45 mm x 15 mm with elastomer gasket. Imaged with Keyence VHX-6000, lens ZS20:x20.

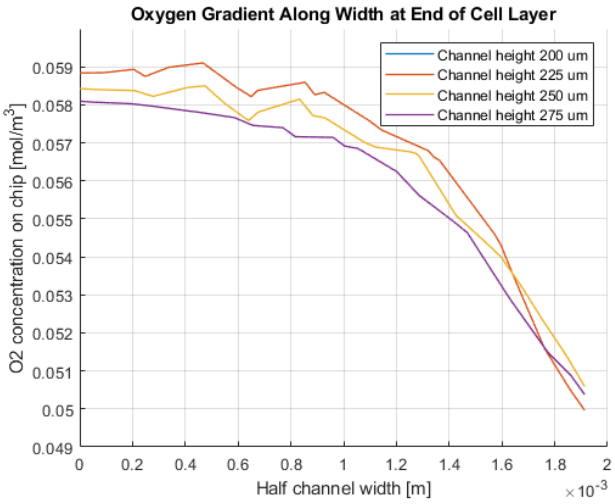

Figure 3.9: COMSOL simulation of lateral oxygen gradient at end of the cell layer for varying chip channel heights.

The elastomer walls of the chip channel are not visible when clamped in the chip holder. In order to identify the channel height, the visible width of the elastomer was measured from a microscope image in uncompressed and compressed configuration. The chip used for the measurement was not clamped before. Additionally, the top glass slide was placed on the bottom slide with the attached elastomer pointing upwards. The following measurements were executed without fluid inside the chip channel, since the open medium outlet during cell experiments does not built up significant pressure in the channel.

In the uncompressed configuration, the height of the elastomer was determined by moving the microscopic lens vertically down (z-stack measurement) on the elastomer wall displayed in Figure 3.8. This rough height measurement of the elastomer, with the round side pointing up, is visualised in Figure 3.10. The difference between the highest and lowest height peak results in a height before compression of 292 μm, which is close to the manufacturer value of 300 μm. For this height measurement, the elastomer was not covered with a glass slide since scattering of the glass disturbs the imaging at different focal distances.

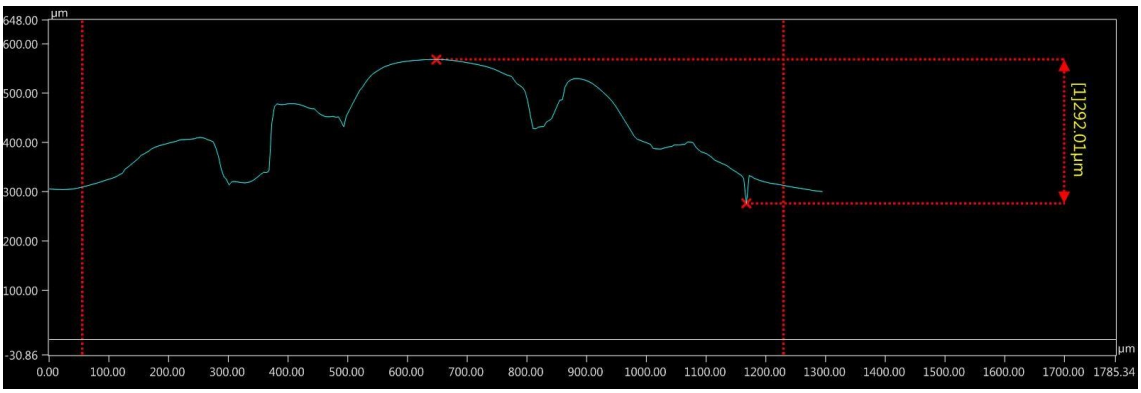

Figure 3.10: Height measurement of elastomer wall on glass plate by vertically moving lens. Imaged with a Keyence VHX-6000, lens ZS20:x150.

Next, the contact width of the elastomer on the bottom glass slide was imaged in compressed and uncompressed configuration. In the uncompressed configuration, the two chip slides were inserted leaving the chip holder fully opened. In the compressed configuration, the two chip slides were clamped by the closing the chip holder. Since the chip holder blocked the view on a large part of the elastomer wall, the elastomer was imaged on three visible points as visualised in Figure A.4. With the VHX software the contact point distances were measured between two parallel lines manually plotted on the optical image. The manually plotting of the points causes a measurement variation of ± 5 μm.

In open configuration (Figure A.5a) the elastomer measured a top width of 1256 μm and a contact width at the elastomer bottom of 93 μm. Table 3.2 displays the width measurements at three points on the elastomer in compressed configuration. The average top width of the compressed elastomer is 1244 μm with an average bottom contact width of 695 μm. There is a slight increase in bottom width of 1244 μm relative to the uncompressed width of 1256 μm, and a significant increase in bottom contact width of 695 μm relative to the uncompressed bottom width of 93 μm.

Point	Top Width Compressed Elastomer [μm]	Bottom Contact Width Compressed Elastomer [μm]
A	1282 ± 5	717 ± 5
B	1215 ± 5	700 ± 5
C	1235 ± 5	670 ± 5
Average	1244 ± 5	695 ± 5

Table 3.2: Measured elastomer widths at three different points (Figure A.4).

With the obtained elastomer width from microscope imaging, the height of the compressed elastomer is estimated. A schematic ellipse of 1250 μm wide with initial uncompressed height of 300 μm (Figure 3.11) is drawn such that the ellipse lines intersect with the glass bottom for a contact width of 700 μm. The resulting Figure 3.12 displays that the change in height of 50 μm would lead to a contact width of 700 μm, resulting in a corresponding compressed channel height of 250 μm.

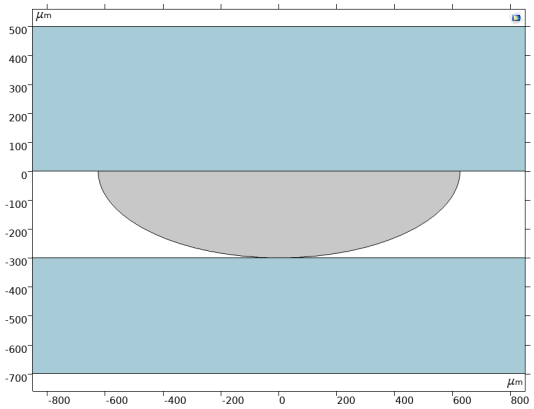

Figure 3.11: Uncompressed elastomer with a height of 300 μm.

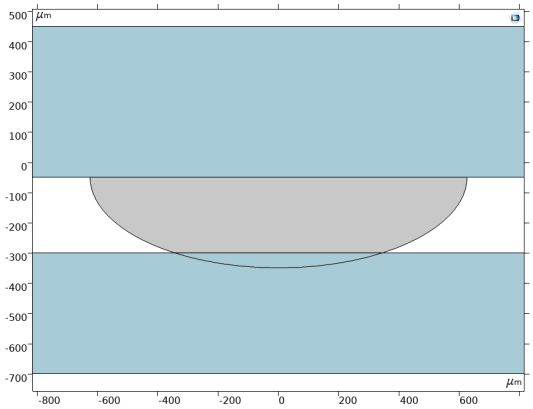

Figure 3.12: Compressed elastomer with a height of 250 μm.

COMSOL simulations of stationary solid mechanics as a linear elastic material were not satisfying. A contact pair was included between the glass bottom and the bottom of the elastomer. With a pre-described displacement of 50 μm, the elastomer moved down with 150 μm as displayed in Figure B.9 Unfortunately, the material specifications of the elastomer were not available to model a hyperelastic material behaviour or adding adhesion between the elastomer and glass bottom slide.

3.3. Chip Elastomer Permeability

To maintain low oxygen conditions (≤ 9 mol/m^3) in the cell medium flow, the oxygen diffusion from outside air through the elastomer wall is quantified. According to Micronit company, the uncompressed elastomer (Figure 3.8) has an oxygen permeability of D = 9.88 $\times 10^{-11}$ m^2/s (data Figure A.6). This provided diffusion constant belongs to a material in the same the material family as the chip elastomer. The chip elastomer is compressed which might vary its diffusion constant. For that reason, the permeability of the chip elastomer was tested for more accurate simulations. Oxygen diffusion through glass is neglected since the diffusion constant is five orders of magnitude smaller [13] compared to the manufacturers elastomer diffusion constant.

To quantify the elastomer oxygen permeability the following experiment was conducted. Starting at low oxygen conditions (< 0.05 mol/m^3) in the cell medium, the increase of oxygen concentration in cell medium was measured at stationary medium. First, the oxygen concentration of the cell medium was lowered by spinning 3 mL of PBS in a glass Eppendorf tube (thin fluid gas exchanger) and purging it with nitrogen gas at a flow rate of 200 mL/min for 6 minutes. Due to the fast spinning of the tube, the fluid forms a thin layer at the outside of the tube creating a large diffusion area for oxygen exchange with the nitrogen gas. Second, the Eppendorf tube was closed with a rubber and the medium is extracted with a needle to a glass syringe. Third, the low oxygen medium was inserted through the Micronit EFTE tubing (ID=0.25 mm) in the Micronit resealable chip, heated on a hot plate at 37 °C. The chip as well as the medium outlet tubing of 10 cm were filled with the medium. Finally, the oxygen concentration was measured every 20 seconds in the middle of the chip channel with the laser-fiber setup described in Section 5.2.

Bodmer *et al.* defined the signal-to-noise ratio (SNR) in the lifetime domain as ratio of maximum fluorescence signal amplitude (at the decay start) to the maximum signal of the noise [14]. The detected fluorescence signal during the measurements in medium with oxygen indicator Palladium Porphyrin was 1.2 V. In an empty chip channel, without oxygen indicator, the initial amplitude of the detected signal (fluorescence intensity) was 0.5 V. This results in a SNR of 2.4.

This chip oxygen permeability experiment was repeated twice, resulting in the increase of oxygen concentration plotted in Figure 3.13. The first measurement interval in blue is shifted forward with 2 minutes time to overlap the second measurement interval in red with a relative lower initial concentration. The steep initial increase of oxygen in the first 10 minutes is explained by the relative large gradient at the lowest oxygen level with respect to the outside air. The first interval curve starts to flatten after 25 minutes at 0.12 mol/m^3, and the second interval curve starts to flatten after 35 minutes at 0.13 mol/m^3.

The measurement points at higher oxygen concentrations show a relative larger variation over time compared to the measurement points at low oxygen concentrations < 0.10 mol/m^3. A lower oxygen concentration lead to a higher lifetime determined from the decay in fluorescence signal. Longer lifetimes are determined more accurately from the exponentially decaying signal than low lifetimes, resulting in smaller measurement variation at low oxygen concentrations. This variation in measurement values might suggest flattening of the blue curve, while oxygen concentration might still be increasing as shown by the red curve.

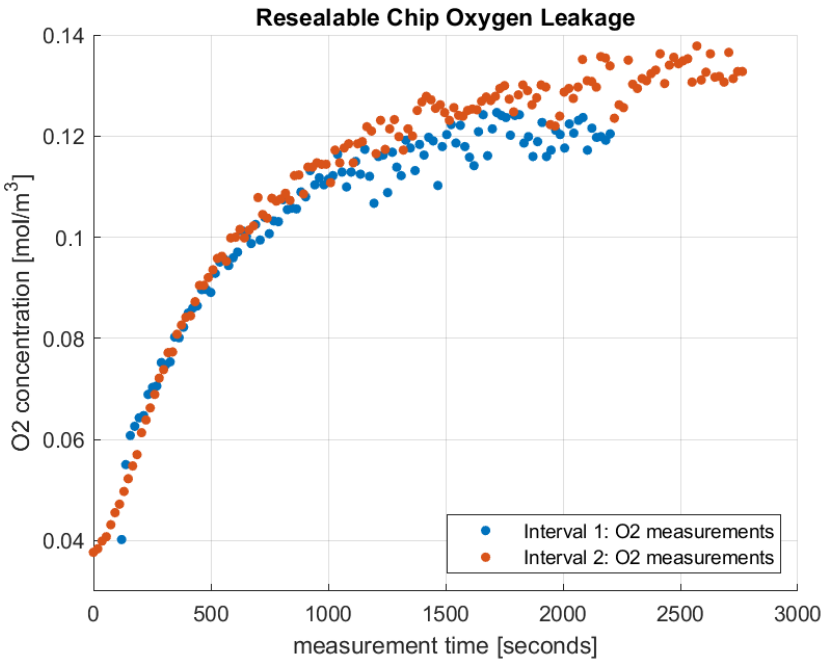

Figure 3.13: Oxygen measurements in static medium of the Micronit resealable chip.

For diffusive mass transfer, the oxygen concentration c (mol/m^3) over time t (s) through the elastomer thickness, noted by x (m), is described by the complementary error function in Equation 3.1. In this equation, c_0 is the initial concentration (mol/m^3), c_s is the saturation concentration (mol/m^3) and D is the diffusion constant (m^2/s). Further mass transfer theory is stated in Section 4.1.

The measurement points in Figure 3.13 are fitted with the MATLAB fittype function of Equation 3.2 to obtain the factor n relating to the diffusion constant. The resulting fits of the two measurements intervals with their coefficient are stated in Figure A.7 and Figure A.8. The obtained coefficients n with 95% confidence bounds for interval 1 and 2 are 11.73 (11.41, 12.05) and 12.91 (12.63, 13.19) respectively. For the total elastomer thickness of 2 mm (both sides channel), the resulting diffusion constants for interval 1 and 2 are 7.27 $\times 10^{-9} \pm$ 0.38 m^2/s and 6.0 $\times 10^{-9} \pm$ 0.27 m^2/s respectively.

$$c(x,t) = c_0 + (c_s - c_0) \cdot erfc\left(\frac{x}{\sqrt{4\,D\,t}}\right) \tag{3.1}$$

$$myfittype(a,b,n,t) = a + (b-a) \cdot erfc\left(n \cdot \frac{1}{\sqrt{t}}\right) \tag{3.2}$$

The obtained diffusion constants were verified with COMSOL simulations of the chip channel model, presented in Section 4.2 without flow of medium. Following from previous Section 3.2, the elastomer shape was defined as 250 μm high with a top and bottom width of 1244 μm and 696 μ respectively. Further, the oxygen concentration in the middle of the chip was evaluated by the average of a 10 mm long x 1 mm wide x 0.25 mm high volume (Figure B.10) representing the laser-fiber measurement volume. The manufacturers diffusion constant as well as the two diffusion constants obtained from fitting resulted in oxygen concentrations > 0.50 mol/m^3 after 30 minutes as visualised in Figure B.11. Although the saturation concentration was not taken into account in COMSOL, the initial increase from 0.04 to 0.15 mol/m^3 was not along the shape of the measurement intervals. Therefore, these diffusion coefficients are not representative.

Further simulations show that the initial oxygen concentration in the elastomer determines the steepness of the curve in the first 10 minutes as displayed in Figure B.12. Finally, the best fitting of interval 1 (Figure 3.14) and 2 (Figure 3.15) was found with an initial elastomer concentration of 0.65 mol/m^3 and diffusion constants of D = 8.0 $\times 10^{-12}$ m^2/s and D = 1.0 $\times 10^{-11}$ m^2/s respectively. The second measurement interval shows a continuous increase after 1500 seconds as expected to reach a saturation concentration of 0.20 mol/m^3 at 37 °C. Therefore, the second interval diffusion constant of D = 1.0 $\times 10^{-11}$ m^2/s is chosen for further simulations of the chip channel.

The elastomer diffusion constant D = 1.0 $\times 10^{-11}$ m^2/s obtained from the COMSOL simulation is almost one order lower than the Micronit diffusion constant of D = 9.88 $\times 10^{-11}$ m^2/s. One reason could be that the Micronit value is not specific for this elastomer type. Another reason could be that compression of the chip lowers the diffusion constant. Besides, the assumption that the oxygen concentration reaches 0.20 mol/m^3 is not verified with a prolonged duration of the permeability experiments.

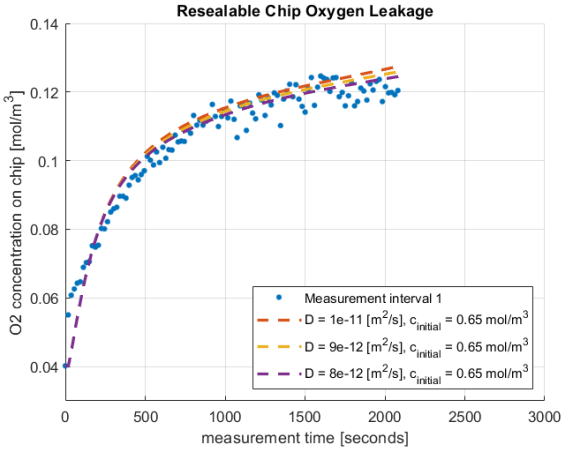

Figure 3.14: Measurement interval 1 fitted with COMSOL simulation values.

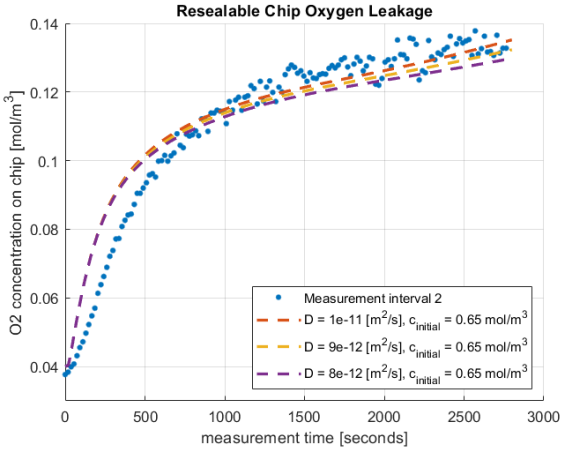

Figure 3.15: Measurement interval 2 fitted with COMSOL simulation values.

3.4. Summary Experiments

First of all, confocal imaging of the HepaRG cell layer with fluorescence staining revealed an uneven cell layer with an average thickness of 31.5 μm. Second, the chip channel height was estimated by measuring the increase in contact width of the round elastomer side under compression. This resulted in an channel height estimation of 250 μm under compression with respect to the 300 μm in uncompressed configuration. Third, the oxygen permeability of the elastomer was tested by measuring increase of oxygen with initial low oxygen concentration on the Micronit chip. The resulting diffusion constant of the compressed elastomer following from COMSOL simulations is D = 1.0 $\times 10^{-11}$ m^2/s with respect to the manufacturers value of D = 9.88 $\times 10^{-11}$ m^2/s.

4

Modelling & Simulation

In this chapter, the chip channel and gas exchanger are modelled and simulated in COMSOL to achieve a design according to the requirements of Chapter 2. First, Section 4.1 introduces the theory of laminar flow and oxygen mass transfer. Second, in Section 4.2 the chip channel is modelled to simulated the oxygen concentrations in the medium flow. Third, Section 4.3 presents a 2D gas exchanger model to simulate the effect of the silicone tubing dimensions. Fourth, Section 4.4 presents the simulated performance of the gas exchanger box design presented in Chapter 6. Lastly, Section 4.5 presents the simulated oxygen increase in 12 cm of Micronit EFTE tubing.

4.1. Theory: Laminar Flow and Mass Transfer

This section describes the theory of laminar flow and mass transfer for modelling the chip channel and gas exchanger. To start, the Reynolds number (Re) in Equation 4.1 determines the type of flow as laminar or turbulent. In the equation, ρ is the density (kg/m^3), U the characteristic flow speed (m/s), ζ the characteristic length (m) and μ the dynamic viscosity (Pa· s). The flow of cell medium at 35 μL/min in Micronit channel is laminar (Re < 1000) as indicated by the evaluated Reynolds number of 0.96 derived in Section 4.2.1 [15]. The flow of gas in the gas exchanger is also laminar as indicated by the Reynolds number of 16 derived in Section 4.3.1. For a channel geometry with a low height-to-width aspect ratio, 0.25 mm height to 4 mm width, the parallel plate approximation results in a fully developed laminar parabolic velocity profile [16].

The flow in the chip channel is modelled as laminar incompressible flow between two fixed parallel plates including only a pressure gradient along the channel length. The corresponding Navier-Stokes momentum equations with assumptions of no gravity, zero velocity profile in y or z direction and no-slip at each wall lead to velocity profile stated in Equation 4.2 [15]. In this equation, p is the pressure (Pa), x is the channel length (m), h is the channel height (m), y the coordinate along the height (m) and μ is the dynamic viscosity (Pa· s). The shear stress profile along the channel height y is described by Equation 4.3, relating to the flow velocity in x-direction u (m/s) and dynamic viscosity μ (Pa· s).

$$Re = \frac{\rho\, U\, \zeta}{\mu} \tag{4.1}$$

$$u(y) = -\frac{dp}{dx}\,\frac{h^2}{2\,\mu}\left(1-\frac{y^2}{h^2}\right) \tag{4.2}$$

$$\tau(y) = \mu \frac{du}{dy} \tag{4.3}$$

For oxygen mass transfer, it is assumed that the solute oxygen is sufficiently dilute such that is does not affect the motion of the solvent, for instance the cell medium. The mass transfer of dissolved oxygen, through for instance the cell medium or oxygen permeable membrane, is the transport of a dilute species described by the convection-diffusion equation in Equation 4.4. In the equation, c is the concentration (mol/m^3), t is time (s), $\mathbf{u}$ is the velocity field (m/s), D is the diffusion constant (m^2/s) and R is the sink term (mol/m^3/s). The term $\mathbf{u} \cdot \nabla c$ relates to convection, the term $D\nabla^2 c$ relates to diffusion and the term R relates to a reaction, for instance cellular oxygen consumption [16].

$$\frac{\partial c}{\partial t} + \mathbf{u} \cdot \nabla c = D\nabla^2 c + R \tag{4.4}$$

Further, Equation 4.5 presents the three dimensionless parameters c^*, t^* and u^*. First, the dimensionless concentration c^* is scaled with the channel inlet concentration c_0. Second, the dimensionless time t^* scaled with the diffusion coefficient D (m^2/s) in one dimension of interest. The characteristic length ζ (m) is either the channel height or channel width. This choice depends on the interest of evaluating the diffusion in vertical (height) or lateral (width) direction [16]. Third, the dimensionless speed u^* is scaled with the characteristic speed U (m/s). Substitution of the these three dimensionless parameters in Equation 4.4 results in the dimensionless convection-diffusion equation of Equation 4.6.

In Equation 4.6, the dimensionless Péclet (Pe) number describes the ratio of convective to diffusive transport. The Péclet number, stated in Equation 4.7, is obtained with the characteristic flow velocity U (m^2/s), the characteristic length ζ (m) and the diffusion constant D (m^2/s). The Péclet number for cell medium with a diffusion constant of 2.69×10^{-9} m^2/s in a 250 μm high channel with a flow speed of 1.1 mm/s is 102, indicating the dominance of convection over diffusion (Pe $\gg$ 1).

$$c^* = \frac{c}{c_0} \quad , \quad t^* = t\left(\frac{D}{\zeta^2}\right) \quad , \quad u^* = \frac{\mathbf{u}}{U} \tag{4.5}$$

$$\frac{\partial c^*}{\partial t^*} + \mathrm{Pe}\, \mathrm{u}^* \cdot \nabla c^* = \nabla^{*2} c^* + R^* \tag{4.6}$$

$$\mathrm{Pe} = \frac{U\,\zeta}{D} \tag{4.7}$$

For transient diffusion over time (excluding convection), Fick's second law of diffusion for the concentration c in one dimension x is stated in Equation 4.8. Fick's second law can be solved with the complementary error function in Equation 4.9. In this equation, c_s is the saturation concentration (mol/m^3), c_0 is the initial concentration (mol/m^3), x the diffusion length (m), D the diffusion constant (m^2/s) and t the time (s) [17].

$$\frac{\partial c}{\partial t} = D\,\frac{\partial^2 c}{\partial x^2} \tag{4.8}$$

$$c(x,t) = c_0 + (c_s - c_0) \cdot erfc\left(\frac{x}{\sqrt{4\,D\,t}}\right) \tag{4.9}$$

4.2. Chip Channel

The design objective for the chip channel is to form an oxygen gradient along the length of the channel due to cellular oxygen consumption. The geometry of the microfluidic chip channel is displayed in Figure 4.1 according to the dimensions of the Micronit resealable flow cell (Appendix Figure B.1). For all chip channel simulations, half the chip channel is modelled since the channel is symmetric along the length reducing the computational simulation time.

4.2.1. Chip Model

The chip channel consists of two borosilicate glass slides, with fluidic inlets at the top slide of 0.8 mm diameter. The elastomer is modelled as a silicone material in compressed configuration. The height of the elastomer, defining the channel height, is 250 μm, as experimentally determined in Section 3.2. This elastomer geometry includes a 1.244 mm wide flat side to the top glass slide and a 0.695 mm wide flat contact to the bottom glass slide. Further, half the cell layer is defined as a square of 2 mm wide and 25 mm long, which is visible through the open space of the chip holder and meets the requirement of a minimum cell layer of 1 cm^2 for a whole cell layer (req. 2.2 Table A.1). The height of the cell layer is 50 μm, defined by the experimentally defined HepaRG cell layer height of 31.5 μm (Section 3.1) with an additional thin layer of collagen underneath. The model is defined at a temperature of 310.15 K (37° C , req. 2.4) and a pressure of 1 atm. The complete set of modelling parameters is listed in Appendix Table B.1.

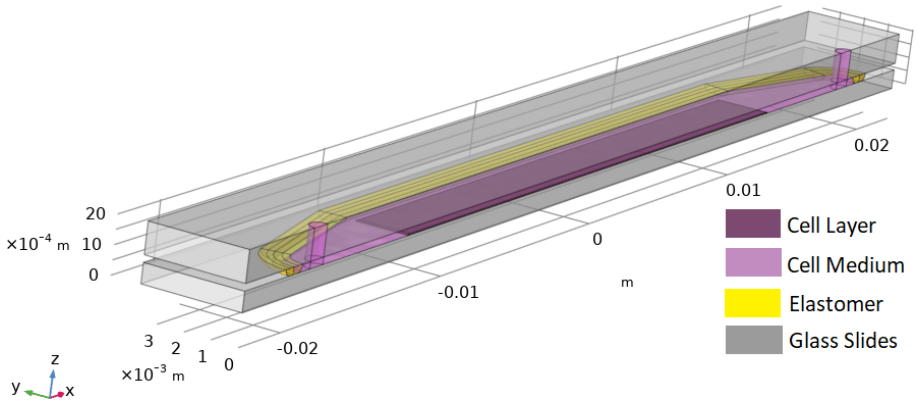

Figure 4.1: Geometry of the channel model, dimensions according to the Micronit resealable flow cell (Appendix Figure B.1).

The cell medium flow, modelled as water with a medium viscosity, in the chip channel is assumed laminar according to the Reynolds number in Equation 4.1. With the water density of ρ = 993 kg/m^3 at 37 °C [18], average fluidic inlet velocity of U = 1.16 mm/s (flow rate of 35 μL/min), characteristic inlet diameter of ζ=0.8 mm and dynamic viscosity of μ = 0.958 mPa*s at 37 °C [18], the resulting Reynolds number is 0.96 which states laminar flow. Further, the modelled fluid properties of water are adjusted with the density at 37 °C and cell medium viscosity of RPMI +10% FBS cell medium which is 45% higher than water at 37 °C [18].

For laminar medium , the flow rate is set as fully developed flow at the inlet. At the outlet the pressure is set at 0 Pa relative to the ambient pressure with suppressed backflow. For modelling half of the channel, the flow rate is also set to be half the Q_{med}. Further, at the chip walls, chip top and cell layer top surface no-slip conditions are applied. Lastly, symmetry conditions are applied to the side of the half-channel geometry. These boundary conditions result in the following flow velocity profile in Figure 4.2. The velocity profile above the cell layer shows u_{max} of 1.1 mm/s and the velocity at the relative narrow inlet shows a velocity of 1.4 mm/s.

For the medium thickness of 200 μm above the cell layer in the 4 mm wide channel, the shear stress resulted in 0.015 Pa (Figure 4.3) which is well below the maximum of 0.05 Pa and in the range of minimal 0.01-0.05 Pa as set by design requirement 2.11 (Table A.1). From literature it is known that a shear stress exceeding 0.50 Pa reduces the cellular function [11], however in general a shear stress near 0.01-0.05 is not a common standard to cause reduced cell function. For this reason, the flow rate is not increased to increase the shear stress.

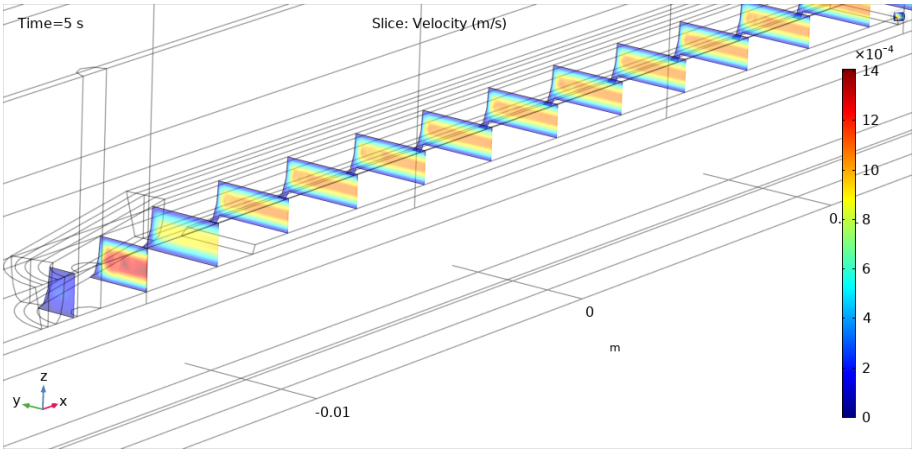

Figure 4.2: Velocity profile along the chip channel at a flow rate of 35 μL/min. In this view, the z-axis is scaled four times relative to the x- and y-axis.

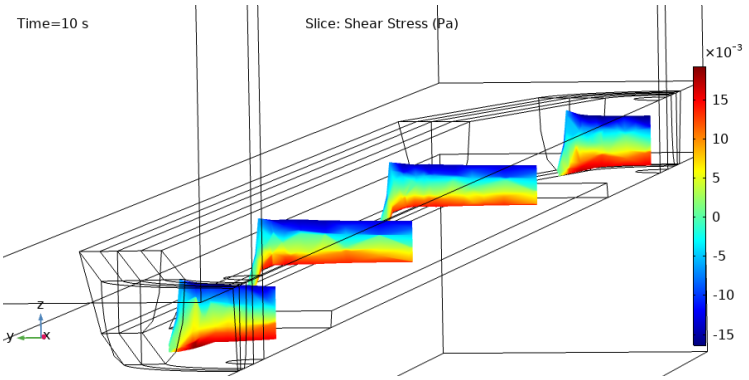

Figure 4.3: Shear stress profile of chip channel at a flow rate of 35 μL/min. In this view, the z-axis is scaled four times compared to the x- and y-axis.

Regarding the mass transport of oxygen, the following the conditions are applied for the chip channel model. First, in the water flow both diffusion and convection are applied with the diffusion coefficient and viscosity of cell medium. Second, diffusion is applied for oxygen transfer through the elastomer and cell layer with the corresponding material diffusion constants (Appendix Table B.1). Third, the initial concentrations in the medium, cell layer, glass and elastomer are set to 0.20 mol/m^3. Fourth, the oxygen consumption of liver cells of 5 nmol O_2/(min $\cdot$ 1$\times$ 10^6 cells) [11] is modelled as a negative reaction rate R_{O2}. Fifth, the concentration of outside air of 8.4 mol/m^3 [3] is set on the outside of the side of elastomer walls and glass slides. Lastly, for half the channel modelled symmetry conditions are applied. The mesh settings of the chip channel model are stated in Section B.3.1

4.2.2. Oxygen gradient

To replicate the oxygen gradient along the length of the cell layer, as described by design requirement 2.8, the oxygen concentration is evaluated on the top surface of the cell layer.

For the 45 μL chip channel, the simulation shows that it takes 60 seconds at 35 μL/min flow to lower the oxygen concentration on the cell layer from the initial saturated condition (0.20 mol/m^3) to physiological conditions (0.09 mol/m^3). After that, a stationary longitudinal oxygen gradient along the cell layer appears after 230 seconds. This longitudinal oxygen gradient over the cell layer centre from 0.09 mol/m^3 to 0.058 mol/m^3 is visualised in Figure 4.4. In this figure, the lateral difference from the channel centre at 1.0 mm width is not significant. The channel side at 1.5 mm to 1.9 mm from the centre show a lower concentration at the end of the cell layer of 0.055 to 0.052 mol/m^3 respectively. This effect is due to lower medium flow speed in the range of 1.5 to 1.9 mm from the channel centre visible in Figure B.6c. This effect should be considered for lateral oxygen measurement halfway or at the end of the chip channel. Additionally, an oxygen gradients is present over the height of the channel due to oxygen consumption of the cells on the bottom as visualised in Figure 4.5.

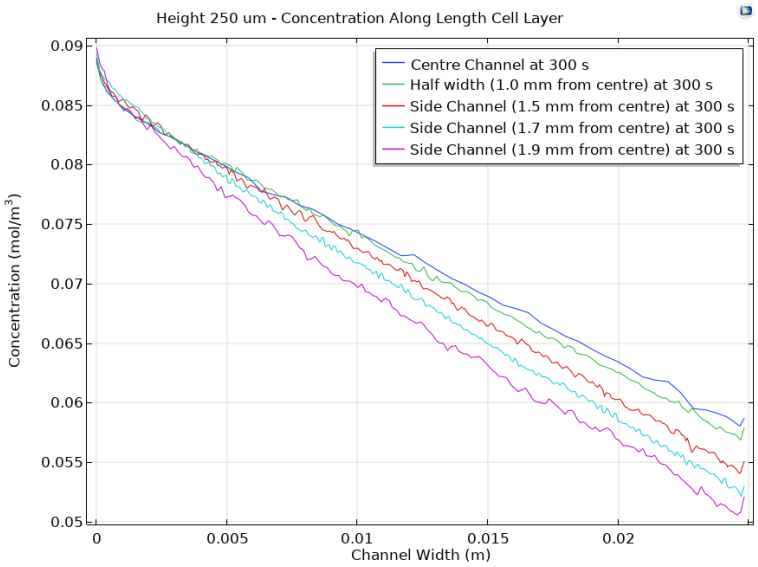

Figure 4.4: Longitudinal oxygen gradients along the cell layer length for three widths at a flow rate of 35 μL/min.

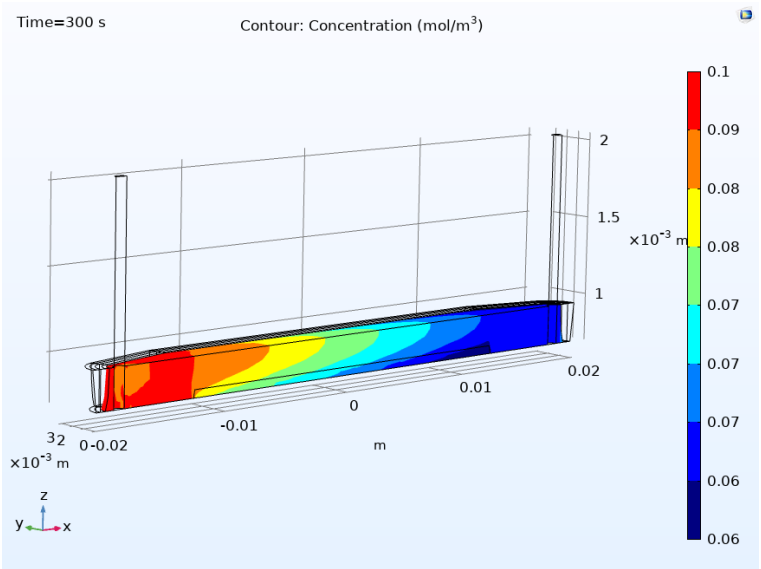

Figure 4.5: 3D oxygen gradient in the chip channel volume. In this view, the z-axis is scaled 10 times relative to the x- and y-axis.

4.2.3. Flow stop

In a cell experiment, the oxygen consumption of cells is estimated by a decay in measured oxygen concentration in the cell medium during a cell medium flow stop of 30 seconds (req. 2.7 , Table A.1). In COMSOL, a medium flow was simulated for 250 seconds after which the medium flow was stopped. Figure 4.6 displays the established oxygen gradient after 250 seconds of medium flow. After a flow stop of 30 seconds the longitudinal oxygen gradient drops with 0.02 mol/m^3. After a 60 seconds flow stop, the gradient drops 0.045 mol/m^3 which leads to oxygen concentrations in the hypoxia regime. Remarkably, the concentrations at the start and end of the cell layer decreases less rapid since the 25 mm long cell layer only partially cover the 40 mm chip channel.

These results are based on a cellular oxygen consumption of 5 nmol O_2/(min*1 $\times 10^6$ cells) which might vary for experiments in chip. The > 0.02 mol/m^3 decrease in oxygen concentration within 30 seconds fulfils design requirement 2.7 (Table A.1) which described a decrease of > 0.007 mol/m^3 during 0.5-1 min for detection by the laser setup.

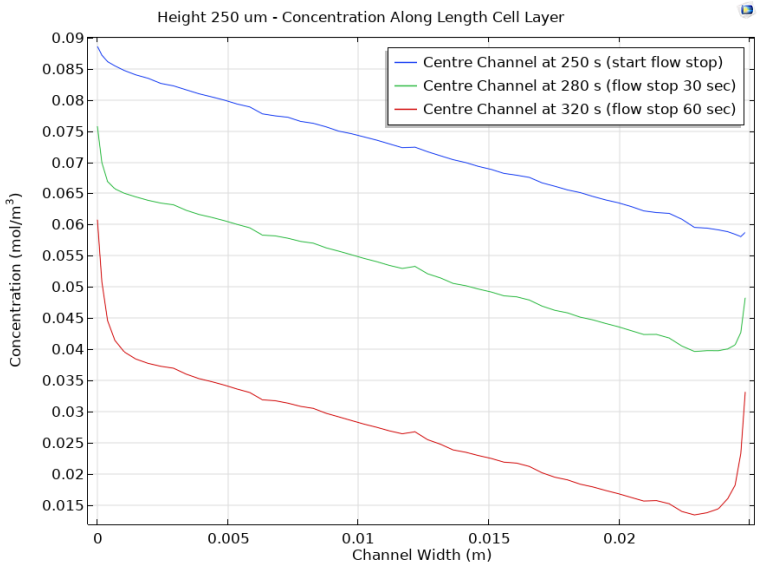

Figure 4.6: COMSOL simulation of the oxygen gradient along the cell layer centre length during a medium flow stop.

4.3. Tubular Gas Exchanger

The design objective of the gas exchanger is to set the dimensions and determine the settling time of the preferred oxygen concentration in the cell medium. The gas exchanger relies on the principle of oxygen exchange between liquid and gas through a membrane as described in Chapter 1. This straight tube model is also representative for a bend silicone tubing shape, as long as the nitrogen gas flow lowers the oxygen concentration on the outside of the silicone tubing.

4.3.1. Tubular Model

Figure 4.7 visualises the COMSOL tubular model, where the liquid cell medium (pink) modelled as water flows in the oxygen permeable silicone tubing (dark blue). The tubing is surrounded by nitrogen gas (light blue) situated in the covering gas tube (grey) modelled as PMMA. With an oxygen gradient between the cell medium liquid and the gas, the oxygen is extracted from the cell medium. The circular gas exchanger is modelled in 2D as axisymmetric around the middle of the silicone tubing length. For that reason, the gas inlet and outlet are modelled very small in diameter since these also revolve around the axis of symmetry.

The design parameters in the exchanger model are the length L, inner diameter ID and wall thickness h of the silicone tubing, as well as the flow rates of the medium Q_{med} and gas Q_{gas}. The inner diameter and wall thickness of the tubing are interdependent given by the choice of commercial tubing. The flow rate of medium in the range of 25-45 μL/min should be met as described by design requirement 1.3. The minimum flow rate is set by the mass flow controller (described Section 5.3), therefore a flow rate Q_{gas} = 200 mL/min is chosen. Further, the gas tube in grey has an inner diameter of 7.5 mm and wall thickness of 2 mm. The silicone tubing has a inner diameter of 0.8 mm and a wall thickness of 0.4 mm with a length of 37 cm.

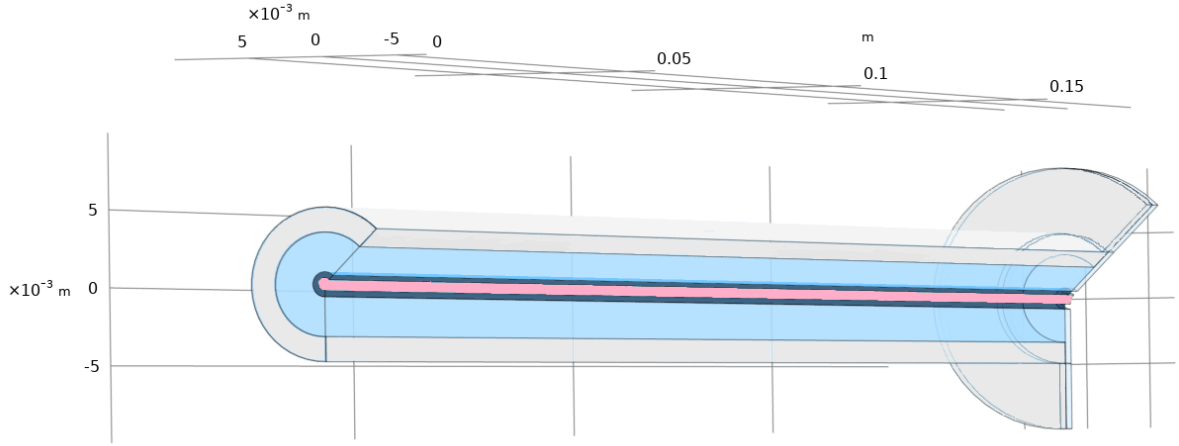

Figure 4.7: COMSOL 2D axisymmetric tubular gas exchanger model (in 3D presentation). Cell medium (pink), silicone tubing (dark blue), gas flow (light blue) and gas tubing (grey).

Laminar flow is applied for the cell medium in the silicone tubing and the gas flow of nitrogen, flowing at 35 μL/min and 200 mL/min respectively. The Reynolds number for medium at 37 °C in tubing, with a characteristic length ζ = 0.8 mm, is similar to Re = 0.96 calculated value at the Micronit inlet in Section 4.2.1. The nitrogen gas with density ρ = 1.091 kg/m^3, flow rate of 200 mL/min results in a characteristic flow speed U=79.0 mm/s. For the characteristic length ζ between the tubes of 3.35 mm and dynamic viscosity μ = 1.82 $\times 10^{-5}$ Pa·s, the Reynolds number is 16 within the laminar regime.

Regarding mass transport, there is only diffusion through the silicone membrane, and both diffusion and convection for the flow of medium and nitrogen. The oxygen concentration 8.4 mol/m^3 of air is applied on the outside of the gas tube. Initial concentration conditions are set to 0.20 mol/m^3 for cell medium at 37 °C and silicone tubing. Variation between 0.15 and 0.30 mol/m^3 in the initial tubing concentration influences the exchanger medium outlet concentration with 0.03 mol/m^3 after 100 seconds and is insignificant after 300 seconds as shown by Figure 4.8. The model is defined at a temperature of 310.15 K (37° C , req. 2.4) and a pressure of 1 atm.

Presence of air with a high oxygen concentration (8.4 mol/m^3) with respect to nitrogen causes a oxygen flux into the oxygen permeable tubing, which increases the medium concentration at the simulation start. This resulting peak at the start is physically not possible since the saturation concentration in medium at 37 °C is 0.20 mol/m^3. Future research should include the saturation concentration in COMSOL to prevent oxygen concentrations > 0.20 mol/m^3.

Additionally, the initial concentration of PMMA is set to be 0.32 mol/m^3 [19]. Variation of this gas tube initial concentration does not influence the medium outlet concentration as shown in Appendix Figure B.14. The complete set of modelling parameters is stated in Appendix Table B.2.

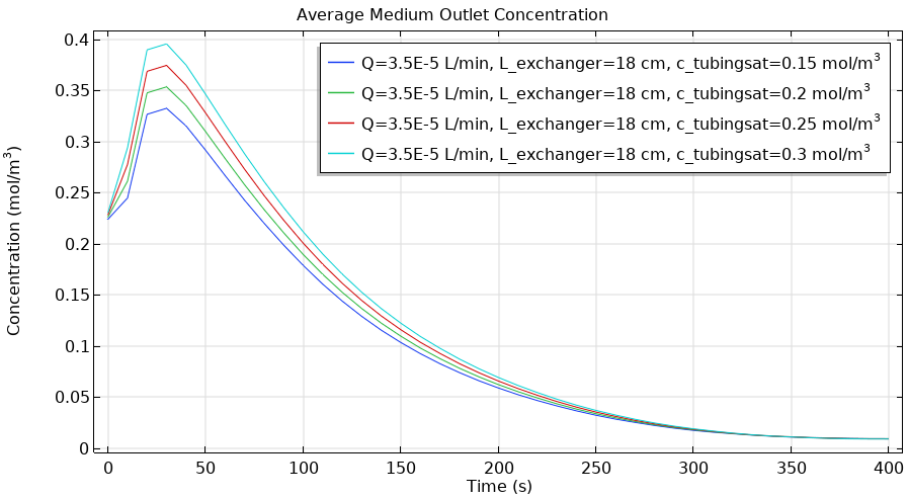

Figure 4.8: COMSOL simulation average medium outlet concentration of the 18 cm tubular exchanger. Including 35 μL/min medium flow and 200 mL/min gas flow for varying initial silicone tubing concentrations.

4.3.2. Tubular Exchanger Simulation

This section presents the results of COMSOL simulations of the tubular model to determine the effect of the tubing length L, flow rate Q_{med} and the choice of commercial tubing on the oxygen concentration at the exchanger medium outlet.

First, the influence of the tubing length is evaluated at a medium flow rate Q_{med} = 35 μL/min. For a larger tubing length the cell medium has more time to exchange oxygen, therefore a lower concentration is expected. The silicone tubing length was adjusted to 53, 33 and 18 cm and the average concentration of the medium outlet surface was derived. The resulting Figure 4.9 shows an increase in concentration during the first 80 seconds above the saturated medium concentration of 0.20 mol/m^3. As previously discussed, this increase is physically not possible. The three lengths follow the same curve until 400 seconds, after which the shortest length of 18 cm exchanger reached a minimum of 0.018 mol/m^3 while the longer exchanger reach lower towards 0 mol/m^3. Further, the three tubing lengths reach conditions below 0.02 mol/m^3 within 300 seconds, which characterises the time to reach low oxygen concentrations.

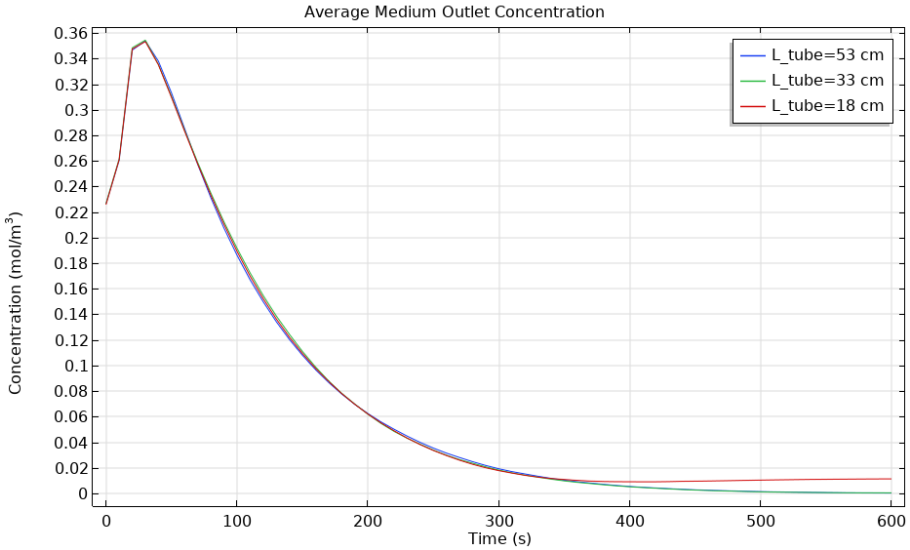

Figure 4.9: COMSOL tubular exchanger simulation of the average medium outlet concentration at varying tubing lengths at 35 μL/min medium flow rate.

Second, the relation between the medium flow rate and the outlet concentration of the gas exchanger is evaluated. Figure 4.10 shows that the outlet concentration for 18 cm tubing shows slight deviation for varying flow rates in the stationary value after 300 seconds. The decay in oxygen concentration is not influenced by a flow rate between 25 and 45 μL/min fulfilling design requirement 1.3. Yet the stationary low oxygen concentration varies with 0.02 mol/m^3 for this flow rate range.

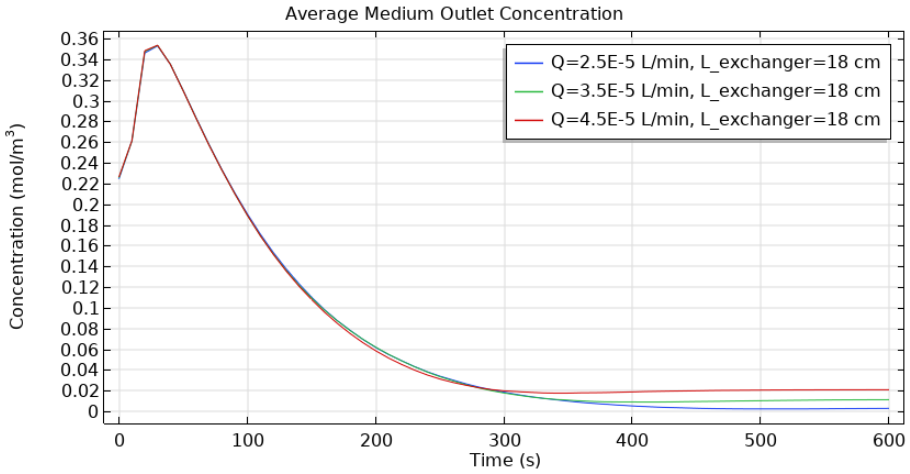

Figure 4.10: COMSOL 18 cm tubular exchanger simulation of the average medium outlet concentration length at at varying medium flow rates.

Third, two commercial tubing choices with different inner diameter and wall thickness are evaluated. The first tubing is the VMQ silicone tubing with inner diameter 0.8 mm and wall thickness 0.40 mm (Section 5.3). The second tubing is the platina cured silicone tubing with inner diameter 0.31 mm and wall thickness 0.15 mm (VWR website link). In the complementary error function (Equation 4.9), describing oxygen diffusion through a membrane, the concentration changes linearly with the tubing wall thickness x in the factor $x/\sqrt{4\,D\,t}$. Reduction of the wall thickness relates to a lower oxygen concentration over time, therefore low oxygen concentration can be realised within a shorter time.

For this COMSOL simulation the experimentally determined diffusion coefficient D = 1.1 $\times 10^{-9}$ m^2/s (Section 5.5) is assumed for both tubing types. Evaluating the average concentration at the medium outlet in Figure 4.11, the first tubing with a wall thickness of 0.4 mm a concentration < 0.01 mol/m^3 after 340 seconds. In comparison, the tubing with a wall thickness of 0.15 mm already reaches low oxygen < 0.01 mol/m^3 after 50 seconds, within the desired of 1 minute response time as described by requirement 1.1. The tubing with thinner wall thickness leads to more rapid diffusion of oxygen, therefore the initial air conditions in the tube cause a relative larger medium concentration peak with respect to the tubing with thicker wall thickness. Additionally, Figure B.15 shows a significantly more rapid decrease of oxygen when reducing the wall thickness of a 0.8 mm inner diameter tubing from 0.40 mm to 0.15 mm.

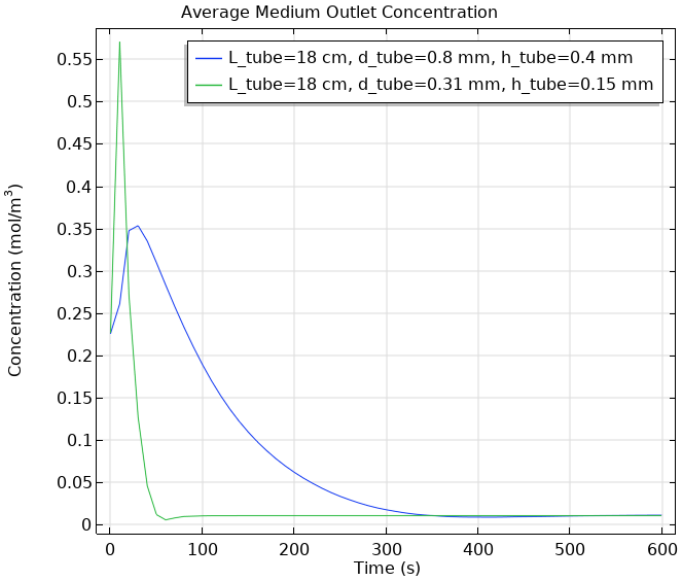

Figure 4.11: COMSOL tubular exchanger simulation of average medium outlet concentration for two silicone tubing types at 35 μL/min medium flow rate.

4.4. Gas Exchanger Box

The functioning prototype with 18 cm silicone tubing (Chapter 5) showed resulting oxygen concentration of < 0.01 mol/m^3 within 5 minutes. This low oxygen medium provided by the tubular gas exchanger is not transferred to the microfluidic chip, since the microfluidic connectors are oxygen permeable.

Besides, the design objective of the gas exchanger box is to minimise the dimensions of the module connected to the microfluidic setup of the Micronit. The dimensions of the Micronit chip holder are 128 mm x 85 mm x 21 mm (Section 5.3) and it would be beneficial if the additional gas exchanger could be placed on top of this chip holder realising a compact system relative to the chip channel glass slides of 45 x 15 x 2.1 mm. Minimising the gas exchanger dimensions allows placing the system in an incubator to grow cell culture or in a microscopic setup for imaging the cells.

The design requirement 1.1 states that low oxygen concentration of 0.01 mol/m^3 should be reached within time of 1-5 minutes. This section presents the gas exchanger 3D model to provide insight on the gas flow within box and evaluate the decrease in medium oxygen concentration. The gas exchanger box, presented in Chapter 6, contains a gas volume inside of 50 x 50 x 17 mm and 18 cm tubing length. Only the bottom half of the gas exchanger box design is modelled for symmetry.

At the start of the simulation, the nitrogen gas flushes out the air present in the box. A 3D simulation with convective mass transfer for cell medium and nitrogen gas is performed to reach low oxygen concentration <0.01 mol/m^3 on the outside boundary of the silicone tubing. The height of the gas is adjusted to 8 mm instead of 17 mm, since no variation on the very top and bottom of the gas flow are expected. For this 3D model it is assumed that there is no change in the silicone diffusion constant caused by material tension of the bend tubing.

Figure 4.12 presents the top view on the bottom half of the box. At t = 0, Figure 4.12a indicates the presence of air with a concentration of 8.4 mol/m^3 and the inlet of nitrogen in the lower left. Second, Figure 4.12b indicates that the box is filled with nitrogen after 40 seconds. The following Figure 4.12c and Figure 4.12d show decay in the oxygen concentration in the tubing. Remarkably the tubing on the lower right is quicker lowered in concentration prior to the lower left positioned, which is closer to the nitrogen inlet. Further, the streamline velocity profile of nitrogen in Figure 4.13 shows a flow direction straight along the diagonal and bend along the corners with only at the inlet some swirls in velocity direction. The flow speed magnitude profile is displayed in Figure B.17.

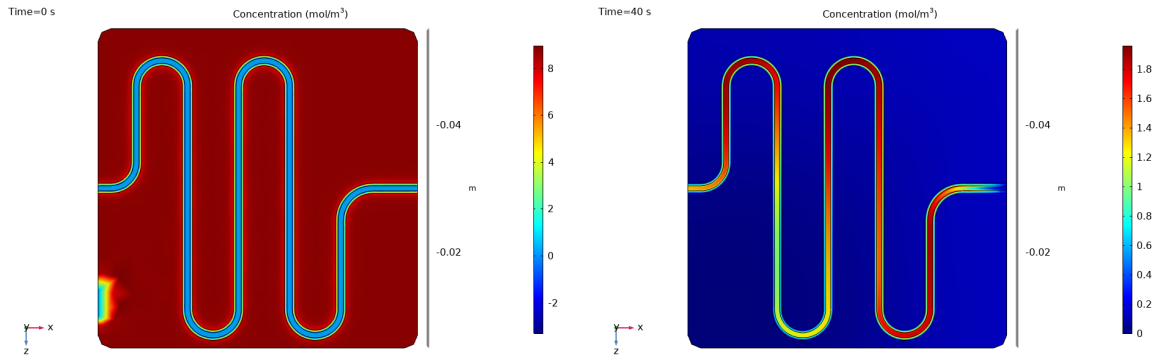

(a) Time = 0 sec, air inside box.

(b) Time = 40 sec, box filled with nitrogen.

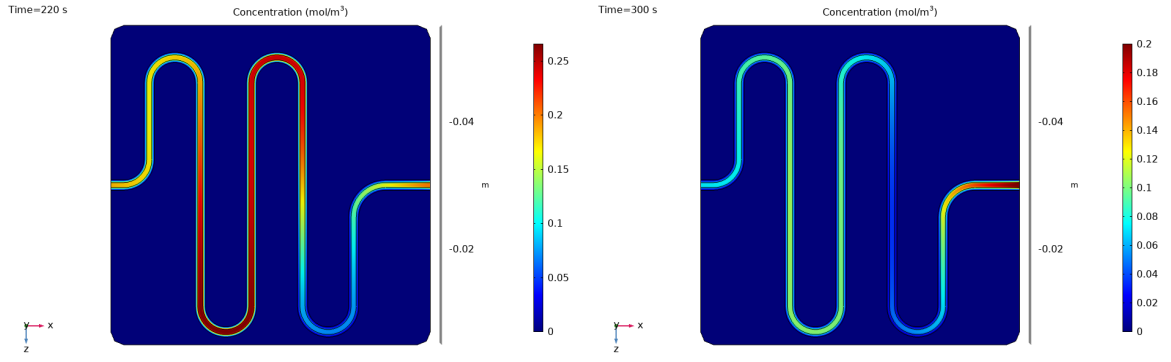

(c) Time = 220 sec, medium concentration decay in lower right tubing.

(d) Time = 300 sec, concentration medium outlet (left side) reaches 0.07 mol/m^3.

Figure 4.12: Top view of COMSOL 3D simulation of the bottom half of the exchanger design with convective nitrogen gas flow.

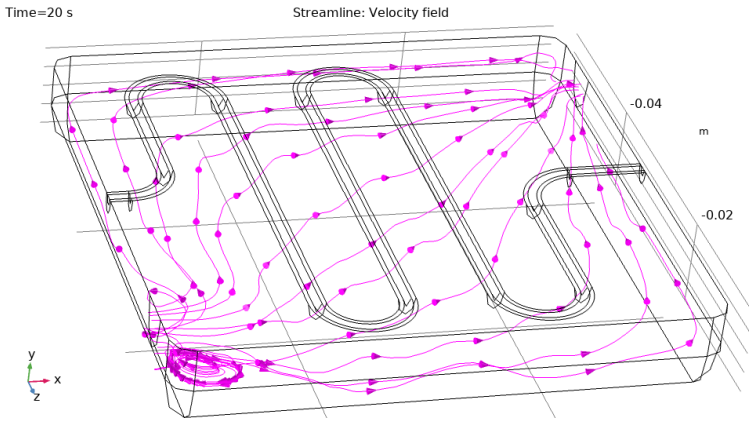

Figure 4.13: COMSOL simulation of nitrogen gas velocity streamline profile in the bottom half of the gas exchanger box.

Although symmetry conditions are applied, the model including nitrogen flow still contains 44911 elements with 76344 DOF taking 3 hours to solve a COMSOL study of 300 seconds. To simplify the model, the time required to reach a conditions < 0.01 mol/m^3 on the silicone tubing outside boundary is determined with this 3D model including nitrogen gas flow. The membrane concentration < 0.0018 mol/m^3 on the membrane outside is reaches within 100 seconds. These 100 seconds should be added to the simulations assuming 0 mol/m^3 on the membrane outside boundary. Figure B.16 visualises the outside silicone membrane after 100 seconds.

For the 3D model without nitrogen gas flow, the initial conditions in the medium and membrane should be determined to include the concentration peak seen in the previous 3D model including nitrogen gas flow. Figure 4.14 shows the average concentration of the total medium and silicone membrane length on the symmetric surface. After 100 seconds of nitrogen flow through the box, the medium reaches 0.75 mol/m^3 and the membrane reaches 0.35 mol/m^3. These concentrations are used as initial concentrations for the model without nitrogen flow.

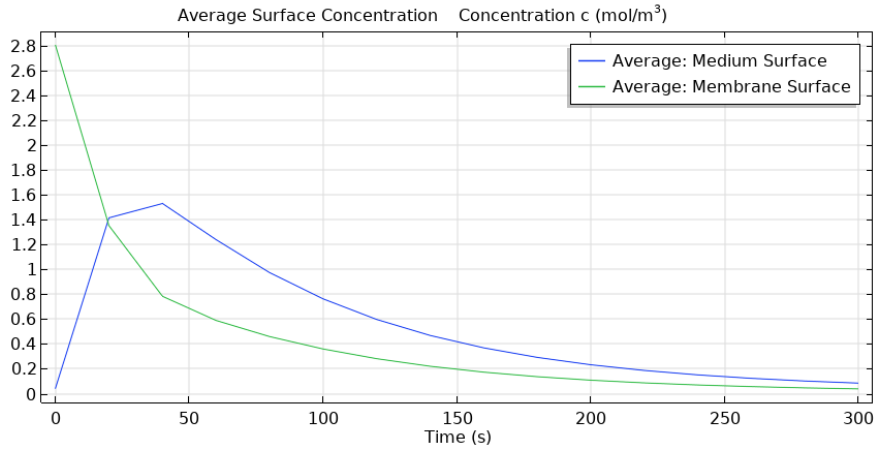

Figure 4.14: COMSOL simulation of the average medium and membrane surface concentration along the symmetric gas exchanger bottom half.

The 3D COMSOL simulation without gas flow shows that the outlet concentration decreases to physiological 0.09 mol/m^3 within 160 seconds and to low oxygen conditions of 0.01 mol/m^3 within 330 seconds. It is important to note that these times require an additional 100 seconds to lower

the concentration on the outside of the membrane. The computational time to solve 300 seconds of simulation reduced from 3 hours to 3 minutes with respect to the nitrogen flow model. Additionally, mesh convergence is shown for a normal size mesh as shown in Figure B.18.

Overall, the simulations of the 3D gas exchanger model demonstrate low oxygen conditions (0.01 mol/m^3) within 430 seconds. This satisfies the design requirement 1.1 of reaching the low oxygen concentrations, however the time takes about 7 minutes instead of the desired 1-5 minutes.

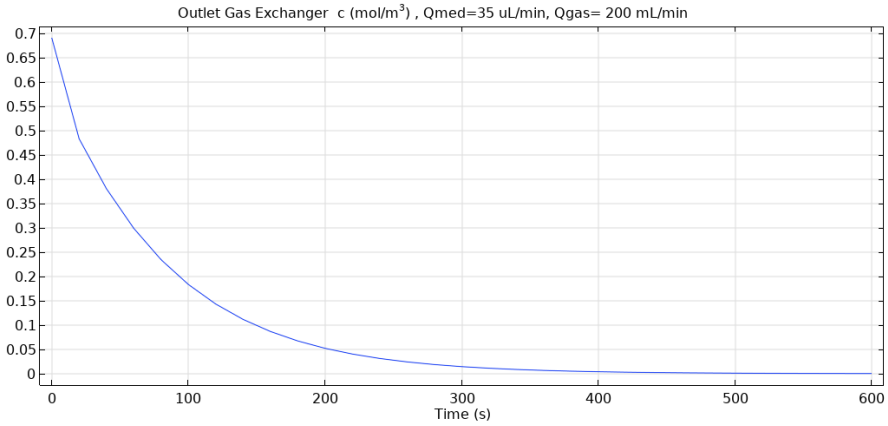

Figure 4.15: COMSOL simulation of the gas exchanger average medium outlet concentration with the boundary condition of 0 mol/m^3 on the tubing outside. To note: an additional 100 seconds is required to reach 0 mol/m^3 on the silicone tubing outside.

4.5. Microfluidic Connectors

The prototype test described in Section 5.5 revealed increase in oxygen concentration in the microfluidic connection from the exchanger outlet towards the microfluidic chip. The microfluidic connection, converting silicone tubing to the Micronit ETFE tubing, exist of tubing as well as connector parts. With a flow rate of 35 μL/min, the flow speed for the ETFE tubing (ID = 0.25 mm, OD = 1.58 mm) is 11.8 mm/s. In 12 cm of EFTE tubing, the low oxygen medium would be transferred for 12 seconds in tubing surrounded by air. In COMSOL the increase in concentration during the transfer of medium through the oxygen impermeable EFTE tubing is modelled. The diffusion constant is chosen to be D = 1.0 $\times 10^{-12}$ m^2/s (CES Edupack: unfilled ETFE [20]) and the tubing length is 12 cm.

Figure 4.16 presents the increase of oxygen for the lowest required oxygen concentration of 0.01 mol/m^3 at the tubing start for varying initial EFTE tubing concentrations. A higher initial tubing concentration increases the outlet concentration for 60 seconds, after which the effect is neglectable to concentrations (< 0.012 mol/m^3) at the tube end. These results show that the initial concentration of the EFTE causes a temporary increase in the first 60 seconds of low oxygen conditions, after which the oxygen concentration stays around the desired 0.01 mol/m^3.

For an initial concentration of 0.20 mol/m^3, the concentration increases from 0.01 mol/m^3 with 7% towards 0.0107 mol/m^3. These temporary losses can be be compensated by setting the concentration of the gas exchanger module. Since the Micronit tubing is able to transfer very low oxygen concentrations, the connectors might cause an oxygen increase into the medium. In order to eliminate this effect, the microfluidic connectors are placed inside the gas exchange module as explained in the detailed design of Chapter 6.

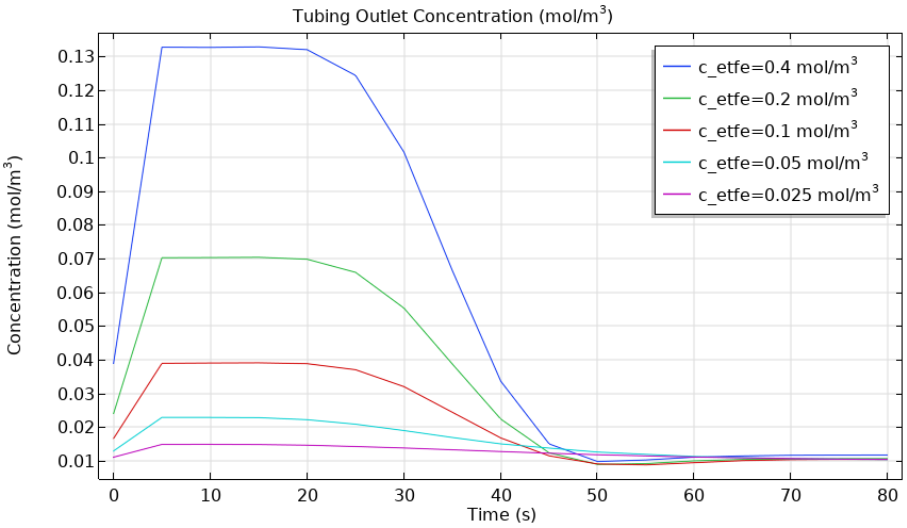

Figure 4.16: COMSOL simulation of oxygen concentrations at end of 120 mm EFTE Micronit tubing, with continuous medium inlet concentration of 0.01 mol/m^3 and varying initial tubing concentration.

5

Tubular Exchanger Prototype

This chapter describes the test of a tubular gas exchanger, which test the gas exchange with cell medium flowing through an oxygen permeable silicone tubing surrounded by nitrogen. With this prototype, the medium flow rate, length of tubing and the oxygen tightness of the connection towards the Micronit chip are tested. First, Section 5.1 describes the background of oxygen measurements. Second, Section 5.2 describes the laser-fiber experimental setup. Third, Section 5.3 states the prototype materials. Fourth, Section 5.4 describes the test protocol for the tubular gas exchanger as well as the processing of the measurement data. Lastly, Section 5.5 presents the test results of the tubular exchanger.

5.1. Oxygen Measurement Method

The optical luminescence detection method of oxygen deploys the oxygen quenching principle of fluorescence dyes. The luminescence response of these dyes, after light pulse excitation, is sensitive to dissolved oxygen in liquid [1]. Oxygen acts as an energy acceptor, leading to a decrease in intensity and lifetime of the fluorescence or phosphorescence types of photoluminescence which is proportional to the concentration of molecular oxygen described by the Stern-Volmer equation stated in Equation 5.1. In this equation τ_0 and I_o are detected excited fluorescence lifetime and intensity respectively in absence of O_2, where τ and I are lifetime and intensity at a certain oxygen concentration, and k_q is the quenching rate constant [9]. The Stern-Volmer equation can be rewritten as stated in Equation 5.2 obtaining the oxygen concentration O_2 from the fluorescence lifetime τ.

$$\frac{I_0}{I} = \frac{\tau_0}{\tau} = 1 + k_q\, \tau_0\, [\mathrm{O_2}] \qquad (5.1)$$

$$O_2 = \frac{1}{k_q}\,(\frac{1}{\tau} - \frac{1}{\tau_0}) \qquad (5.2)$$

The time-gated detection principle (Figure 5.1) of the fluorescence is based on exponentially fitting the decay in emission along a set of time intervals. The ratio of emission signal over several time points in the microseconds range determines the lifetime which links to the oxygen concentration dissolved in the cell medium. This method is preferred over intensity detection, since this method is not influenced by variation in indicator concentration, photo-bleaching or light scattering. [1].

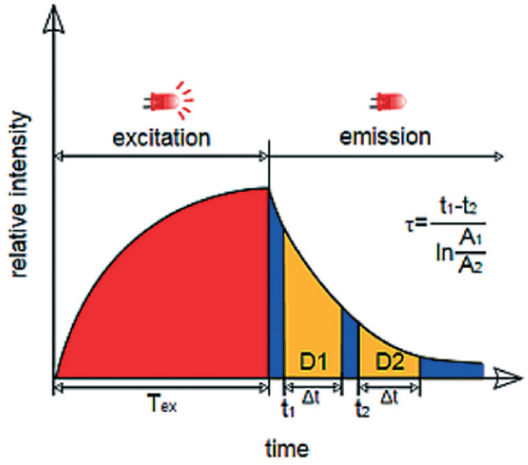

Figure 5.1: Gated detection optical measurement method for optical sensing of oxygen. Figure by Gruber *et al.* [1].

For this research, optical luminescence is detected with the sensor format of the dissolved indicator dye in the cell medium to measure the oxygen concentration. This indicator dye does not require integration in the Micronit chip channel compared to an oxygen indicator incorporates in a sensor layer. Low oxygen concentrations (0.01 mol/m^3) should be measured to validate the low oxygen concentration on chip (req. 2.8, Table A.1) and at the gas exchange outlet (req. 1.1). A dissolved oxygen sensitive indicator in the metallopophyrin complex is chosen that can detect oxygen concentration below 1 ppm (0.03 mol/m^3), which is not reached with ruthenium-based oxygen indicators [9].

Further, oxygen measurements are taken in moving cell medium at 1.1 mm/s flow speed as explained in Section 4.2.1. The emitted fluorescence signal is read for 50,000 samples at a rate of 10 MS/s , which leads to a total data acquisition time of 5 ms [14]. At a flow speed of 1 mm/s during 5 ms, the fluid will move a distance of 5 μm with respect to the read fiber of 200 μm core diameter, therefore the emitted signal is detected well.

The HepaRG liver cell viability is validated for the oxygen indicator: palladium porphryin (PP) dye ((Pd(II) meso-Tetra(4-carboxyphenyl)porphine)). In the concentration range of 0.1-100 μM PP, neither a decrease in ATP concentration is measured over 2 and 4 days, nor morphological changes are seen with respect to the control volume without palladium porphyrin. ATP indicates the energy level in the cell and is therefore an indicator for cell viability. Experimental data and experimental method is stated in Section A.3. This cell viability test shows that PP is not toxic to cells for 0.1-100 μM concentration and can be applied as indicator for the oxygen measurements.

5.2. Laser-Fiber Experimental Setup

The delayed luminescence measurement setup present at the Erasmus MC is similar to the setup described in the paper of Bodmer *et al.* [14], of which only the phospherescence detection channel of the delayed fluorescence detector is used. Also, this research utilises the luminescence indicator palladium porphyrin instead of protopophyrin IX in the publication of Bodmer *et al.* A system overview of the experimental setup is stated in Figure 5.2.

To start, the excitation light source consists of a tunable laser (Opolette 355-I, Opotek, Carlsbad) providing pulses of 2-10 ns with 2-4 mJ/pulse in the wavelength range of 410-670 nm. Next, the laser is coupled to a Fiber Delivery System (FDS) (Opotek, Carlsbad) consisting of a 50 mm planoconvex

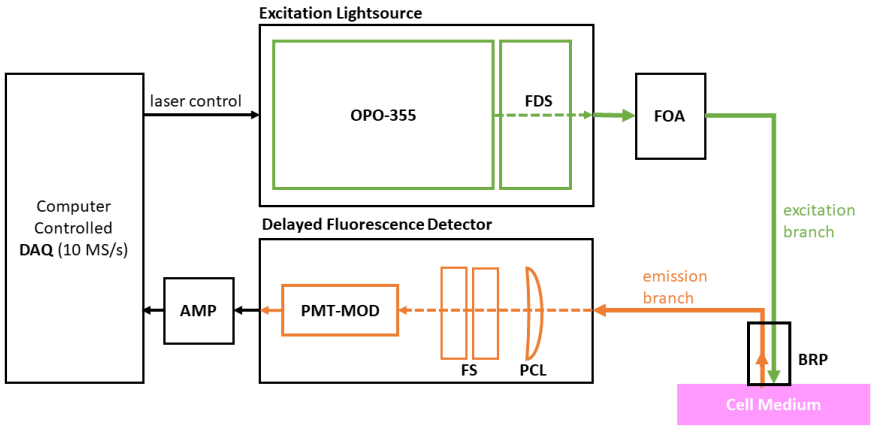

Figure 5.2: Schematic drawing of the laser-fiber experimental setup for measuring oxygen in cell medium. OPO-355: Opolette 355-I, FDS: Fiber Delivery System, FOA: Fiber Optic Attenuator, BRP: Bifurcated Reflection Probe, PCL: Plano Convex Lens, FS: Filter Set, PMT-MOD: Photo Multiplier Module, AMP: Amplifier, DAQ: Data Acquisition.

lens, XY-fibermount and a 2 meter long fiber with a core diameter of 1000 μm. The fiber was connected to a bifurcated reflection probe including 6 light-fibers and 1 read fiber each of 200 μm core diameter (FCR-7IR400-2-2.5x20, Avantes b.v., Eerbeek).

After exciting of the the indicator, the emission signal is detected by a photomultiplier module (PMT) with gate function (H10304-20-NN, Hamamatsu Photonics) by in-house built optics consisting of a filter-holder, a plano convex lens (BK-7, OptoSigma, Santa Ana) with focal length of 90 mm. The emitted light was filtered by a combination of a 590 nm long pass filter (OG590, Newport) and a broadband 675 nm ±25 nm bandpass filter (Omega Optical, Brattleboro).

Subsequently, the output currents of the photomultipliers were voltage-converted by in-house built amplifiers with an input impedance of 440 ohm, 400 times voltage amplification and a bandwidth around 20 MHz. Data-acquisition was performed by a PC-based data acquisition system containing a 10 MS/s simultaneous sampling data acquisition board (NI-PCI-6115, National Instruments). The amplifiers were coupled to the DAQ-board by a BNC interface (BNC-2090A, National Instruments). The data acquisition ran at a rate of 10 mega samples per second. Control of the setup and analysis of the data was performed with software written in LabView (Version 13.0, National Instruments, Austin).

For the palladium porphyrin oxygen indicator, the quenching rate constant is $k_q = 356\ \mathrm{s}^{-1}\ \mathrm{mmHg}^{-1}$ and the lifetime in absence of oxygen is $\tau_0 = 550\ \mu$s determined for the palladium porphyrin by Mik *et al.* [21]. Further the settings in the LabView were as follows: The laser provided 1 shot, channel settings are set to palladium porphyrin for the right values of k_q and τ_0, for lifetime analysis fitting settings start fit after 150 samples with 50,000 samples, and a channel sensitivity is set to 2.0 V. Time between measurement intervals is set to 20 seconds.

The temperature dependent quenching rate constant k_q of Pd-porphyrin is 115 at 21.5 °C room temperature and 190 at 37°C in air-saturated water according to Sinaasappel *et al.* [22]. Therefore the oxygen values provided by the setup at room temperature are calibrated for 37 °C by multiplication with a factor 190/115 = 1.65.

5.3. Tubular Exchanger Materials

This section lists the materials of the gas exchanger prototype depicted in Figure 5.3.

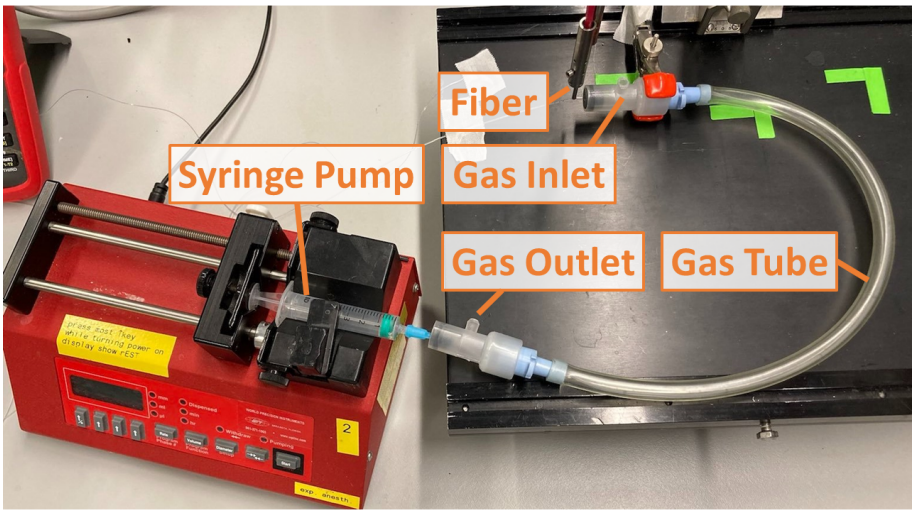

Figure 5.3: Tubular gas exchanger setup. Syringe pump lets medium flow through the silicone tubing of 53 cm inside a PVC gas tube. Gas flow is inserted at the connecting pieces at the end of the gas tube. Fiber measures oxygen at end of the medium flow.

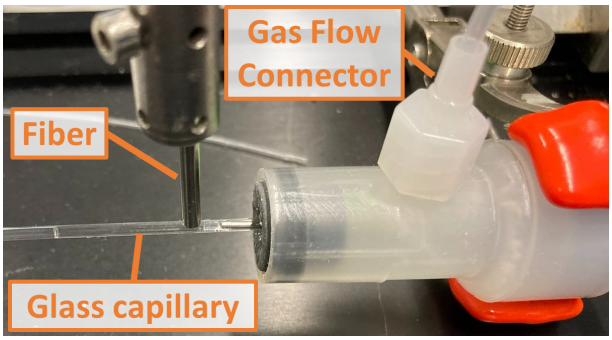

Figure 5.4: Tubular exchanger medium outlet with fiber placed on a glass capillary.

- Microfluidic pump: Single syringe pump (type NE-1000) with a BD 5 mL syringe
  Website: www.newerainstruments.com/products/syringe-pumps/pumps/syringeone.
- Syringe to silicone tube connection: Blunt Luer needle 23G (blue), stainless steel, is pushed into the rubber and silicone tubing is pushed over the needle end.
- Silicone tubing: translucent VMQ silicone tubing with ID = 0.8 mm and wall thickness of 0.4 mm. Website: www.nl.vwr.com/store/product/8563104/tubing-silicone.
- Gas tube: oxygen impermeable PVC tube with ID = 7.5 mm, wall thickness 1.6 mm and length of 37 cm.
  Website: www.fishersci.fi/shop/products/nalgene-non-phthalate-pvc-tubing-25/16595110
- Gas inlets: 3-way gas tube adapters (OD=15 mm, length of 75 mm) with closing rubbers.
- Gas flow connectors: luer extension line V-green extension 71100.10, connecting nitrogen supply to gas flow adapters with male luer. Visualised on the right in Figure 5.4.
- Glass capillary: capillary micropipettes of 55 μL inner volume and measured outer diameter of 1.68 mm and length 60 mm, therefore assumed ID = 1.1 mm.
  Website store: www.nl.vwr.com/store/product/574921/capillaire-micropipetten
  Fluorescence peak intensity on glass capillary filled with PBS (without PP) is 0.35 V compared to 0.60 V of fine bore polystyrene tubing (Portex, ID = 0.58 mm) with laser-fiber described in Section 5.2. Glass capillary visualised on the left in Figure 5.4.

- Gas control nitrogen and air: thermal mass controllers of Bronckhorst (type F-201CV-5K0-RAD-22-V adjusted for low flow range.
  Website: www.bronkhorst.com/int/products/gas-flow/el-flow-select/f-201cv/
  Flow range of 40 mL/min to 2 L/min for normal conditions (1 atm and 0 °C) with an accuracy of 0.5% off from reading. The four gas controllers for O_2, N_2, CO_2 and air are combined with a single channel module (E-7000) for modular digital readout of the analogue mass controller. The different gasses are mixed to a single PVC tube with a tube splitter.
- Microfluidic channel: straight Micronit resealable flow cell 45 mm x 15 mm (Figure 3.5) including borosilicate glass slides with a 700 μm bottom and 1100 μm thick top. This forms a 40 mm long and 4 mm wide microfluidic channel with a height of 300 μm before compression in the chip holder.
  Website: wwww.store.micronit.com/resealable_flow_cell.html
  The price of 6 slides is 500 euros (Micronit store, 12th of June 2021).
- Chip holder: Micronit Fluidic Connect Pro Chip Holder - top connect, chip holder (128 mm x 85 mm x 21 mm) to insert the resealable flow cells, displayed in Figure 3.6. Exact dimensions are given on the following Micronit website.
  Website: www.store.micronit.com/fluidic_connect_pro_resealable_flow_cells.html
  The price of the holder is 1950 euros (Micronit store, 12th of June 2021).
- Micronit EFTE tubing: Fluidic Connect Pro EFTE connection kit including 5 m of Teflon tubing with ID = 0.25 mm, OD = 1.58 mm. Also includes 5 FFKM ferrules for fluidic connection towards fluidic inlet holes on top of glass chip channel slide.
  Website: www.store.micronit.com/fluidic_connect_pro_etfe_connection_kit.html
  Price of tubing is 159 euros (Micronit store, 12th of June 2021).
- Oxygen indicator: Palladium Porphyrin (Pd(II) meso-Tetra(4-carboxyphenyl)porphine), manufacturer name: PdT790.
  Website: www.orders.frontiersci.com/Orders/WebPlugin/ProdDetail.aspx?cat=PdT790

5.4. Test Protocol and Data Processing

This test protocol is applied for the tubular gas exchanger experiments, measuring decrease or increase of oxygen with varying duration after starting or stopping nitrogen gas flow respectively.
1. Prepare medium. Mixing 3 or 5 mL PBS with 5 mM PP.
2. Choose the laser Labview settings of Palladium Porphyrin, wavelength 524 nm, laser power 90%, channel sensitivity of 2.0 V, one laser pulse and 0.2 min measurement interval.
3. Set PhotoMultiplierTube (PMT) between 150-300 to detect a initial peak of the fluorescent signal > 1 V (at saturated oxygen) of the 0-2 V sensitive channel.
4. Flush whole tubing with cell medium (syringe pump 'purge' option).
5. Start air flow of 200 mL/min for 1 minute (to flush out remaining nitrogen).
6. Start medium flow rate of syringe pump at a medium flow rate of 35 μL/min.
7. Obtain stable oxygen interval measurements at gas exchanger medium outlet for 9 measurements (3 minutes) expected around 100 mmHg (saturated oxygen at 23.3 °C, with laser setup quenching constant of 37 °C).
8. Start nitrogen flow of Bronckhorst controller at 200 mL/min.
9. Wait for stationary value at low oxygen (after 10-20 minutes).
10. Stop nitrogen flow, and start air flow at 200 mL/min for 120 seconds.
11. Wait for increase in oxygen concentrations towards initial oxygen concentration measured at step 7.

The laser-fiber setup controlled with Labview provides a .txt file containing the measurement number, time of measurement, fluorescence lifetime (μs) and the resulting oxygen concentration (mmHg).

Work of Oomen *et al.* provides the conversion from mmHg to mol/m^3 at aqueous solutions at 37 °C, displayed in the Table D.1. Oxygen concentrations in mmHg are converted to mol/m^3 with a multiplication with a factor 1.4005 $\times 10^{-3}$. Only the conversion ratios of Oomen *et at.* should be used for changing units, the exact values for oxygen concentration are given for aqueous solutions and not specific for cell medium [2].

In MATLAB, the laser data is read and oxygen concentrations (mmHg) values are rounded to one digit behind the decimal point. In the dataset the oxygen concentration is converted to mol/m^3 and if needed adjusted for temperature when not measured at 37 °C. In a MATLAB for loop, the measurement points are selected for measurement intervals with the time of measurement set to duration in minutes. The MATLAB code used for processing and plotting the data is stated in Appendix E.

5.5. Test Results

This section presents and interprets the gas exchanger prototype tests measuring the decrease in oxygen concentrations for varying flow rates, tubing length and gas ratio of air/nitrogen.

To start, the 53 cm tubing prototype shows a decrease in oxygen concentration at the outlet after 1 minute as presented in Figure 5.5 and Figure 5.6. Figure 5.5 shows consistent behaviour of two tests after starting the nitrogen gas flow, reaching an oxygen concentrations below 0.01 mol/m^3 within 8 minutes. Figure 5.6 shows that an increased medium flow rate of 45 μL/min leads to low oxygen concentration < 0.01 mol/m^3 within 5 minutes, relative to 8 minutes at 35 μL/min. This could be explained with the faster flow speed less influenced by oxygen leakage of the microfluidic connector as explained later in this section.

COMSOL simulations of the tubular gas exchanger model (Section 4.3.1) with the silicone tubing diffusion constant D = 2.54 $\times 10^{-10}$ m^2/s (VMQ silicone CES Edupack [20]) showed a less steep oxygen decrease relative to the testing results. Therefore, this diffusion constant is increased with a few iterations to fit the measurement curves in Figure 5.6. This resulted in an approximation for the VMQ silicone diffusion constant of D = 1.1 $\times 10^{-9}$ m^2/s.

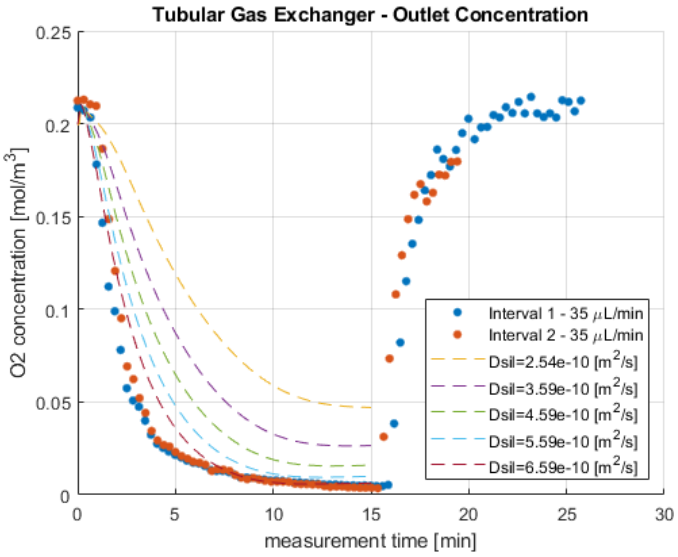

Figure 5.5: Tubular 53 cm exchanger at 35 μL/min medium flow rate. Outlet measurements after starting nitrogen flow compared to COMSOL simulation to determine silicone diffusion constant.

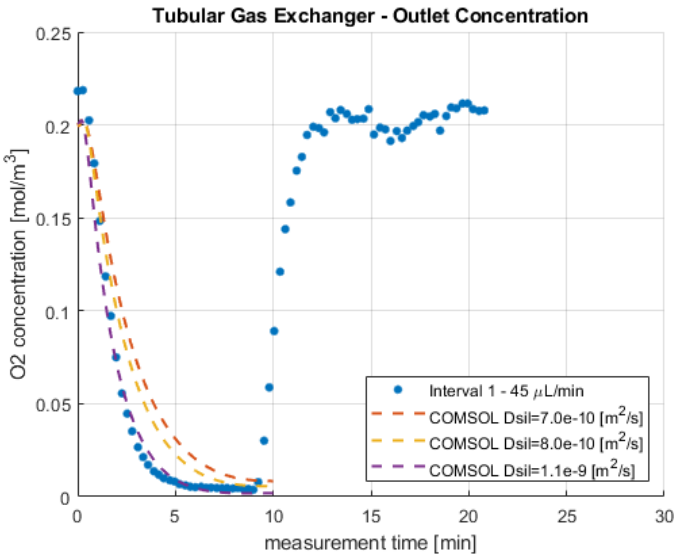

Figure 5.6: Tubular 53 cm exchanger at 45 μL/min medium flow rate. Outlet measurements after starting nitrogen flow compared to COMSOL simulation to determine silicone diffusion constant.

With the achieved low oxygen conditions proving the principle of gas exchange, the tubing length is reduced to test the influence on the achieved concentration range. The lengths of 33 cm (Figure 5.7) and 18 cm (Figure 5.8) reach an oxygen concentration below 0.01 mol/m^3 within 6 minutes and 5 minutes respectively. The stationary oxygen concentrations are around 0 mol/m^3. In the second interval of Figure 5.8, three blue measurement points after 4 minutes do not follow the expected decay, this might be due to an air bubble or accidental leakage in the system. Given these results, the system can be reduced in tubing length towards 18 cm still meeting the requirement 1.1 of low oxygen range of 0.01 mol/m^3 within 5 minutes.

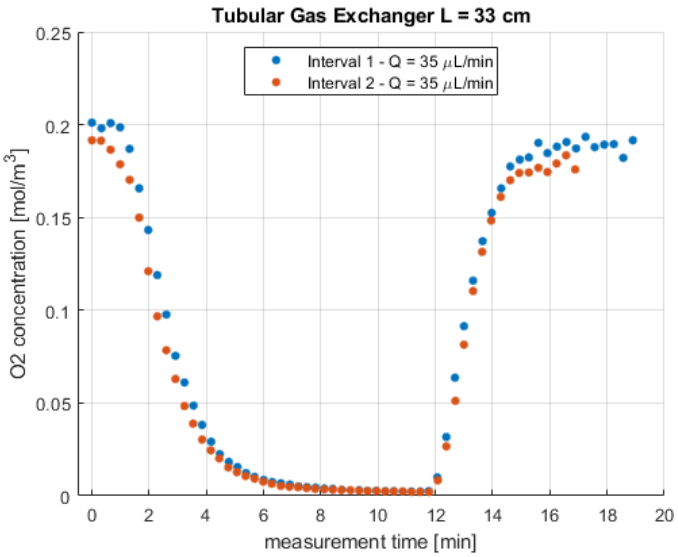

Figure 5.7: Tuber exchanger medium outlet concentration with 33 cm tubing at 35 μL/min medium flow rate.

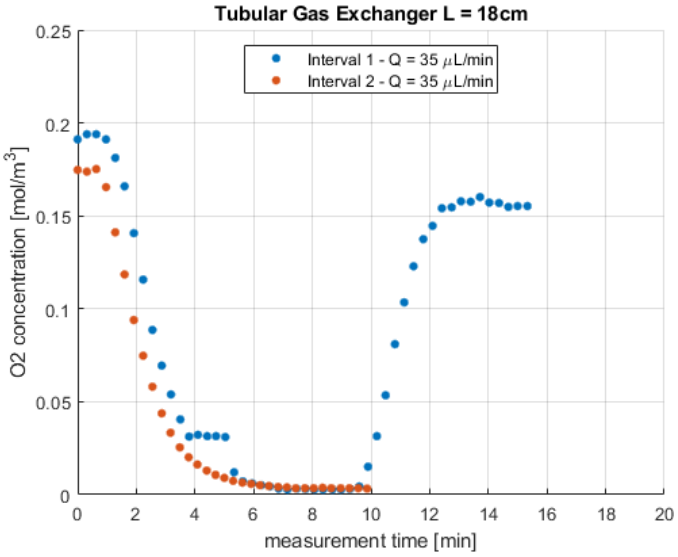

Figure 5.8: Tubular exchanger medium outlet concentration with 18 cm tubing at 35 μL/min medium flow rate.

With the functioning gas exchanger prototype, the Micronit chip is connected to the exchanger outlet to verify low oxygen concentrations on chip. The Micronit chip was connected to the 53 cm long tubular exchanger, which was tested most frequent therefore reliable, to reach oxygen concentrations of 0.01 mol/m^3. The resulting decay in oxygen concentration on chip is displayed in Figure 5.9. In this figure, the oxygen concentration reaches 0.14 mol/m^3 and 0.12 mol/m^3 with a nitrogen flow of 200 mL/min and 400 mL/min respectively. These oxygen concentrations are higher than the oxygen concentration of 0.01 mol/m^3 measured at the exchanger medium outlet. This result shows that the connection is not oxygen tight and that increase of the gas flow slightly lowers the oxygen concentration. Besides, the gas exchanger shows an oxygen decrease within 1 minute, whereas the chip shows an decrease after 4 minutes time. This could be due to the time required to fill the Micronit channel with low oxygen medium.

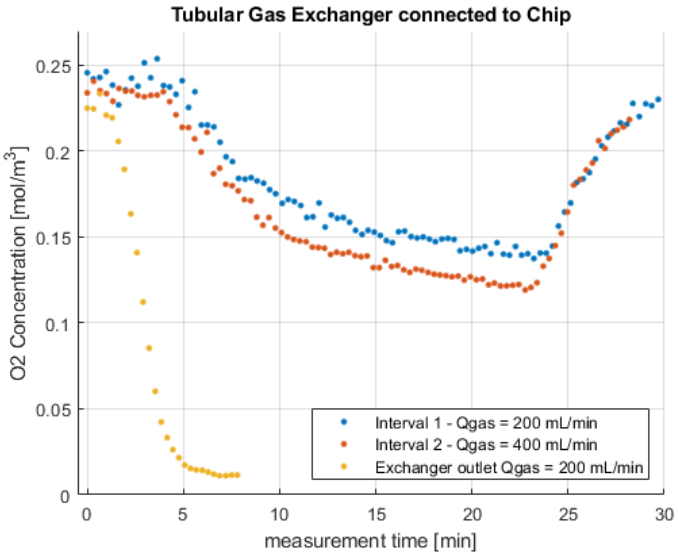

Figure 5.9: On chip medium oxygen concentration compared to exchanger outlet. Tubing length is 53 cm and medium flow rate is 35 μL/min.

In the previous tubular exchanger experiments pure nitrogen containing no oxygen is used as gas flow. To be able to set the oxygen concentration in the medium at a desired value, the gas flow ratio of air/nitrogen is adjusted to tune the oxygen concentration. Figure 5.10 shows the increases in oxygen concentration at the exchanger outlet, by increase of the air/nitrogen ratio with a consistent total gas flow rate of 200 mL/min. Every 18 measurements (6 minutes) the air/nitrogen fraction is increased to increase the oxygen content of the gas mixture with steps of 1% O_2. After changing the gas mixture, the medium outlet showed increase of concentration within 80 seconds with a settling time of 3-4 minutes for a stationary concentration. After setting gas oxygen concentration to 9% the medium concentration shows a small dip at 27 minutes due to a small medium leakage at the tubing connector.

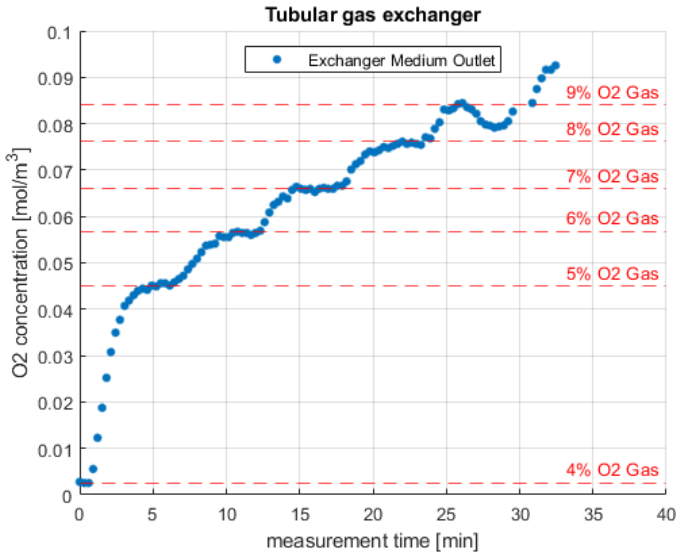

Figure 5.10: Gas exchanger outlet oxygen concentration with varying nitrogen/air ratio in the 200 mL/min gas flow rate. Exchanger tubing length of 18 cm and medium flow of 35 μL/min.

5.6. Prototype Conclusion

All in all, the test results proof the principle of gas exchange through 0.4 mm thick silicone tubing reaching the desired low oxygen medium concentration of 0.01 mol/m^3 for hypoxia experiments. The silicone tubing length can be reduced towards 18 cm for a faster system response towards 5 minutes for concentrations below 0.01 mol/m^3. These low concentrations allow adding a fraction of air to the nitrogen gas flow, realising the tuning of desired oxygen concentrations. The microfluidic connectors from the gas exchanger outlet to the chip channel were not oxygen tight, resulting in oxygen concentration of only 0.15 mol/m^3 on the Micronit chip channel compared to 0.01 mol/m^3 at the outlet. Countermeasures to prevent oxygen leakage are presented in Chapter 6.

6

Gas Exchanger Design

Based on the tubular prototype proving the gas exchange concept (Chapter 5) and the 3D simulations (Section 4.4) demonstrating low oxygen conditions, this chapter presents the detailed design of the gas exchanger. In short, the gas exchanger concept utilises the method of cell medium flow separated by an oxygen permeable membrane from a flow nitrogen gas flow. First, the Section 6.1 discusses the design choices for the detailed design. Second, Section 6.2 presents the gas exchanger geometry and dimensions. Third, Section 6.3 presents the choice of materials and manufacturing method.

6.1. Design Considerations

To begin with, the design choice of a separate module gas exchanger not integrated with the microfluidic chip is motivated. The state-of-the-art integrated gas exchange implementation on chip was reported by Busek *et al.* to create hypoxia conditions in cell medium [12]. Although this implementation incorporates a microfluidic pump and valve manufactured with laser cut foils [23], the tested system only reaches 0.11 mol/m^3 within 300 seconds. The author states that this is most likely due to oxygen entry through the incorporated pump. The design requirement 1.1 states low oxygen conditions of 0.01 mol/m^3 which cannot be satisfied with this design, and besides the laser cutting of thin foils requires more intensive manufacturing expertise for biologist researchers. Adding to this, the medium flow rates applied by Busek *et al.* in the order of 360 μL/min are not preferred, since the Erasmus MC design does not apply recirculating flow. These high flow rates pose too high amounts of cell medium used in experiments.

A gas exchanger module apart from the microfluidic channel allows biologists researchers in cell research to have freedom of choice regarding the microfluidic chip channel. At the Erasmus MC, the departments of lung, bone or vascular cell research interested in hypoxia conditions are experimenting with diverse microfluidic chips, or organ chips, which is not yet a standard in cell culture. Providing a functioning gas exchanger module allows for a cell experiment setup at low oxygen conditions compatible with a diverse range of microfluidic chips or pump types. In the design, the manufacturing method and materials should be available to biologists researchers without dependence on advanced manufacturing methods only available at research facilities of the TU Delft.

Lastly, the tube model of the gas exchanger in Section 4.3.2 indicated faster decay in oxygen concentration for a 0.31 mm inner diameter tubing with a 0.15 mm wall thickness. Although this improves the system settling time, the microfluidic connection from silicone tubing with an outer diameter

0.6 mm towards the Micronit tubing of 1.58 mm outer diameter forms a new challenge, since the available microfluidic luer connectors are not fitting this relative small diameter. A sharp Birmingham gauge needles, that could connect the two tubings, should be smaller than the 30G type, meaning a inner diameter of 0.159 mm, that could harm the silicone. For this reason of microfluidic connectors size, in the design the relative larger tubing with inner diameter of 0.8 mm and wall thickness of 0.4 mm is applied.

6.2. Gas Exchanger Box

This section presents the geometry of the gas exchanger module and the according dimensions. Figure 6.1 visualises the SolidWorks model of the gas exchanger with in front the gas inlet and medium outlet, and in the back the gas outlet and medium inlet. The module consist of a PMMA box of 60 x 60 x 27 mm, with a volume inside of 50 x 50 x 17 mm. In the gas volume the 18 cm long silicone tubing is placed with an additional tubing guidance in the shape of a heat exchanger as visualised in Figure 6.2. The tubing guidance part in blue is not modelled in the 3D COMSOL model. The silicone tubing is inserted through a tubing hole of 1.6 mm diameter. Next, the microfluidic adapters (NanoTight Fitting PEEK/EFTE, ColeParmer) connect the silicone tubing to the Micronit EFTE tubing, after which the EFTE tubing leaves the gas volume through a similar tubing hole of 1.6 mm diameter.

Applying counterflow of the gas with respect to the medium, the gas inlet is placed on the side of the medium outlet to assure the lowest oxygen concentration around the end of the medium tubing. The gas inlet of 4 mm diameter is able to fit a male luer lock connector providing gas through the coupled extension line. On the opposite side, the gas outlet is a 10 mm diameter hole fits a tapered rubber through which a blunt needle or EFTE tubing can provide an outlet to not build significant pressure. Technical drawings of the gas exchanger are stated in Appendix C.

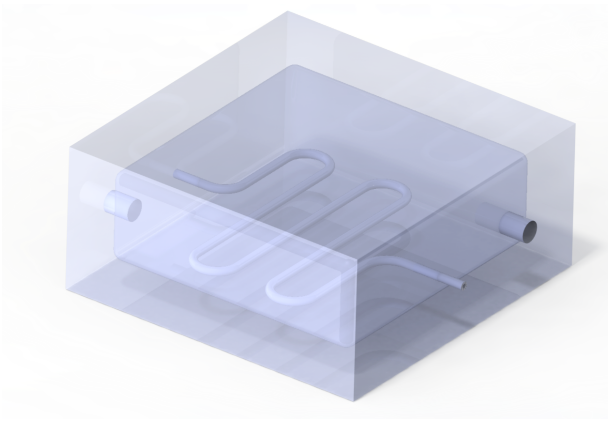

Figure 6.1: SolidWorks render of gas exchanger design

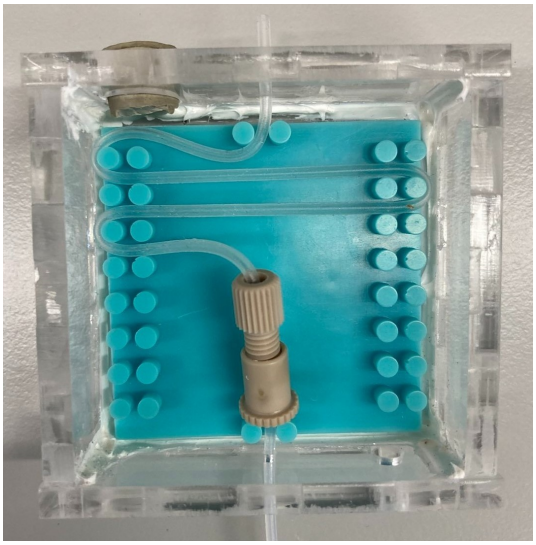

Figure 6.2: Manufactured gas exchanger box.

Further, for flexibility of choice in silicone tubing length and shape, a tube guiding part (Figure 6.3) was designed with 4 mm high pillars along which the silicone tubing can be aligned. Pillars with 2 mm spacing allow to clamp the tubing at the medium start and end. In additions, eight pairs of pillars (2 mm spacing) at two box sides allows silicone tubing of different lengths to be aligned in an alternating path from side to side.

6.3. Materials and Fabrication

This section motivates the choice of materials and most suitable manufacturing method. The complete set of materials is stated in Section C.1.

For cell research application, the microfluidic tubing, microfluidic connectors and gas box should be sterilised prior to the experiment to avoid contamination of the cell medium flowing over the cells (req. 2.3 Table A.1). Additionally, it would be beneficial to replace the silicone tubing as silicone might absorb certain molecules similarly to the PDMS absorbing small hydrophobic molecules (such as drugs) [24] [9]. As medium tubing, the commercial biocompatible VMQ silicone is chosen similar to the tubular gas exchanger (Section 5.3) with the smallest available inner diameter of 0.8 mm and wall thickness 0.4 mm. VMQ silicone contains a high oxygen permeability (experimentally determined D = 1.1 $\times 10^{-9}$ m^2/s). Additional, VMQ silicone holds satisfactory resistance to ethanol according to CES Edupack material library [20], therefore ethanol can be used to sterilise the tubing.

The walls of the gas exchanger box should be oxygen impermeable and allow manufacturing with a low cost manufacturing method preferably available in Erasmus MC. A sheet of 4 mm thick Arylic PMMA is chosen as an oxygen impermeable material with a diffusion constant of 5.0-8.3 $\times 10^{-14}$ m^2/s (CES Edupack, PMMA (molding and extrusion) [20]) and compatibility with laser cutting available at Erasmus MC. Besides, PMMA is optically clear for visual inspection of the tubing during experiments and holds sufficient strength for robust handling. Further, PMMA holds excellent durability of water, however for cleaning purposes limited use of ethyl alcohol (ethanol) and aceton is unsatisfactory which might result in dissolution or chemical reaction. PMMA can be cleaned with iso-propyl alchol (iso-propanol) which is satisfactory for chemical durability [20].

The PMMA sheet was lasercut with interlocking indents (SolidWorks 'tab and slot feature') at the sides of the walls and bottom parts of the box. This allows to assemble the PMMA parts by sliding the parts together with glue in between. The glue chosen is one component transparent acrifix glue (type 0192) suitable for plexiglas. After curing of 3 hours at ambient room temperature and light, the edges on the inside of the box were sealed with Bison mounting kit. The top lid was mechanically clamped with thin rubber sheets in between as visualised in Chapter 7. The rubber sheets were cut in a rectangular wall profile of 5 mm thick.

Finally, the tube guiding part with the smallest feature size of 3 mm pillars diameter requires an realised offset of 0.2 mm to let the silicone tubing fit in. This part was 3D printed at the facility of Hightech Engineering at TU Delft with a Trusa SL1 printer.

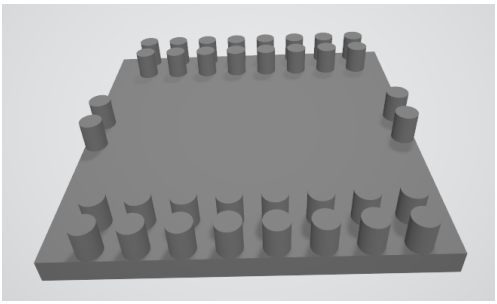

Figure 6.3: Tubing guiding part with a 3 mm thick bottom, 4 mm high pillars of 3 mm diameter. Dimensions stated in Figure C.4.

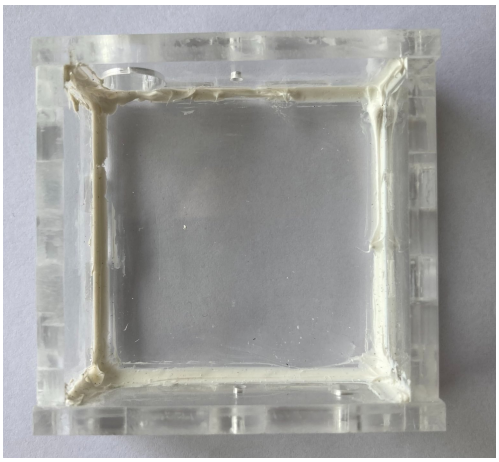

Figure 6.4: Manufactured gas exchanger box of PMMA sheets with mounting kit sealing at the inside edges.

7

System Validation

This chapter presents the system validation of the gas exchanger design with and without integration of the Micronit chip. First, Section 7.1 presents the experimental setup. Second, Section 7.2 presents and discusses the validation of the gas exchanger box described in Chapter 6, according to the expected functioning simulated with the COMSOL model in Section 4.4. Prior to a cell layer test on chip, the oxygen concentrations in the Micronit chip connected to the gas exchanger are characterised in Section 7.3. Finally, the cell layer test is presented in Section 7.4 proving the gas exchanger functionality for biological experiments.

7.1. Experimental Setup

The gas exchanger box is built according to the detailed description of Chapter 6, including the microfluidic adapter inside the gas volume to connect the silicone with the Micronit EFTE tubing. The oxygen is measured with the laser-fiber setup previously introduced in Section 5.2. Different to previous experiments, the concentration of indicator dye was increased from 5 mM Palladium Porhyrin (PP) to 45 mM, since the signal intensity at the fluorescence peak was 1.2 V (of 2 V sensitive channel) with a high signal amplification signal (PMT 150). The increased Palladium Porphyrin concentration allowed almost half the signal amplification (PMT 275) to obtain a signal of 1.2 V.

The gas controllers, syringe pump and Micronit system used are described in Section 5.3. Further, the syringe pump is directly attached to the the silicone tubing with a blunt tip luer needle as the medium inlet of the gas exchanger.

To test the functionality of the gas exchanger module, the oxygen concentration of the end of the silicon exchanger tubing was measured. The silicone tubing of the gas exchanger was connected to a glass capillary (Section 5.3) inserted in a fiber holder. The fiber holder allows alignment of the fiber with respect to the small glass capillary. The fiber holder, displayed in Figure C.5, consists of a 35 mm x 15 mm x 35 mm block with a circular insert at the side for the glass capillary and a circular insert for a fiber from the top.

To test the oxygen concentrations in the chip channel, the gas exchanger was connected to the Micronit system with 10 cm EFTE tubing towards the inlet. The Micronit system outlet contained 8 cm EFTE tubing with an open end. The resulting experimental setup is visualised in Figure 7.2. Figure 7.3 displays the 25 mm x 4 mm viewing window for transparent access to the 40 mm x 5 mm chip channel clamped in the chip holder. To measure longitudinal oxygen gradients along the cell layer, the fiber is placed at the start, middle and end position of the viewing window.

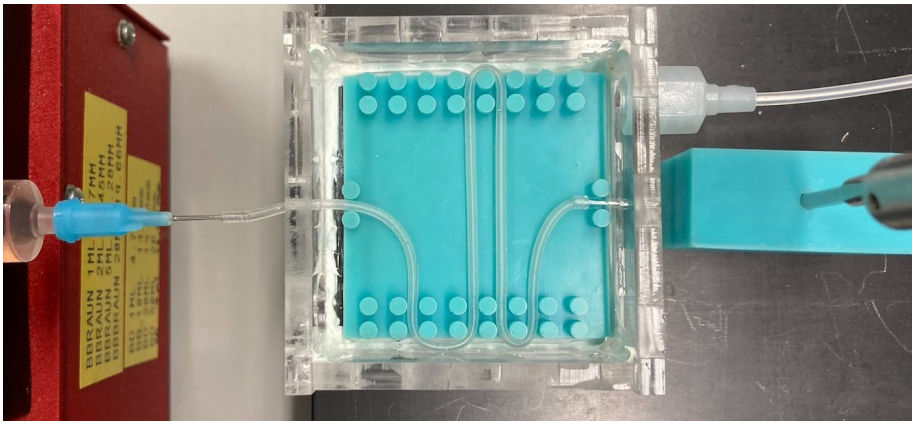

Figure 7.1: Experimental setup for gas exchanger box validation. Syringe pump (left) for medium flow, gas exchanger module (centre) with gas inlet on top right and fiber holder (right).

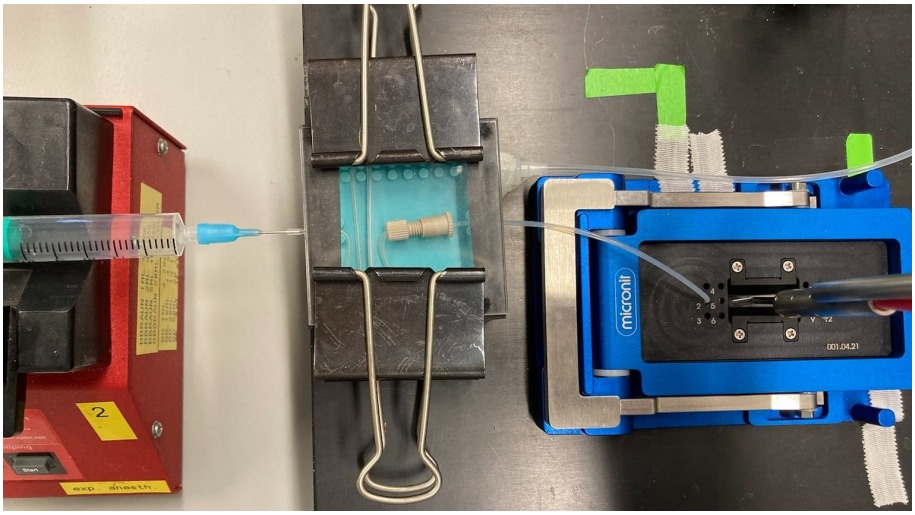

Figure 7.2: Experimental setup for system validation. Syringe pump (left), gas exchanger box (centre) with gas inlet on top right and Micronit chip holder with fiber on top (right).

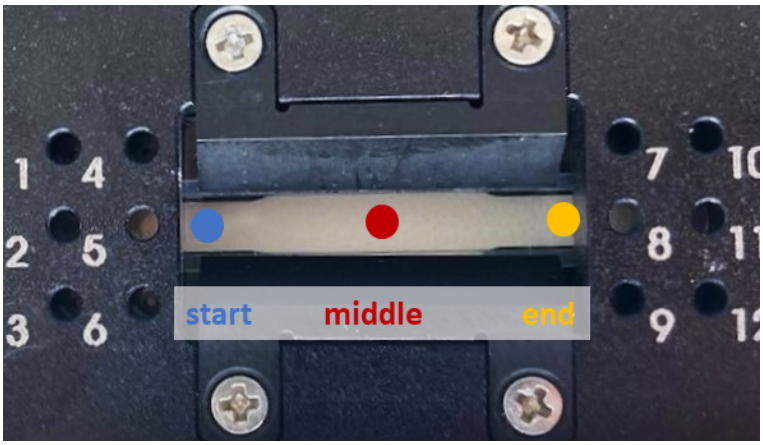

Figure 7.3: Viewing window of Micronit chip holder for fiber access to the Micronit resealable microfluidic chip.

7.2. Gas Exchanger Test

This section first validates the functioning of the gas exchanger box by measuring the oxygen concentration at the gas exchanger medium outlet. Second, the gas flow composition is varied by choosing different fractions of air/nitrogen gas with a consistent gas flow of 400 mL/min. The gas controller of air requires a minimum of 40 mL/min, therefore a lower ratio air/nitrogen than 0.1 cannot be tested. Third, the transfer of low oxygen medium to the Micronit chip channel is validated by measuring the oxygen concentrations on chip.

7.2.1. Method: Exchanger Module Test

The testing procedure to measure low oxygen at the medium outlet of the gas exchanger box is described in Appendix Section D.2.1. In short, the fiber and glass capillary are placed in the fiber holder. Measurements intervals are conducted with a nitrogen gas flow of 200 mL/min and 400 mL/min with a duration of 20 minutes. For tuning of low oxygen concentration, the ratio of air/nitrogen is increased from 0.1 to 0.2, with steps of 0.025, remaining a constant total gas flow of 400 mL/min.

The testing procedure to measure low oxygen concentrations in the Micronit chip channel connected to the gas exchanger is described in Appendix Section D.2.3. In short, the fiber is placed on the middle of the chip channel. Oxygen measurements are for two intervals of nitrogen gas flow of 400 mL/min for 18 minutes.

7.2.2. Results

The design requirement 1.1 states that the gas exchanger should reach the lowest oxygen concentration of 0.01 mol/m^3 within 5 minutes. The COMSOL simulation (Section 4.4) of the gas exchanger box shows lowered oxygen concentrations at the outlet to 0.05 mol/m^3 after 300 seconds and to 0.01 mol/m^3 after 430 seconds.

Regarding the measurements at the gas exchanger outlet, Figure 7.4 visualises the decrease in oxygen concentration at the medium outlet of the gas exchanger after starting the nitrogen gas flow. The two intervals show a start of decreasing oxygen concentration after 2.5 minutes. Next, the first interval with 200 mL/min nitrogen gas flow resulted in a decreased concentration of only 0.05 mol/m^3 after 20 minutes. The second interval at 400 mL/min nitrogen gas flow resulted in 0.05 mol/m^3 within 5 minutes and the desired low oxygen conditions of 0.01 mol/m^3 within 12.5 minutes.

Additionally, the 400 mL/min interval is consistent for two repetitions as displayed in figure D.5. Not only the decrease in oxygen is slower at 200 mL/min compared to 400 mL/min, also the increase in oxygen is slower after starting the air flow. The increased gas flow rate increases the convective mass transfer along the silicone exchanger tubing, which might result in these more rapid changes in oxygen concentration. Compared to the 18 cm prototype with a gas volume of 8 mL, the gas exchanger has a larger gas volume of 37.5 mL which requires a higher gas flow rate for the similar results.

Similar to the COMSOL simulations at 200 mL/min, the test with 400 mL/min nitrogen flow achieves a decrease towards 0.05 mol/m^3 within 5 minutes. The further reduction in concentration towards 0.01 mol/m^3 takes 12.5 minutes instead of the simulated 7.2 minutes. Besides, the COMSOL modelling of the gas exchanger did not take into account the tube guiding elements with pillars (Figure 6.2) or the 2 cm long microfluidic connector (Figure 6.2). These two elements might block the flow of nitrogen requiring more time to lower the oxygen concentration on the outside of the silicone tubing.

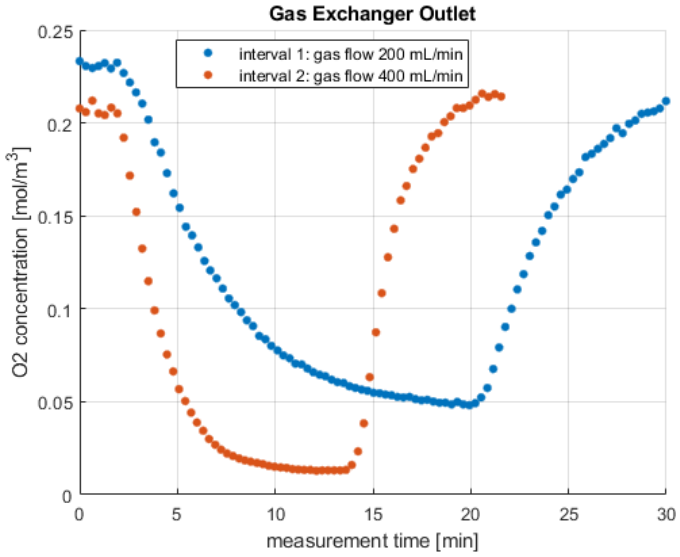

Figure 7.4: Measurements at gas exchanger box medium outlet with flow rates of 200 mL/min and 400 mL/min nitrogen gas.

To reach specific low oxygen concentration for biological hypoxia experiments, the gas flow composition is changed from pure nitrogen to a gas flow including a fraction of air as well as nitrogen. Figure 7.5 visualises the increase in oxygen concentration at the gas exchanger medium outlet when stepwise increasing the fraction of air/nitrogen. The outlet concentration responds after 2 minutes and reaches a stationary value after approximately 5 minutes. This is the similar range of the prototype with a response time of 80 seconds and stationary values after 3-4 minutes. Besides the gas exchanger box reaching low oxygen concentration of 0.01 mol/m^3, this test shows the possibility to tune hypoxia oxygen concentrations between 0.035 mol/m^3 and 0.055 mol/m^3 with steps of about 0.005 mol/m^3.

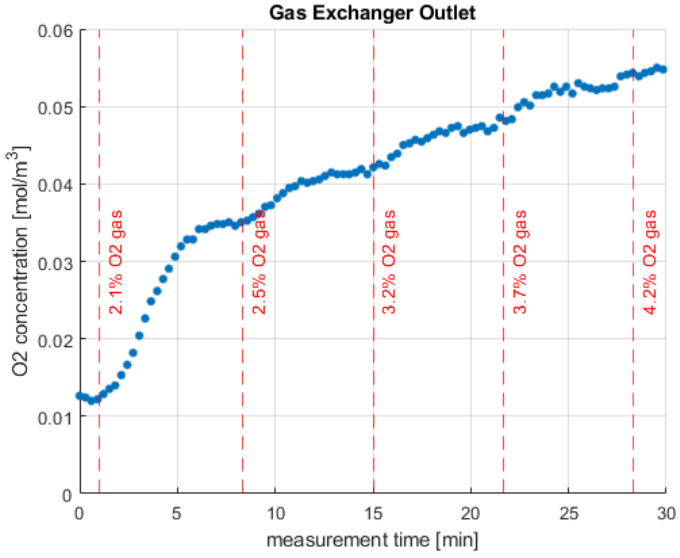

Figure 7.5: Gas exchanger medium outlet concentrations with different ratio's of air/nitrogen in 400 mL/min gas flow.

For measurements on chip, Figure 7.6 visualises the decrease of oxygen of in the Micronit chip channel compared to the measurements at the gas exchanger outlet. The two measurement intervals on chip show a less steep decrease in oxygen compared to the gas exchanger outlet after 4 minutes time. Where the gas exchanger reaches 0.01 mol/m^3 in 14 minutes, the concentrations on chip reach only 0.04 mol/m^3. Further, a concentration of 0.031 mol/m^3 is reached in 21 minutes time. This test reveals that the the low oxygen conditions with a minimum of 0.05 mol/m^3 can be transferred on chip within reasonable time of 14 minutes.

This slower decay of oxygen concentration could be due to the relative higher initial oxygen concentration in the elastomer chip walls compared to the medium. The fact that the chip does not reach the desired 0.01 mol/m^3 could be due to an oxygen leakage in the microfluidic connectors towards the Micronit chip.

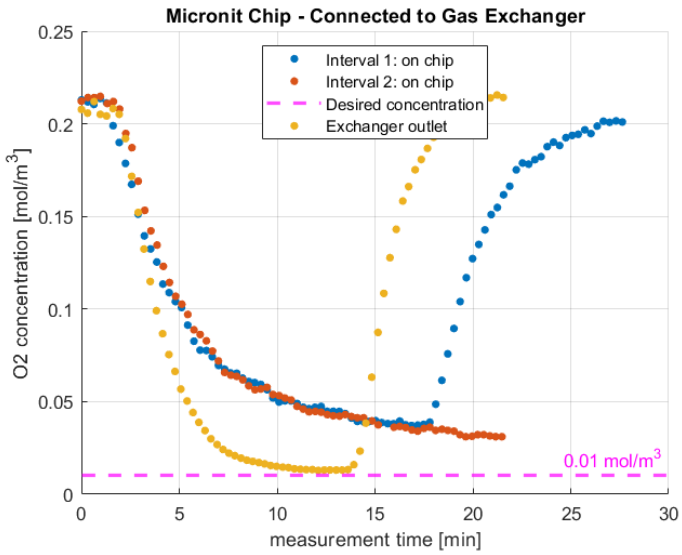

Figure 7.6: Oxygen concentrations in the Micronit chip channel connected to the gas exchanger with only nitrogen gas.

7.3. Characterisation Chip Channel

Prior to the system test including a cell layer in the chip channel, the chip channel without the presence of cells is characterised to later indicate the influence of the cell layer. First, this validation identifies the air/nitrogen ratio of gas flow for a physiological medium inlet on chip. Second, the oxygen gradient along the channel length is measured. The Micronit channel is 40 mm long x 4 mm wide, however the chip holder allows a viewing area on top of 25 mm long x 4 mm wide (Figure 7.3). Therefore the oxygen gradient is measured over a 25 mm length. Third, a 1 minute medium flow stop is used in cell experiments determines the oxygen consumption of the cell layer (req. 2.7 Table A.1). The decrease in medium oxygen concentration indicates the oxygen consumed by the cells. In this validation, a medium flow stop is performed to identify a possible change in oxygen concentration without the presence of cells.

7.3.1. Method: Oxygen Gradient and Flow Stop

To create physiological inlet oxygen conditions on chip, a concentration of 0.09 mol/m^3 is preferred at the start of the channel. This is achieved by testing three ratio's of air/nitrogen to reach the 0.09 mol/m^3. In the gas flow, there is the presence of CO_2 as required for cell tests.

The testing procedure to characterise oxygen concentration on the Micronit resealable chip without the presence of cells is described in Appendix Section D.3. In short, the chip slide is heated at 37 °C and the gas flow is set to 10% oxygen gas (setting 190 mL/min air, 190 mL/min nitrogen and 20 mL/min CO_2) without starting the medium flow. After starting the flow, oxygen measurements are taken for 5 minutes and if the oxygen level does not reach the preferred 0.09 mol/m^3 the ratio of air/nitrogen is adjusted with the remaining flow of 20 mL/min CO_2. The oxygen gradient is measured by moving the fiber along the start, middle and end of the viewing area length. During a medium flow stop, 10 single oxygen measurements are taken in the 'continuous flash' mode of the laser.

7.3.2. Results

The oxygen gradient during flow of cell medium along the length of the 25 mm chip channel is displayed in Figure 7.7. The mean concentration of 0.0956 ± 0.0008 mol/m^3 (mean ± SD) at the channel start decreases slightly towards a mean concentration of 0.0892 ± 0.0006 mol/m^3 at the middle of the chip. At the end of the channel, the mean concentration of 0.0952 ± 0.0008 mol/m^3 is reached similar to the channel start. The oxygen concentrations along the channel are not measured simultaneously, however over time the slight decrease in the middle is also noted (Figure D.6). The uneven surface of the aluminium foil under the chip holder might contribute to this slight decrease in the chip middle.

Although the oxygen decrease of 0.005 mol/m^3 in the middle of the chip, an expected oxygen gradient from 0.090 to 0.058 mol/m^3 (Section 4.2.2) can be identified along the channel length for a physiological medium inlet around 0.095 mol/m^3.

The resulting oxygen measurements in the middle of the channel during a medium flow stop are visualised in Figure 7.8. The oxygen concentration slightly increases after 1.5 minute from 0.089 mol/m^3 to 0.096 mol/m^3 in 2.1 minutes time. This slight increase in oxygen concentration during 3.6 minutes could be due to oxygen leakage through the elastomer walls and is not disturbing a flow stop of 1 minute.

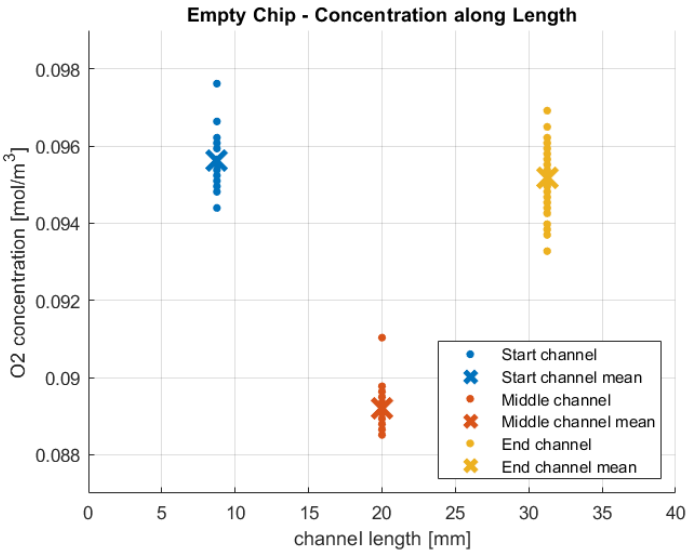

Figure 7.7: Oxygen gradient along length of Micronit chip channel without the presence of cells.

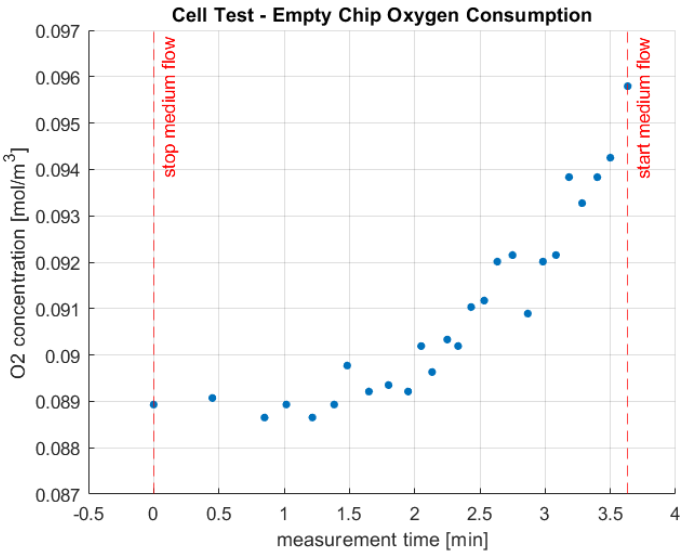

Figure 7.8: Oxygen concentration in Micronit chip channel during a medium flow stop without the presence of cells.

7.4. Cell Layer Test

This section presents the system test in which the Micronit chip channel including a liver cell layer is connected to the gas exchanger box. The previous Section 7.3 demonstrated no disturbances by the chip channel to measure the oxygen gradient along the length or to measure oxygen during flow stops.

In this cell test, it is expected that the oxygen concentration decreases due to cellular oxygen consumption, creating a negative gradient of 0.032 mol/m^3 as modelled in Section 4.2.2. Additionally, a decrease in oxygen concentration of about 0.045 mol/m^3 is expected during a 60 seconds medium flow stop due to cellular oxygen consumption as modelled in Section 4.2.3.

7.4.1. Method: Cell Test

The testing procedure to measure the oxygen gradient and oxygen concentrations during a flow stop in the Micronit resealable chip with presence of cells is described in Appendix Section D.4. In short, the cells are cultured on the bottom Micronit chip slide a week prior to the experiment to create a confluent cell layer. The chip is heated to 37 °C and the medium in the gas exchanger tubing is equilibrated with 7% oxygen gas (setting 134 mL/min air, 246 mL/min nitrogen and 20 mL/min CO_2) for 5 minutes. Next, the chip slides including the cell layer are inserted in the Micronit chip holder and the medium flow is started. After 20 minutes of medium flow, the oxygen gradient is measured along the start, middle and end of the viewing area length. Then, three flow stop are executed measurement, with 14 minutes intermittent time, by taking 10 single oxygen measurements in the 'continuous flash' mode of the laser.

7.4.2. Results

To start, the oxygen gradient over the cell layer length of 25 mm is displayed in Figure 7.9. The concentration at the start of the cell layer is 0.1085 ± 0.0015 mol/m^3 (mean ± SD) which is higher than the chip without cells. This might be due measurement after a different gas exchanger operation time of 20 minutes compared to 40 minute at measurement of the empty chip channel. Further, the concentration shows a linear decrease towards 0.0803 ± 0.0019 mol/m^3 in the middle and towards 0.0601 ± 0.0022 mol/m^3 at the end of the cell layer. These results show a clear decrease in oxygen along the cell layer with respect to the chip channel without cells. This oxygen gradient is larger than the chip simulation of 0.09 mol/m^3 to 0.058 mol/m^3, indicating a higher cellular oxygen consumption.

In the human liver, physiological inlet conditions 0.084-0.098 mol/m^3 decrease towards outlet conditions of 0.035-0.045 mol/m^3 [11]. This physiological decreasing gradient of about 0.055 mol/m^3 is nearly realised on the Micronit chip from 0.11 mol/m^3 to 0.06 mol/m^3 along the cell layer. This show the ability for biologists to create physiological oxygen gradients on the Micronit chip channel.

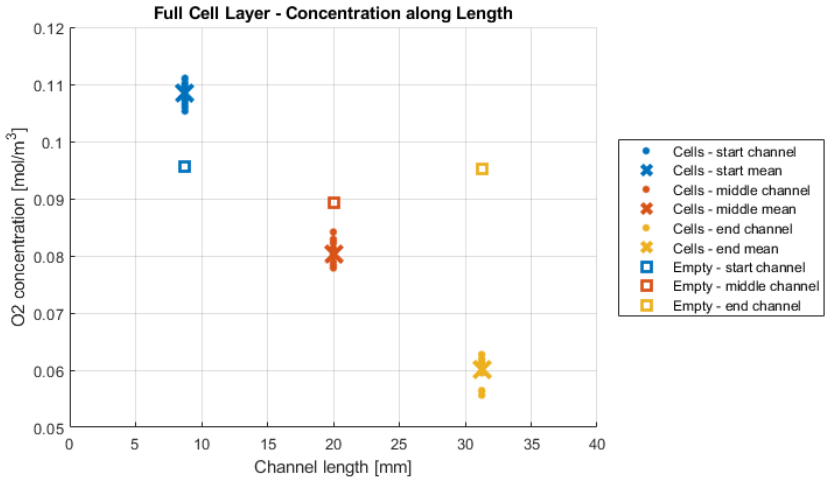

Figure 7.9: Oxygen gradient in Micronit chip channel along the length of the cell layer.

The oxygen concentrations at the middle of the cell layer during three independent medium flow stops of 1 minute is presented in Figure 7.10. For all three measurement intervals there is a clear steep decrease in oxygen from 0.08 mol/m^3 towards values below 0.02 mol/m^3. Since the Labview software only allows manual single measurements shortly after each other, the time between the measurement points is not equal. This decay in oxygen is stronger than the modelled 0.02 mol/m^3 decrease after 30 second and the 0.045 mol/m^3 decrease after 60 seconds. This indicated that the cellular oxygen consumption is higher than modelled.

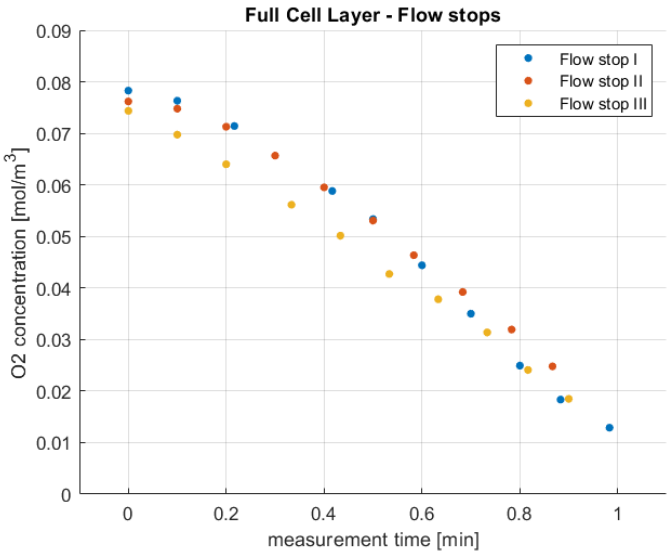

Figure 7.10: Oxygen concentration in the Micronit chip channel during a medium flow stop to determine the oxygen consumption of the cell layer.

7.5. System Validation Conclusion

All in all, the gas exchanger box demonstrated low oxygen conditions of 0.01 mol/m^3 within 12.5 minutes with 400 mL/min nitrogen flow which allows the tuning of concentrations in the hypoxia domain. On chip the oxygen concentration decreases less rapid towards 0.05 mol/m^3 within 14 minutes and the lowest concentration after 21 minutes is 0.031 mol/m^3. Further, the Micronit chip shows no significant change > 0.005 mol/m^3 in oxygen concentration along the 25 mm length and no significant change in concentration during a 1.5 minute medium flow stop. The system test with cell layer on chip supplied with physiological oxygen concentrations showed a longitudinal oxygen gradient from 0.11 mol/m^3 to 0.06 mol/m^3. Adding to this, after 30 minutes of medium flow three flow stops were performed every 15 minutes with repeatable decrease of 0.06 mol/m^3 during 1 minute. The realised oxygen gradient and the performance of flow stops both validate the functionality of the gas exchanger box for oxygen consumption experiments with a liver cell layer on chip.

8

Summary & Conclusion

Section 8.1 summarises the obtained design requirements and Section 8.2 presents the gas exchanger design conclusions.

8.1. Summary

A gas exchanger for liver cell experiments at the Erasmus MC shall be designed according the following identified design requirements. The gas exchanger should supply the organ chip channel with a medium concentration between the physiological 0.10 mol/m^3 to low oxygen conditions of 0.01 mol/m^3. It is desired that the gas exchanger reaches the set oxygen concentration within 1-5 minute to induce hypoxia conditions at varying pace. Depending on the numbers of cells in the chip channel consuming oxygen, the gas exchanger shall supply a medium flow rate between 25-45 μL/min. Further, the gas exchanger shall operate at 37 °C, have the ability to replace the gas-liquid membrane and be sterile to avoid contamination of the cell medium. The gas exchanger shall be operated by a non-technician, requiring ease-of-use in exchanger operation during cell experiments.

8.2. Conclusion

For an adequate Micronit chip channel model, experimental work resulted in a HepaRG cell layer height of 31.5 μm, an elastomer wall shape with a height of 250 μm and an elastomer diffusion constant of D = 1.1 $\times$ 10^{-11} m^2/s. Chip simulations with a physiological inlet concentration demonstrated a longitudinal oxygen gradient (0.090 to 0.058 mol/m^3) along the cell layer at 35 μL/min medium flow rate. A slight lateral gradient (max. 0.006 mol/m^3) exists on the cell layer sides within 0.5 mm of the elastomer due to lateral variation in the medium flow speed.

The tubular prototype exchanges oxygen in cell medium flow through an oxygen permeable silicone tubing with surrounding nitrogen counterflow. The tubing length of 18 cm lowers the oxygen concentration to 0.01 mol/m^3 within the desired 5 minutes. The microfluidic connection between the prototype and the chip hinders oxygen concentrations < 0.15 mol/m^3 on chip within 10 minutes and is therefore critical in the exchanger design.

The designed and fabricated gas exchanger box (60 x 60 x 27 mm) consists of a 37.5 mL gas volume in which a 18 cm long silicone tubing is guided. The silicone tubing, with 0.4 mm wall thickness, can be rapidly replaced and changed in length with access provided by the lid on top. The microfluidic connectors are placed inside the gas volume to prevent oxygen leakage. The box consists of lasercut PMMA sheets, which is a fabrication method available at the Erasmus MC.

COMSOL simulation of the 3D exchanger box shows an oxygen concentration < 0.0018 mol/m^3 on the silicone tubing outside after 100 seconds at 200 mL/min of nitrogen flow. With this knowledge, 0 mol/m^3 can be assumed on the silicone tubing outside for simulation times > 100 seconds. After a total of 430 seconds a medium oxygen concentration of < 0.01 mol/m^3 is realised.

The tested gas exchanger box provides a desired oxygen concentration of 0.01 mol/m^3 within 12.5 minutes at 400 mL/min nitrogen flow. This measured time is longer than the modelled time due to the absence of the tube guiding part and microfluidic connector in the model. Further, by tuning the air/nitrogen ratio in the gas flow hypoxia oxygen concentrations can be provided by the gas exchanger between 0.035-0.055 mol/m^3 with steps of 0.005 mol/m^3. The oxygen concentration transferred on chip was 0.05 mol/m^3 after 14 minutes. The relative slower decay is most likely due to the initial concentration of the chip elastomer being relatively higher than the cell medium initial concentration. Not reaching the concentration of 0.01 mol/m^3, might be due to the presence of an oxygen leakage at the microfluidic connectors clamped on the chip slide.

Without the presence of a cell layer, at a physiological 0.096 mol/m^3 inlet concentration the Micronit chip channel shows no significant longitudinal oxygen gradient over 25 mm length. Also, during a medium flow stop the oxygen concentration does not change within 1.5 minute, which enables an oxygen consumption measurement of a cell layer. With a cell layer presence, a longitudinal oxygen gradient from 0.11 mol/m^3 to 0.06 mol/m^3 is realised with a medium flow rate of 35 μL/min. Additionally, three medium flow stops with 15 minutes intermittent time showed a consistent decrease from 0.08 mol/m^3 to 0.02 mol/m^3 within 1 minute. This system validation demonstrates the gas exchanger box functioning in the relevant lab environment for microfluidic flow over cell layers on chip.

Overall, this generic gas exchanger design provides a gas control module that can be integrated with microfluidic organ chips for the purpose of physiological as well as hypoxia cell experiments.

9

Recommendations

For further research in the field of oxygen control and measurements in microfluidic channels applied in cell research the following recommendations are proposed.

To start, to reduce the time from 12.5 to the required 5 minutes for the gas exchanger box to provide oxygen concentrations of 0.01 mol/m^3 the following research directions could be considered. First, the tubular exchanger prototype did realise a more rapid decay in oxygen, therefore the silicone tubing path in the gas volume could be investigated. If the tubing is lifted off the box bottom, the gas can more rapidly flow along the tubing bottom. Also, adding elements on the PMMA sheets could (equally) spread the nitrogen flow over the silicone tubing. Second, the effect of tube guiding elements or microfluidic connectors should be modelled, which might alter the nitrogen flow pattern or speed in the gas exchanger box. Third, including the saturation concentration in the COMSOL model eliminates oxygen concentrations > 0.20 mol/m^3 which are physically not possible at 37 °C.

Moreover, to realise medium oxygen concentrations (<0.05 mol/m^3) on chip for hypoxia experiments the following could be considered. First, the minimum oxygen concentration on chip can be identified with prolonged oxygen measurements indicating a possible oxygen leakage in the connector on top of the chip inlet and outlet. Second, before inserting the cell layer attached to the bottom chip slide, the empty chip channel might be flushed with low oxygen medium at a high flow rate lowering the initial oxygen concentration of the elastomer. This might results in a more rapid decay in oxygen concentration on chip.

Next, a smaller silicone tubing, in terms of inner diameter and wall thickness, could lead to a more rapid decay in oxygen concentration which would also require less tubing length. Further research might solve the challenge of integrating this smaller silicone tubing with different microfluidic tubing considering the fragile silicone tubing and ability of rapid replacement by biologists. One approach could be to 3D print a cone-shaped connector with fastening similar to the NanoFit used in this research. Another approach could be to decrease the oxygen leakage in the connectors, for instance through a seal or material choice.

To monitor the inlet oxygen concentration at the start of the chip channel, a miniature oxygen sensor at the microfluidic chip flow inlet would be beneficial. It would be recommended to use a dissolved indicator or sensor layer with the detection of lifetime which is independent of fluctuating light sources, interference of ambient light and differences in dye concentration [1]. Preferably, the oxygen indicator is excited independent of the laser, for instance with a LED in combination with phase-modulated light [25]. Gruber *et al.* provides further information for robust sensor integration [1].

Adding to this, the measured oxygen concentration at the chip inlet, allows feedback control to the gas exchanger to compensate for deviations in temperature, oxygen leakage or medium flow rate. This results into further regulation of the oxygen concentration during the cell experiments. The Bronckhorst gas controllers can be controlled with the FlowPlot software, that is compatible with Labview software used to control the laser-fiber oxygen measurements. Feedback control would require more tests to identify the response time and settling time of realised oxygen concentration between 0.10-0.01 mol/m^3 at different flow rates. Also, a suitable control loop is required for to the sensor signal.

Regarding oxygen measurements across the cell layer, measuring on multiple points spatially arranged over the cell layer would improve the identified oxygen gradients since the cells form a heterogeneous layer. This sensor format, allowing spatial-temporal oxygen measurements, is preferably compatible with multiple types of microfluidic chips.

Besides, the first 10 minutes after starting the gas exchanger the cell medium flow over the cells contains a higher oxygen concentration than the oxygen physiological oxygen concentration. If the cells are also grown (cultured) prior to the experiment at physiological oxygen concentrations, a valve between the gas exchanger and chip channel might be considered. This valve could discard the cell medium at oxygen concentrations above the physiological value.

In this research, the Micronit resealable channel height was defined by experimentally estimating the width of the elastomer channel wall. This measurement can be validated with an additional measurement of the channel height. One way could be the imaging of coloured strips on the top and bottom glass slide by changing the focal length moving the microscope lens vertically. The difference in focal length between the imaged strips leads to the channel height.

For optical oxygen measurements with the laser-fiber method the variation in measurements at higher oxygen concentration (> 0.10 mol/m^3) could be reduced by fitting the detected signal on a smaller sampling interval. For this research 50,000 points are incorporated in the exponential fitting of the detected signal. Reduction of this amount of points might reduce the fitting error of the detected signal at shorter fluorescence lifetimes (for higher oxygen concentrations).

10

Self Reflection

After this mechanical research project in the biological domain, this section reflects on my research approach and learning.

During the time at Erasmus, I was curious and stayed open-minded to get familiar with the biological need for control of cell layers on chip. Interviewing biologists in different cell research domains helped to understand the motivation behind the technical request, understand the future wishes and gather the lessons learned from failed technical projects. Incrementally increasing the complexity of the chip setup and testing it with cells is crucial to obtain a functioning organ chip.

At the start, I defined the specific scope of an oxygen control module to be implemented with existing microfluidic setups. After the prototype tests, the priority of oxygen leakage in the connectors distracted me from other gas exchanger box features oxygen, such as automatic gas control or tubing path geometry. On one hand, intermediate revision of the design would have been beneficial to progress towards further design improvements. On the other hand, this relatively simple initial system could be verified with a cell test to show functionality in a biological setup.

For experimental procedures, a balance between planning beforehand and creativity during the moment is required. I learned that apart from expected measurement values, also a change in measurement plan during the experiment is beneficial in case the experiment fails or shows different behaviour. After all, questioning the new knowledge obtained in a new measurement guided me in decisions on what to measure.

During the research project unknowns, such as initial material oxygen concentrations or chip channel height, appeared. The trade off between conducting own measurements or taking a rough approximation was sometimes difficult. By proving the influence of the unknown parameter, time could be efficiently dedicated in the research project.

Lastly, in this individual project I learned to present scientific simulation results and measurement setups in online video meetings. With clear visualisations and careful choice of content I tried to give a vivid impression of the research. Overall, the power of presenting, in person or on paper, is providing the critical picture with little words. Grateful am I to be educated at TU Delft, where the critical matters.

A

Appendix: Requirements, Experiments and Prototype

A.1. Design Requirements: Chip Channel

Table A.1: Chip channel requirements.

Functional Requirements	**Performance Requirements**
2.1 Cell Type - Chip shall allow cell culture of the HepaRG cell line, containing both hepatocyte (liver) cells and cholangiocytes (bile) cells, for cell behaviour experiments. Cells should show viability for 2-3 days during long term cell experiments.	
2.2 Cell Number - Chip shall host a certain amount of hepatocytes in order to have enough material for protein, metabolism or DNA analysis after the experiment as well as have the density of confluent layer.	Cell layer shall be 1 cm^2 with a minimum number of 200,000 cells.
2.3 Sterile - Chip shall be sterilised before seeding of cells, for example by flushing with ethanol, exposure to UV-light or treatment in autoclave, to prevent contamination of the cells by fungi or bacteria.	
2.4 Temperature - Temperature shall be 37 °C at the cells, since this significantly influences cell function.	System shall operate at 37 °C.
2.5 Direct Access - Chip shall allow open access to the channel in order to seed the cells with a pipette or take out the cells for after experiment analysis.	
2.6 Transparency - One side of the chip shall be transparent, in order to perform optical oxygen measurements with a laser-fiber setup or optical imaging of the cells.	
2.7 Flow Stop - A medium flow stop (0.5 - 1 min) shall allow measuring the decrease in medium oxygen concentration. This leads to an estimation of the oxygen consumption of the cells.	The decrease in oxygen concentration shall be > 0.007 mol/m^3, to be detectable by the laser-fiber setup.

2.8 Surface - The chip shall allow proper adherence of the cells to the surface, e.g. allowance of glass coating with collagen type one.	
2.9 Oxygen Gradient - Medium at the chip inlet shall contain a physiological concentration of oxygen, and oxygen consumption of the cells shall lead to a gradient of oxygen towards the outlet.	The physiological oxygen concentration of medium inlet shall be 0.091 mol/m^3 with a decrease in oxygen gradient along the chip length [26] [9].
2.10 Oxygen Barrier - The chip shall be oxygen tight, in order to control the oxygen concentration at the inlet with pre-mixed medium.	The oxygen concentration in the chip channel shall not increase with $\geq$ 0.01 mol/m^3, which is more than the physiological variation of oxygen concentration at the inlet [9].
2.11 Shear Stress - The shear stress on the cell layer surface shall be evaluated, since above a certain threshold the hepatocytes show dysfunction.	Shear stress on cell layer is < 0.5 Pa [11] and minimal 0.01-0.05 Pa [27].
1.12 Material - The chip material shall not interact with the medium, for instance by absorbing cell medium particles or changing concentrations of chemicals.	Biocompatible materials shall be used for parts in contact with cell medium. PDMS shall be avoided for absorption of hydrophobic molecules [9] [24].

A.2. Cell Layer Height: Cell Culture & Fluorescent Staining

For the experimental estimaton of the HepaRG cell layer, a glass slide with 1.1 mm thickness is covered with a 280 μm high PMMA mould with the shape of a 0.96 cm^2 chip channel (Figure A.1). The glass plate is coated with Collagene I (Rat Tail) with 150 μL with dilluted concentration of 70 μg/ml. After a few hours, the Hepa RG cells are seeded with 150 μL at 9.3 $\times 10^5$ cells/ml resulting in a number of 139,500 cells. After a week, the cell medium is changed for 1 mL WME cell medium containing 5 μM calcein AM. The non-fluorescent calcein AM (website link) is a cell-permeant dye which is converted to green-fluorescent in live cells. The fluorescent dye will be absorped by both the hepatocytes as well as the cholangiocytes, which are the epithelial cells of the bile duct. After adding adding the dye to the cells, the cells are incubated for 30 minutes at 37 °C to let the fluorescent calcein develop inside the cells. After the cell incubation, the mould is carefully removed to image only the cells on the glass slide.

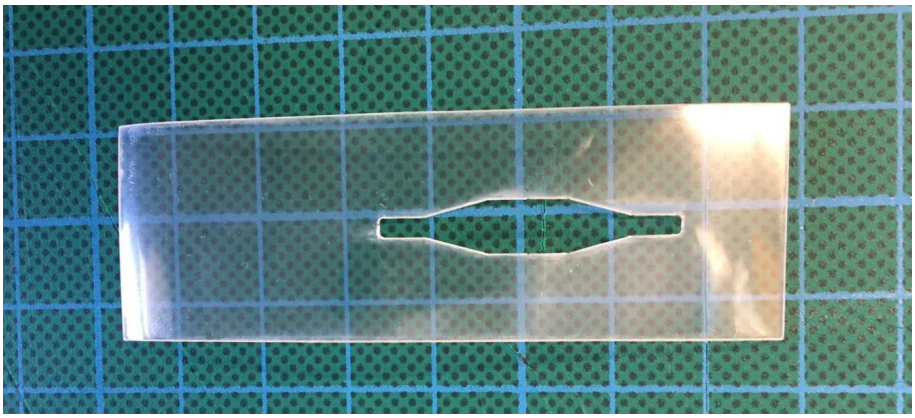

Figure A.1: PMMA mould of 76 x 26 mm for culturing cell layer in a Erasmus MC chip channel. The grid in the background measures 10 x 10 mm.

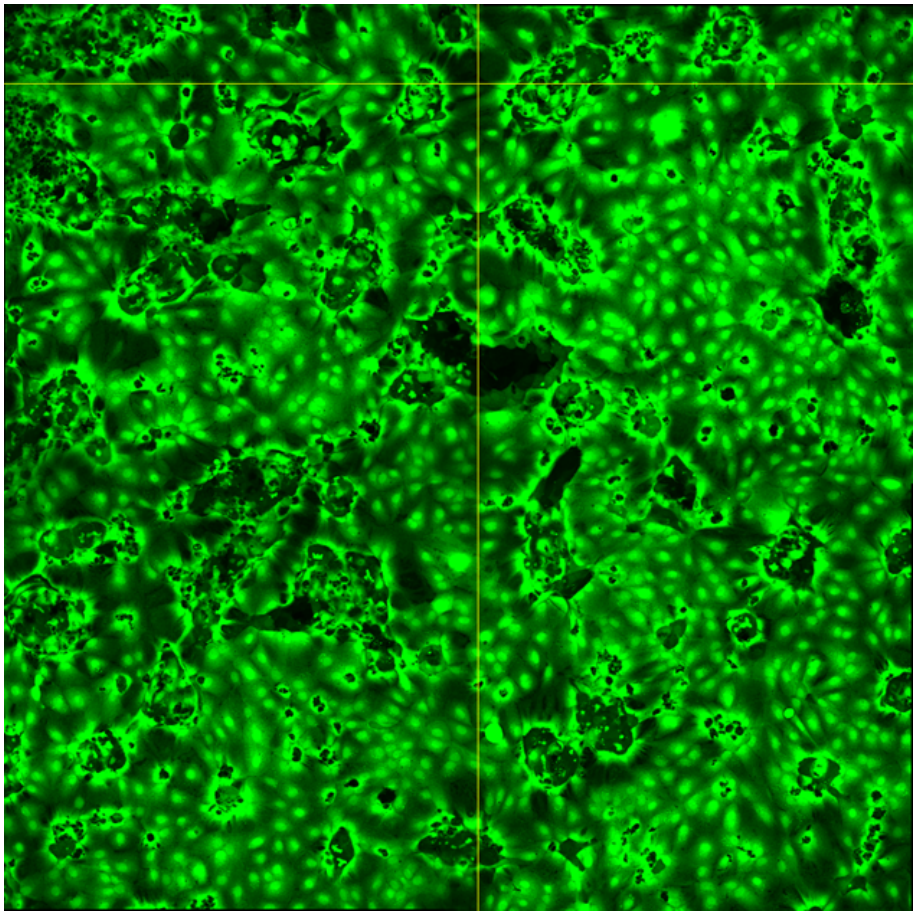

Figure A.2: Fluorescent imaging of 1476 x 1476 μm HepaRG cell layer, image is a z-projection with max intensity settings. In the image both hepatocytes and cholangiocytes are visible.

A.3. Palladium Porphyrin Cell Viability

This appendix section describes the experimental procedure to evaluate the viability of HepaRG cells with concentrations of Palladium Porphyrin (PP) as luminescence indicator dye for measuring oxygen concentrations. To evaluate the effect of the PP dye on the cells, the ATP concentration in the cell is measured with the luminescence kit (CellTiter-Glo 2.0 Cell Viability Assay). The ATP is an molecule that provides overall energy to the cell and the ATP concentration might decrease when PP would be toxic to the mitochondria. ATP tests the viability of the cell and is a selective parameter that does not exclude all toxic effects to the cell. HepaRG cells were distributed on a 96-well plate with the following concentrations of PP: 0.1, 0.1, 10, 50 and 100 μM. The luminescence kit is is used next to measure the Relative Light Units (RLU) in respect to the control volume without PP. Graph A.3 states the RLU with respect to the luminescence of the control volume, defined as 100%, for the five concentrations of PP measured after 2 and 4 days. For all the concentrations of PP no difference in ATP concentration is seen with respect to the control volume. Also no morphological differences of the cells exposed to PP were noticed with respect to the control volume.

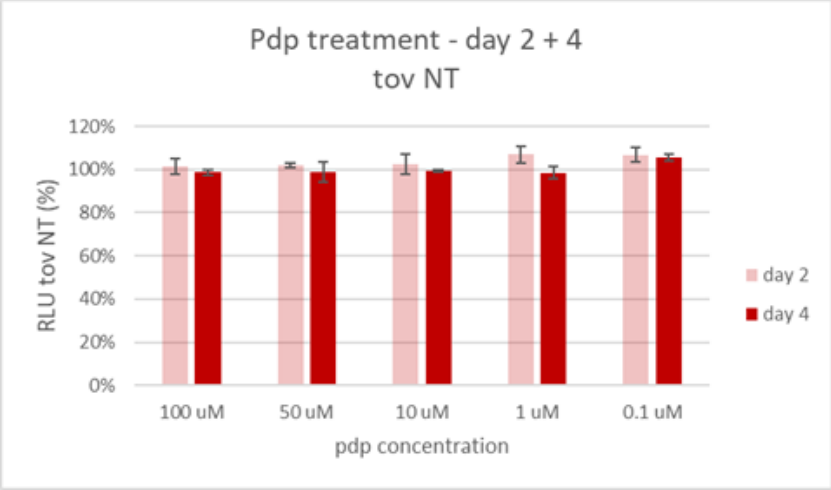

Figure A.3: Luminescence measurement for ATP concentration in HepaRG cells. Relative Light Units (RLU) are identified with respect to luminescence of control volume (NT).

A.4. Chip Channel Height

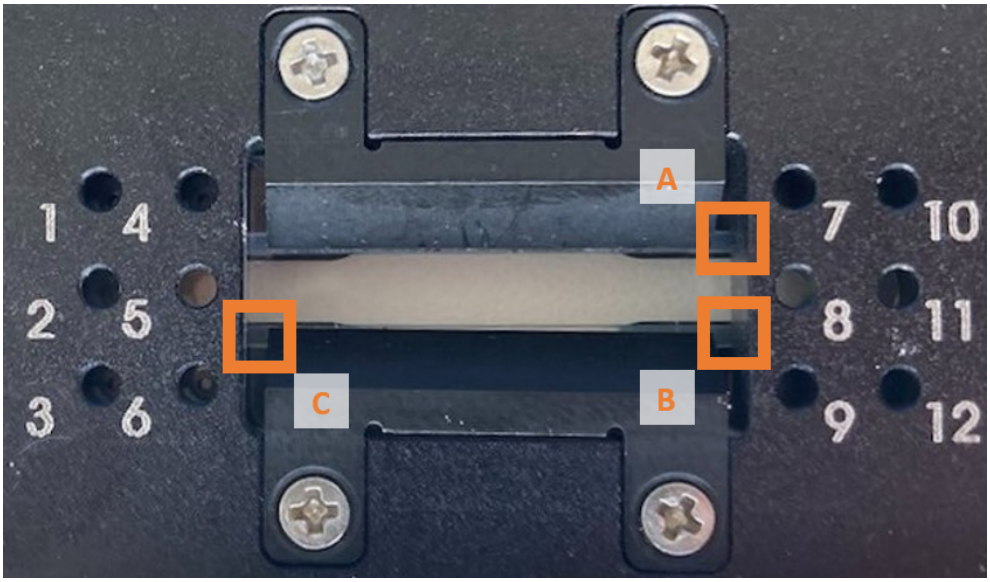

Figure A.4: Imaging points on top of chip holder to the define the elastomer width in compressed configuration.

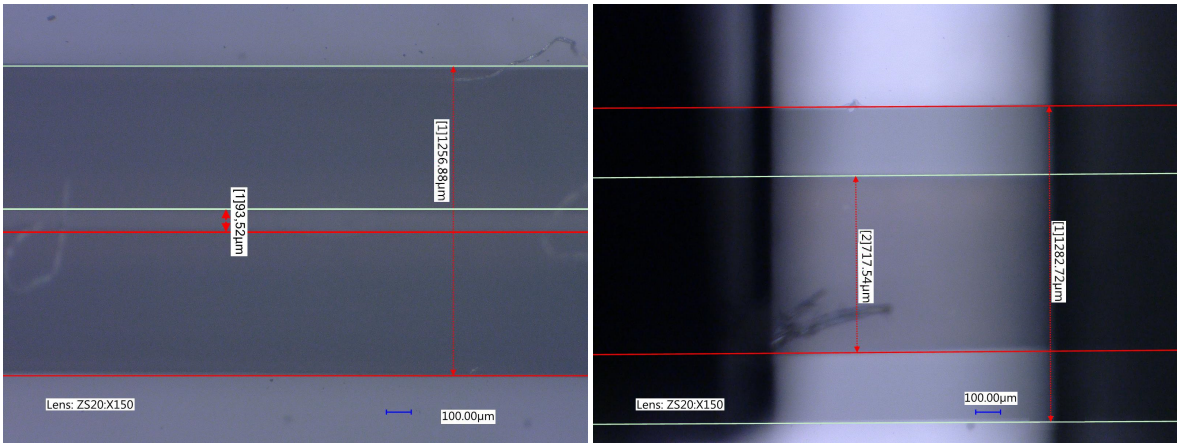

(a) Uncompressed configuration

(b) Compressed configuration with clamping parts in black

Figure A.5: Optical imaging of elastomer width of the Micronit resealable chip elastomer in dark grey. Imaged with a Keyence VHX-6000, lens ZS20:x150.

A.5. Chip Elastomer Permeability

Gas permeability test (temp:30degC, area: 15.2cm^2, gas pressure :0.5kgf/cm^2)

	Gas Transmission rate (GTR) [cm^3/(m^2·24h·atm)]			Permeability Coefficient (P) [cm^3·cm/(cm^2·s·cmHg)]		
Type of gas	Sample1	Sample2	Ave	Sample1	Sample2	Ave
O2	8.3E+03	8.2E+03	8.3E+03	1.3E-08	1.3E-08	1.3E-08

Figure A.6: Gas permeability data of a material in the same family as elastomer Micronit resealable channel provided by the Micronit company.

A.5.1. Fitting Measurement Data

Both measurement intervals of oxygen increase are fitted in MATLAB with the function: $myfit(time) = a + (b-a) * erfc(n * (1/\sqrt{time}))$.

Interval 1: Coefficients (with 95% confidence bounds): a = 0.05406 (0.05091, 0.05722), b = 0.1498 (0.1471, 0.1526) and n = 11.73 (11.41, 12.05). Fitted curve visualised in Figure A.7.

Interval 2: Coefficients (with 95% confidence bounds): a = 0.03653, b = 0.1728 , n = 12.91 (12.63, 13.19). Fitted curve visualised in Figure A.8

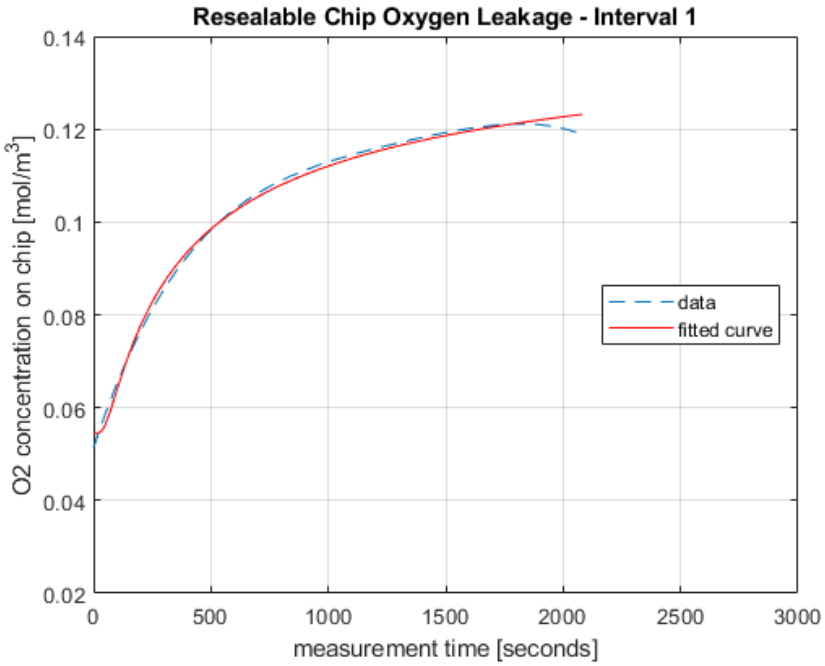

Figure A.7: MATLAB fittype function applied on measurement data interval 1.

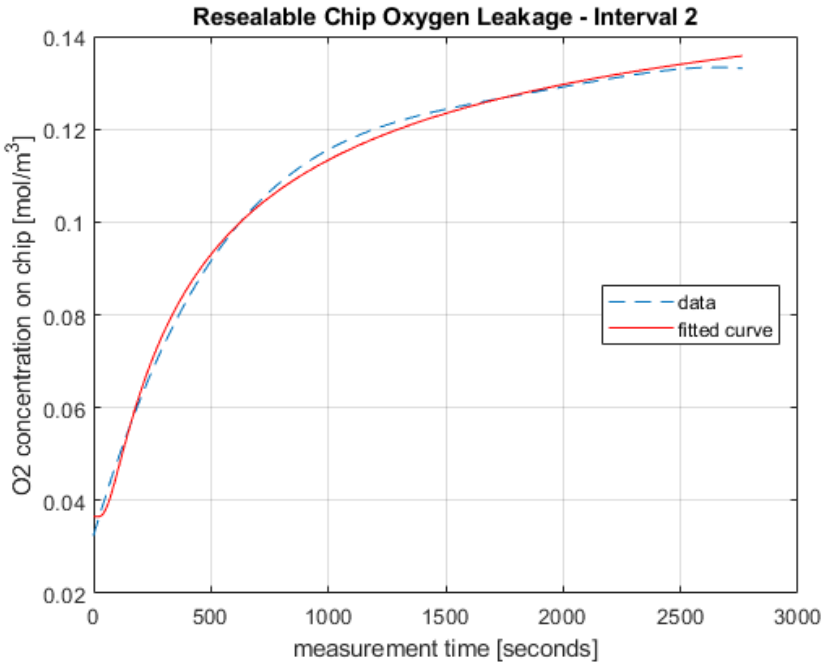

Figure A.8: MATLAB fittype function applied on measurement data interval 2.

B

Appendix: Modelling & Simulation

B.1. Micronit Resealable Chip Channel

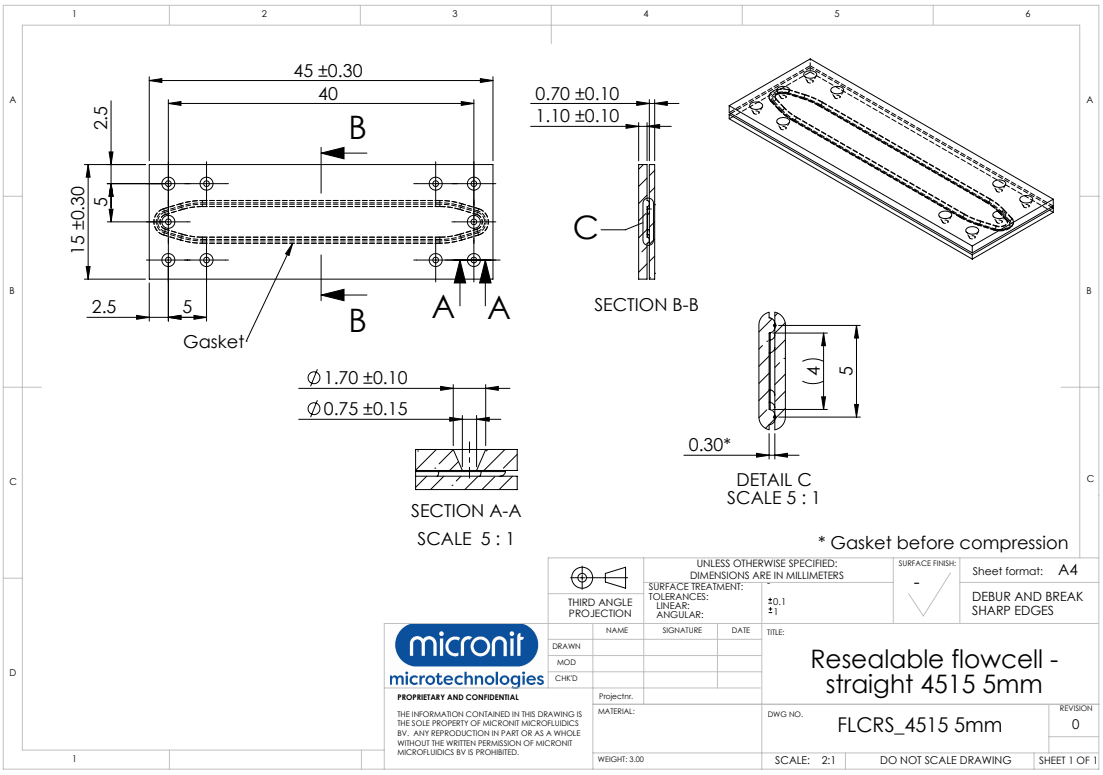

Figure B.1: Micronit resealable flowcell straight (45x15x5 mm) technical drawings.

B.2. Chip Channel Model Geometry

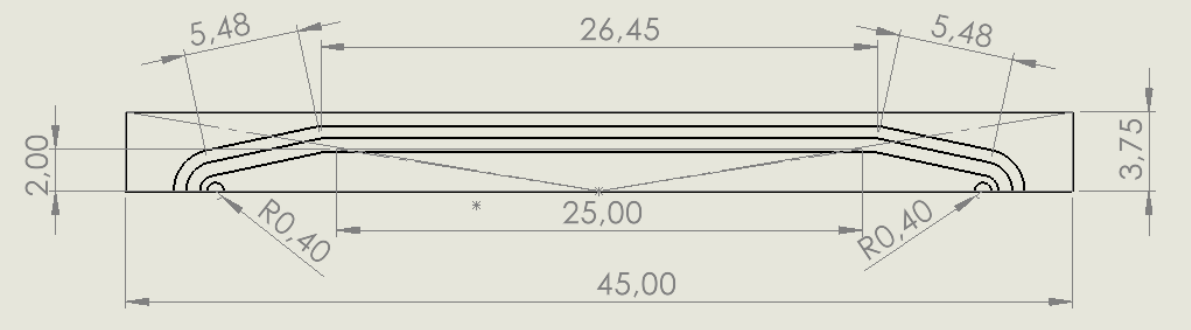

Figure B.2: Micronit half chip channel model top view. Elastomer on bottom glass slide of 45 mm x 3.75 mm. Including cell layer of 25 mm x 2 mm.

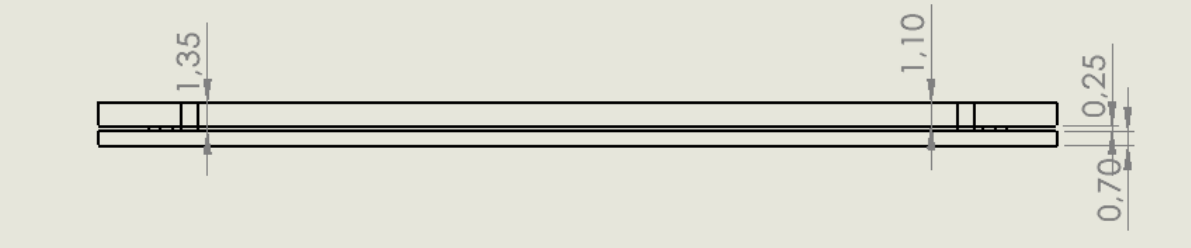

Figure B.3: Micronit chip channel model front view. Thickness top glass slide 1.1 mm, bottom glass slide 0.70 mm and elastomer height of 0.25 mm.

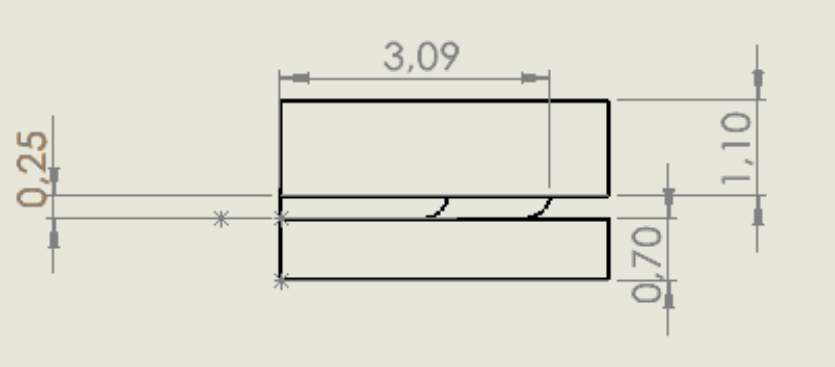

Figure B.4: Micronit chip channel model view on the right. Displaying the 0.25 mm elastomer in between chip slides.

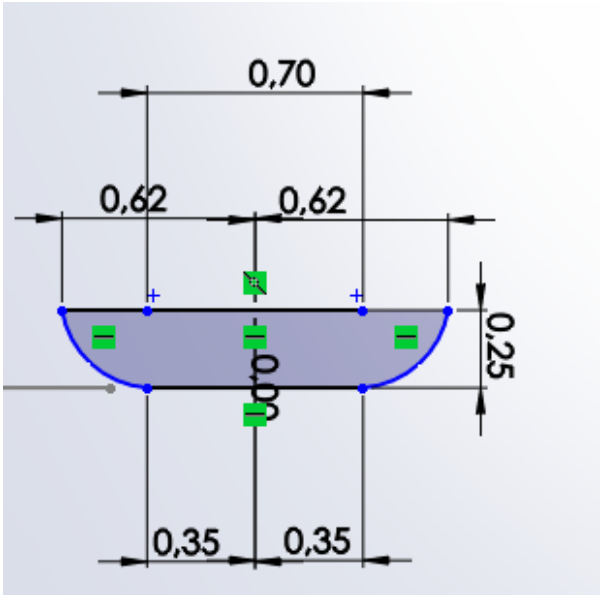

Figure B.5: Micronit chip channel model elastomer geometry. Top width of 1.244 mm, bottom width of 0.695 mm and height of 0.25 mm.

B.3. Chip Channel Model

Name	Value	Description
Q_{med}	5.833E-10 m^3/s	Medium flow rate of 35 μL/min
c_{satmed}	0.20 mol/m^3	Saturated O2 concentration in air 37 ° Celsius, Place2017 [3]
c_{lowmed}	0.090 mol/m^3	Physiological O2 concentration medium inlet, Riveria2019 [9]
c_{satair}	8.84 mol/m^3	O2 concentration in air, Place2017 [3]
$D_{O2cells}$	9.5E-10 m^2/s	O2 diffusion constant in cells, Kim2013 [28]
D_{O2med}	2.69E-9 m^2/s	O2 diffusion constant medium, Poon2020 [18]
$D_{O2elastomer}$	1.0E-11 m^2/s	O2 diffusion constant of elastomer family Micronit chip
$D_{O2glass}$	1.0E-15 m^2/s	O2 diffusion constant in glass, Norton1957 [13]
R_{O2}	0.00334 $mol/(m^2\ s)$	O2 consumption 200k hepatocyte cells, Ehrlich2019 [11]

Table B.1: COMSOL chip channel simulation parameters.

B.3.1. Chip Channel Mesh Settings

Initial physics controlled mesh size settings were decreased until no COMSOL warnings occurred for regions smaller than specified minimum element size. The user controlled size of the mesh for the fluid domain is set to extremely coarse and the glass substrate is set to extra coarse. The fluid boundaries are set to coarse and the elastomer wall to normal element size. Further, corner refinements are applied to all domains and boundaries with fluidic contact. This user-controlled mesh results in a total of 75901 elements and 17369 boundary elements, with a total of 68571 DOF (plus 130913 internal DOF).

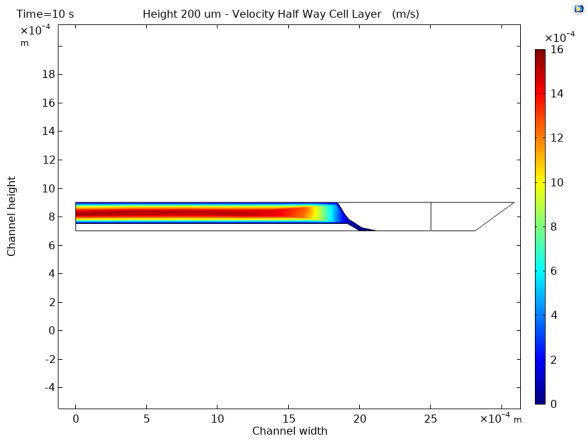

(a) 200 μm channel height.

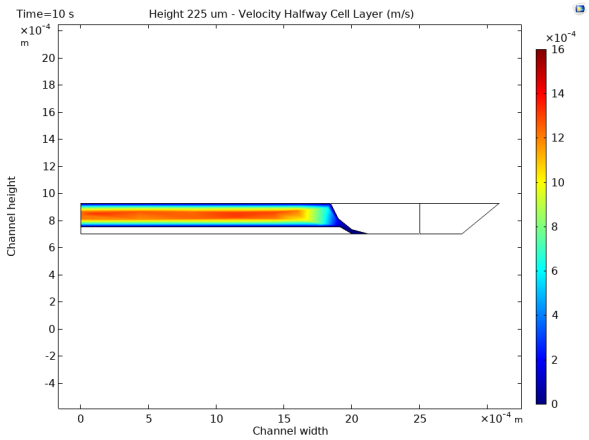

(b) 225 μm channel height.

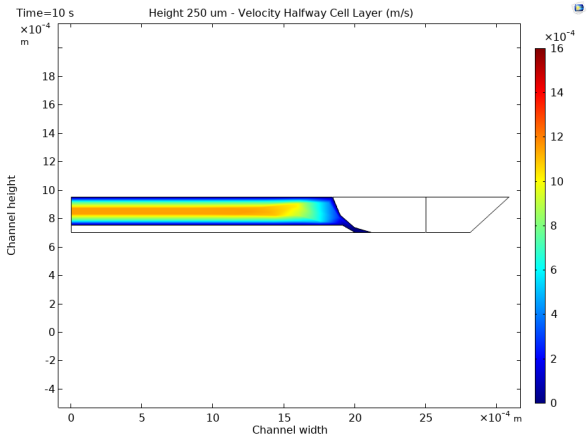

(c) 250 μm channel height.

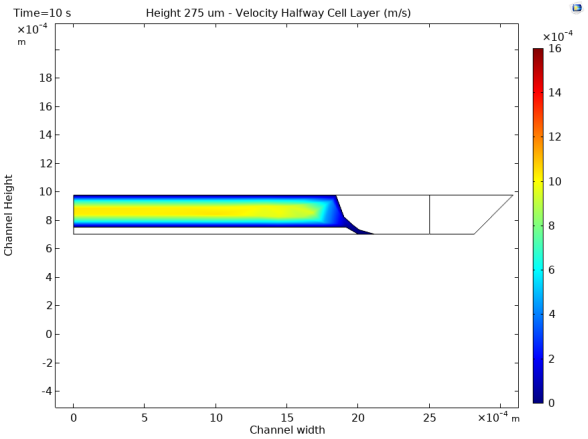

(d) 275μm channel height.

Figure B.6: COMSOL simulation of half the velocity profile (m/s) after 10 seconds in the symmetric chip channel at different heights.

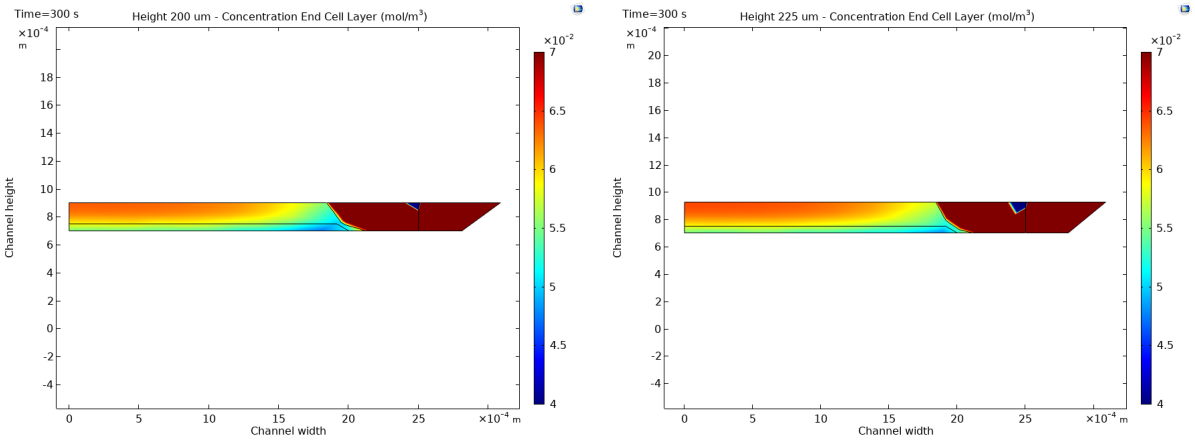

(a) 200 μm channel height.

(b) 225 μm channel height.

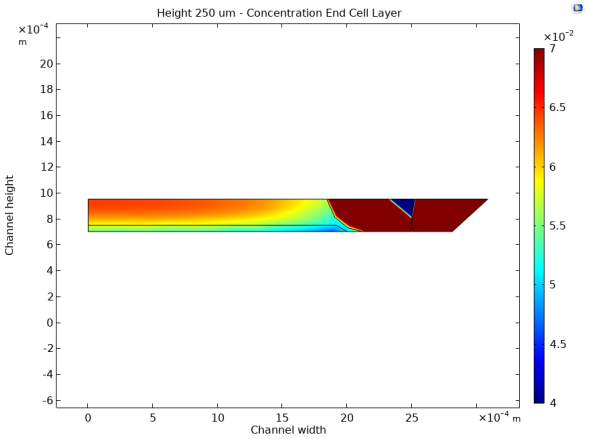

(c) 250 μm channel height.

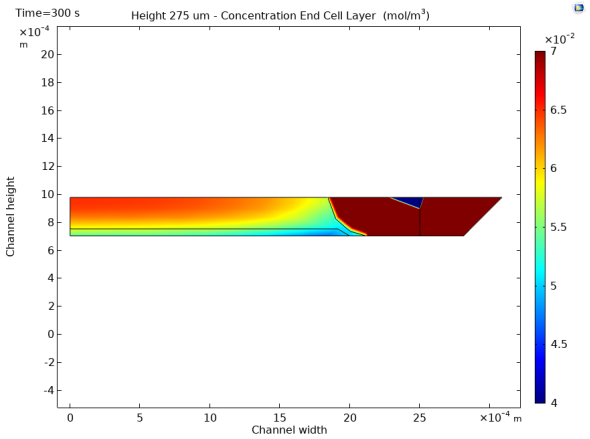

(d) 275 μm channel height.

Figure B.7: COMSOL simulation of oxygen concentration after 300 seconds of half symmetric channel cross section at end of the cell layer.

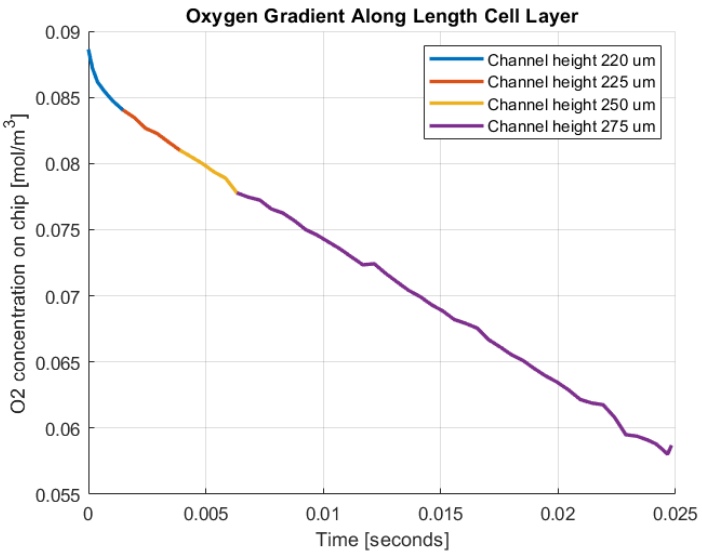

Figure B.8: COMSOL simulation of oxygen gradient along cell layer surface length for varying channel heights after 300 seconds.

B.4. Channel Height COMSOL simulation

In COMSOL Solid Mechanics, an ellipse geometry with a-radius 1250 μm, b-radius 300 μm and sector angel of 180° is modelled as linear elastic silicone. On the top and bottom of the ellipse the glass top and bottom slide are placed. The contact pair is chosen with the bottom glass slide as source and the round ellipse as destination. A 50 μm pre-described displacement downwards of the elastomer top is chosen. The resulting displacement with corresponding stresses is visualised in figure B.9.

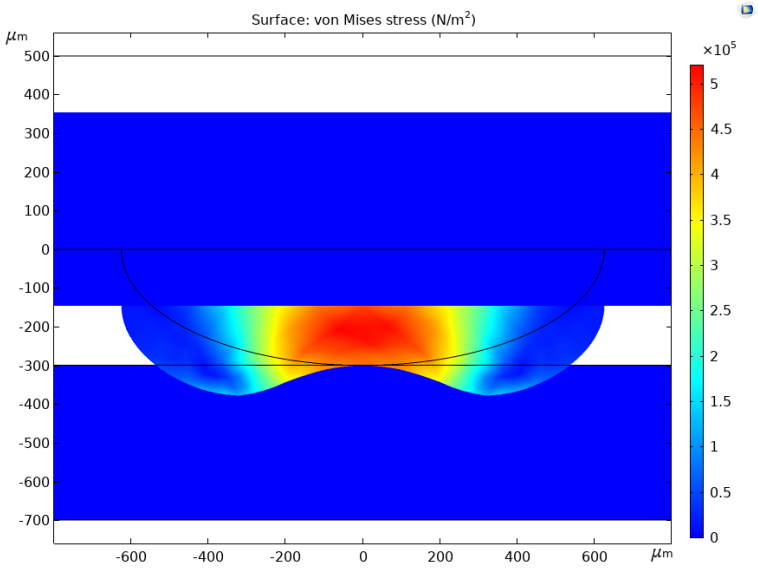

Figure B.9: COMSOL simulation of chip channel elastomer with pre-described displacement of 50 μm of the elastomer top.

B.5. Chip Elastomer Permeability

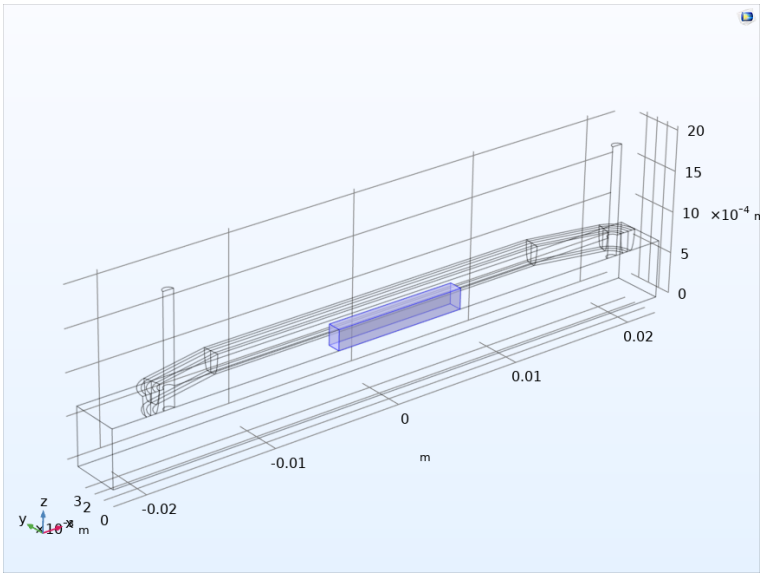

Figure B.10: COMSOL evaluated volume (in blue) for the simulation of oxygen increase in Micronit chip channel with stationary medium.

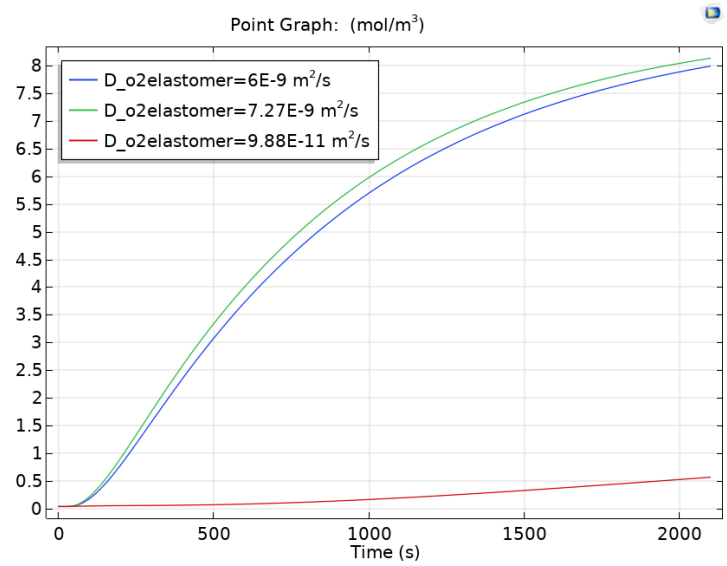

Figure B.11: COMSOL simulation of oxygen concentration in stationary medium with manufacturer and fitting diffusion constants.

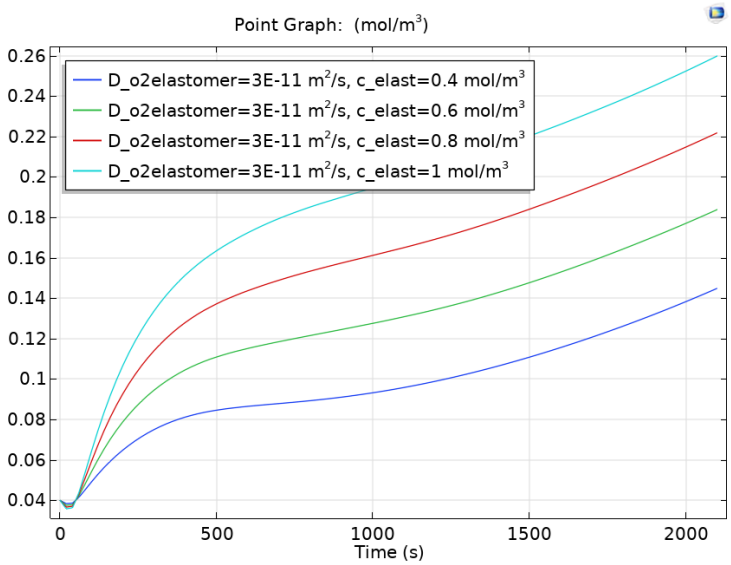

Figure B.12: COMSOL simulation of oxygen concentration in stationary medium with varying initial concentration of the chip elastomer.

B.6. Gas Exchanger Simulation

Name	Value	Description
d_{tube}	8E-4 m	Silicon inner diameter tube, VMQ silicon tubing
h_{tube}	4E-4 m	Silicon tubing wall thickness, VMQ silicon tubing
L_{tube}	0.18 m	Silicon tubing length
$L_{exchanger}$	0.2 m	Length gas volume
$H_{exchanger}$	0.0075 m	Height gas volume
h_{cover}	0.002 m	Thickness covering PVC tube
L_{gas}	1.3E-4 m	Diameter gas inlet/outlet for axisymmetric model
$D_{O2silicon}$	2.54E-10 m^2/s	O2 diffusion coefficient VMQ silicon elastomer VWL data sheet
$D_{o2siliconfit}$	1.1E-9 m^2/s	O2 diffusion coefficient silicone (determined with prototype)
$D_{o2water}$	2.69E-9 m^2/s	O2 diffusion coefficient medium, Place2017 [3]
D_{O2PMMA}	2.7E-12 m^2/s	O2 diffusion coefficient PMMA, Riveria2017 [9]
D_{O2AIR}	1.76E-5 m^2/s	O2 diffusion coefficient in air
D_{O2N2}	0.3473	diffusion coefficient in nitrogen at 310K, Winkelmann2007 [29]
mu_{med}	9.58E-4 Pa·s	dynamic viscosity cell medium at 37 °C, Poon2020 [18]
Q_{med}	5.8333E-10 m^3/s	Medium flow rate at 35 uL/min
Q_{gas}	3.3333E-6 m^3/s	Flow rate nitrogen at 200 mL/min
c_{airsat}	8.74 mol/m^2	Saturated oxygen concentration in air, Place2017 [3]
c_{medsat}	0.2 mol/m^2	Saturated oxygen concentration, 37 °C, Place2017 [3]

Table B.2: COMSOL gas exchanger simulation parameters.

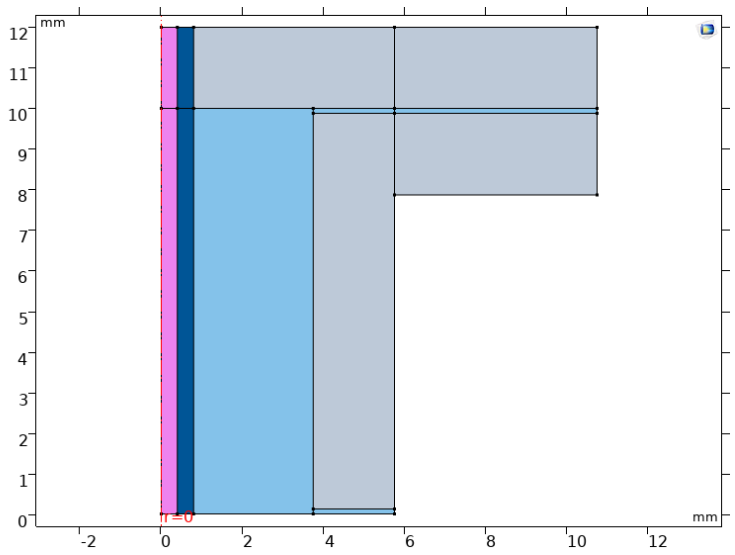

Figure B.13: 2D axisymmetric tubular gas exchanger model with the following dimensions along horizontal axis. Cell medium 0.4 mm (pink), silicone tubing 0.4 mm (darkblue), nitrogen gas 3.35 mm (lightblue) and PVC tube cover 2 mm (grey).

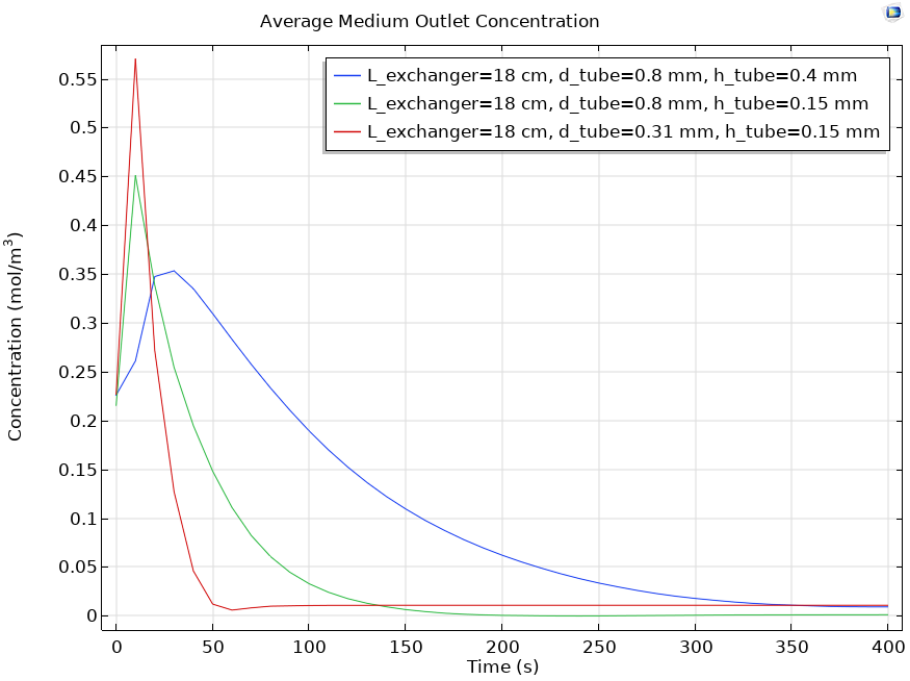

Figure B.15: COMSOL simulation of tubular exchanger with varying wall thickness for the ID = 0.8 mm tubing, compared to the ID=0.31 tubing with a wall thickness of 0.15 mm.

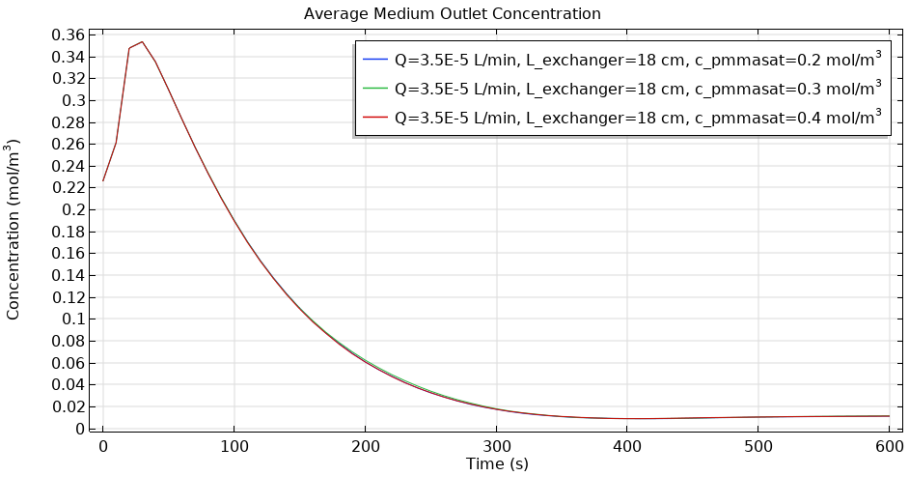

Figure B.14: COMSOL simulation of average medium outlet concentration for different initial concentrations of the PMMA representing the covering gas tube. The three initial gas tube concentrations show no influence on the medium outlet concentration.

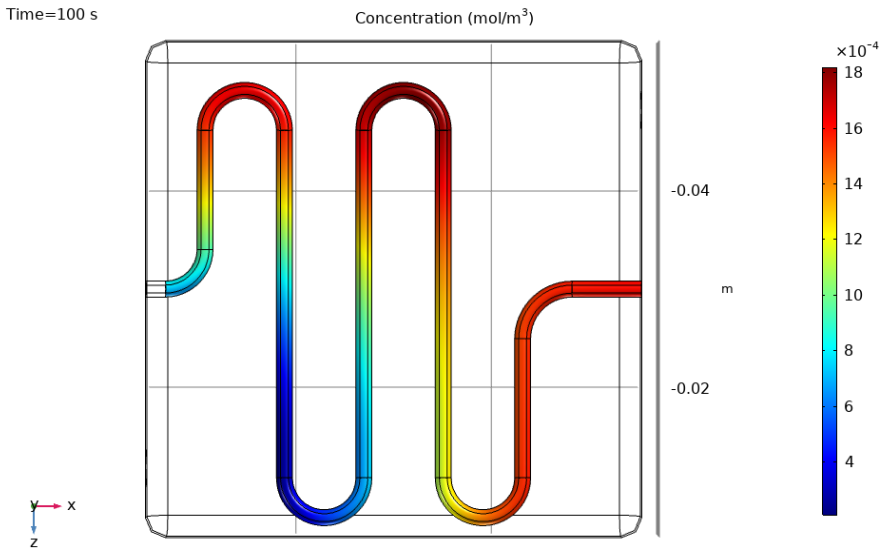

Figure B.16: COMSOL simulation of the silicon outside membrane concentration after 100 seconds including convective nitrogen gas flow. View from the bottom of the gas exchanger box.

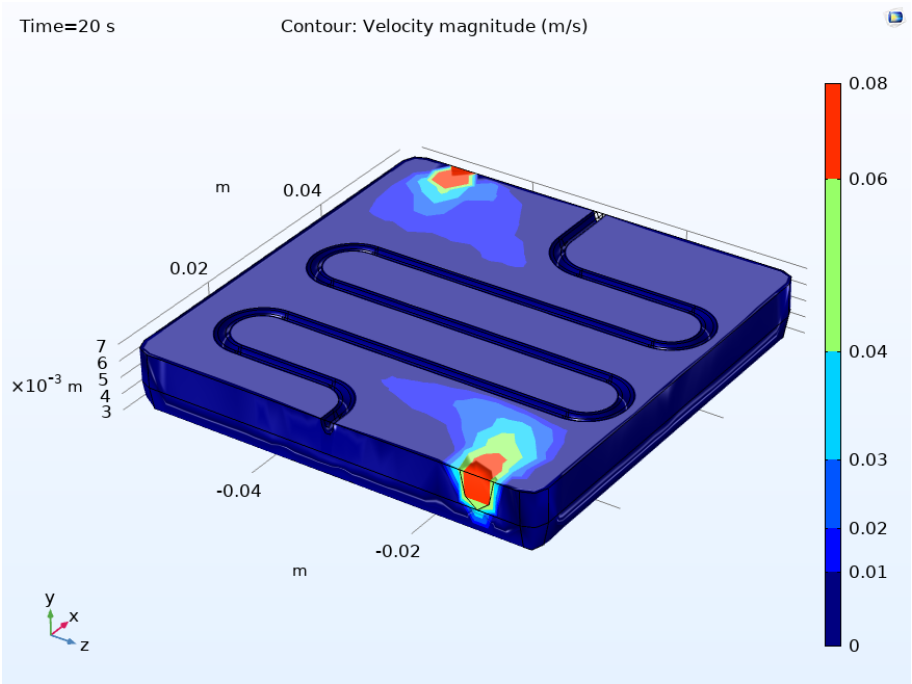

Figure B.17: COMSOL simulation contour plot of nitrogen flow speed magnitude (m/s) with logarithmic scale.

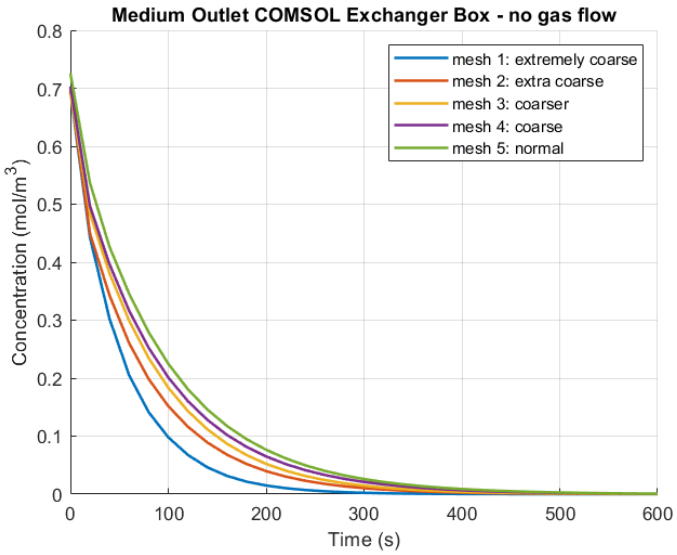

Figure B.18: COMSOL simulation mesh convergence evaluating the average medium outlet concentration for the exchanger model without nitrogen flow.

C

Appendix: Gas Exchanger Design

C.1. Material List

- PMMA 4 mm thick sheet: RS Pro Extruded Acrylic PMMA sheet. Optically clear material, 4 mm thick, density 1.41 g/cm^3, clear finish and machineable.
  Website: https://nl.rs-online.com/web/p/plastic-sheets/0824660/
- Silicone tubing: translucent VMQ silicone tubing with ID = 0.8 mm and wall thickness of 0.4 mm. Website: www.nl.vwr.com/store/product/8563104/tubing-silicone.
- Micronit EFTE tubing: Fluidic Connect Pro EFTE connection kit including 5 m of Teflon tubing with ID = 0.25 mm, OD = 1.58 mm. Also 5 FFKM ferrules for fluidic connection towards fluidic inlet holes on top of glass chip channel slide.
  Website: www.store.micronit.com/fluidic_connect_pro_etfe_connection_kit.html
  Price of tubing is 159 euros (Micronit store, 12th of June 2021).
- Gas flow connectors: luer extension line V-green extension 71100.10, connecting nitrogen supply to gas flow adapters with male luer. Visualised on the right in Figure 5.4.
- Acrifix glue: Acrifix type 1R 0192, transparent 1 component glue for Plexiglass and polycarbonate. Curing by exposure to daylight. Website: www.deplasticwinkel.nl/shop/lijm-voor-plexiglas-14317p.html
- Bison mounting kit: kit for mounting and sealing, can be found at the DIY store Gamma. Website: www.gamma.nl/assortiment/bison-poly-max-crystal-universeelkit-transparant-300-gram/p/B366645 . Other available kits for sealing, website: www.gamma.nl/assortiment/bouwmaterialen/lijmen-kitten/montagekit/merk-bison?f_toepassing=Afdichtenf_toepassingsgebied_lijm_kleefstof=Binnenscrolltofacet=toepassing
- Tapered rubbers: rubbers with a diameter of 10 mm for closing the gas outlet.
- Microfluidic Connector: NanoPort connector also called 'NanoTight' including the following parts:
  - F-142N: Fingertight Ferrule 10-32 Coned, for 1/16" OD Natural Tefzel (ETFE) Website: www.idex-hs.com/store/fingertight-ferrule-10-32-coned-for-1-16-od-natural-tefzel-etfe.html
  - F-333-01: NanoTight PEEK Headless, Short, 10-32 Coned, for 1/16" OD Single. Website: www.idex-hs.com/store/nanotighttm-peek-headless-short-10-32-coned-for-1-16-od-single.html
  - Optional: rubber ring with number N-123-02 Website: www.coleparmer.co.uk/i/idex-n-123-02-nanoport-gasket-flat-bottom/0202426
  - N-333-01: NanoPort Assembly Headless, 10-32 Coned, for 1/16" OD Website: www.idex-hs.com/store/nanotighttm-peek-headless-short-10-32-coned-for-1-16-od-single.html

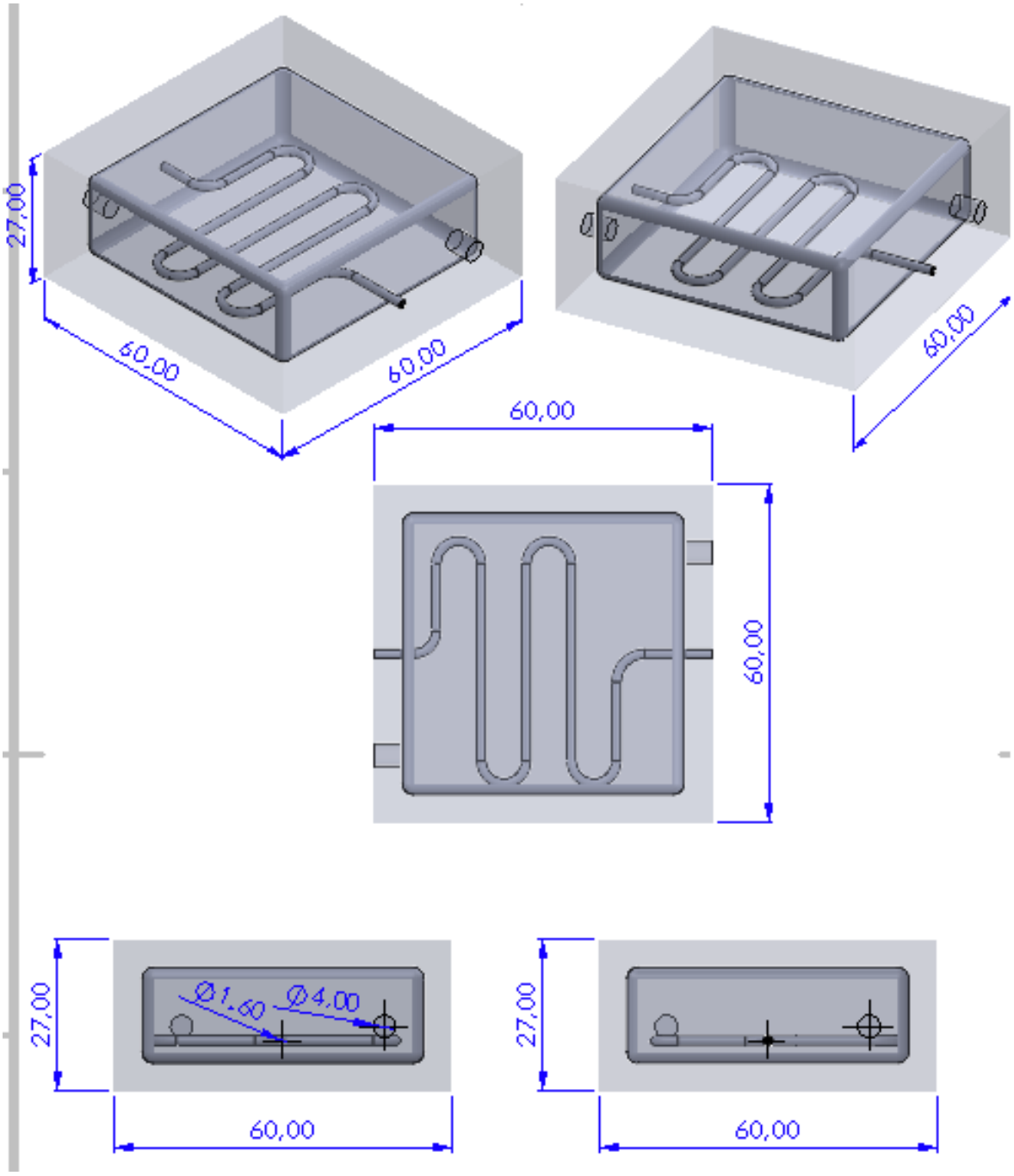

Figure C.1: SolidWorks 60 x 60 x 27 mm gas exchanger design dimensions (mm).

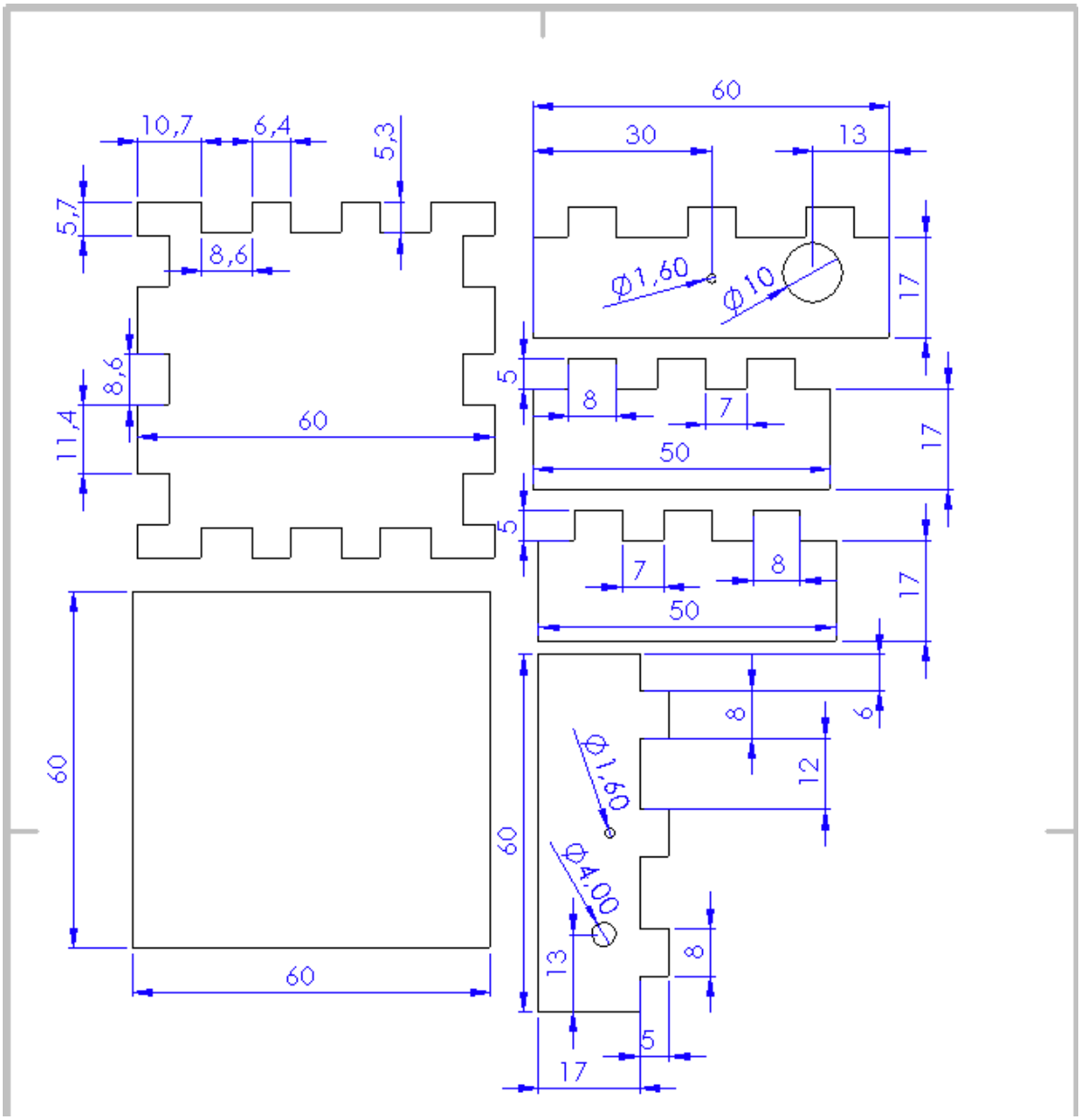

Figure C.2: Gas exchanger box PMMA sheets for manufacturing with lasercutting dimensions (mm).

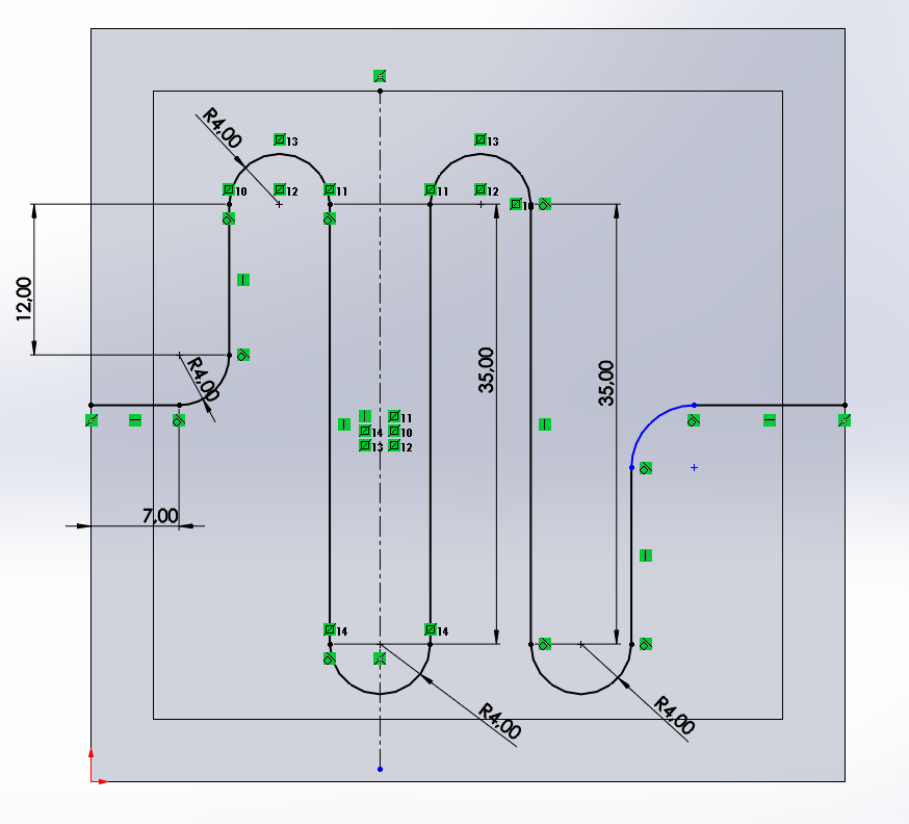

Figure C.3: Solidworks drawing of gas exchanger box silicone tubing path dimensions (mm).

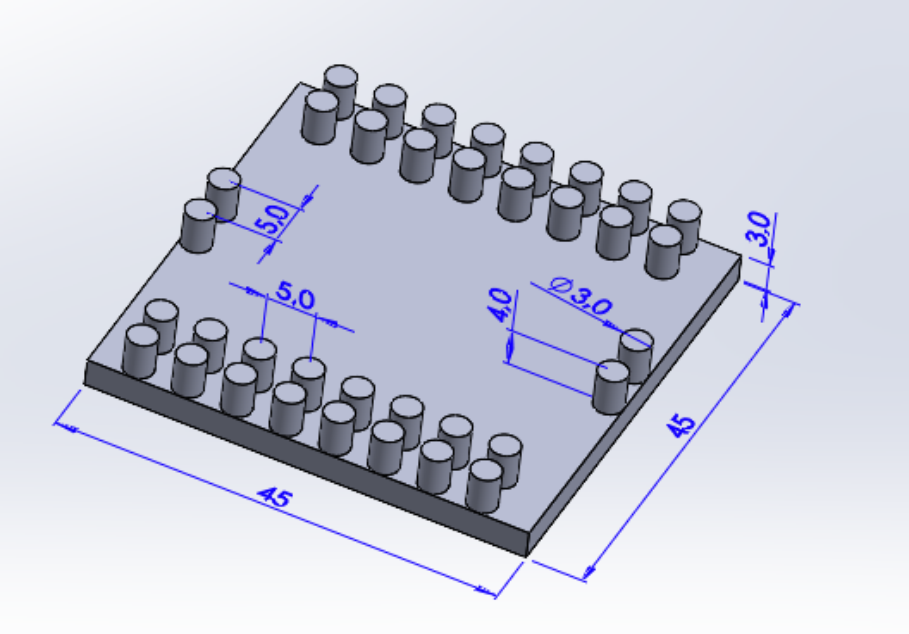

Figure C.4: Tube guiding part dimensions (mm).

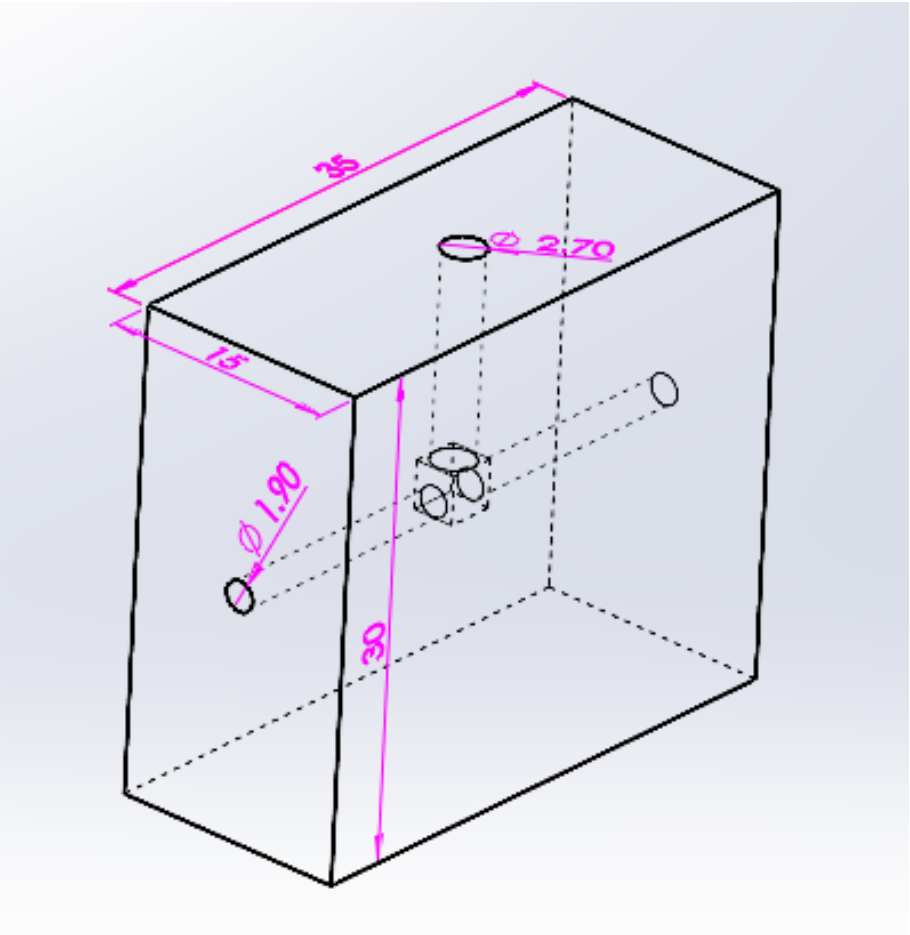

Figure C.5: Fiber holder drawing with a 2.7 mm insert for the fiber and a 1.9 mm insert for the glass fiber.

D

Appendix: Gas Exchanger Validation

Temp 37 °C					
% O_2	5	10	21	50	100
µmol L^{-1}	53.5	107.0	224.7	535.0	1070.0
mg L^{-1} (ppm)	1.7	3.3	7.0	16.7	33.4
hPa	50.9	101.9	213.9	509.4	1018.8
Torr ≈ mmHg	38.2	76.4	160.5	382.1	764.3

Figure D.1: Overview by Oomen *et al.* to convert units of dissolved oxygen concentration in aqueous solution at 37 °C for several oxygen partial pressures [2]. Oxygen concentrations in cell medium are different from this aqueous solutions [3].

D.1. Prototype Test with Integrated Chip

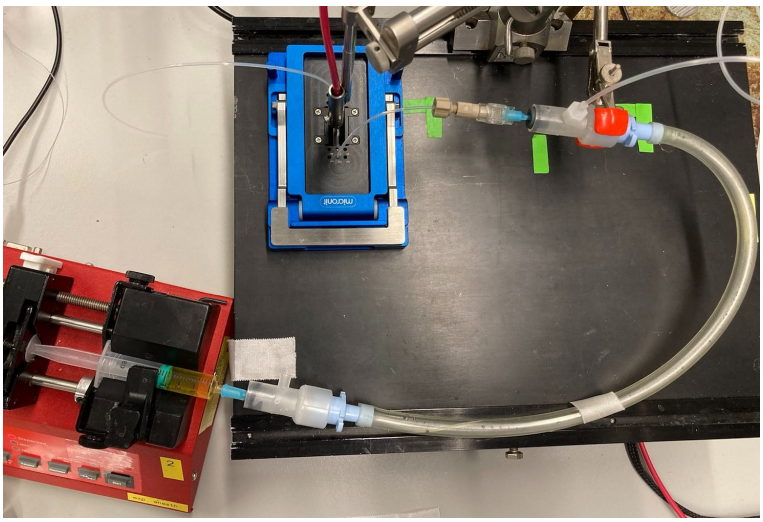

Figure D.2: Prototype setup of 53 cm length connected to the Micronit chip channel.

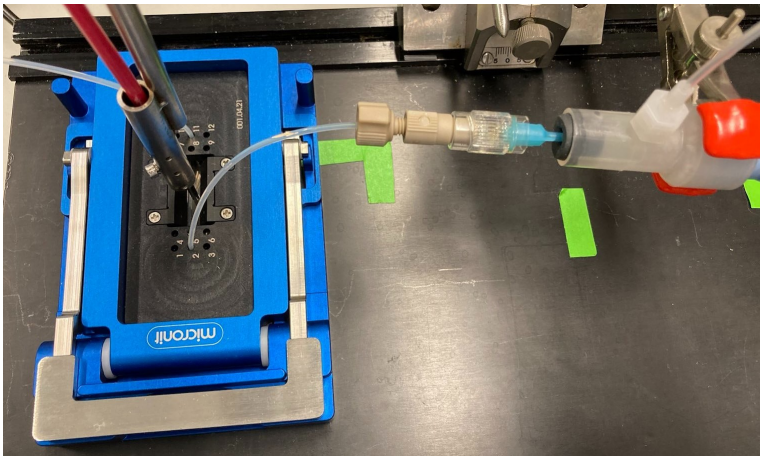

Figure D.3: Prototype setup of 53 cm length, showing microfluidic connection from gas exchanger end to Micronit chip channel

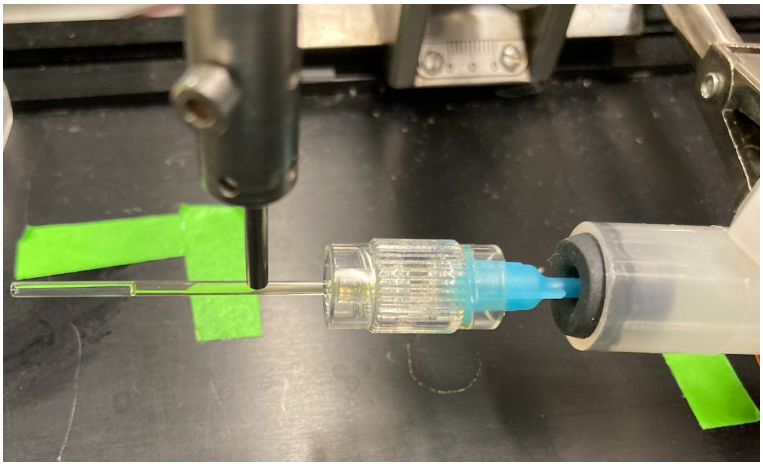

Figure D.4: Laser fiber measurement on gas exchanger prototype outlet, to verify functioning of gas exchanger connected to Micronit chip.

D.2. Validation Method: Gas Exchanger Test

D.2.1. Testing Procedure: Gas Exchanger Outlet

The testing procedure to measure low oxygen concentrations at the medium outlet of the gas exchanger box is as follows.
1. Place the fiber and glass capillary in the fiber holder.
2. Choose the Laser Labview settings of Palladium Porphyrin, wavelength 524 nm, laser power 90%, one laser pulse, channel sensitivity of 2.0 V and 0.2 min measurement interval.
3. Prepare medium. Mix 5 mL PBS with 45 mM PP, and insert this is a 5 mL BD syringe.
4. Fill whole tubing sequence with cell medium until the medium reached the end of the glass capillary (syringe pump, 'purge' option).
5. Set PhotoMultiplierTube (PMT) to 275, perform 3 single measurements to obtain maximum signal amplitude (fluorescence intensity) of 1.2 V.
6. Start medium flow rate of syringe pump at 35 μL/min.
7. Obtaining stable oxygen measurements for 2 minutes around the expected 0.20 mol/m^3.
8. For low oxygen conditions, start nitrogen flow of Bronckhorst controller at 200 mL/min.
9. Take measurements for 20 minutes, until an oxygen concentration of 0.01 mol/m^3 is reached.
10. Stop nitrogen flow, and start air flow at 400 mL/min. Continue measurements until oxygen concentration reaches value of step 7.
11. For a repetition of saturated to low oxygen conditions, repeat step 8 to step 10. If 0.01 mol/m^3 not reached, increase nitrogen gas flow to 400 mL/min.
12. For tuning hypoxia oxygen concentration, the ratio of air/nitrogen is increased from 0.1 to 0.2, with steps of 0.025, remaining a constant total gas flow of 400 mL/min. Wait for 7 minutes after a change in gas composition.

D.2.2. Gas Exchanger Outlet

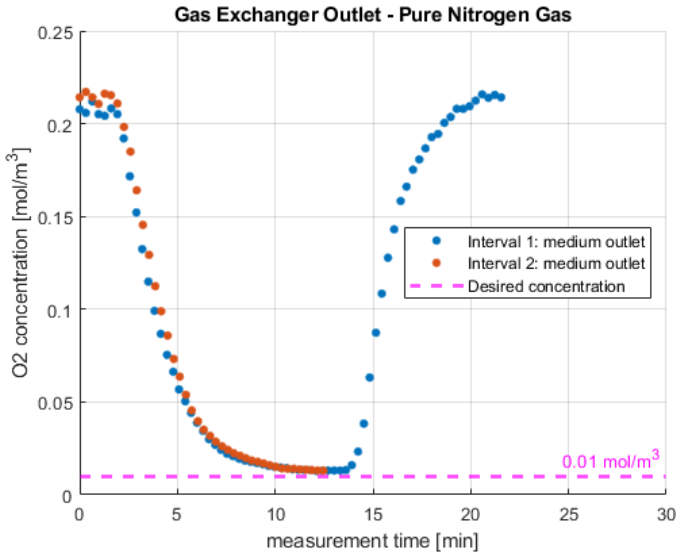

Figure D.5: Oxygen concentration at the gas exchanger box medium outlet with 400 mL/min nitrogen gas.

D.2.3. Testing Procedure: on Chip Measurements

The testing procedure to measure low oxygen concentrations in the Micronit chip channel connected to the gas exchanger is as follows.
1. Choose the Laser Labview settings of Palladium Porphyrin, wavelength 524 nm, laser power 90%, one laser pulse, channel sensitivity of 2.0 V and 0.2 min measurement interval.

2. Prepare medium. Mix 5 mL PBS with 45 mM PP, and insert this is a 5 mL BD syringe. Place aluminium foil under the Micronit chip holder.
3. Fill whole tubing sequence with cell medium until the medium reached the Micronit outlet tubing (syringe pump, 'purge' option).
4. Place the fiber on top of the chip, in the middle of the viewing area.
5. Set PhotoMultiplierTube (PMT) to 275, perform 3 single measurements to obtain maximum signal amplitude (fluorescence intensity) of 1.8 V.
6. Obtaining stable oxygen measurements for 2 minutes around the expected 0.20 mol/m^3.
7. Start medium flow rate of syringe pump at 35 μL/min.
8. For low oxygen conditions, start nitrogen flow of the Bronckhorst controller at 400 mL/min.
9. Take measurements for 18 minutes.
10. Stop nitrogen flow, and start air flow at 400 mL/min. Continue measurements until oxygen concentration reaches value of step 6.
11. For a repetition of saturated to low oxygen conditions, repeat step 8 to step 10. The measurement time may be prolonged to 22 minutes.

D.3. Validation Method: Characterisation Chip Channel

The testing procedure to characterise oxygen concentration on the Micronit resealable chip without the presence of cells is as follows.

1. Turn on heating plate at 38 °C and let the Micronit system heat for 10 minutes. After that, the upper side of the bottom chip slide with open holder reaches 36 °C.
2. Choose the Laser Labview settings of Palladium Porphyrin, wavelength 524 nm, laser power 90%, one laser pulse, channel sensitivity of 2.0 V and 0.2 min measurement interval.
3. Prepare medium. Mix 5 mL PBS with 45 mM PP, and insert this is a 5 mL BD syringe. Place aluminium foil under the Micronit chip.
4. Fill whole tubing sequence with cell medium until the medium reached the Micronit outlet tubing (syringe pump, 'purge' option).
5. Place the fiber at the start of the channel, as close to the medium inlet as allowed by the viewing window.
6. Set PhotoMultiplierTube (PMT) to 220, perform 3 single measurements to obtain maximum signal amplitude (fluorescence intensity) of 1.6 V. 7. Obtaining stable oxygen measurements for 2 minutes around the expected 0.20 mol/m^3.
8. For physiological conditions, start gas flow with 10% oxygen (setting 190 mL/min air, 190 mL/min nitrogen and 20 mL/min CO_2), and wait for 5 minutes.
9. Start medium flow rate of syringe pump at 35 μL/min.
10. After that, take measurements for 5 minutes. If the oxygen concentration is not around 0.09 mol/m^3, the oxygen concentration of gas is decreased to 8% or 7% by decreasing the air/nitrogen ratio with remaining 20 mL/min CO_2.
11. Wait for 10 minutes after last change of gas flow mixture.

Measure oxygen gradient:
12. For the oxygen concentration at the start of the channel, take 18 measurements during 6 minutes time.
13. For the oxygen concentration at end of the channel, place the fiber as close to the medium outlet as allowed by the viewing area. Obtain 48 measurements during 16 minutes time.
14. For the oxygen concentration at the middle (halfway) the channel, place the fiber in the centre of the viewing area. Obtain 20 measurements during 7 minutes time.

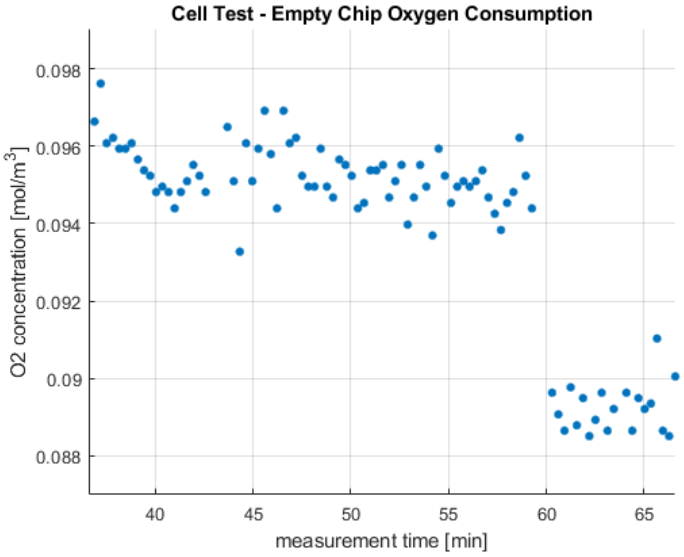

Figure D.6: Chip characterisation oxygen gradient measurements over time. Begin of the channel (37 to 42 min), the end of the channel (43 and 59 min) and the middle of the channel is measured (60 to 67 min).

Flow stop measurement:
15. Change the Labview settings to 'continuous flash'.
16. Stop the medium flow, and manually take oxygen measurements until an increase of > 0.005 mol/m^3 is obtained with at least 10 measurements.
17. Start flow of medium and change the Labview settings to intermittent flash', and obtain 20 measurements during 7 minutes time.

D.4. Validation Method: Cell Layer Test

This section describes the testing method to measure the oxygen gradient and oxygen concentrations during a flow stop in the Micronit resealable chip with presence of cells.

At least one week before the cell layer is cultured of HepaRG cells on the bottom slide of the Micronit resealable chip channel. A 33 mm long x 3 mm wide x 280 μm high PMMA mould (appendix Figure D.7) is glued to the bottom Micronit glass slide of 0.7 mm thickness. The glass slide is coated with Collagene I (Rat Tail) with 150 μL with dilluted concentration of 70 μg/ml. After a few hours, the Hepa RG cells are seeded with 150 μL at 9.3 $\times 10^5$ cells/ml resulting in a confluent cell layer of 150,000 cells/cm^2.

The top glass slide of the Micronit resealable should be cleaned with ethanol. For this cell experiment of one hour, cleaning of the tubing with ethanol and gas exchanger with iso-propanol is not required.

The testing procedure to characterise oxygen concentration on the Micronit resealable chip with the presence of the HepaRG cell layer is as follows.
1. Clean the top glass slide of the chip channel with ethanol. Take 18 cm new long silicone tubing for the gas exchanger. Flush the silicone and Micronit EFTE tubing with water.
2. Turn on heating plate at 38 °C and let the Micronit system heat for 10 minutes. After that, the upper side of the chip slide with open holder reaches 36 °C.
3. Choose the Laser Labview settings of Palladium Porphyrin, wavelength 524 nm, laser power 90%,

one laser pulse, channel sensitivity of 2.0 V and 0.2 min measurement interval.
4. Prepare medium. Mix 15 mL PBS with 45 mM PP, and insert this is a 15 mL BD syringe. Place aluminium foil under the Micronit chip.
5. Fill whole tubing sequence with cell medium until the medium reached the Micronit inlet tubing (syringe pump, 'purge' option).
6. For physiological conditions, start gas flow with 7% oxygen (setting 134 mL/min air, 246 mL/min nitrogen and 20 mL/min CO_2), and wait for 5 minutes.
7. Prepare cell layer. Remove the PMMA mould from the Micronit bottom chip glass slide with a pipette. Place the bottom glass slide (incl. cell layer) in the holder and carefully cover with the top glass slide. Be careful to not damage the cell layer with with the elastomer walls of the top glass slide.
8. Place the fiber at the start of the channel, as close to the medium inlet as allowed by the viewing window.
9. Start medium flow rate of syringe pump at 35 μL/min to supply the cells with medium. Do not use the 'purge' option to quickly fill the chip channel in a few seconds, since this might flush away the cell layer.
10. Set PhotoMultiplierTube (PMT) to 320, perform 3 single measurements to obtain maximum signal amplitude (fluorescence intensity) of 0.7 V. This low amplification should not saturated the 2.0 V sensitivity at expected low oxygen during flow stops.
11. Perform oxygen measurements for 20 minutes to stabilise the oxygen concentration at the channel start and let the cell layer adapt to new environment.

Measure oxygen gradient along length:
12. For the oxygen concentration at the start of the channel, take 30 measurements during 10 minutes time.
13. For the oxygen concentration at the middle (halfway) the channel, place the fiber in the centre of the viewing area. Obtain 18 measurements during 6 minutes time.
14. For the oxygen concentration at end of the channel, place the fiber as close to the medium outlet as allowed by the viewing area. Obtain 18 measurements during 6 minutes time.

Measure oxygen gradient along width at end channel:
15. For the oxygen concentration at the left, take 10 measurements during 3 minutes time.
16. For the oxygen concentration at the right, take 10 measurements during 3 minutes time.

Flow stop measurement:
17. Change the Labview settings to 'continuous flash'.
18. Stop the medium flow, and manually take 10 single oxygen measurements.
19. Start flow of medium and change the Labview settings to intermittent flash', and obtain oxygen measurement during 14 minutes before the next flow stop.

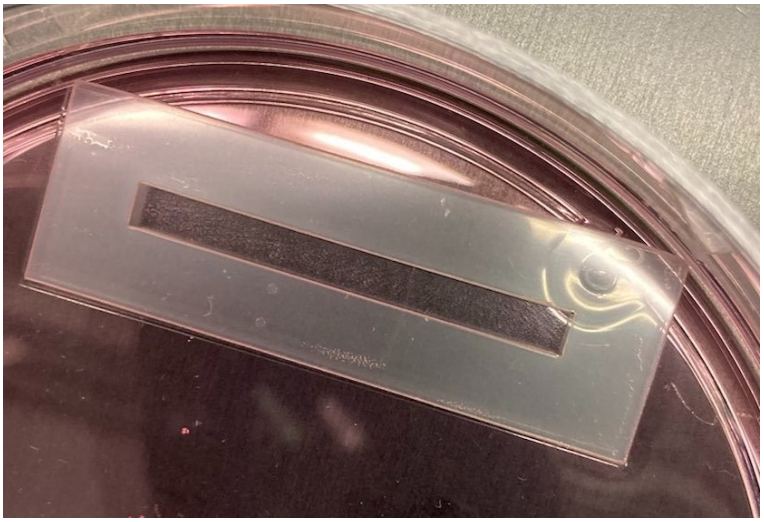

Figure D.7: Cultured HepaRG cell layer with surrounding mould (33 mm x 3 mm) on a Micronit resealable flow cell glass slide covered with cell medium.

D.5. Extra: Cell Test Width Channel

Figure D.8 displays the oxygen measurements along the width at the end of the cell layer. There is a clear variation in the oxygen concentration along the width of the cell layer with a increased concentration at the sides, of 0.075 mol/m^3 and 0.068 mol/m^3, compared to the 0.06 mol/m^3 in the centre. This demonstrates the existence of variations in oxygen along the width, which could occur due to inhomogeneities in the cell layer. Further research in oxygen measurements along the width of the chip channel and cell layer is required to provide an improved understanding of the oxygen variation.

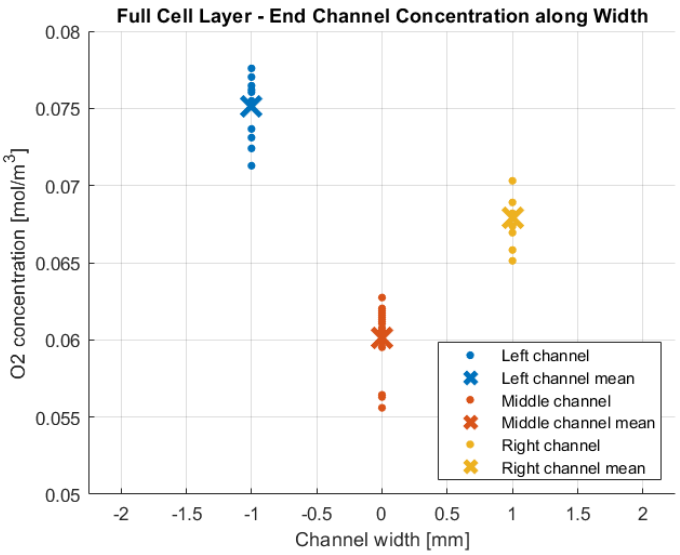

Figure D.8: Oxygen variation along the width at the end of the cell layer in Micronit chip channel.

E

Appendix: MATLAB Code

This appendix states the MATLAB code to process the laser measurement data.

E.1. Chip Elastomer Permeability Test

```
%ProcessingLaserData, experiment 28 april 2021, Matthijs van Reeuwijk
clear all
close all
%% import laser data from .txt file
opts = detectImportOptions('20210428-micronitchip45uLchiplekmeten-
    interval1', ...
    'DecimalSeparator',','); %set comma as decimal seperator
LaserData1 = readtable('20210428-micronitchip45uLchiplekmeten-interval1
    ',...
    opts); %read .txt file second interval
DataSet = LaserData1(:,[1,5,11,12,22]);        %select desired columns
DataSet.Properties.VariableNames = {'MeasurementNr', 'Time', 'Lifetime'
    ,'pO2', 'Notes'};
DataSet( ismember(DataSet.MeasurementNr,1:12) , :) = []; %delete values
DataSet.Time = datetime(DataSet.Time,'Format','hh:mm:ss');
DataSet.Lifetime = round(DataSet.Lifetime,1); %round values to 1
    decimal
DataSet.pO2 = round(DataSet.pO2,1);           %round values to 1
    decimal
%% Special laser data import since first value dataset gives NAN
opts = detectImportOptions('20210428-micronitchip45uLchiplekmeten-
    interval2', ...
    'DecimalSeparator',','); %set comma as decimal seperator
LaserData2 = readtable('20210428-micronitchip45uLchiplekmeten-interval2
    ',...
    opts); %read .txt file of the measurement data first interval
LaserData2(1,:) = [];                    %delete first because NaN value
DataSet = LaserData2(:,[1,8,12,13,23]); %select desired columns
DataSet.Properties.VariableNames = {'MeasurementNr', 'Time', 'Lifetime'
    ,'pO2', 'Notes'};

%% Adapt Dataset
DataSet.Lifetime = round(DataSet.Lifetime,1); %round values to 1
    decimal
```

```
DataSet.pO2 = round(DataSet.pO2,1);           %round values to 1
    decimal
%convert mmHg to mol/m^3, with factor 1.4005e-3
DataSet.pO2 = DataSet.pO2 * 1.4005e-3; %set pO2 to mol/m^3

%% import Comsol Simulations 20210625
    %simulation of chip channel stationary oxygen leakage
%interval 1 (35min) - c_intial medium 0.04 mol/m3, vary c_initial
    elastomer
%ModelData = readtable('20210625-ResealableFlowCellLeakage_D1e-11
    _cinitial0.6_cmed0.04.txt');
%ModelData = readtable('20210625-ResealableFlowCellLeakage_D1e-11
    _cinitial0.65_cmed0.04.txt');
%ModelData = readtable('20210625-ResealableFlowCellLeakage_D1e-11
    _cinitial0.7_cmed0.04.txt');

%interval 1 - vary D with c_intial elastomer 0.065 mol/m3
ModelData = readtable('20210625-ResealableFlowCellLeakage_D1e-11
    _cinitial0.65_cmed0.04.txt');
%ModelData = readtable('20210625-ResealableFlowCellLeakage_D9e-12
    _cinitial0.65_cmed0.04.txt');
%ModelData = readtable('20210625-ResealableFlowCellLeakage_D8e-12
    _cinitial0.65_cmed0.04.txt');
ModelData = ModelData([6:end],[1:2]); %delete first 5 rows of comments

%interval 2 (45 min) - c_intial medium 0.04 mol/m3, vary D
ModelData = importdata('20210625-ResealableFlowCellLeakage_D1e-11
    _cinitial0.65_cmed0.04_t45min.mat');
%ModelData = importdata('20210625-ResealableFlowCellLeakage_D1e-11
    _cinitial0.60_cmed0.04_t45min.mat');
%ModelData = importdata('20210625-ResealableFlowCellLeakage_D9e-12
    _cinitial0.65_cmed0.04_t45min.mat');
%ModelData = importdata('20210625-ResealableFlowCellLeakage_D8e-12
    _cinitial0.65_cmed0.04_t45min.mat');

ModelData.Properties.VariableNames = {'Time', 'Concentration'}; %name
    var

%% Interval Structure
%Interval structure needs to contain measurementnr, time, lifetime and
    pO2
%StartN2 defines the starting time of N2 gas flow
StartN2 = [1,length(DataSet.MeasurementNr)];
IntCount = ["one","two","three","four","five","six"];
for i = 1:1:length(StartN2)-1 %minus one for end value last loop
    nr = IntCount(i);
    Interval.(nr) = DataSet(ismember(DataSet.MeasurementNr,StartN2(i):
        StartN2(i+1)),:);
    Interval.(nr) = removevars(Interval.(nr),'Notes');
    Interval.(nr).Time = Interval.(nr).Time(:) - Interval.(nr).Time(1);
        %create duration array
    Interval.(nr).Time = minutes(Interval.(nr).Time);%convert hh:mm:ss
        to minutes
    Interval.(nr).Time = Interval.(nr).Time * 60;
end
```

```
figure; title('Resealable Chip Oxygen Leakage')
grid on; hold on;
for i = 1:1:length(StartN2)-1 %plot pO2 values along time in minutes
    nr = IntCount(i);
    plot(Interval.(nr).Time,Interval.(nr).pO2,'.','MarkerSize',12)
    grid on; hold on;
end

%% plot model data
plot(ModelData.Time,ModelData.Concentration,'--','linewidth',2)
xlabel('measurement time [seconds]'); ylabel('O2 concentration on chip
   [mol/m^3]')
legend('Measurement interval 2', ...
       'D = 1e-11 [m^2/s], c_{initial} = 0.65 mol/m^3', ...
       'D = 9e-12 [m^2/s], c_{initial} = 0.65 mol/m^3', ...
       'D = 8e-12 [m^2/s], c_{initial} = 0.65 mol/m^3', ...
        'Location','southeast')
axis([0 3000 0.03 0.14])

%% Fitting measurement points - obtain diffusion constant
myfittype = fittype ('a + (b-a) * erfc(n * (1/sqrt(time)) )',...
             'independent','time','dependent','y');
x = Interval.one.Time;
y = Interval.one.pO2;
myfit = fit(x,y,myfittype);
plot(myfit,x,y,'--')

clear i nr;
xlabel('measurement time [seconds]'); ylabel('O2 concentration on chip
   [mol/m^3]')
legend('Interval 1: pO2 measurements', 'Interval 1: polyfit 6th order',
    ...
       'Interval 2: pO2 measurements', 'Interval 2: polyfit 6th order',
           ...
       'Location','southeast')
axis([0 45 0.02 0.14])
```

E.2. Tubular Exchanger Prototype

E.2.1. Prototype 53 cm tube at 35 μL/min

```
%ProcessingLaserData, Experiment 2 april 2021, Matthijs van Reeuwijk
clear all
close all

%import laser data from .txt file
opts = detectImportOptions('20210402
    GasExchangerExperiment35uLminL60cmPBSmetPP_datalog', ...
     'DecimalSeparator',','); %set comma as decimal seperator
LaserData = readtable('20210402
    GasExchangerExperiment35uLminL60cmPBSmetPP_datalog',...
     opts); %read txt file of the measurement data
DataSet = LaserData(:,[1,5,11,12,22]);        %select desired columns
DataSet.Properties.VariableNames = {'MeasurementNr', 'Time', 'Lifetime'
    ,'pO2', 'Notes'};
DataSet.Time = datetime(DataSet.Time,'Format','hh:mm:ss'); %hours,min,
    sec format
DataSet.Lifetime = round(DataSet.Lifetime,1); %round values to 1
    decimal
DataSet.pO2 = round(DataSet.pO2,1);           %round values to 1
    decimal

%convert pO2 value with quenching constant; from 37 to 21 deg Celsius
     %sinaasappe1996; k_quench at 21.5 deg is 115, at 37 deg is 190
DataSet.pO2 = DataSet.pO2*(190/115); %correct quenching constant
%convert mmHg to mol/m^3, with factor 1.4005e-3
DataSet.pO2 = DataSet.pO2 * 1.4005e-3; %set pO2 to mol/m^3

%% import Comsol Average Outlet Concentration 20210408
%medium flow 35 uL/min, parallel gas flow of 200 mL/min, no inlet or
    outlet
%tubing h=0.4mm, ID=0.8mm
ModelData = readtable('20210413GasExchangerExportOutletConcDsil6dot59e
    -6');
ModelData = ModelData([6:end],[1:2]); %delete first 5 rows of comments
ModelData.Properties.VariableNames = {'Time', 'Concentration'}; %name
    var
ModelData.Time = ModelData.Time*(1/60); %convert seconds to minutes
%% Clean LaserData to create DataSet, delete 44 values
%remove measurements with polymer outlet, since low signal of 0.3V,
    glas cappilair 1.3V
DataSet( ismember(DataSet.MeasurementNr,1:4) , :) = [];
%remove since still N2 in tube, at 28 flush with air and at 45
    measurements stable again
DataSet( ismember(DataSet.MeasurementNr,5:44) , :) = [];
%% Interval Structure
%Interval structure needs to contain measurementnr, time, lifetime and
    pO2
%StartN2 defines the starting time of N2 gas flow
StartN2 = [53,136,218,length(DataSet.MeasurementNr)];
IntCount = ["one","two","three","four","five","six"];
for i = 1:1:length(StartN2)-1 %minus one for end value last loop
     nr = IntCount(i);
     Interval.(nr) = DataSet(ismember(DataSet.MeasurementNr,StartN2(i):
         StartN2(i+1)),:);
```

```
    Interval.(nr) = removevars(Interval.(nr),'Notes');
    Interval.(nr).Time = Interval.(nr).Time(:) - Interval.(nr).Time(1);
        %create duration array
    Interval.(nr).Time = minutes(Interval.(nr).Time);%convert hh:mm:ss
       to minutes
    clear i nr;
end

figure; title('02 April Gas Exchanger Prototype Experiment - Intervals'
   )
grid on; hold on;
for i = 1:1:length(StartN2)-1 %plot pO2 values along time in minutes
    nr = IntCount(i);
    plot(Interval.(nr).Time,Interval.(nr).pO2,'b')
    grid on; hold on; clear i nr;
end
xlabel('measurement time [min]')
ylabel('O2 concentration [mol/m^3]')
legend('pO2 interval 1', 'pO2 interval 2', 'pO2 interval 3', ...
       'Location','northwest')
%% plot Model Data
plot(ModelData.Time,ModelData.Concentration,'--')
title('Tubular Gas Exchanger - Outlet Concentration')
legend('Interval 1 - 35 \muL/min', 'Interval 2 - 35 \muL/min', ...
       'Dsil=2.54e-10 [m^2/s]', ...
       'Dsil=3.59e-10 [m^2/s]', ...
       'Dsil=4.59e-10 [m^2/s]', ...
       'Dsil=5.59e-10 [m^2/s]', ...
       'Dsil=6.59e-10 [m^2/s]', 'Location','southeast')
```

E.2.2. Prototype 53 cm tube at 45 μL/min

```
%ProcessingLaserData, experiment 28 april 2021
%micronit chip connected to gas exchanger
%Matthijs van Reeuwijk, 3 April 2021
clear all
close all

%import laser data from .txt file
opts = detectImportOptions('20210428-
   GasExchangerExperiment35uLminL60cmPBSmetPP-chipconnected', ...
    'DecimalSeparator',',');%set comma as decimal seperator
LaserData = readtable('20210428-
   GasExchangerExperiment35uLminL60cmPBSmetPP-chipconnected',...
    opts); %read .txt file of the measurement data
DataSet = LaserData(:,[1,5,11,12,22]);        %select desired columns
DataSet.Properties.VariableNames = {'MeasurementNr', 'Time', 'Lifetime'
   ,'pO2', 'Notes'};
DataSet.Time = datetime(DataSet.Time,'Format','hh:mm:ss'); %hours,min,
   sec format
DataSet.Lifetime = round(DataSet.Lifetime,7); %round values to 1
   decimal
DataSet.pO2 = round(DataSet.pO2,7);           %round values to 1
   decimal

%convert pO2 value with quenching constant; from 37 to 21 deg Celsius
    %sinaasappe1996; k_quench at 22.5 deg is 125, at 37 deg is 190
```

```
DataSet.pO2 = DataSet.pO2*(190/125); %correct quenching constant
%convert mmHg to mol/m^3, with factor 1.4005e-3
DataSet.pO2 = DataSet.pO2 * 1.4005e-3; %set pO2 to mol/m^3

%% Clean Data
%first values of gas exchanger outlet without flow, delete for equal
%start with previous two intervals
DataSet( ismember(DataSet.MeasurementNr,199:212) , :) = [];

%% Interval Structure
%Interval structure needs to contain measurementnr, time, lifetime and
   pO2
%StartN2 defines the starting time of N2 gas flow
StartN2 = [12,110,(212-13),length(DataSet.MeasurementNr)];
IntCount = ["one","two","three","four","five","six"];
for i = 1:1:length(StartN2)-1 %minus one for end value last loop
    nr = IntCount(i);
    Interval.(nr) = DataSet(ismember(DataSet.MeasurementNr,StartN2(i):
       StartN2(i+1)),:);
    Interval.(nr) = removevars(Interval.(nr),'Notes');
    Interval.(nr).Time = Interval.(nr).Time(:) - Interval.(nr).Time(1);
        %create duration array
    Interval.(nr).Time = minutes(Interval.(nr).Time);%convert hh:mm:ss
       to minutes
    clear i nr;
end

figure; title('Tubular Gas Exchanger connected to Chip')
grid on; hold on;
for i = 1:1:length(StartN2)-1 %plot pO2 values along time in minutes
    nr = IntCount(i);
    plot(Interval.(nr).Time,Interval.(nr).pO2,'.','MarkerSize',10)
end
xlabel('measurement time [min]'); ylabel('O2 Concentration [mol/m^3]')
legend('Interval 1 - Qgas = 200 mL/min', ...
       'Interval 2 - Qgas = 400 mL/min', ...
       'Exchanger outlet Qgas = 200 mL/min','Location','southeast')
axis([-0.5 30 0 0.27])
```

E.2.3. Prototype 33 cm tube at 35 μL/min

```
%ProcessingLaserData, experiment 03 May 2021, Matthijs van Reeuwijk
clear all
close all

%import laser data from .txt file
opts = detectImportOptions('20210503-
   GasExchangerExperiment35uLminL33cmPBSmetPP-outletTRIAL4', ...
    'DecimalSeparator',','); %set comma as decimal seperator
LaserData = readtable('20210503-
   GasExchangerExperiment35uLminL33cmPBSmetPP-outletTRIAL4',...
    opts); %read .txt file of the measurement data
DataSet = LaserData(:,[1,5,11,12,22]);        %select desired columns
DataSet.Properties.VariableNames = {'MeasurementNr', 'Time', 'Lifetime'
   ,'pO2', 'Notes'};
DataSet.Time = datetime(DataSet.Time,'Format','hh:mm:ss'); %hours,min,
   sec format
```

```
DataSet.Lifetime = round(DataSet.Lifetime,1); %round values to 1
    decimal
DataSet.pO2 = round(DataSet.pO2,1);           %round values to 1
    decimal

%convert pO2 value with quenching constant; from 37 to 21 deg Celsius
    %sinaasappe1996; k_quench at 21.5 deg is 115, at 37 deg is 190
DataSet.pO2 = DataSet.pO2*(190/115); %correct quenching constant
%convert mmHg to mol/m^3, with factor 1.4005e-3
DataSet.pO2 = DataSet.pO2 * 1.4005e-3; %set pO2 to mol/m^3

%% Clean Data: need for air flow and closed PMT
%remove measurements with cleaning air flow for resting N2
DataSet( ismember(DataSet.MeasurementNr,1:19) , :) = [];
%remove for closed PMT
DataSet( ismember(DataSet.MeasurementNr,20:22) , :) = [];
%remove for stopping gas flow after 25
DataSet( ismember(DataSet.MeasurementNr,23:25) , :) = [];
%remove noise measurements on capillary
DataSet( ismember(DataSet.MeasurementNr,146:149), :) = [];
%% Interval Structure
%Interval structure needs to contain measurementnr, time, lifetime and
    pO2
%StartN2 defines the starting time of N2 gas flow
StartN2 = [31,91,DataSet.MeasurementNr(end)];
IntCount = ["one","two","three","four","five","six"];
for i = 1:1:length(StartN2)-1 %minus one for end value last loop
    nr = IntCount(i);
    Interval.(nr) = DataSet(ismember(DataSet.MeasurementNr,StartN2(i):
        StartN2(i+1)),:);
    Interval.(nr) = removevars(Interval.(nr),'Notes');
    Interval.(nr).Time = Interval.(nr).Time(:) - Interval.(nr).Time(1);
        %create duration array
    Interval.(nr).Time = minutes(Interval.(nr).Time);%convert hh:mm:ss
        to minutes
    clear i nr;
end

figure; title('Tubular Gas Exchanger L = 33 cm')
grid on; hold on;
for i = 1:1:length(StartN2)-1 %plot pO2 values along time in minutes
    nr = IntCount(i);
    plot(Interval.(nr).Time,Interval.(nr).pO2,'.','MarkerSize',15)

    grid on; hold on; clear i nr;
end
xlabel('measurement time [min]')
ylabel('O2 concentration [mol/m^3]')
legend('Interval 1 - Q = 35 \muL/min', ...
       'Interval 2 - Q = 35 \muL/min', ...
       'Location','north')
axis([-0.5 20 0 0.25])
```

E.2.4. Prototype 18 cm tube at 35 μL/min

```
%ProcessingLaserData, experiment 03 May 2021
%Matthijs van Reeuwijk, 3 April 2021
```

```
clear all
close all

%import laser data from .txt file
opts = detectImportOptions('20210503-
    GasExchangerExperiment35uLminL20cmPBSmetPP-outlet', ...
     'DecimalSeparator',',');%set comma as decimal seperator
LaserData = readtable('20210503-
    GasExchangerExperiment35uLminL20cmPBSmetPP-outlet',...
     opts); %read .txt file of the measurement data
DataSet = LaserData(:,[1,5,11,12,22]);        %select desired columns
DataSet.Properties.VariableNames = {'MeasurementNr', 'Time', 'Lifetime'
    ,'pO2', 'Notes'};
DataSet.Time = datetime(DataSet.Time,'Format','hh:mm:ss'); %hours,min,
    sec format
DataSet.Lifetime = round(DataSet.Lifetime,7); %round values to 1
    decimal
DataSet.pO2 = round(DataSet.pO2,7);           %round values to 1
    decimal

%convert pO2 value with quenching constant; from 37 to 21 deg Celsius
     %sinaasappe1996; k_quench at 21.5 deg is 115, at 37 deg is 190
DataSet.pO2 = DataSet.pO2*(190/115); %correct quenching constant
%convert mmHg to mol/m^3, with factor 1.4005e-3
DataSet.pO2 = DataSet.pO2 * 1.4005e-3; %set pO2 to mol/m^3

%% Clean Data: need for air flow and closed PMT
%remove measurements since old medium in first three measurements
DataSet( ismember(DataSet.MeasurementNr,1:3) , :) = [];
%remove measurements, since takes long time for interval 1 to reach
    0.17
%therefore cut off at 15 min, 60 measurements
DataSet( ismember(DataSet.MeasurementNr,61:76) , :) = [];

%remove measurements in interval 2, for stepwise increase n2/air ratio
%DataSet( ismember(DataSet.MeasurementNr,0:112) , :) = [];
%delete last three capillary noise measurements
DataSet( ismember(DataSet.MeasurementNr,242:245) , :) = [];
%% Interval Structure
%Interval structure needs to contain measurementnr, time, lifetime and
    pO2
%StartN2 defines the starting time of N2 gas flow
 %end number 111 since after that stepwise increasing air/n2 ratio
%StartN2 = [11,76,109]; %interval 1 and 2
%StartN2 = [112,245]; %stepwise increase air/n2 ratio
StartN2 = [112,213]; %stepwise increase air/n2 ratio until 9% air

IntCount = ["one","two","three","four","five","six"];
for i = 1:1:length(StartN2)-1 %minus one for end value last loop
    nr = IntCount(i);
    Interval.(nr) = DataSet(ismember(DataSet.MeasurementNr,StartN2(i):
       StartN2(i+1)),:);
    Interval.(nr) = removevars(Interval.(nr),'Notes');
    Interval.(nr).Time = Interval.(nr).Time(:) - Interval.(nr).Time(1);
        %create duration array
    Interval.(nr).Time = minutes(Interval.(nr).Time);%convert hh:mm:ss
```

```
        to minutes
    clear i nr;
end

%StopN2 defines the time at which N2 gas flow is stopped, for polyfit
    decay
%StartFit = [13,80];
%StopFit = [41,110];
figure; title('Tubular Gas Exchanger L = 18cm')
grid on; hold on;
for i = 1:1:length(StartN2)-1 %plot pO2 values along time in minutes
    nr = IntCount(i);
    plot(Interval.(nr).Time,Interval.(nr).pO2,'.','MarkerSize',15)
    %for j = 1:1:length(StopFit)-1
    %    polytime = Interval.(nr).Time(ismember(Interval.(nr).
        MeasurementNr,StartFit(i):StopFit(i)));
    %    polypO2 = Interval.(nr).pO2(ismember(Interval.(nr).
        MeasurementNr,StartFit(i):StopFit(i)));
    %    p = polyfit(polytime,polypO2,4);
    %    y = polyval(p,polytime);
    %    plot(polytime,y,'g-','linewidth',1);
    %end
    grid on; hold on; %clear i j nr polytime polypO2 p y
end
xlabel('measurement time [min]')
ylabel('O2 concentration [mol/m^3]')
legend('Interval 1 - Q = 35 \muL/min', ... %'Interval 1 - polyfit 4th
    order',...
        'Interval 2 - Q = 35 \muL/min', ... %'Interval 1 - polyfit 4th
            order',
        'Location','north')
%axis([0 20 0 0.25]) %on chip intervals

%% plot tune air/nitrogen
title('Tubular gas exchanger')
axis([0 40 0 0.1]) %tune air/nitrogen
yline(0.0025,'r--',{'4% O2 Gas'},'labelhorizontalalignment','right')
yline(0.0449,'r--',{'5% O2 Gas'},'labelhorizontalalignment','right')
yline(0.0567,'r--',{'6% O2 Gas'},'labelhorizontalalignment','right')
yline(0.0659,'r--',{'7% O2 Gas'},'labelhorizontalalignment','right')
yline(0.0761,'r--',{'8% O2 Gas'},'labelhorizontalalignment','right')
yline(0.084,'r--',{'9% O2 Gas'},'labelhorizontalalignment','right')
%yline(0.0920,'r--',{'10% O2 Gas'},'labelhorizontalalignment','left')
%yline(0.0972,'r--',{'start 11% O2 Gas'},'labelhorizontalalignment','
    left')
legend('Exchanger Medium Outlet','Location','North')
```

E.2.5. Prototype 53 cm tube with chip at 35 μL/min

```
%ProcessingLaserData, experiment 28 april 2021, Matthijs van Reeuwijk
clear all
close all

%import laser data from .txt file
opts = detectImportOptions('20210428-
    GasExchangerExperiment35uLminL60cmPBSmetPP-chipconnected', ...
     'DecimalSeparator',',');%set comma as decimal seperator
```

```
LaserData = readtable('20210428-
    GasExchangerExperiment35uLminL60cmPBSmetPP-chipconnected',...
     opts); %read .txt file of the measurement data
DataSet = LaserData(:,[1,5,11,12,22]);        %select desired columns
DataSet.Properties.VariableNames = {'MeasurementNr', 'Time', 'Lifetime'
    ,'pO2', 'Notes'};
DataSet.Time = datetime(DataSet.Time,'Format','hh:mm:ss'); %hours,min,
    sec format
DataSet.Lifetime = round(DataSet.Lifetime,7); %round values to 1
    decimal
DataSet.pO2 = round(DataSet.pO2,7);           %round values to 1
    decimal

%convert pO2 value with quenching constant; from 37 to 21 deg Celsius
    %sinaasappe1996; k_quench at 22.5 deg is 125, at 37 deg is 190
DataSet.pO2 = DataSet.pO2*(190/125); %correct quenching constant
%convert mmHg to mol/m^3, with factor 1.4005e-3
DataSet.pO2 = DataSet.pO2 * 1.4005e-3; %set pO2 to mol/m^3

%% Clean Data
%first values of gas exchanger outlet without flow, delete for equal
%start with previous two intervals
DataSet( ismember(DataSet.MeasurementNr,199:212) , :) = [];

%% Interval Structure
%Interval structure needs to contain measurementnr, time, lifetime and
    pO2
%StartN2 defines the starting time of N2 gas flow
StartN2 = [12,110,(212-13),length(DataSet.MeasurementNr)];
IntCount = ["one","two","three","four","five","six"];
for i = 1:1:length(StartN2)-1 %minus one for end value last loop
    nr = IntCount(i);
    Interval.(nr) = DataSet(ismember(DataSet.MeasurementNr,StartN2(i):
        StartN2(i+1)),:);
    Interval.(nr) = removevars(Interval.(nr),'Notes');
    Interval.(nr).Time = Interval.(nr).Time(:) - Interval.(nr).Time(1);
        %create duration array
    Interval.(nr).Time = minutes(Interval.(nr).Time);%convert hh:mm:ss
        to minutes
    clear i nr;
end

figure; title('Tubular Gas Exchanger connected to Chip')
grid on; hold on;
for i = 1:1:length(StartN2)-1 %plot pO2 values along time in minutes
    nr = IntCount(i);
    plot(Interval.(nr).Time,Interval.(nr).pO2,'.','MarkerSize',10)
end
xlabel('measurement time [min]'); ylabel('O2 Concentration [mol/m^3]')
legend('Interval 1 - Qgas = 200 mL/min', ...
       'Interval 2 - Qgas = 400 mL/min', ...
       'Exchanger outlet Qgas = 200 mL/min','Location','southeast')
axis([-0.5 30 0 0.27])
```

E.3. System Validation: Gas Exchanger Box Validation

```
%ProcessingLaserData, experiment 14th of June 2021, Matthijs van
```

```
    Reeuwijk
clear all
close all

%import 1-200 ml/min laser data from .txt file
opts = detectImportOptions('1-20210614-gasexchangerbox-55
    uLcapillairoutlet-35uLmin200mlmingas17cmtube_v1', ...
    'DecimalSeparator',',');        %set comma as decimal seperator
LaserData = readtable('1-20210614-gasexchangerbox-55uLcapillairoutlet
    -35uLmin200mlmingas17cmtube_v1',...
    opts);                          %read .txt file of the measurement
        data
DataSet = LaserData(:,[1,5,11,12,22]); %select desired columns
DataSet.Properties.VariableNames = {'MeasurementNr', 'Time', 'Lifetime'
    ,'pO2', 'Notes'};
DataSet.Time = datetime(DataSet.Time,'Format','hh:mm:ss'); %hours,min,
    sec format

%import 3-gas exchanger 400 ml/min laser data from .txt file
opts = detectImportOptions('3-20210614-gasexchangerbox-55
    uLcapillairoutlet-35uLmin400mlmingas17cmtube_v2', ...
    'DecimalSeparator',','); %set comma as decimal seperator
LaserData2 = readtable('3-20210614-gasexchangerbox-55uLcapillairoutlet
    -35uLmin400mlmingas17cmtube_v2',...
    opts); %read .txt file of the measurement data
DataSet = LaserData2(2:228,[1,8,12,13,23]); %select desired columns

%import 4-chipconnect laser data from .txt file
opts = detectImportOptions('4-20210614-gasexchangerbox-55
    uLcapillairoutlet-35uLmin400mlmingas17cmtubeCHIPconnect_v1', ...
    'DecimalSeparator',','); %set comma as decimal seperator
LaserData3 = readtable('4-20210614-gasexchangerbox-55uLcapillairoutlet
    -35uLmin400mlmingas17cmtubeCHIPconnect_v1',...
    opts); %read .txt file of the measurement data
DataSet = LaserData3(2:258,[1,8,12,13,23]); %select desired columns


DataSet.Properties.VariableNames = {'MeasurementNr', 'Time', 'Lifetime'
    ,'pO2', 'Notes'};
DataSet.Lifetime = round(DataSet.Lifetime,1); %round values to 1
    decimal
DataSet.pO2 = round(DataSet.pO2,1);           %round values to 1
    decimal
%convert pO2 value with quenching constant; from 37 to 22.5 deg Celsius
    %sinaasappe1996; k_quench at 22.5 deg is 120, at 37 deg is 190
    %sinaasappel1996: k_q at 25 deg is 132 for first chip interval
    %sinaasappel1996: k_q at 24 deg is 125 for second chip interval
DataSet.pO2 = DataSet.pO2*(190/120); %correct quenching constant
%convert mmHg to mol/m^3, with factor 1.4005e-3
DataSet.pO2 = DataSet.pO2 * 1.4005e-3; %set pO2 to mol/m^3

%% Clean Data
%1-remove first 5 measurements because set PMT and flush tube with air
DataSet( ismember(DataSet.MeasurementNr,1:5) , :) = [];
head(DataSet) %show first 5 values dataset
```

```
%3-gas exchanger: remove first 7 values since nitrogen left in tube
DataSet( ismember(DataSet.MeasurementNr,1:7) , :) = [];

%4-chip: remove first 90 measurements since warm chip and forgot alu
    foil
DataSet( ismember(DataSet.MeasurementNr,1:90) , :) = [];
%% Interval Structure
%Interval structure needs to contain measurementnr, time, lifetime and
    pO2
%StartN2 defines the starting time of N2 gas flow
StartN2 = [6,122]; %1- gas exchanger 200 mlL/min
%StartN2 = [11,80,120] %3-gas exchanger pure nitrogen 400 mL/min
%StartN2 = [120, 225] %3-increase air to gas mixture
%StartN2 = [100,188,255];   %4-onchip
IntCount = ["one","two","three","four","five","six"];
for i = 1:1:length(StartN2)-1 %minus one for end value last loop
    nr = IntCount(i);
    Interval.(nr) = DataSet(ismember(DataSet.MeasurementNr,StartN2(i):
        StartN2(i+1)),:);
    Interval.(nr) = removevars(Interval.(nr),'Notes');
    Interval.(nr).Time = Interval.(nr).Time(:) - Interval.(nr).Time(1);
        %create duration array
    Interval.(nr).Time = minutes(Interval.(nr).Time);%convert hh:mm:ss
        to minutes
    clear i;
end
%Start and Stop fit for defining the interval of fitting
%StartFit = [19, 38, 119];
%StopFit = [36, 55, 119];
figure;
%title('Micronit Chip - Connected to Gas Exchanger')
title('Gas Exchanger Outlet - Pure Nitrogen Gas')
grid on; hold on;
for i = 1:1:length(StartN2)-1 %plot pO2 values along time in minutes
    nr = IntCount(i);
    plot(Interval.(nr).Time,Interval.(nr).pO2,'.','MarkerSize',15)
    %for j = 1:1:length(StartFit)-1
    %    polytime = Interval.(nr).Time(ismember(Interval.(nr).
        MeasurementNr,StartFit(j):StopFit(j)));
    %    polypO2 = Interval.(nr).pO2(ismember(Interval.(nr).
        MeasurementNr,StartFit(j):StopFit(j)));
    %    p = polyfit(polytime,polypO2,1);
    %    y = polyval(p,polytime);
        %polytime_e = polytime(1)+2:0.2:polytime(end)+2;
        %y = @(x) p(1)*x + p(2); y = y (polytime_e);
    %    plot(polytime,y,'g-','linewidth',1.5);
    %end
    %grid on; hold on; %clear i j nr polytime polypO2 p y
end
xlabel('measurement time [min]')
ylabel('O2 concentration [mol/m^3]')
axis([0 30 0 0.25])
legend('Interval 1: medium outlet', 'Interval 2: medium outlet',....
       'Desired concentration', 'Location','east')

%legend('interval 1: gas flow 200 mL/min', ...
```

```
%       'interval 2: gas flow 400 mL/min',...
%         'location','southeast')
%legend('Interval 1: on chip', 'Interval 2: on chip',...
%       'Desired concentration','Exchanger outlet','Location','north')
yline(0.01, '--m',{'0.01 mol/m^3'}, 'linewidth',2)

%% additional for tuning air/N2
%start plot at 120 measurements
xline(1,'--r',{'2.1% O2 gas'},'labelverticalalignment','middle'); % first step 40/400 air
xline(8.33,'--r',{'2.5% O2 gas'},'labelverticalalignment','middle'); %second step 50/400 air
xline(15,'--r',{'3.2% O2 gas'},'labelverticalalignment','middle'); %third step 60/400
xline(21.67,'--r',{'3.7% O2 gas'},'labelverticalalignment','middle'); %fourth step 70/400
xline(28.3,'--r',{'4.2% O2 gas'},'labelverticalalignment','middle'); %fifth step 80/400
axis([0 30 0 0.06])
```

E.4. System Validation: Characterisation Chip Channel

```
%ProcessingLaserData, empty chip experiment 21st of June 2021
%Matthijs van Reeuwijk
clear all
close all

%import Empty Chip Validation
opts = detectImportOptions('20210621-ExchangertoChip-ValidateEmptyChip-35uLmin45mMPP-gasflow400mlmin', ...
    'DecimalSeparator',',');        %set comma as decimal seperator
LaserData = readtable('20210621-ExchangertoChip-ValidateEmptyChip-35uLmin45mMPP-gasflow400mlmin',...
    opts);                          %read .txt file of the measurement data

DataSet = LaserData(:,[1,5,11,12,22]); %select desired columns
DataSet.Properties.VariableNames = {'MeasurementNr', 'Time', 'Lifetime','pO2', 'Notes'};
DataSet.Time = datetime(DataSet.Time,'Format','hh:mm:ss'); %hours,min,sec format
DataSet.Lifetime = round(DataSet.Lifetime,1); %round values to 1 decimal
DataSet.pO2 = round(DataSet.pO2,1);           %round values to 1 decimal
DataSet.pO2 = DataSet.pO2 * 1.4005e-3; %set pO2 to mol/m^3

%% Clean Data
%empty chip - remove first 6 measurements, for setting PMT value
DataSet( ismember(DataSet.MeasurementNr,1:6) , :) = [];
%% Interval Structure
%Interval structure contains measurementnr, time, lifetime and pO2
%StartInt defines selection measurement points
StartInt = [7,221];    %all measurement points
%StartInt = [7,36];     %measure after 5 min wait 190air/90N2/20CO2 and flow stop
%StartInt = [9,110];    %from 10% O2 in gas towards 8% O2 in gas
```

```
%StartInt = [180, 221]; %flow stop continous flash whole measurement
%StartInt = [185,210];  %flow stop continous flash; only continous data

IntCount = ["one","two","three","four","five","six"];
for i = 1:1:length(StartInt)-1 %minus one for end value last loop
    nr = IntCount(i);
    Interval.(nr) = DataSet(ismember(DataSet.MeasurementNr,StartInt(i):
       StartInt(i+1)),:);
    Interval.(nr) = removevars(Interval.(nr),'Notes');
    Interval.(nr).Time = Interval.(nr).Time(:) - Interval.(nr).Time(1);
        %create duration array
    Interval.(nr).Time = minutes(Interval.(nr).Time);%convert hh:mm:ss
       to minutes
    clear i;
end

figure;
title('Cell Test - Empty Chip Oxygen Consumption')
grid on; hold on;
for i = 1:1:length(StartInt)-1 %plot pO2 values along time in minutes
    nr = IntCount(i);
    plot(Interval.(nr).Time,Interval.(nr).pO2,'.','MarkerSize',15)
end
xlabel('measurement time [min]')
ylabel('O2 concentration [mol/m^3]')

    %% empty chip - 10% gas flowstop
xline(9.4667,'--r',{'start medium flow'})       %start medium flow
xline(14.267,'--r',{'stop medium flow'});       %stop medium flow
    %% empty chip - varying o2 concentration gas
xline(0,'--r',{'10% O2 gas'});          %10% o2 gas after calibration
xline(9.25,'--r',{'8% O2 gas'});        %8% o2 gas
xline(16.583,'--r',{'7% O2 gas'});      %7% o2 gas
axis([-1 35 0.09 0.19]);
    %% empty chip - continous flash extra measurements
%including measurements before and after flow stop
xline(1.5667, '--r', {'stop medium flow'})
xline(5.3167, '--r',{'start medium flow'})
axis([-1 12 0.087 0.097])
    %% empty chip - continous flash only contious measurements
xline(0, '--r', {'stop medium flow'})
xline(3.6333, '--r',{'start medium flow'})
axis([-0.5 4 0.087 0.097])

    %% empty chip - gradient
%full channel is 40 mm long; measured from inlet to outlet,
   measurements
%through open windows of 25 mm long and 4.5 mm wide
%window start at 8.75 mm of channel
ChannelStart = DataSet( ismember(DataSet.MeasurementNr,92:110) , :);
ChannelStartO2 = ChannelStart.pO2(:); %oxygen concentrations
ChannelStartMean = mean(ChannelStartO2); %mean start channel
ChannelStartStd = std(ChannelStartO2); %standard deviation start
   channel
%window middle at 20 mm of channel
ChannelMiddle = DataSet( ismember(DataSet.MeasurementNr,162:180) , :);
```

```
ChannelMiddleO2 = ChannelMiddle.pO2(:); %oxygen concentrations
ChannelMiddleMean = mean(ChannelMiddleO2); %mean start channel
ChannelMiddleStd = std(ChannelMiddleO2); %standard deviation start
    channel
%window end at 31.25 mm of channel
ChannelEnd = DataSet( ismember(DataSet.MeasurementNr,111:159) , :);
ChannelEndO2 = ChannelEnd.pO2(:); %oxygen concentrations
ChannelEndMean = mean(ChannelEndO2); %mean start channel
ChannelEndStd = std(ChannelEndO2); %standard deviation start channel

%plot measurement points
figure; hold on; grid on; title('Empty Chip - Concentration along
    Length')
plot(ones(length(ChannelStartO2),1)*8.75, ChannelStartO2,'.','Color',[0
     0.4470 0.7410],'Markersize',15);
plot(8.75, ChannelStartMean, 'x','color',[0 0.4470 0.7410],'Markersize'
    ,15,'Linewidth',3)
plot(ones(length(ChannelMiddleO2),1)*20, ChannelMiddleO2,'.','Color'
    ,[0.8500 0.3250 0.0980],'Markersize',15);
plot(20, ChannelMiddleMean, 'x','Color',[0.8500 0.3250 0.0980],'
    Markersize',15,'Linewidth',3)
plot(ones(length(ChannelEndO2),1)*31.25, ChannelEndO2,'.','Color'
    ,[0.9290 0.6940 0.1250],'Markersize',15);
plot(31.25, ChannelEndMean, 'x','Color',[0.9290 0.6940 0.1250],'
    Markersize',15,'linewidth',3)

xlabel('channel length [mm]')
ylabel('O2 concentration [mol/m^3]')
legend('Start channel','Start channel mean',...
       'Middle channel','Middle channel mean',...
       'End channel','End channel mean','Location','southeast')
axis([0 40 0.087 0.099])
```

E.5. System Validation: Cell Test

```
%ProcessingLaserData, experiment 21st of June 2021, full cell layer
%Matthijs van Reeuwijk
clear all
close all

%import Full Cell Layer Chip Validation
    %reading data from .txt file not working due to continious flash
        use
    %therefore manually adjusted measurement data in excel
LaserData = importdata('20210621-ExchangertoChip-ValidateCELLSChip2-35
    uLmin45mMPP-gasflow400mlminV2-matlabdataset.mat');
DataSet = LaserData(:,[1,8,12,13,23]); %select desired columns
DataSet.Properties.VariableNames = {'MeasurementNr', 'Time', 'Lifetime'
    ,'pO2', 'Notes'};
DataSet.Lifetime = round(DataSet.Lifetime,1); %round values to 1
    decimal
DataSet.pO2 = round(DataSet.pO2,1);           %round values to 1
    decimal
DataSet.pO2 = DataSet.pO2 * 1.4005e-3; %set pO2 to mol/m^3

%% Interval Structure
%Interval structure contains measurementnr, time, lifetime and pO2
```

```
%StartInt defines selection measurement points
StartInt = [1,333];  %full dataset
%StartInt = [1,93];   %start channel - initial start stabilising with 7% gas
%StartInt = [62,93];  %start channel - 10 minutes of steady state at 7% gas
%StartInt = [152,333]; %middle channel - oxygen consumption measurements
%StartInt = [171,181]; %flow stop I
%StartInt = [238,248]; %flow stop II
%StartInt = [292,301]; %flow stop III
IntCount = ["one","two","three","four","five","six"];
for i = 1:1:length(StartInt)-1 %minus one for end value last loop
    nr = IntCount(i);
    Interval.(nr) = DataSet(ismember(DataSet.MeasurementNr,StartInt(i):StartInt(i+1)),:);
    Interval.(nr) = removevars(Interval.(nr),'Notes');
    Interval.(nr).Time = Interval.(nr).Time(:) - Interval.(nr).Time(1);
     %create duration array
    Interval.(nr).Time = minutes(Interval.(nr).Time);%convert hh:mm:ss to minutes
    clear i;
end

figure;
%title('Full Cell Layer - Flow stops')
title('Full Cell Layer - System Startup')
grid on; hold on;
for i = 1:1:length(StartInt)-1 %plot pO2 values along time in minutes
    nr = IntCount(i);
    plot(Interval.(nr).Time,Interval.(nr).pO2,'.','MarkerSize',15)
end
xlabel('measurement time [min]')
ylabel('O2 concentration [mol/m^3]')

%axis([-1 31 0.09 0.14]) %intitial start gas 7% oxygen 30 minutes
legend('Flow stop I','Flow stop II', 'Flow stop III','location','northeast')
axis([-0.1 1.1 0 0.09]) %flow stops

    %% steady state - 20 to 30 minutes
axis([19.5 30 0.10 0.13]) %7% gas steady from 20-30 minutes
Steady7 = DataSet(ismember(DataSet.MeasurementNr,62:93) , :);
Steady7O2 = Steady7.pO2(:); %oxygen concentrations
Steady7Mean = mean(Steady7O2); %mean 0.1084
Steady7Std = std(Steady7O2); %standard deviation 0.0016

yline(0.1085,'--','linewidth',2,'color',[0.8500 0.3250 0.0980]); %mean 10 min
yline((0.1085+0.0015),'--','linewidth',1.5,'color',[0.9290 0.6940 0.1250]);
yline((0.1085-0.0015),'--','linewidth',1.5,'color',[0.9290 0.6940 0.1250]);
legend('Measurements start channel','Mean value (0.109 mol/m^3)',...
    'Standard deviation (0.0015 mol/m^3)','Location','Northeast')

```

```
    %% full cell layer - oxygen gradient
%window start at 8.75 mm of channel
ChannelStart = DataSet( ismember(DataSet.MeasurementNr,62:93) , :);
ChannelStartO2 = ChannelStart.pO2(:); %oxygen concentrations
ChannelStartMean = mean(ChannelStartO2); %mean start channel
ChannelStartStd = std(ChannelStartO2); %standard deviation start
    channel
%window middle at 20 mm of channel
ChannelMiddle = DataSet( ismember(DataSet.MeasurementNr,94:111) , :);
ChannelMiddleO2 = ChannelMiddle.pO2(:); %oxygen concentrations
ChannelMiddleMean = mean(ChannelMiddleO2); %mean start channel
ChannelMiddleStd = std(ChannelMiddleO2); %standard deviation start
    channel
%window end at 31.25 mm of channel
ChannelEnd = DataSet( ismember(DataSet.MeasurementNr,112:130) , :);
ChannelEndO2 = ChannelEnd.pO2(:); %oxygen concentrations
ChannelEndMean = mean(ChannelEndO2); %mean start channel
ChannelEndStd = std(ChannelEndO2); %standard deviation start channel

%plot measurement points and mean values
figure; hold on; grid on; title('Full Cell Layer - Concentration along
    Length')
plot(ones(length(ChannelStartO2),1)*8.75, ChannelStartO2,'.','Color',[0
     0.4470 0.7410],'Markersize',15);
plot(8.75, ChannelStartMean, 'x','color',[0 0.4470 0.7410],'Markersize'
    ,15,'Linewidth',3)
plot(ones(length(ChannelMiddleO2),1)*20, ChannelMiddleO2,'.','Color'
    ,[0.8500 0.3250 0.0980],'Markersize',15);
plot(20, ChannelMiddleMean, 'x','Color',[0.8500 0.3250 0.0980],'
    Markersize',15,'Linewidth',3)
plot(ones(length(ChannelEndO2),1)*31.25, ChannelEndO2,'.','Color'
    ,[0.9290 0.6940 0.1250],'Markersize',15);
plot(31.25, ChannelEndMean, 'x','Color',[0.9290 0.6940 0.1250],'
    Markersize',15,'linewidth',3)

xlabel('Channel length [mm]')
ylabel('O2 concentration [mol/m^3]')
legend('Cells - start channel', 'Cells - start mean', 'Cells - middle
    channel',...
        'Cells - middle mean', 'Cells - end channel','Cells - end mean'
            ,...
        'Empty - start channel', 'Empty - middle channel','Empty - end
            channel',...
        'Location','eastoutside')
axis([0 40 0.05 0.12])
plot(8.75, 0.0956, 's','Color',[0 0.4470 0.7410],'Markersize',8,'
    linewidth',2)
plot(20, 0.0892, 's','Color',[0.8500 0.3250 0.0980],'Markersize',8,'
    linewidth',2)
plot(31.25, 0.0952, 's','Color',[0.9290 0.6940 0.1250],'Markersize',8,'
    linewidth',2)
    %% full cell layer - variation width
%window start at end chip - left
ChannelEndLeft = DataSet( ismember(DataSet.MeasurementNr,131:141) , :);
ChannelEndLeftO2 = ChannelEndLeft.pO2(:); %oxygen concentrations
ChannelEndLeftMean = mean(ChannelEndLeftO2); %mean left
```

```
ChannelEndleftStd = std(ChannelEndLeftO2); %standard deviation left
%window start at end chip - middle
ChannelEndMid = DataSet( ismember(DataSet.MeasurementNr,112:130) , :);
ChannelEndMidO2 = ChannelEndMid.pO2(:); %oxygen concentrations
ChannelEndMidMean = mean(ChannelEndMidO2); %mean middle
ChannelEndMidStd = std(ChannelEndMidO2); %standard deviation middle
%window middle at end chip - right
ChannelEndRight = DataSet( ismember(DataSet.MeasurementNr,142:151) , :)
    ;
ChannelEndRightO2 = ChannelEndRight.pO2(:); %oxygen concentrations
ChannelEndRightMean = mean(ChannelEndRightO2); %mean right
ChannelEndRightStd = std(ChannelEndRightO2); %standard deviation right

%plot measurement points and mean values
figure; hold on; grid on; title('Full Cell Layer - End Channel
    Concentration along Width')
plot(ones(length(ChannelEndLeftO2),1)*-1, ChannelEndLeftO2,'.','Color'
    ,[0 0.4470 0.7410],'Markersize',15);
plot(-1, ChannelEndLeftMean, 'x','color',[0 0.4470 0.7410],'Markersize'
    ,15,'Linewidth',3)
plot(ones(length(ChannelEndMidO2),1)*0, ChannelEndMidO2,'.','Color'
    ,[0.8500 0.3250 0.0980],'Markersize',15);
plot(0, ChannelEndMidMean, 'x','Color',[0.8500 0.3250 0.0980],'
    Markersize',15,'Linewidth',3)
plot(ones(length(ChannelEndRightO2),1)*1, ChannelEndRightO2,'.','Color'
    ,[0.9290 0.6940 0.1250],'Markersize',15);
plot(1, ChannelEndRightMean, 'x','Color',[0.9290 0.6940 0.1250],'
    Markersize',15,'linewidth',3)

xlabel('Channel width [mm]')
ylabel('O2 concentration [mol/m^3]')
legend('Left channel','Left channel mean','Middle channel',...
       'Middle channel mean','Right channel', 'Right channel mean',...
       'Location','southeast')
axis([-2.25 2.25 0.05 0.08])


%% full cell layer - compare flow stops
%sequence over time of two measurements with measurements in between
xline(2.2167,'--',{'stop flow'},'linewidth',2,'color',[0.8500 0.3250
    0.0980]); %start medium flow
xline(12.2,'--',{'start flow'},'linewidth',2,'color',[0.9290 0.6940
    0.1250]) %start medium flow
xline(3.5167,'--',{'start flow'},'linewidth',2,'color',[0.8500 0.3250
    0.0980]); %stop medium flow
xline(14.733,'--',{'stop flow'},'linewidth',2,'color',[0.9290 0.6940
    0.1250]); %stop medium flow
legend('Middle channel','Medium flow stop I','Medium flow Stop II','
    Location','south');

    %% half cell layer - compare flow stops
%plot: start measurement at flow stop, and end measurement at start
    flow
legend('Flow stop I','Flow stop II','Location','northeast')
axis([-0.1 2.6 0 0.10])
```

F

Appendix: Measurement Data

F.1. Abbreviations

Abbreviation	Name	Explanation
LP90	Laser Power	Laserpower set to 90%.
PP524	Palladium Porphyrin 'wavelength [nm]'	Oxygen indicator excited at 524 nm wavelength.
PMT	PhotoMultiplierTube	Laser setup module described in 5.2.

Table F.1: Abbreviations used in the laser measurement data.

F.2. Chip Elastomer Permeability Test

F.2.1. Interval 1: Elastomer Permeability

Oxygen measured on the middle of the chip channel. Laser settings: LP90, PP524. Medium with 10 mM PP.

Table F.2: First measurement of oxygen increase in Micronit chip channel.

MeasurementNr	Time [hh:mm:ss]	Lifetime [μs]	O2 [mmHg]	Notes
13	01:32:41	83.143164	28.677711	PMT150, chip fully inserted with fluid
14	01:32:59	63.315331	39.257813	
15	01:33:18	57.876399	43.427018	
16	01:33:37	56.399751	44.697733	
17	01:33:56	55.065304	45.904702	
18	01:34:15	54.722873	46.223911	
19	01:34:34	51.735169	49.188284	
20	01:34:53	50.76032	50.231027	
21	01:35:11	50.590248	50.417061	
22	01:35:30	47.79181	53.668274	
23	01:35:49	47.970579	53.449238	
24	01:36:08	47.66878	53.819969	
25	01:36:27	44.988527	57.330639	
26	01:36:46	45.078492	57.20603	
27	01:37:05	44.050464	58.660266	
28	01:37:25	42.697428	60.68099	
29	01:37:44	42.223489	61.419433	

30	01:38:03	42.029283	61.726835
31	01:38:22	40.631783	64.025544
32	01:38:42	40.634294	64.021272
33	01:39:01	40.899291	63.573371
34	01:39:20	39.344573	66.287315
35	01:39:39	38.497904	67.857467
36	01:39:58	38.289107	68.255357
37	01:40:17	38.720662	67.437704
38	01:40:36	38.155555	68.512139
39	01:40:55	37.729209	69.34405
40	01:41:14	36.31076	72.252427
41	01:41:33	36.682747	71.46795
42	01:41:53	37.137595	70.530085
43	01:42:12	35.878533	73.184375
44	01:42:31	36.90607	71.004584
45	01:42:51	35.441067	74.150766
46	01:43:10	36.48792	71.876823
47	01:43:29	35.626045	73.739243
48	01:43:49	35.687706	73.603011
49	01:44:08	34.329323	76.717513
50	01:44:27	34.927674	75.31576
51	01:44:47	34.863228	75.464425
52	01:45:06	34.87183	75.444551
53	01:45:25	33.895396	77.765027
54	01:45:45	34.184016	77.065327
55	01:46:04	32.679683	80.84795
56	01:46:24	33.490474	78.767009
57	01:46:43	33.076668	79.816319
58	01:47:03	33.457633	78.849338
59	01:47:22	33.166794	79.58555
60	01:47:41	32.95159	80.138671
61	01:48:01	31.828893	83.145542
62	01:48:20	32.792021	80.553487
63	01:48:39	33.60465	78.482034
64	01:48:59	32.773864	80.600945
65	01:49:18	32.206108	82.111879
66	01:49:38	32.883218	80.315918
67	01:49:57	31.601847	83.779603
68	01:50:17	33.012897	79.980366
69	01:50:36	34.535737	76.22846
70	01:50:55	31.944794	82.825348
71	01:51:15	31.897266	82.956369
72	01:51:34	33.909295	77.73106
73	01:51:54	31.745491	83.377402
74	01:52:13	32.494445	81.337946
75	01:52:32	32.957236	80.12407
76	01:52:52	31.151644	85.064192
77	01:53:11	31.525251	83.995567
78	01:53:31	32.709343	80.770007

79	01:53:50	31.338567	84.526354
80	01:54:09	31.867444	83.038782
81	01:54:29	31.01754	85.454049
82	01:54:48	31.171571	85.00655
83	01:55:08	33.531308	78.664867
84	01:55:27	31.46429	84.168202
85	01:55:46	30.869494	85.888369
86	01:56:05	30.387205	87.332602
87	01:56:25	31.263262	84.742259
88	01:56:44	30.415451	87.246754
89	01:57:03	31.437269	84.244936
90	01:57:23	31.990159	82.700651
91	01:57:42	32.446895	81.464629
92	01:58:01	30.720572	86.329481
93	01:58:21	29.955743	88.664042
94	01:58:40	31.933778	82.85568
95	01:59:00	30.603046	86.68063
96	01:59:19	29.838278	89.033194
97	01:59:38	29.961592	88.645737
98	01:59:58	30.065183	88.322706
99	02:00:17	30.892232	85.821391
100	02:00:36	29.985604	88.57066
101	02:00:55	29.956609	88.661329
102	02:01:15	31.262328	84.744943
103	02:01:34	30.964624	85.608811
104	02:01:53	31.945483	82.823451
105	02:02:13	31.202566	84.917034
106	02:02:32	30.284136	87.64721
107	02:02:51	31.9498	82.811569
108	02:03:10	31.640606	83.670717
109	02:03:30	30.662637	86.502245
110	02:03:49	30.856952	85.925355
111	02:04:08	31.534354	83.969848
112	02:04:28	30.349372	87.447834
113	02:04:47	30.781234	86.149283
114	02:05:07	30.195404	87.919777
115	02:05:26	30.068041	88.313825
116	02:05:45	31.631026	83.697605
117	02:06:04	30.549269	86.842206
118	02:06:24	31.011568	85.471489
119	02:06:43	30.965059	85.607537
120	02:07:03	31.147835	85.075221
121	02:07:22	30.825293	86.01885
122	02:07:41	29.297431	90.771077
123	02:08:01	29.602417	89.783267
124	02:08:20	30.456689	87.121708
125	02:08:39	29.940992	88.710238
126	02:08:58	29.809457	89.124212
127	02:09:17	31.880107	83.003769

128	02:09:37	31.357837	84.471271
129	02:09:56	29.206694	91.068945
130	02:10:16	29.369981	90.534239
131	02:10:35	30.475519	87.064722
132	02:10:55	30.916854	85.748978
133	02:11:14	31.395898	84.362677

F.2.2. Interval 2: Elastomer Permeability

Oxygen measured on the middle of the chip channel. Laser settings: LP90, PP524. Medium with 10 mM PP.

Table F.3: Second measurement of oxygen increase in Micronit chip channel.

MeasurementNr	Time [hh:mm:ss]	Lifetime [μs]	O2 [mmHg]	Notes
1	'12:38:15'	87.67451	26.93158	PMT150, fluid inserted on chip.
2	'12:38:33'	86.30986	27.43815	
3	'12:38:52'	83.68639	28.45841	
4	'12:39:10'	82.02028	29.14024	
5	'12:39:29'	78.16355	30.83007	
6	'12:39:47'	74.7709	32.46069	
7	'12:40:06'	72.40403	33.68877	
8	'12:40:25'	69.24064	35.46125	
9	'12:40:43'	66.23829	37.30008	
10	'12:41:02'	63.55882	39.08785	
11	'12:41:21'	61.36351	40.66896	
12	'12:41:40'	57.38337	43.84402	
13	'12:41:59'	55.41753	45.58048	
14	'12:42:17'	53.55377	47.34449	
15	'12:42:36'	51.67762	49.24875	
16	'12:42:55'	49.61238	51.51146	
17	'12:43:14'	48.55762	52.74131	
18	'12:43:33'	46.6887	55.05696	
19	'12:43:52'	46.613	55.15466	
20	'12:44:11'	44.7416	57.67523	
21	'12:44:30'	43.8426	58.96259	
22	'12:44:49'	43.091	60.08012	
23	'12:45:09'	42.92	60.33982	
24	'12:45:28'	41.70064	62.25355	
25	'12:45:47'	40.28224	64.62544	
26	'12:46:05'	40.31866	64.56244	
27	'12:46:24'	39.6566	65.72557	
28	'12:46:44'	39.06748	66.7937	
29	'12:47:03'	38.20043	68.42565	
30	'12:47:22'	38.07097	68.67571	
31	'12:47:41'	38.40904	68.02629	
32	'12:48:00'	36.78703	71.25088	
33	'12:48:20'	36.72168	71.38677	
34	'12:48:39'	36.21102	72.4655	
35	'12:48:58'	36.76514	71.29634	
36	'12:49:18'	36.25805	72.36489	

37	’12:49:37’	35.94922	73.03044
38	’12:49:56’	34.21443	76.99229
39	’12:50:16’	35.21958	74.64921
40	’12:50:35’	35.44607	74.13959
41	’12:50:55’	34.26809	76.86373
42	’12:51:14’	34.43628	76.46338
43	’12:51:33’	34.30128	76.7844
44	’12:51:53’	33.95919	77.60935
45	’12:52:12’	34.36571	76.63088
46	’12:52:31’	32.94982	80.14325
47	’12:52:50’	32.94525	80.15507
48	’12:53:10’	33.99714	77.51702
49	’12:53:29’	32.52515	81.25634
50	’12:53:48’	32.49388	81.33945
51	’12:54:07’	32.29682	81.86691
52	’12:54:27’	32.35205	81.71842
53	’12:54:46’	32.35663	81.70614
54	’12:55:05’	33.37479	79.05774
55	’12:55:24’	31.63622	83.68303
56	’12:55:44’	32.28653	81.89463
57	’12:56:03’	31.53831	83.95868
58	’12:56:22’	31.30573	84.62039
59	’12:56:42’	32.30263	81.85127
60	’12:57:01’	31.31335	84.59853
61	’12:57:20’	31.22266	84.85911
62	’12:57:40’	30.4984	86.99558
63	’12:57:59’	30.70437	86.37773
64	’12:58:19’	31.81292	83.18986
65	’12:58:38’	30.20541	87.88897
66	’12:58:58’	31.57905	83.84378
67	’12:59:17’	30.58157	86.74508
68	’12:59:37’	30.17684	87.97702
69	’12:59:56’	30.9521	85.64551
70	’13:00:15’	31.64021	83.67184
71	’13:00:35’	30.60227	86.68295
72	’13:00:54’	30.92166	85.73485
73	’13:01:14’	29.7613	89.27668
74	’13:01:34’	29.37086	90.53137
75	’13:01:53’	29.13541	91.30425
76	’13:02:13’	29.28513	90.81135
77	’13:02:32’	29.67318	89.55699
78	’13:02:52’	29.51128	90.0763
79	’13:03:11’	29.85924	88.96711
80	’13:03:31’	30.18681	87.94626
81	’13:03:50’	29.61373	89.74702
82	’13:04:10’	29.98409	88.57538
83	’13:04:29’	30.01809	88.46928
84	’13:04:49’	29.75919	89.28338
85	’13:05:09’	29.67675	89.54561

86	’13:05:28’	29.7147	89.42471
87	’13:05:48’	29.35159	90.59417
88	’13:06:08’	29.16038	91.22169
89	’13:06:27’	29.33383	90.65211
90	’13:06:47’	29.13632	91.30124
91	’13:07:06’	28.80046	92.42554
92	’13:07:26’	28.70263	92.75797
93	’13:07:46’	29.25591	90.90714
94	’13:08:05’	29.80637	89.13397
95	’13:08:25’	29.08265	91.47915
96	’13:08:44’	28.66712	92.87919
97	’13:09:04’	28.90148	92.0846
98	’13:09:23’	29.4914	90.14046
99	’13:09:43’	29.18388	91.14414
100	’13:10:02’	28.66364	92.89107
101	’13:10:22’	28.76198	92.556
102	’13:10:41’	30.40313	87.28419
103	’13:11:01’	30.45261	87.13407
104	’13:11:21’	30.01181	88.48885
105	’13:11:40’	28.94734	91.93063
106	’13:12:00’	28.80834	92.39885
107	’13:12:19’	29.24241	90.95148
108	’13:12:39’	28.74827	92.60259
109	’13:12:58’	27.64478	96.50286
110	’13:13:18’	28.47554	93.53843
111	’13:13:37’	28.50199	93.44689
112	’13:13:57’	28.736	92.64429
113	’13:14:16’	27.54075	96.88666
114	’13:14:36’	27.59151	96.69904
115	’13:14:55’	27.8889	95.61342
116	’13:15:14’	30.08875	88.24953
117	’13:15:34’	29.50617	90.09278
118	’13:15:53’	29.63668	89.67357
119	’13:16:13’	27.6823	96.36513
120	’13:16:32’	28.62312	93.02982
121	’13:16:52’	28.79509	92.44371
122	’13:17:12’	28.39743	93.80975
123	’13:17:31’	28.4982	93.45998
124	’13:17:50’	28.18972	94.5386
125	’13:18:10’	28.04843	95.04054
126	’13:18:29’	27.41905	97.33935
127	’13:18:48’	28.61021	93.07411
128	’13:19:08’	27.86005	95.71771
129	’13:19:27’	27.56917	96.78151
130	’13:19:47’	27.80379	95.92175
131	’13:20:06’	27.69527	96.31762
132	’13:20:26’	27.61165	96.62477
133	’13:20:45’	28.53151	93.34492
134	’13:21:05’	27.14773	98.36323

135	’13:21:24’	28.44339	93.64991
136	’13:21:44’	28.1376	94.72317
137	’13:22:03’	27.42204	97.32819
138	’13:22:22’	28.35662	93.95211
139	’13:22:41’	28.31426	94.10033
140	’13:23:01’	28.55204	93.27413
141	’13:23:21’	27.38506	97.46651
142	’13:23:40’	28.39421	93.82096
143	’13:23:59’	28.10199	94.84969
144	’13:24:19’	28.10468	94.84012

F.3. Tubular Exchanger Prototype

F.3.1. Prototype 53 cm tube at 35 μL/min

Oxygen measured on glass capillary. Laser settings: LP90, PP524. Medium with 5 mM PP.

Table F.4: Measurement data of 53 cm prototype at 35 μL/min.

MeasurementNr	Time [hh:mm:ss]	Lifetime [μs]	O2 [mmHg]	Notes
1	01:33:09	28.553139	93.270329	Measure glass capillary
2	01:34:00	30.084668	88.262193	PMT150
3	01:38:43	24.018786	111.842404	
4	01:39:32	28.681452	92.830216	
5	01:55:22	29.489699	90.145966	
6	02:00:20	29.561347	89.915103	
7	02:00:38	30.181555	87.962464	
8	02:00:57	30.227955	87.819602	
9	02:01:14	29.432893	90.329808	
10	02:01:30	30.057681	88.346025	
11	02:01:48	29.737411	89.35251	
12	02:02:59	29.128193	91.328143	Start med flow 35 uL/min, no gas flow
13	02:03:18	28.268672	94.260299	
14	02:03:37	28.68561	92.816018	
15	02:03:56	27.154688	98.33672	
16	02:04:15	28.149384	94.681389	
17	02:04:34	27.828967	95.830336	
18	02:04:53	29.182931	91.147257	
19	02:05:12	28.474333	93.542601	
20	02:05:31	28.148112	94.685896	
21	02:05:50	28.468897	93.561438	
22	02:06:09	27.930588	95.46309	
23	02:06:28	30.181887	87.961441	
24	02:06:47	32.723135	80.733814	
25	02:07:06	35.515699	73.984214	
26	02:07:25	37.061291	70.68581	
27	02:07:44	38.00035	68.812823	
28	02:08:03	38.365067	68.110104	
29	02:08:22	39.752905	65.553968	
30	02:08:41	39.731322	65.592352	
31	02:09:00	40.136858	64.878015	
32	02:09:19	36.420494	72.019345	
33	02:09:37	33.311447	79.217778	
34	02:09:56	32.765454	80.622943	
35	02:10:15	31.722211	83.442338	
36	02:10:34	30.732875	86.292877	
37	02:10:53	30.223126	87.834449	
38	02:11:12	30.094083	88.232983	
39	02:11:31	30.212497	87.867147	
40	02:11:50	30.664138	86.497761	
41	02:12:09	28.957642	91.896115	
42	02:12:28	29.723752	89.395916	
43	02:12:47	28.404992	93.783421	

44	02:13:06	29.761643	89.2756	
45	02:13:26	27.95884	95.361463	
46	02:13:45	28.453007	93.616539	
47	02:14:04	27.132774	98.420268	
48	02:14:23	27.797876	95.943231	
49	02:14:42	28.097836	94.864459	
50	02:15:01	28.444901	93.644675	
51	02:15:20	27.90235	95.56487	
52	02:15:39	27.414912	97.354824	
53	02:15:58	28.324535	94.064323	Start N2 flow 200 mL/min
54	02:16:17	28.519899	93.384989	
55	02:16:37	29.013379	91.709764	
56	02:16:56	32.903501	80.263261	
57	02:17:14	39.461864	66.075112	
58	02:17:33	50.43871	50.583878	PMT250
59	02:17:52	56.564006	44.553105	
60	02:18:10	69.703387	35.19192	
61	02:18:29	90.489547	25.934883	
62	02:18:48	100.184797	22.930822	
63	02:19:06	105.907576	21.415768	PMT200
64	02:19:25	121.729733	17.968365	
65	02:19:43	142.883149	14.55209	
66	02:20:02	160.163997	12.430951	
67	02:20:20	169.880525	11.427832	
68	02:20:38	179.531358	10.538977	
69	02:20:57	189.638696	9.705066	
70	02:21:15	197.787303	9.094816	
71	02:21:33	209.324767	8.312033	
72	02:21:52	216.875322	7.844838	
73	02:22:10	221.104892	7.597074	
74	02:22:28	232.531685	6.972774	
75	02:22:47	253.816116	5.959771	
76	02:23:05	256.478955	5.84487	
77	02:23:23	257.927527	5.78336	
78	02:23:42	263.653268	5.54685	
79	02:24:00	281.091082	4.88591	
80	02:24:18	303.068031	4.161257	
81	02:24:36	301.913727	4.196693	
82	02:24:55	306.585297	4.054925	
83	02:25:13	313.625799	3.849245	
84	02:25:31	320.647139	3.653121	
85	02:25:49	325.167076	3.531349	
86	02:26:07	327.687157	3.464914	
87	02:26:26	329.849363	3.408722	
88	02:26:44	339.791816	3.159541	
89	02:27:02	348.41185	2.955013	
90	02:27:20	344.594604	3.044323	
91	02:27:38	349.6698	2.926009	Stop N2 flow
92	02:27:56	355.471576	2.794895	

93	02:28:15	361.21779	2.669189	
94	02:28:33	369.310702	2.498779	
95	02:28:51	368.709711	2.511177	
96	02:29:09	369.042523	2.504306	
97	02:29:27	372.025988	2.443265	
98	02:29:45	378.269281	2.318645	
99	02:30:03	377.725516	2.329335	
100	02:30:21	382.529627	2.23594	
101	02:30:39	381.610967	2.253618	
102	02:30:57	385.630389	2.176896	
103	02:31:15	391.065131	2.075666	
104	02:31:33	387.474489	2.142228	
105	02:31:51	372.60575	2.431517	
106	02:32:09	125.371792	17.298017	
107	02:32:28	66.722571	36.992276	
108	02:32:46	49.265997	51.909533	
109	02:33:05	42.501797	60.983807	
110	02:33:24	39.050082	66.825728	
111	02:33:43	35.520616	73.973267	
112	02:34:02	33.917111	77.71197	
113	02:34:21	31.548637	83.929519	
114	02:34:40	32.396981	81.598011	
115	02:35:00	33.078062	79.81274	
116	02:35:19	31.609361	83.758472	
117	02:35:38	30.214321	87.861534	
118	02:35:57	29.109001	91.391723	
119	02:36:16	30.700843	86.388241	
120	02:36:36	29.768919	89.252532	
121	02:36:55	29.722879	89.398691	
122	02:37:14	28.836032	92.305205	
123	02:37:33	29.013446	91.709539	
124	02:37:52	28.292743	94.175761	
125	02:38:12	28.682066	92.828117	
126	02:38:31	27.926247	95.478722	
127	02:38:50	28.712113	92.725628	
128	02:39:09	27.587692	96.713111	
129	02:39:28	28.70862	92.737533	
130	02:39:48	28.977004	91.831297	
131	02:40:07	28.707935	92.739867	
132	02:40:26	29.012608	91.712335	
133	02:40:45	27.816873	95.874219	
134	02:41:04	27.926603	95.477439	
135	02:41:23	28.566151	93.225518	
136	02:41:42	27.83144	95.821367	Start N2 gas flow at 200 mL/min
137	02:42:01	27.771101	96.040656	
138	02:42:20	28.099189	94.859647	
139	02:42:39	28.192457	94.52893	
140	02:42:58	31.496912	84.075737	
141	02:43:18	38.941444	67.026404	

142	02:43:37	47.182179	54.4277	
143	02:43:56	58.558892	42.86136	
144	02:44:14	77.43376	31.16877	
145	02:44:33	84.652317	28.075404	
146	02:44:52	98.055668	23.539626	
147	02:45:10	112.464583	19.8694	
148	02:45:29	136.601646	15.456107	
149	02:45:47	153.097481	13.240461	
150	02:46:06	163.178968	12.106907	
151	02:46:24	167.395622	11.673287	
152	02:46:42	181.486149	10.370451	
153	02:47:01	194.152546	9.360695	
154	02:47:19	201.329862	8.844919	
155	02:47:37	213.641889	8.040866	
156	02:47:56	217.659622	7.798167	
157	02:48:14	227.134395	7.259826	
158	02:48:33	256.428346	5.847031	
159	02:48:51	248.695259	6.18765	
160	02:49:09	249.992289	6.129049	
161	02:49:28	257.323822	5.808911	
162	02:49:46	284.612852	4.762256	
163	02:50:04	303.084222	4.160762	
164	02:50:22	316.123271	3.778486	
165	02:50:41	305.093804	4.099715	
166	02:50:59	319.35099	3.688677	
167	02:51:17	328.391787	3.446521	
168	02:51:36	338.203501	3.198365	
169	02:51:54	338.588338	3.188925	
170	02:52:12	337.452074	3.216859	
171	02:52:30	341.740561	3.112401	
172	02:52:49	358.027438	2.738484	
173	02:53:07	362.458453	2.64257	
174	02:53:25	365.302023	2.582245	
175	02:53:43	366.964718	2.547404	
176	02:54:01	371.44778	2.455019	
177	02:54:19	389.834644	2.098338	
178	02:54:37	399.054182	1.931864	
179	02:54:56	392.57251	2.048085	
180	02:55:14	396.716906	1.973335	Stop N2 flow
181	02:55:32	404.595113	1.835463	
182	02:55:50	405.952355	1.812251	
183	02:56:08	413.11785	1.692233	
184	02:56:26	412.542634	1.701714	
185	02:56:44	413.427879	1.687134	
186	02:57:03	416.911101	1.630368	
187	02:57:21	146.520469	14.064054	
188	02:57:39	73.592593	33.062197	
189	02:57:58	52.243648	48.659835	
190	02:58:17	44.400982	58.15686	

191	02:58:36	38.970583	66.972469	
192	02:58:55	36.013941	72.890009	
193	02:59:14	34.857095	75.478601	
194	02:59:33	36.784369	71.2564	
195	02:59:52	35.761784	73.43997	
196	03:00:11	33.896351	77.762693	
197	03:00:30	33.976959	77.566091	
198	03:00:48	32.644043	80.941795	
199	03:01:07	32.637584	80.958824	
200	03:01:26	31.331546	84.546439	
201	03:01:46	30.658102	86.515795	
202	03:02:05	31.065892	85.313095	
203	03:02:24	31.871585	83.027327	
204	03:02:43	29.968392	88.624462	
205	03:03:02	29.367032	90.543841	
206	03:03:22	29.591061	89.819686	
207	03:03:41	29.983252	88.578007	
208	03:04:00	28.518242	93.390712	
209	03:04:19	29.206343	91.070102	
210	03:04:38	28.288749	94.189777	
211	03:04:57	28.426036	93.710211	
212	03:05:16	28.25606	94.304654	
213	03:05:35	29.126356	91.334224	
214	03:05:55	29.5159	90.061412	
215	03:06:14	29.061079	91.550851	
216	03:06:33	28.83452	92.310315	
217	03:06:52	27.902294	95.565072	
218	03:07:11	29.119026	91.358501	Start N2 gas flow at 200 mL/min
219	03:07:30	27.996074	95.227845	
220	03:07:50	29.476672	90.188064	
221	03:08:09	28.082398	94.919418	
222	03:08:28	28.117606	94.794169	
223	03:08:47	31.574023	83.857933	
224	03:09:06	36.308019	72.258268	
225	03:09:25	43.776823	59.058865	
226	03:09:44	43.446696	59.546427	
227	03:10:03	40.094835	64.951366	
228	03:10:22	39.058759	66.809747	
229	03:10:41	66.442674	37.169625	
230	03:11:00	80.041806	29.986768	
231	03:11:18	114.052633	19.521629	
232	03:11:37	131.551981	16.245438	
233	03:11:55	141.251977	14.779115	
234	03:12:14	156.961596	12.788773	
235	03:12:32	165.985216	11.815874	
236	03:12:51	182.217733	10.30831	
237	03:13:09	191.957932	9.526104	
238	03:13:27	207.918599	8.402789	
239	03:13:46	215.611073	7.920783	

240	03:14:04	225.221207	7.36488	
241	03:14:22	239.80394	6.606437	
242	03:14:41	243.872012	6.411039	
243	03:14:59	255.070825	5.905331	
244	03:15:18	273.881464	5.148969	
245	03:15:36	290.031086	4.577878	
246	03:15:54	306.593093	4.054692	
247	03:16:12	312.410856	3.884077	
248	03:16:31	314.26428	3.831049	
249	03:16:49	328.714988	3.43811	
250	03:17:07	336.09991	3.250348	
251	03:17:25	344.044181	3.057364	
252	03:17:44	358.798476	2.721624	
253	03:18:02	357.324794	2.753912	
254	03:18:20	364.711857	2.594688	
255	03:18:38	356.764032	2.766268	
256	03:18:56	370.546274	2.473417	
257	03:19:14	383.762844	2.212343	
258	03:19:32	392.837659	2.043256	
259	03:19:50	403.519044	1.853977	
260	03:20:09	409.278883	1.756011	
261	03:20:27	414.794001	1.664757	
262	03:20:45	419.45696	1.589475	
263	03:21:03	423.754593	1.521558	
264	03:21:21	426.430589	1.47996	
265	03:21:40	436.819623	1.323294	
266	03:21:58	441.069006	1.26134	
267	03:22:16	443.124037	1.231805	
268	03:22:34	440.951057	1.263044	
269	03:22:52	448.566832	1.154889	
270	03:23:11	446.371729	1.185684	
271	03:23:29	449.697183	1.139148	
272	03:23:47	454.347627	1.075214	
273	03:24:05	463.051258	0.959006	
274	03:24:24	466.279756	0.917004	
275	03:24:42	466.314333	0.916557	
276	03:25:00	465.846627	0.922605	
277	03:25:18	473.435114	0.825955	
278	03:25:37	472.062925	0.843202	
279	03:25:55	479.188898	0.754713	
280	03:26:13	478.449903	0.763767	
281	03:26:31	476.349345	0.789657	
282	03:26:49	477.101831	0.780356	
283	03:27:08	476.153471	0.792083	
284	03:27:26	477.096022	0.780428	Stop N2 flow
285	03:27:44	330.877208	3.382268	
286	03:28:02	110.836405	20.236305	
287	03:28:21	67.280076	36.643426	
288	03:28:39	51.656082	49.271413	

289	03:28:58	43.122137	60.033044	
290	03:29:17	41.058884	63.306413	
291	03:29:36	38.030228	68.75475	
292	03:29:56	35.907803	73.120558	
293	03:30:14	35.398457	74.246171	
294	03:30:33	34.322941	76.732726	
295	03:30:52	34.64193	75.979129	
296	03:31:11	33.704603	78.234147	
297	03:31:30	33.619557	78.444971	
298	03:31:50	33.003171	80.005442	
299	03:32:09	33.112929	79.72332	
300	03:32:28	36.050752	72.810366	
301	03:32:47	36.027661	72.860306	
302	03:33:06	36.673272	71.487733	
303	03:33:25	37.412228	69.974851	
304	03:33:44	35.890531	73.158204	
305	03:34:03	35.423212	74.190716	
306	03:34:22	36.010245	72.898013	
307	03:34:41	35.31202	74.440413	
308	03:35:01	34.345213	76.679655	
309	03:35:20	35.636564	73.71597	
310	03:35:38	34.957273	75.247664	
311	03:35:57	35.462217	74.103497	
312	03:36:16	34.368394	76.624492	
313	03:36:35	33.418633	78.947316	
314	03:36:54	33.917568	77.710853	
315	03:37:13	33.586655	78.52682	
316	03:37:32	34.014458	77.474948	
317	03:37:51	34.214955	76.991023	
318	03:38:10	33.287127	79.279387	
319	03:38:29	33.535494	78.654412	
320	03:38:49	32.240695	82.018313	
321	03:39:08	32.953191	80.134532	
322	03:39:27	32.845414	80.414238	
323	03:39:46	33.126037	79.689753	
324	03:40:05	32.486133	81.360064	
325	03:40:25	31.725745	83.432472	
326	03:40:44	31.238625	84.813118	Start air flow at 200 mL/min
327	03:41:03	31.416161	84.304969	
328	03:41:22	31.458729	84.183984	
329	03:41:41	32.088471	82.431626	
330	03:42:01	31.883423	82.994606	
331	03:42:20	32.281864	81.907203	
332	03:42:39	31.08782	85.249318	
333	03:42:58	30.48611	87.032702	
334	03:43:17	31.206338	84.906154	
335	03:43:37	31.234075	84.826219	
336	03:43:56	30.905666	85.781866	
337	03:44:15	30.620671	86.627797	

338	03:44:34	31.073799	85.290088
339	03:44:54	31.325111	84.564857
340	03:45:13	30.661322	86.506175
341	03:45:32	30.61933	86.631814
342	03:45:51	30.855848	85.928612
343	03:46:11	30.223132	87.834432
344	03:46:30	29.531131	90.012327
345	03:46:49	31.074374	85.288416
346	03:47:08	30.026941	88.441696
347	03:47:28	29.426562	90.35034
348	03:47:47	30.448566	87.146313
349	03:48:06	29.880659	88.899668
350	03:48:25	30.583694	86.738708
351	03:48:44	29.808916	89.12592
352	03:49:03	30.175889	87.97994
353	03:49:22	30.367587	87.392317
354	03:49:42	30.447735	87.14883
355	03:50:01	30.107961	88.189957
356	03:50:20	30.25113	87.74841
357	03:50:39	29.833504	89.048257

F.3.2. Prototype 53 cm tube at 45 μL/min

Oxygen measured on glass capillary. Laser settings: LP90, PP524. Medium with 5 mM PP.

Table F.5: Measurement data of 53 cm prototype at 45 μL/min.

MeasurementNr	Time [hh:mm:ss]	Lifetime [μs]	O2 [mmHg]	Notes
1	02:45:56	27.515911	96.978728	Measure glass capillary, PMT150
2	02:46:20	28.687412	92.809869	
3	02:46:37	28.736369	92.64305	
4	02:46:53	29.219212	91.027741	
5	02:47:12	28.724736	92.682637	
6	02:47:29	28.376855	93.881477	
7	02:47:45	28.475792	93.537545	
8	02:48:04	28.512487	93.410592	
9	02:48:21	28.05044	95.033379	
10	02:48:37	28.292768	94.175674	
11	02:48:56	28.027911	95.113873	
12	02:49:13	28.254544	94.309988	Start N2 flow at 200 mL/min
13	02:49:29	28.203988	94.488194	
14	02:49:48	30.344421	87.462937	
15	02:50:04	34.000288	77.509364	
16	02:50:21	40.578327	64.116617	
17	02:50:39	49.84458	51.247697	
18	02:50:55	59.582637	42.037166	
19	02:51:11	74.957841	32.366996	
20	02:51:29	96.400594	24.031456	
21	02:51:45	115.274553	19.260561	
22	02:52:00	138.161368	15.223965	
23	02:52:18	168.730431	11.540538	

24	02:52:34	196.643649	9.177413	
25	02:52:49	224.196556	7.421882	
26	02:53:07	254.836502	5.915457	
27	02:53:22	275.011741	5.106816	
28	02:53:37	297.325681	4.340262	
29	02:53:56	316.490099	3.768187	
30	02:54:11	327.197141	3.477752	
31	02:54:26	348.888144	2.944007	
32	02:54:44	362.843067	2.634356	
33	02:54:59	376.878007	2.346058	
34	02:55:14	384.135292	2.205246	
35	02:55:32	380.738191	2.270491	
36	02:55:47	388.669226	2.119944	
37	02:56:02	391.993982	2.058645	
38	02:56:20	395.952707	1.987001	
39	02:56:36	396.87433	1.970527	
40	02:56:51	394.728039	2.009011	
41	02:57:09	402.18564	1.877057	
42	02:57:24	395.084687	2.002587	Start air flow at 200 mL/min
43	02:57:39	401.810839	1.883571	
44	02:57:57	406.406199	1.804524	
45	02:58:12	417.700406	1.617636	
46	02:58:27	331.957201	3.354648	
47	02:58:45	154.894909	13.027551	
48	02:59:01	92.18602	25.363623	
49	02:59:16	64.481725	38.455304	
50	02:59:34	48.959014	52.26704	Stop air flow
51	02:59:50	41.742846	62.185447	
52	03:00:06	38.199695	68.427072	
53	03:00:25	34.709198	75.82198	
54	03:00:41	33.379552	79.045728	
55	03:00:57	31.473391	84.142386	
56	03:01:16	30.825039	86.019599	
57	03:01:33	30.926144	85.721684	
58	03:01:49	31.289853	84.665901	
59	03:02:08	29.717977	89.414282	
60	03:02:24	30.16342	88.01842	
61	03:02:40	29.560815	89.916811	
62	03:02:59	29.853389	88.985542	
63	03:03:15	30.286989	87.638474	
64	03:03:31	30.224854	87.829136	
65	03:03:50	30.203392	87.895176	
66	03:04:06	29.492104	90.138198	
67	03:04:22	31.454868	84.194942	
68	03:04:41	30.889253	85.83016	Start air flow at 200 mL/min again.
69	03:04:57	31.04126	85.384847	
70	03:05:13	31.978891	82.731589	
71	03:05:32	31.185366	84.966686	
72	03:05:48	31.74468	83.379661	

73	03:06:04	31.123788	85.144898
74	03:06:23	30.751451	86.237666
75	03:06:38	30.46259	87.103842
76	03:06:54	29.945202	88.697049
77	03:07:14	30.031598	88.42719
78	03:07:29	29.853896	88.983942
79	03:07:45	31.145373	85.08235
80	03:08:04	30.005736	88.507808
81	03:08:19	29.372201	90.527009
82	03:08:35	29.4564	90.253645
83	03:08:54	29.114827	91.372413
84	03:09:10	29.112561	91.379922
85	03:09:26	29.506524	90.091651
86	03:09:45	29.619588	89.728259
87	03:10:01	29.591528	89.818187

F.3.3. Prototype 33 cm tube at 35 μL/min

First 25 measurements there was remaining nitrogen in gas tube and a closed PMT, therefore these measurements are deleted. Oxygen measured on glass capillary. Laser settings: LP90, PP524. Medium with 5 mM PP.

Table F.6: Measurement data of 33 cm prototype at 35 μL/min.

MeasurementNr	Time [hh:mm:ss]	Lifetime [μs]	O2 [mmHg]	Notes
26	01:51:19	31.242603	84.801671	PMT226
27	01:51:38	31.126148	85.138053	
28	01:51:58	30.785573	86.13642	PMT200
29	01:52:18	31.044825	85.374454	
30	01:52:37	31.284012	84.682662	Start N2 flow at 200 mL/min
31	01:52:56	30.545187	86.854494	
32	01:53:16	30.980384	85.562662	
33	01:53:35	30.566527	86.790291	
34	01:53:55	30.898177	85.803897	
35	01:54:15	32.690649	80.819116	
36	01:54:35	36.607231	71.625915	
37	01:54:54	41.945443	61.860423	
38	01:55:13	49.740694	51.365397	
39	01:55:32	59.3822	42.196296	
40	01:55:51	74.451708	32.621751	
41	01:56:10	89.145261	26.40299	
42	01:56:29	107.525747	21.016619	
43	01:56:47	129.947534	16.509078	
44	01:57:06	158.346319	12.632274	
45	01:57:24	189.993199	9.677428	PMT225
46	01:57:43	215.594598	7.921779	
47	01:58:01	238.303863	6.680172	
48	01:58:19	269.419801	5.318814	
49	01:58:37	295.270119	4.406033	
50	01:58:56	318.685452	3.707046	
51	01:59:14	337.382068	3.218587	

52	01:59:32	350.852813	2.898922	
53	01:59:51	365.950029	2.568628	
54	02:00:09	382.496687	2.236573	
55	02:00:27	393.842207	2.025017	
56	02:00:45	403.621739	1.852206	
57	02:01:03	411.763126	1.714604	
58	02:01:21	420.6987	1.569709	
59	02:01:40	431.955395	1.395708	
60	02:01:58	438.768145	1.294737	
61	02:02:16	441.174393	1.259819	
62	02:02:34	442.340681	1.243031	
63	02:02:52	448.292793	1.158717	
64	02:03:11	451.056353	1.120326	
65	02:03:29	455.870102	1.054566	Stop N2 flow
66	02:03:47	458.025725	1.025566	Start air flow at 200 mL/min
67	02:04:06	459.811105	1.001754	
68	02:04:24	461.811612	0.97529	
69	02:04:42	455.293478	1.06237	
70	02:05:00	300.011575	4.255682	
71	02:05:19	149.555174	13.675038	
72	02:05:37	86.042404	27.539311	
73	02:05:56	62.905149	39.547101	Stop air flow
74	02:06:15	50.841815	50.142325	
75	02:06:35	43.609386	59.305229	
76	02:06:54	39.580291	65.862129	
77	02:07:14	36.620635	71.597828	
78	02:07:33	34.333216	76.708234	
79	02:07:53	33.692226	78.264762	
80	02:08:12	33.481471	78.789563	
81	02:08:32	32.182189	82.176704	
82	02:08:51	33.074661	79.821471	
83	02:09:11	32.513224	81.288018	
84	02:09:31	32.09964	82.401166	
85	02:09:51	32.662704	80.892632	
86	02:10:11	31.678559	83.564355	
87	02:10:30	32.565169	81.150209	
88	02:10:50	32.309834	81.831876	
89	02:11:10	32.290059	81.885117	
90	02:11:30	33.53062	78.666586	Start N2 flow at 200 mL/min
91	02:11:50	31.949709	82.81182	
92	02:12:09	31.972739	82.748491	
93	02:12:29	32.79279	80.551477	
94	02:12:49	34.133395	77.187191	
95	02:13:09	35.687329	73.603843	
96	02:13:29	40.206465	64.756855	
97	02:13:48	48.962633	52.262799	
98	02:14:07	59.845087	41.830414	
99	02:14:26	72.01597	33.897829	
100	02:14:45	86.927825	27.206783	

101	02:15:04	107.980688	20.906555	
102	02:15:22	128.083274	16.823705	
103	02:15:41	154.465502	13.077965	
104	02:15:59	178.914859	10.59289	
105	02:16:17	204.064002	8.657982	
106	02:16:36	239.359084	6.628207	
107	02:16:54	265.092139	5.489021	
108	02:17:12	289.708109	4.588675	
109	02:17:31	308.323302	4.003278	
110	02:17:49	332.583657	3.338709	
111	02:18:07	355.640721	2.791137	
112	02:18:26	376.678892	2.349998	
113	02:18:44	388.951078	2.114707	
114	02:19:02	397.00237	1.968244	
115	02:19:20	407.869676	1.779724	
116	02:19:38	417.275806	1.624479	
117	02:19:57	426.298386	1.482003	
118	02:20:15	431.931072	1.396074	
119	02:20:33	435.292392	1.345856	
120	02:20:52	440.429032	1.270594	
121	02:21:10	444.017696	1.219047	
122	02:21:28	451.565817	1.1133	
123	02:21:47	452.186475	1.104762	
124	02:22:05	457.369959	1.03436	
125	02:22:23	460.958348	0.986549	Stop N2 flow
126	02:22:42	463.57089	0.952207	Start air flow at 200 mL/min
127	02:23:00	467.866598	0.896572	
128	02:23:18	468.934131	0.882904	
129	02:23:37	467.061887	0.906916	
130	02:23:55	322.406681	3.605311	
131	02:24:13	169.064304	11.507661	
132	02:24:32	103.371175	22.066559	
133	02:24:50	69.742913	35.16908	Stop air flow
134	02:25:09	53.21483	47.678574	
135	02:25:28	45.407384	56.754685	
136	02:25:47	40.581678	64.110901	
137	02:26:07	37.613373	69.573334	
138	02:26:27	35.715338	73.542115	
139	02:26:46	34.981317	75.192435	
140	02:27:06	34.928415	75.314055	
141	02:27:26	34.472817	76.376914	
142	02:27:45	34.880469	75.424599	
143	02:28:04	34.029917	77.437432	
144	02:28:24	33.285443	79.283655	
145	02:28:43	34.621084	76.027954	
146	02:29:03	34.194558	77.039994	Stop medium flow at measure noise capillary
147	02:31:04	228.937044	7.162447	Signal 0.35 V
148	02:31:43	228.181405	7.203079	Signal 0.35 V
149	02:32:04	218.260052	7.762665	Signal 0.35 V

F.3.4. Prototype 18 cm tube at 35 μL/min

Interval with pure nitrogen gas flow. After 112 measurements start tuning air/nitrogen ratio. Oxygen measurement on glass capillary. Laser settings: LP90, PP524, 5 mM PP.

Table F.7: Measurement data of 18 cm prototype at 35 μL/min.

MeasurementNr	Time [hh:mm:ss]	Lifetime [μs]	O2 [mmHg]	Notes
1	03:10:18	32.474228	81.391763	PMT 224
2	03:11:09	32.693284	80.812192	
3	03:11:28	32.705048	80.781285	
4	03:11:47	31.492328	84.088718	
5	03:12:07	31.623782	83.717947	
6	03:12:26	31.274194	84.710851	
7	03:12:45	32.198836	82.131578	
8	03:13:04	31.697462	83.511476	
9	03:13:23	32.218922	82.07719	
10	03:13:43	32.286698	81.894174	
11	03:14:02	32.034823	82.578225	Start N2 flow at 200 mL/min
12	03:14:21	31.595312	83.797987	
13	03:14:40	31.610026	83.756601	
14	03:15:00	32.040079	82.56384	
15	03:15:19	33.672041	78.314742	
16	03:15:38	36.578031	71.687169	
17	03:15:57	42.601796	60.828671	
18	03:16:16	50.970253	50.003103	
19	03:16:35	64.772862	38.259501	
20	03:16:54	79.925109	30.038008	
21	03:17:13	98.994199	23.268034	
22	03:17:32	124.408696	17.471465	
23	03:17:50	151.262424	13.463049	
24	03:18:08	148.173288	13.850205	
25	03:18:27	150.103594	13.606415	
26	03:18:45	150.544597	13.551596	
27	03:19:04	151.742547	13.404291	
28	03:19:22	272.680825	5.194128	
29	03:19:40	344.207758	3.053484	
30	03:19:59	364.303115	2.603329	
31	03:20:17	381.835615	2.249287	PMT 250
32	03:20:35	398.728735	1.937609	
33	03:20:53	430.81125	1.412978	
34	03:21:11	444.403267	1.213558	
35	03:21:30	430.53172	1.417212	
36	03:21:48	440.273032	1.272854	
37	03:22:06	447.162324	1.174558	
38	03:22:24	444.694072	1.209425	
39	03:22:43	445.205728	1.202165	
40	03:23:01	444.793898	1.208007	Stop N2 flow
41	03:23:19	441.767457	1.251271	Start air flow at 200 mL/min
42	03:23:38	399.973555	1.915684	
43	03:23:56	242.560324	6.473326	

44	03:24:14	150.10507	13.606231	
45	03:24:32	99.533849	23.11419	
46	03:24:51	70.094841	34.966864	
47	03:25:10	56.448391	44.654817	Stop air flow
48	03:25:29	48.225211	53.140057	
49	03:25:49	43.558191	59.380934	
50	03:26:08	41.525339	62.537922	
51	03:26:27	39.180481	66.586323	
52	03:26:47	39.085364	66.760795	
53	03:27:06	38.295012	68.244045	
54	03:27:26	38.351895	68.135251	
55	03:27:45	37.811988	69.18106	
56	03:28:04	38.487548	67.877099	
57	03:28:24	38.545674	67.767041	
58	03:28:43	38.986385	66.943253	
59	03:29:02	38.889907	67.121997	
60	03:29:22	38.899468	67.104243	
61	03:29:41	39.623125	65.785409	Start air flow at 200 mL/min
62	03:30:01	39.536353	65.941	
63	03:30:20	38.799363	67.290555	
64	03:30:39	38.379401	68.082758	
65	03:30:59	38.018133	68.778247	
66	03:31:18	37.38514	70.029253	
67	03:31:38	36.790505	71.243665	
68	03:31:57	35.533459	73.944684	
69	03:32:16	34.971178	75.215714	
70	03:32:36	35.336263	74.385838	
71	03:32:55	35.143215	74.822509	
72	03:33:14	35.574161	73.854238	
73	03:33:34	34.901495	75.376085	
74	03:33:53	35.118089	74.879695	
75	03:34:12	34.708042	75.824675	
76	03:35:49	35.473592	74.078098	Start N2 flow at 200 mL/min
77	03:36:08	34.829729	75.541918	
78	03:36:27	35.007082	75.133332	
79	03:36:46	34.763212	75.696236	
80	03:37:06	36.644156	71.548594	
81	03:37:25	42.462407	61.045116	
82	03:37:44	49.906078	51.178251	
83	03:38:03	61.486823	40.57715	
84	03:38:22	75.019	32.336446	
85	03:38:41	92.98378	25.102197	
86	03:39:00	116.95121	18.911215	
87	03:39:18	143.985398	14.401592	
88	03:39:37	174.390371	11.000224	
89	03:39:55	203.971643	8.664215	
90	03:40:13	231.334975	7.035264	
91	03:40:32	261.74377	5.624574	
92	03:40:50	290.542796	4.56082	

93	03:41:08	313.419209	3.855149	
94	03:41:26	339.4223	3.168541	
95	03:41:45	353.431864	2.8405	
96	03:42:03	368.985165	2.505489	
97	03:42:21	386.905033	2.152898	
98	03:42:39	394.187667	2.018767	
99	03:42:58	407.87368	1.779656	
100	03:43:16	414.515629	1.669305	
101	03:43:34	424.496737	1.509969	
102	03:43:53	427.335173	1.466016	
103	03:44:11	425.155652	1.499713	
104	03:44:29	419.697953	1.585629	
105	03:44:47	423.082264	1.532092	
106	03:45:06	423.956191	1.518406	
107	03:45:24	427.559126	1.462573	
108	03:45:42	428.032012	1.455315	
109	03:46:00	433.918897	1.366282	
110	03:46:19	438.792385	1.294383	
111	03:46:37	442.148764	1.245788	End of pure nitrogen gas flow
112	03:46:55	443.484641	1.226651	Set 160 mL/min N2, 40 mL/min air
113	03:47:14	450.77199	1.124255	
114	03:47:32	453.19901	1.090883	
115	03:47:50	376.501518	2.353511	
116	03:48:08	270.988402	5.258464	
117	03:48:27	212.123682	8.134969	
118	03:48:45	175.583584	10.890762	
119	03:49:03	152.255515	13.341924	
120	03:49:22	139.136775	15.081434	
121	03:49:40	131.302533	16.286004	
122	03:49:59	123.626216	17.614375	
123	03:50:17	121.226152	18.064223	
124	03:50:36	118.69302	18.558746	
125	03:50:54	116.281541	19.049538	
126	03:51:13	115.694641	19.172081	
127	03:51:31	115.884625	19.132277	
128	03:51:50	114.31179	19.465793	
129	03:52:08	114.808708	19.359435	
130	03:52:27	113.439573	19.654731	Set 150 mL/min N2, 50 mL/min air
131	03:52:45	113.142037	19.719849	PMT 225
132	03:53:04	113.979065	19.537526	
133	03:53:22	112.763934	19.803095	
134	03:53:41	111.583967	20.066514	
135	03:53:59	110.33726	20.350954	
136	03:54:18	107.428597	21.040243	
137	03:54:36	105.695362	21.46902	
138	03:54:55	103.52568	22.026003	
139	03:55:13	101.475958	22.574071	
140	03:55:32	99.401098	23.15188	

141	03:55:50	98.744618	23.339754	
142	03:56:09	98.523233	23.403675	
143	03:56:27	96.14428	24.109138	
144	03:56:46	96.356901	24.044669	
145	03:57:04	96.497916	24.002068	
146	03:57:22	95.334029	24.35745	
147	03:57:41	95.005864	24.459225	
148	03:58:00	95.245641	24.384793	Set 140 mL/min N2, 60 mL/min air
149	03:58:18	95.199751	24.399009	
150	03:58:37	95.777099	24.221144	
151	03:58:55	95.236608	24.38759	
152	03:59:14	94.707379	24.552409	
153	03:59:32	92.046045	25.409961	
154	03:59:51	89.478821	26.285526	
155	04:00:09	87.382559	27.038622	
156	04:00:28	86.667432	27.30387	
157	04:00:47	85.279449	27.831384	
158	04:01:05	85.807052	27.628854	
159	04:01:24	83.90435	28.371212	
160	04:01:42	83.134497	28.681234	
161	04:02:01	83.515263	28.527184	
162	04:02:20	83.94896	28.353422	
163	04:02:38	83.530996	28.520849	
164	04:02:57	84.293834	28.216523	
165	04:03:15	83.506881	28.53056	
166	04:03:34	83.402736	28.572563	Set 130 mL/min N2, 70 mL/min air
167	04:03:53	83.648814	28.473484	
168	04:04:11	83.657085	28.470164	
169	04:04:30	82.827642	28.806411	
170	04:04:49	82.924954	28.766613	
171	04:05:07	81.773129	29.243748	
172	04:05:26	79.377609	30.28042	
173	04:05:45	78.148817	30.836846	
174	04:06:04	77.551981	31.11347	
175	04:06:23	76.29304	31.711162	
176	04:06:42	75.608077	32.044714	
177	04:07:01	75.804323	31.948533	
178	04:07:20	75.586545	32.055298	
179	04:07:39	74.79397	32.449101	
180	04:07:58	75.119664	32.286269	
181	04:08:17	74.619178	32.537075	
182	04:08:36	74.209163	32.745065	
183	04:08:55	73.821132	32.94403	
184	04:09:14	74.233248	32.732784	Set 120 mL/min N2, 80 mL/min air
185	04:09:33	74.08363	32.809205	
186	04:09:52	74.228294	32.735309	
187	04:10:11	74.5818	32.555941	
188	04:10:30	73.121599	33.308056	
189	04:10:49	73.300457	33.21432	

190	04:11:08	71.579961	34.135417	
191	04:11:27	70.51073	34.730496	
192	04:11:46	68.445061	35.932798	
193	04:12:05	68.680975	35.791829	
194	04:12:24	68.319096	36.008467	
195	04:12:43	67.597648	36.447282	
196	04:13:01	67.56552	36.467041	
197	04:13:20	68.214184	36.071702	
198	04:13:39	68.482931	35.910104	
199	04:13:58	69.18807	35.49207	
200	04:14:16	70.311003	34.843661	
201	04:14:35	70.9389	34.490046	
202	04:14:53	71.123151	34.387465	Set 110 mL/min N2, 90 mL/min air
203	04:15:12	71.448118	34.207831	
204	04:15:31	71.339395	34.267749	
205	04:15:50	71.164939	34.364274	
206	04:16:08	70.402983	34.791466	
207	04:16:27	68.809334	35.715534	
208	04:17:47	67.503543	36.505212	
209	04:18:05	65.470761	37.797224	
210	04:18:25	64.028653	38.763556	
211	04:18:43	62.873465	39.569604	
212	04:19:03	62.817792	39.609199	
213	04:19:22	62.21281	40.04404	
214	04:19:41	62.514447	39.826181	
215	04:20:00	63.267385	39.291433	Set 100 mL/min N2, 100 mL/min air
216	04:20:19	63.359248	39.227061	
217	04:20:38	63.264742	39.293289	
218	04:20:57	62.595436	39.768044	
219	04:21:16	63.210181	39.331613	
220	04:21:34	62.738157	39.665959	
221	04:21:53	62.331331	39.958186	
222	04:22:13	61.592929	40.49845	
223	04:22:32	59.07817	42.439731	
224	04:22:51	58.551427	42.867476	
225	04:23:10	59.052628	42.460297	
226	04:23:29	59.095085	42.426122	
227	04:23:48	59.611453	42.014376	
228	04:24:07	59.884496	41.799526	
229	04:24:27	59.581039	42.03843	
230	04:24:46	60.68053	41.184182	Set 90 mL/min N2, 110 mL/min air
231	04:25:05	60.582177	41.259334	
232	04:25:24	60.283606	41.488978	
233	04:25:43	59.853485	41.823829	
234	04:26:02	57.891992	43.413945	
235	04:26:21	57.929468	43.382555	
236	04:26:40	57.384185	43.843321	
237	04:27:00	56.298209	44.787563	
238	04:27:19	57.104434	44.083127	

239	04:27:38	57.88396	43.420678	
240	04:27:57	57.055218	44.125558	
241	04:28:17	56.109656	44.955231	
242	04:28:36	56.309171	44.77785	Stop medium flow for capillary noise
243	04:33:31	357.146535	2.757835	Capillary with water, signal 0.35 V
244	04:33:54	350.537868	2.906115	Capillary with water, signal 0.35 V
245	04:34:13	348.332418	2.956851	Capillary with water, signal 0.35 V

F.3.5. Prototype 53 cm tube with chip at 35 μL/min

Oxygen measured on chip with laser settings: LP90, PP524. Medium with 5 mM PP.

Table F.8: Measurement data of 18 cm prototype integrated with the Micronit resealable chip at 35 μL/min.

MeasurementNr	Time [hh:mm:ss]	Lifetime [μs]	O2 [mmHg]	Notes
1	04:25:05	24.219664	110.872423	PMT150
2	04:25:55	24.407157	109.981481	
3	04:26:15	25.257625	106.106241	
4	04:26:35	23.717841	113.326324	
5	04:26:55	23.933057	112.261322	
6	04:27:14	23.674491	113.543188	
7	04:27:34	24.27992	110.584593	
8	04:27:53	23.355215	115.16519	
9	04:28:13	23.084193	116.577257	
10	04:28:33	24.129796	111.304372	
11	04:28:52	23.623126	113.801173	
12	04:29:12	23.313696	115.379381	Start N2 flow at 200 mL/min
13	04:29:31	23.63988	113.716904	
14	04:29:51	23.564834	114.095319	
15	04:30:11	23.251967	115.69925	
16	04:30:31	23.991883	111.973545	
17	04:30:50	25.144129	106.608239	
18	04:31:11	24.265359	110.654018	
19	04:31:30	23.59503	113.942764	
20	04:31:50	24.041695	111.730965	
21	04:32:10	22.803065	118.077449	
22	04:32:30	23.587868	113.978914	
23	04:32:50	22.605781	119.152502	
24	04:33:10	24.009101	111.889582	
25	04:33:29	24.086393	111.514143	
26	04:33:49	24.518859	109.457165	
27	04:34:08	23.746032	113.185721	
28	04:34:28	25.296573	105.935011	
29	04:34:48	24.350703	110.248298	
30	04:35:08	26.444817	101.113517	
31	04:35:27	26.448179	101.100015	
32	04:35:47	26.573703	100.598332	
33	04:36:06	27.65986	96.447446	
34	04:36:25	28.820781	92.356754	
35	04:36:45	29.208579	91.062737	
36	04:37:04	30.663933	86.498372	

37	04:37:24	30.720377	86.330063	
38	04:37:43	30.60237	86.682656	
39	04:38:02	30.891901	85.822366	
40	04:38:22	31.120027	85.155806	
41	04:38:41	31.721089	83.44547	
42	04:39:00	32.1418	82.286384	
43	04:39:20	33.141478	79.650246	
44	04:39:39	32.731032	80.713101	
45	04:39:58	32.939793	80.169202	
46	04:40:18	33.345356	79.132027	
47	04:40:37	34.713278	75.812468	
48	04:40:56	34.626905	76.014313	
49	04:41:15	33.069288	79.835271	
50	04:41:34	35.857881	73.229468	
51	04:41:53	34.425086	76.489893	
52	04:42:12	34.802828	75.604256	
53	04:42:31	34.713963	75.810871	
54	04:42:50	35.298315	74.471299	
55	04:43:09	36.305349	72.263957	
56	04:43:29	36.791193	71.242236	
57	04:43:48	36.295195	72.285603	
58	04:44:07	36.528484	71.791334	
59	04:44:26	36.963928	70.885449	
60	04:44:45	37.635223	69.529976	
61	04:45:04	37.954375	68.902365	
62	04:45:23	36.500158	71.85101	
63	04:45:42	36.372792	72.120495	
64	04:46:02	37.08551	70.636313	
65	04:46:21	37.300627	70.199491	
66	04:46:40	37.175153	70.453668	
67	04:46:59	37.470435	69.858217	
68	04:47:18	37.817037	69.171142	
69	04:47:38	37.424795	69.949639	
70	04:47:57	37.36143	70.076936	
71	04:48:16	37.515977	69.767215	
72	04:48:35	39.109275	66.716854	Stop N2 flow.
73	04:48:55	38.894249	67.113932	Start air flow at 200 mL/min
74	04:49:14	39.163688	66.617064	
75	04:49:33	38.717382	67.443851	
76	04:49:52	38.488125	67.876007	
77	04:50:11	39.586784	65.850489	
78	04:50:30	37.975289	68.861606	
79	04:50:50	39.608462	65.811653	
80	04:51:09	39.765594	65.53142	Stop air flow
81	04:51:28	38.481409	67.888742	
82	04:51:47	39.75731	65.546138	
83	04:52:06	39.540708	65.933175	
84	04:52:25	40.287014	64.617169	
85	04:52:45	39.472216	66.056444	

86	04:53:04	39.424756	66.142111	
87	04:53:23	38.400316	68.042895	
88	04:53:42	35.743848	73.479384	
89	04:54:01	34.078392	77.320015	
90	04:54:20	33.067977	79.838639	
91	04:54:39	31.020129	85.44649	
92	04:54:59	30.685116	86.435135	
93	04:55:18	30.152147	88.053236	
94	04:55:37	28.974835	91.838554	
95	04:55:57	27.935413	95.445717	
96	04:56:16	27.286788	97.835928	
97	04:56:36	26.847756	99.519324	
98	04:56:55	26.301836	101.690949	
99	04:57:15	26.399365	101.296398	
100	04:57:34	25.048378	107.035291	
101	04:57:54	25.89231	103.380122	
102	04:58:14	25.081589	106.8868	
103	04:58:33	25.199409	106.36317	
104	04:58:53	24.817909	108.076689	
105	04:59:13	25.528355	104.926817	
106	04:59:33	24.340169	110.298221	
107	04:59:53	25.190018	106.404725	
108	05:00:12	24.322855	110.380371	
109	05:00:33	24.629453	108.942735	
110	05:00:52	24.417802	109.931306	Start N2 flow at 400 mL/min
111	05:01:12	23.771369	113.059637	
112	05:01:32	24.29873	110.495037	
113	05:01:52	24.477489	109.650791	
114	05:02:12	24.932963	107.554398	
115	05:02:31	24.181443	111.055742	
116	05:02:51	24.308509	110.44853	
117	05:03:11	24.3262	110.364493	
118	05:03:30	24.58338	109.15648	
119	05:03:50	24.669827	108.756083	
120	05:04:10	24.570126	109.218117	
121	05:04:30	24.549103	109.316022	
122	05:04:49	24.360085	110.203873	
123	05:05:09	24.941009	107.518055	
124	05:05:29	25.77186	103.88716	
125	05:05:48	26.604491	100.476004	
126	05:06:08	26.621327	100.409231	
127	05:06:27	27.42028	97.334764	
128	05:06:47	28.415601	93.746499	
129	05:07:06	26.943837	99.146228	
130	05:07:26	30.226018	87.825556	
131	05:07:45	29.755078	89.296424	
132	05:08:04	31.213026	84.886865	
133	05:08:24	31.354001	84.482233	
134	05:08:43	31.843765	83.104326	

135	05:09:02	32.753224	80.654953	
136	05:09:22	32.842919	80.420734	
137	05:09:41	34.65984	75.93723	
138	05:10:00	35.621465	73.74938	
139	05:10:19	34.733501	75.765355	
140	05:10:39	35.986416	72.949666	
141	05:10:58	36.587354	71.667601	
142	05:11:17	37.130716	70.544098	
143	05:11:36	37.488259	69.822575	
144	05:11:55	37.682082	69.437163	
145	05:12:15	37.794245	69.215935	
146	05:12:34	38.59042	67.682543	
147	05:12:53	38.611718	67.642392	
148	05:13:12	38.759491	67.36503	
149	05:13:31	39.658801	65.721636	
150	05:13:50	39.360188	66.258991	
151	05:14:09	39.553626	65.909973	
152	05:14:28	39.33779	66.299625	
153	05:14:47	39.820507	65.434009	
154	05:15:06	40.002092	65.113794	
155	05:15:25	39.891154	65.30908	
156	05:15:44	41.798916	62.095178	
157	05:16:03	41.809948	62.077447	
158	05:16:22	40.580251	64.113334	
159	05:16:41	41.595562	62.423721	
160	05:17:00	41.398489	62.745194	
161	05:17:19	42.173691	61.497987	
162	05:17:38	42.590016	60.846909	
163	05:17:57	42.059895	61.678192	
164	05:18:16	42.261394	61.359764	
165	05:18:35	42.59887	60.8332	
166	05:18:54	42.969514	60.264414	
167	05:19:12	43.065489	60.118729	
168	05:19:31	43.195067	59.923061	
169	05:19:50	43.40799	59.604077	
170	05:20:09	43.250387	59.839884	Stop N2 flow
171	05:20:28	43.996033	58.739157	Start air flow at 400 mL/min
172	05:20:47	43.432444	59.567643	
173	05:21:06	43.953445	58.801021	
174	05:21:25	43.78311	59.049651	
175	05:21:44	44.970164	57.356134	
176	05:22:02	44.56489	57.924178	
177	05:22:21	45.176365	57.07103	Stop air flow
178	05:22:40	45.120889	57.147478	
179	05:22:59	45.042053	57.256441	
180	05:23:18	44.884233	57.475722	
181	05:23:38	45.966109	56.002744	
182	05:23:56	45.475899	56.661483	
183	05:24:15	44.488011	58.033101	

184	05:24:34	41.569994	62.465256	
185	05:24:53	40.283031	64.624064	
186	05:25:12	38.373977	68.093104	
187	05:25:31	36.658237	71.519148	
188	05:25:50	34.069643	77.341184	
189	05:26:09	31.261355	84.747738	
190	05:26:29	30.75846	86.216852	
191	05:26:48	29.92819	88.75037	
192	05:27:08	29.313461	90.718646	
193	05:27:27	27.567585	96.787374	
194	05:27:47	28.142091	94.707248	
195	05:28:06	27.049094	98.740544	
196	05:28:25	26.804548	99.687979	
197	05:28:44	26.569797	100.613872	
198	05:29:03	26.07704	102.611599	
199	05:29:23	24.909494	107.660544	
200	05:29:42	25.338186	105.752649	
201	05:30:02	25.127278	106.683162	
202	05:30:22	25.601925	104.610623	
203	05:30:41	25.181891	106.440717	
204	05:31:01	24.55337	109.296138	
205	05:31:20	25.47544	105.15537	
206	05:31:40	24.477399	109.651213	
207	05:32:00	24.625014	108.963292	
208	05:32:20	25.45679	105.236146	
209	05:32:39	24.827999	108.030692	Last measurement on chip
210	05:32:59	24.009018	111.889985	Measure capillary outlet gas exchanger
211	05:40:46	24.92177	107.604997	No medium flow, no gas flow
212	05:41:09	24.8908	107.745237	Start N2 flow at 200 mL/min
213	05:41:43	25.358309	105.664675	
214	05:42:03	25.386398	105.542111	
215	05:42:22	24.457035	109.746768	Start medium flow
216	05:42:42	25.78342	103.838294	
217	05:43:01	25.961212	103.092195	
218	05:43:20	27.612854	96.620327	
219	05:43:39	29.842622	89.019489	
220	05:43:59	34.289626	76.812241	
221	05:44:18	39.41184	66.165461	
222	05:44:37	48.600707	52.690029	
223	05:44:56	62.158628	40.083397	
224	05:45:15	84.068376	28.305892	
225	05:45:34	112.454689	19.871597	
226	05:45:52	135.975227	15.55084	
227	05:46:10	161.008612	12.33895	
228	05:46:29	184.607509	10.108753	
229	05:46:47	212.002687	8.142527	
230	05:47:05	228.002049	7.212763	
231	05:47:23	236.439804	6.773102	

232	05:47:42	238.806128	6.65538
233	05:48:00	248.525374	6.195371
234	05:48:18	261.340973	5.641115
235	05:48:36	272.83629	5.188258
236	05:48:55	273.817227	5.151375
237	05:49:13	268.357462	5.360088
238	05:49:31	266.382652	5.437687
239	05:49:49	267.930819	5.376755
240	05:50:08	282.581636	4.833198
241	05:50:26	283.694289	4.794212
242	05:50:44	279.251983	4.951723
243	05:51:02	276.855368	5.038799
244	05:51:21	275.372921	5.093419
245	05:51:39	276.078787	5.067339
246	05:51:57	275.844786	5.07597
247	05:52:15	274.199264	5.137081
248	05:52:34	271.073442	5.255212
249	05:52:52	271.534393	5.237621
250	05:53:10	272.148127	5.214291
251	05:53:28	269.368629	5.320795
252	05:53:47	269.839196	5.30261

F.4. Gas Exchanger Box Validation

F.4.1. Gas Exchanger Box Test at 200 mL/min nitrogen

Measurement on glass capillary. Laser settings: LP90, PP524. Medium at 45 mM PP.

Table F.9: Measurement data of gas exchanger box validation with 200 mL/min nitrogen flow at 35 μL/min medium flow.

MeasurementNr	Time [hh:mm:ss]	Lifetime [μs]	O2 [mmHg]	Notes
1	11:37:14	26.651956	100.287966	PMT300, no medium flow
2	11:38:09	25.584733	104.684349	PMT275
3	11:39:18	25.563339	104.776233	
4	11:40:12	25.948408	103.145586	Start medium flow
5	11:47:36	25.939274	103.183705	Flush tube with air at 200 mL/min
6	11:48:17	25.933773	103.206672	
7	11:48:36	25.477006	105.14859	
8	11:48:55	25.87417	103.456181	
9	11:49:15	25.096488	106.820314	
10	11:49:34	25.910837	103.302553	
11	11:49:53	25.240312	106.182529	
12	11:50:12	25.459993	105.222267	Start N2 flow at 200 mL/min
13	11:50:31	25.733491	104.049675	
14	11:50:51	25.870151	103.473046	
15	11:51:10	25.738162	104.029863	
16	11:51:29	25.584206	104.686609	
17	11:51:48	25.879734	103.432842	
18	11:52:07	25.564131	104.772828	
19	11:52:27	26.143602	102.337346	
20	11:52:46	26.727067	99.991774	
21	11:53:05	27.344154	97.619961	
22	11:53:24	28.088231	94.898645	
23	11:53:43	29.23618	90.971946	
24	11:54:02	30.996245	85.516265	
25	11:54:21	31.871739	83.026902	
26	11:54:40	33.80256	77.992631	
27	11:55:00	35.914445	73.10609	
28	11:55:19	37.610589	69.578861	
29	11:55:38	40.089619	64.960481	
30	11:55:57	41.316745	62.879439	
31	11:56:16	43.155657	59.982447	
32	11:56:35	45.425369	56.730193	
33	11:56:53	47.239399	54.355587	
34	11:57:12	48.750887	52.511981	
35	11:57:31	50.942228	50.033422	
36	11:57:50	53.274174	47.619773	
37	11:58:08	54.985312	45.978914	
38	11:58:27	56.864499	44.290682	
39	11:58:45	59.246874	42.304342	
40	11:59:04	61.11335	40.856334	
41	11:59:23	64.34502	38.547855	
42	11:59:42	65.574724	37.729204	

43	12:00:00	68.186545	36.088393	
44	12:00:19	70.074072	34.978741	
45	12:00:37	72.138495	33.83158	
46	12:00:56	73.428958	33.147257	
47	12:01:14	76.128734	31.790626	
48	12:01:33	76.48146	31.620456	
49	12:01:51	78.648083	30.608669	
50	12:02:09	80.771718	29.669633	
51	12:02:28	82.183758	29.072114	
52	12:02:46	83.069255	28.707771	
53	12:03:05	85.223058	27.853179	
54	12:03:23	86.71227	27.287111	
55	12:03:42	87.245721	27.08904	
56	12:04:00	89.398922	26.313583	
57	12:04:18	90.553061	25.91311	
58	12:04:37	91.671567	25.534623	
59	12:04:55	92.72486	25.186552	
60	12:05:14	94.328546	24.671525	
61	12:05:32	94.591064	24.58888	
62	12:05:50	95.636936	24.264127	
63	12:06:09	96.117007	24.117427	
64	12:06:27	97.459133	23.71497	
65	12:06:45	97.86545	23.595306	
66	12:07:04	97.597886	23.673994	
67	12:07:22	99.315262	23.176303	
68	12:07:41	100.271147	22.906676	
69	12:07:59	99.822752	23.032513	
70	12:08:17	101.280692	22.627439	Stop N2 flow
71	12:08:36	102.45598	22.309291	Start air flow at 200 mL/min
72	12:08:54	102.355056	22.336324	
73	12:09:13	103.852304	21.940667	
74	12:09:31	101.867937	22.467555	
75	12:09:49	104.159958	21.860777	
76	12:10:08	104.735018	21.712706	
77	12:10:26	103.049174	22.151469	
78	12:10:44	97.953899	23.569388	
79	12:11:03	90.67478	25.871469	
80	12:11:21	78.934463	30.479089	
81	12:11:39	68.778711	35.73371	
82	12:11:58	61.303077	40.714081	
83	12:12:17	56.00158	45.051846	
84	12:12:35	51.132333	49.828414	
85	12:12:54	47.948262	53.476493	
86	12:13:13	44.564224	57.92512	
87	12:13:32	42.384097	61.16734	
88	12:13:51	40.652778	63.989841	
89	12:14:10	38.547073	67.764397	
90	12:14:29	37.460498	69.878104	
91	12:14:48	36.036566	72.84104	

92	12:15:07	35.522976	73.968013	
93	12:15:26	34.392785	76.566529	
94	12:15:45	33.729034	78.173781	
95	12:16:04	32.28439	81.900393	
96	12:16:23	32.00032	82.672769	
97	12:16:42	31.546159	83.936512	
98	12:17:01	31.156236	85.050903	
99	12:17:20	30.668553	86.484573	
100	12:17:39	29.87568	88.915335	
101	12:17:58	30.272733	87.682148	
102	12:18:18	29.528666	90.020269	
103	12:18:37	29.274791	90.845227	
104	12:18:56	28.802534	92.4185	
105	12:19:15	28.70681	92.743701	
106	12:19:34	28.621555	93.03517	
107	12:19:52	28.435337	93.677889	
108	12:20:11	27.911192	95.532978	
109	12:20:30	27.790398	95.970422	
110	12:20:49	27.602981	96.656713	
111	12:21:09	27.596642	96.680085	
112	12:21:28	27.686233	96.350709	
113	12:21:47	27.888379	95.615303	
114	12:22:06	26.921926	99.231075	
115	12:22:25	27.24098	98.009037	
116	12:22:44	27.172443	98.269128	
117	12:23:04	27.149873	98.355065	
118	12:23:23	26.595886	100.510162	
119	12:23:42	26.854974	99.491202	
120	12:24:01	27.005332	98.908827	
121	12:24:20	26.625013	100.39462	
122	12:24:40	26.503983	100.876395	Stop air flow
123	12:24:59	27.018427	98.858415	
124	12:25:18	26.679872	100.17769	
125	12:25:37	26.74163	99.934542	

F.4.2. Gas Exchanger Box Test at 400 mL/min nitrogen

First 6 measurements deleted since old medium left in silicone tubing. Measurement on glass capillary. Laser settings: LP90, PP524. Medium at 45 mM PP.

Table F.10: Measurement data of gas exchanger box validation with 400 mL/min nitrogen flow at 35 μL/min medium flow.

MeasurementNr	Time [hh:mm:ss]	Lifetime [μs]	O2 [mmHg]	Notes
7	12:24:33	27.989117	95.252782	PMT275
8	12:24:52	27.922086	95.493712	
9	12:25:11	28.382368	93.862248	
10	12:25:31	28.264449	94.275147	
11	12:25:50	28.415574	93.746594	Start N2 flow at 400 mL/min
12	12:26:09	28.681287	92.83078	
13	12:26:29	27.880967	95.642078	

14	12:26:48	28.782305	92.487044	
15	12:27:07	28.888566	92.128061	
16	12:27:27	28.37785	93.878005	
17	12:27:46	28.767152	92.53845	
18	12:28:05	30.618643	86.633872	
19	12:28:24	34.034792	77.42561	
20	12:28:44	38.125466	68.57024	
21	12:29:02	43.310796	59.749297	
22	12:29:21	49.375818	51.782717	
23	12:29:40	56.381227	44.714096	
24	12:29:59	63.532958	39.105844	
25	12:30:18	71.777778	34.027266	
26	12:30:37	80.319378	29.865488	
27	12:30:55	91.379892	25.632429	
28	12:31:14	101.038306	22.693974	
29	12:31:32	112.170696	19.934839	
30	12:31:50	124.07185	17.532764	
31	12:32:09	136.628096	15.452126	
32	12:32:27	150.861806	13.512363	
33	12:32:46	163.543515	12.068536	
34	12:33:04	175.759908	10.874713	
35	12:33:22	185.703324	10.018965	
36	12:33:40	193.605265	9.401593	
37	12:33:59	201.813885	8.811457	
38	12:34:17	208.794237	8.34613	
39	12:34:35	214.236263	8.004388	
40	12:34:54	219.202298	7.707343	
41	12:35:12	224.982862	7.378093	
42	12:35:30	231.520703	7.025523	
43	12:35:48	234.985323	6.846638	
44	12:36:07	240.764013	6.559727	
45	12:36:25	242.235486	6.488855	
46	12:36:43	249.331542	6.158826	
47	12:37:01	250.259675	6.117044	
48	12:37:19	252.264773	6.027829	
49	12:37:38	252.106522	6.034819	
50	12:37:56	256.56922	5.841016	Stop N2 flow
51	12:38:14	255.153541	5.901761	Start air flow at 400 mL/min
52	12:38:32	255.302442	5.89534	
53	12:38:51	256.035185	5.863852	
54	12:39:09	256.162811	5.858386	
55	12:39:27	252.344862	6.024295	
56	12:39:45	229.040736	7.156893	
57	12:40:04	179.644031	10.529163	
58	12:40:22	125.315493	17.308083	
59	12:40:40	83.617228	28.486169	
60	12:40:59	63.145802	39.37692	
61	12:41:17	52.006767	48.904733	
62	12:41:36	44.828141	57.554029	

63	12:41:55	40.327378	64.547382	
64	12:42:15	36.73244	71.364356	
65	12:42:33	35.092488	74.93805	
66	12:42:53	33.397316	79.000967	
67	12:43:12	32.416923	81.544672	
68	12:43:31	31.452366	84.202046	
69	12:43:50	30.534725	86.886003	
70	12:44:10	30.26248	87.713585	
71	12:44:29	29.396843	90.446843	
72	12:44:48	29.000599	91.752428	
73	12:45:07	28.401054	93.797133	
74	12:45:27	28.398511	93.805987	
75	12:45:46	28.243048	94.350453	
76	12:46:05	27.838053	95.797388	
77	12:46:25	27.422783	97.325413	
78	12:46:44	27.647607	96.492453	
79	12:47:04	27.445746	97.239712	
80	12:47:23	27.625151	96.575042	Start N2 flow at 400 mL/min
81	12:47:42	27.281263	97.856776	
82	12:48:02	27.617118	96.60462	
83	12:48:21	28.049807	95.035639	
84	12:48:40	27.373547	97.509656	
85	12:48:59	27.479177	97.115196	
86	12:49:19	28.018559	95.147323	
87	12:49:39	29.732924	89.366764	
88	12:49:59	31.740334	83.391777	
89	12:50:18	35.504248	74.009726	
90	12:50:37	39.726379	65.601149	
91	12:50:56	44.333213	58.253569	
92	12:51:15	50.319206	50.71614	
93	12:51:33	56.513307	44.597657	
94	12:51:53	64.170707	38.66644	
95	12:52:12	73.764229	32.973384	
96	12:52:30	83.048748	28.71612	
97	12:52:49	95.365774	24.347642	
98	12:53:07	109.550212	20.533855	
99	12:53:26	122.06771	17.904474	
100	12:53:44	134.155574	15.831041	
101	12:54:03	144.946861	14.272186	
102	12:54:21	155.897375	12.910939	
103	12:54:40	165.858688	11.828784	
104	12:54:58	175.522631	10.896318	
105	12:55:16	184.815428	10.091635	
106	12:55:35	192.743251	9.466481	
107	12:55:53	200.195227	8.923995	
108	12:56:11	209.81544	8.280651	
109	12:56:30	213.844361	8.028417	
110	12:56:48	220.840657	7.612275	
111	12:57:06	228.369595	7.192935	

112	12:57:25	236.546908	6.767723	
113	12:57:44	243.262307	6.439908	
114	12:58:02	245.823391	6.319605	
115	12:58:20	247.049467	6.262895	
116	12:58:39	248.717576	6.186637	
117	12:58:57	250.521115	6.105331	
118	12:59:15	253.835294	5.958934	
119	12:59:33	255.453536	5.888833	
120	12:59:51	254.587626	5.926233	
121	13:00:10	257.007815	5.822333	
122	13:00:28	258.842266	5.744873	End of interval measurement
123	13:00:46	259.950818	5.698595	Set 40 mL/min air and 360 mL/min N2
124	13:01:04	262.061026	5.611582	
125	13:01:22	266.275114	5.441945	
126	13:01:41	264.228012	5.523675	
127	13:01:59	257.791677	5.789099	
128	13:02:17	250.272061	6.116489	
129	13:02:35	246.33109	6.296054	
130	13:02:54	234.568477	6.867881	
131	13:03:12	223.625956	7.453851	
132	13:03:30	211.713707	8.160612	
133	13:03:49	196.747216	9.169894	
134	13:04:07	183.005416	10.241959	
135	13:04:25	172.754193	11.15278	
136	13:04:44	166.505566	11.762987	
137	13:05:02	159.36584	12.518788	
138	13:05:20	154.15906	13.114114	
139	13:05:39	148.337448	13.829225	
140	13:05:57	143.896627	14.413627	
141	13:06:16	141.021077	14.811676	
142	13:06:34	141.028337	14.810651	
143	13:06:52	136.789592	15.427854	
144	13:07:11	137.054128	15.388218	
145	13:07:29	135.615352	15.605659	Set 50 mL/min air and 350 mL/min N2
146	13:07:48	135.242608	15.662746	
147	13:08:06	134.746101	15.739279	
148	13:08:24	134.60231	15.761548	
149	13:08:43	135.357605	15.6451	
150	13:09:01	134.123023	15.836123	
151	13:09:20	133.466163	15.939196	
152	13:09:38	132.300404	16.124646	
153	13:09:56	131.393203	16.271241	
154	13:10:15	129.105024	16.650141	
155	13:10:33	128.054596	16.828616	
156	13:10:52	125.780519	17.225211	
157	13:11:10	124.074559	17.53227	
158	13:11:29	122.600036	17.804558	
159	13:11:47	122.13039	17.892664	

160	13:12:06	120.581603	18.188082	
161	13:12:24	121.161014	18.07668	
162	13:12:42	120.355101	18.231923	
163	13:13:01	120.119355	18.277728	
164	13:13:19	118.929997	18.511589	
165	13:13:38	118.145605	18.668399	Set 60 mL/min air and 340 mL/min N2
166	13:13:56	118.526566	18.591981	
167	13:14:15	118.62733	18.571851	
168	13:14:33	118.635693	18.570181	
169	13:14:52	117.774107	18.743396	
170	13:15:10	116.892957	18.923184	
171	13:15:29	118.572572	18.582786	
172	13:15:47	116.436885	19.017309	
173	13:16:05	115.733582	19.163912	
174	13:16:24	115.870731	19.135184	
175	13:16:42	113.867971	19.56157	
176	13:17:01	112.619553	19.835031	
177	13:17:19	110.761141	20.253526	
178	13:17:38	110.160522	20.391799	
179	13:17:56	109.230248	20.608965	
180	13:18:15	109.823562	20.470035	
181	13:18:33	108.780518	20.715283	
182	13:18:52	108.033501	20.893837	
183	13:19:10	107.235481	21.087331	
184	13:19:29	107.396268	21.048114	
185	13:19:47	106.485876	21.271727	Set 70 mL/min air and 330 mL/min N2
186	13:20:06	105.929368	21.410311	
187	13:20:24	107.56099	21.008059	
188	13:20:43	106.803758	21.193215	
189	13:21:01	106.187759	21.345785	
190	13:21:20	106.044908	21.381419	
191	13:21:38	107.161341	21.105454	
192	13:21:57	106.253586	21.329397	
193	13:22:15	104.152298	21.86276	
194	13:22:34	104.913613	21.66705	
195	13:22:52	104.269196	21.832524	
196	13:23:11	101.829918	22.477851	
197	13:23:30	100.71769	22.782474	
198	13:23:48	101.299979	22.622159	
199	13:24:07	99.281594	23.185895	
200	13:24:25	99.306556	23.178783	
201	13:24:44	98.759344	23.335512	
202	13:25:02	97.418983	23.726848	
203	13:25:21	98.667594	23.361961	
204	13:25:39	97.531701	23.693525	
205	13:25:58	99.006747	23.264438	Set 80 mL/min air and 320 mL/min N2
206	13:26:16	97.000889	23.851129	
207	13:26:35	97.514195	23.698695	
208	13:26:53	97.829593	23.605826	

209	13:27:12	98.038696	23.544585
210	13:27:30	97.679658	23.6499
211	13:27:49	97.780001	23.620389
212	13:28:07	97.581015	23.67897
213	13:28:26	95.667298	24.254806
214	13:28:45	95.24439	24.385181
215	13:29:03	94.917868	24.486636
216	13:29:22	95.669987	24.253981
217	13:29:40	94.89891	24.492548
218	13:29:59	94.654763	24.568896
219	13:30:17	93.936792	24.795714
220	13:30:36	94.298798	24.680919
221	13:30:54	93.052817	25.079784
222	13:31:13	94.520168	24.611154
223	13:31:31	94.684625	24.559536
224	13:31:50	93.445118	24.953053
225	13:32:08	93.504495	24.933964
226	13:32:27	93.992842	24.777883
227	13:32:45	93.494939	24.937034

F.4.3. Gas Exchanger Box with Chip Test at 400 mL/min nitrogen

First 90 measurements are deleted since the chip was slightly heated and measured without aluminium foil underneath. Oxygen measurement on the middle of the channel with laser settings: LP90, PP524. Medium at 45 mM PP.

Table F.11: Measurement data of gas exchanger box integrated with the Micronit resealable chip with 400 mL/min nitrogen flow at 35 μL/min medium flow.

MeasurementNr	Time [hh:mm:ss]	Lifetime [μs]	O2 [mmHg]	Notes
91	15:09:42	26.564094	100.636567	PMT275
92	15:10:02	26.389203	101.337371	
93	15:10:21	26.636269	100.350038	
94	15:10:40	26.112207	102.466524	
95	15:11:00	25.989773	102.973289	
96	15:11:19	25.612047	104.56726	
97	15:11:38	25.386534	105.541517	
98	15:11:58	25.861777	103.508205	
99	15:12:17	25.569054	104.751673	Top of chip holder 26 °C
100	15:12:37	25.367742	105.623487	Start nitrogen flow at 400 mL/min
101	15:12:56	25.497129	105.061575	
102	15:13:15	25.652414	104.394674	
103	15:13:35	25.291031	105.959344	
104	15:13:54	25.564836	104.769796	
105	15:14:14	27.058077	98.706066	
106	15:14:33	28.297819	94.157952	
107	15:14:52	29.963664	88.639253	
108	15:15:11	31.894351	82.964417	
109	15:15:31	35.070659	74.987872	
110	15:15:50	37.819608	69.166091	
111	15:16:09	39.652808	65.732341	

112	15:16:28	41.747998	62.177143	
113	15:16:47	45.75739	56.281493	
114	15:17:06	47.489839	54.042006	
115	15:17:25	49.54332	51.590376	
116	15:17:44	51.005163	49.965383	
117	15:18:03	55.711181	45.313304	
118	15:18:22	60.857406	41.04964	
119	15:18:41	64.252664	38.610605	
120	15:19:00	64.423175	38.494895	
121	15:19:18	66.987269	36.825921	
122	15:19:37	70.877568	34.52431	
123	15:19:56	72.762225	33.49779	
124	15:20:14	74.760439	32.465946	
125	15:20:33	74.842169	32.424914	
126	15:20:51	77.490196	31.14235	
127	15:21:10	79.570831	30.194488	
128	15:21:28	80.295045	29.876087	
129	15:21:47	81.377442	29.410775	
130	15:22:06	84.902254	27.977721	
131	15:22:24	90.820037	25.821922	
132	15:22:43	94.366715	24.65948	
133	15:23:01	93.42386	24.959893	
134	15:23:20	93.311139	24.996214	
135	15:23:38	95.577689	24.282334	
136	15:23:57	98.974403	23.27371	
137	15:24:15	100.428876	22.862679	
138	15:24:33	98.885645	23.299184	
139	15:24:52	98.293704	23.470252	
140	15:25:10	102.795645	22.218699	
141	15:25:29	102.900311	22.190904	
142	15:25:48	102.765836	22.226625	
143	15:26:06	105.109132	21.617246	
144	15:26:25	110.193599	20.384145	
145	15:26:43	114.035374	19.525356	
146	15:27:02	114.706687	19.381196	
147	15:27:20	114.334773	19.460853	
148	15:27:39	113.142403	19.719768	
149	15:27:57	115.663415	19.178636	
150	15:28:16	117.072767	18.886276	
151	15:28:34	117.172373	18.86588	
152	15:28:53	113.821896	19.571556	
153	15:29:11	118.506976	18.595899	Stop N2 flow
154	15:29:29	119.700637	18.35953	Start air flow at 400 mL/min
155	15:29:48	119.080994	18.48164	
156	15:30:06	117.920265	18.713834	
157	15:30:25	114.9503	19.329298	
158	15:30:43	96.336886	24.050725	
159	15:31:02	78.995985	30.451375	
160	15:31:20	65.698401	37.648564	

161	15:31:39	56.764669	44.377556	
162	15:31:58	49.517143	51.620349	
163	15:32:17	44.517913	57.990691	
164	15:32:36	41.160231	63.137962	
165	15:32:55	39.000161	66.917803	
166	15:33:14	37.02649	70.757047	
167	15:33:33	35.089226	74.94549	
168	15:33:52	34.310686	76.761959	
169	15:34:11	32.93339	80.185781	
170	15:34:30	32.056442	82.51909	
171	15:34:50	30.537833	86.876641	
172	15:35:09	29.941079	88.709967	
173	15:35:28	30.046365	88.381221	
174	15:35:47	29.661795	89.593312	
175	15:36:06	29.423478	90.360344	
176	15:36:25	28.608772	93.079021	
177	15:36:44	28.26965	94.256864	
178	15:37:03	28.505647	93.434233	
179	15:37:22	27.91929	95.503785	
180	15:37:41	27.759287	96.083701	
181	15:38:00	27.684654	96.356495	
182	15:38:20	27.359667	97.561715	
183	15:38:39	27.605903	96.645942	
184	15:38:58	27.082792	98.611328	
185	15:39:17	26.745862	99.91792	
186	15:39:36	26.820066	99.627342	
187	15:39:56	26.737206	99.951922	
188	15:40:15	26.811166	99.662111	Start N2 flow at 400 mL/min
189	15:40:35	26.564792	100.633789	
190	15:40:54	26.575275	100.592079	
191	15:41:13	26.503725	100.877425	
192	15:41:34	26.942952	99.149653	
193	15:41:53	26.830976	99.584758	
194	15:42:12	27.323849	97.696299	
195	15:42:31	29.086014	91.467987	
196	15:42:50	30.203614	87.894491	
197	15:43:09	33.225448	79.436041	
198	15:43:29	36.422627	72.014829	
199	15:43:48	39.063318	66.801354	
200	15:44:07	41.120746	63.203491	
201	15:44:26	44.62113	57.844735	
202	15:44:45	47.744034	53.727088	
203	15:45:04	50.814512	50.172011	
204	15:45:23	52.704388	48.189805	
205	15:45:41	55.418322	45.579752	
206	15:46:00	59.976609	41.727486	
207	15:46:19	61.579356	40.508502	
208	15:46:38	63.901302	38.850988	
209	15:46:57	67.88673	36.27033	

210	15:47:15	72.1677	33.815822	
211	15:47:34	78.007393	30.902011	
212	15:47:53	79.583534	30.188852	
213	15:48:11	80.137305	29.944947	
214	15:48:30	82.28377	29.03057	
215	15:48:48	86.058574	27.533177	
216	15:49:07	88.833141	26.513703	
217	15:49:25	88.426242	26.659209	
218	15:49:44	87.30947	27.065532	
219	15:50:02	92.466669	25.27114	
220	15:50:21	93.3232	24.992324	
221	15:50:39	95.054533	24.444087	
222	15:50:58	96.958225	23.863872	
223	15:51:16	102.638271	22.260597	
224	15:51:35	104.98568	21.648671	
225	15:51:53	108.133285	20.869844	
226	15:52:12	107.708011	20.972412	
227	15:52:30	108.231942	20.846165	
228	15:52:49	111.024335	20.193406	
229	15:53:07	112.158664	19.937525	
230	15:53:26	112.694584	19.818424	
231	15:53:44	111.104168	20.175226	
232	15:54:03	113.385504	19.666539	
233	15:54:21	114.664391	19.390229	
234	15:54:40	114.821375	19.356736	Adjust to 3000 analyses points
235	15:55:06	118.722568	18.552856	
236	15:55:25	123.6637	17.607487	
237	15:56:13	126.944362	17.020463	
238	15:56:31	126.148895	17.159996	
239	15:56:49	127.655206	16.897246	
240	15:57:08	131.145567	16.311609	
241	15:57:26	132.84845	16.037057	
242	15:57:45	128.840657	16.694785	
243	15:58:03	127.291423	16.960132	
244	15:58:21	132.126525	16.152588	
245	15:58:40	129.99962	16.500417	
246	15:58:58	131.580217	16.240856	
247	15:59:17	132.989953	16.01456	
248	15:59:35	139.010605	15.099758	
249	15:59:53	142.370565	14.622871	Adjust to standard 5000 analyses points
250	16:00:12	142.139443	14.654952	
251	16:00:30	139.066776	15.091596	
252	16:00:48	139.329762	15.053471	
253	16:01:07	141.013628	14.812729	
254	16:01:25	142.843919	14.557489	Top of chip holder 23.3 °C
255	16:01:44	142.683375	14.579616	
256	16:02:02	139.892896	14.972315	
257	16:02:20	144.276631	14.362212	

F.5. System Validation: Characterisation Chip Channel

Measure oxygen on the Micronit chip channel. Laser settings: LP90, PP524. Medium at 45 mM PP.

Table F.12: Measurement data of chip channel characterisation with 10%, 8% and 7% oxygen gas flow at 35 μL/min medium flow.

MeasurementNr	Time [hh:mm:ss]	Lifetime [μs]	O2 [mmHg]	Notes
3	10:48:57	18.584221	146.041874	Fiber begin channel, PMT200
4	10:49:35	18.418601	147.401009	
5	10:50:54	18.487397	146.833488	
6	10:51:42	18.612219	145.814507	PMT220
7	10:52:00	18.513119	146.622384	Set gas[mL/min]: 190 air, 190 N_2, 20 CO_2
8	11:01:28	19.461129	139.231177	
9	11:01:47	22.163326	121.633148	
10	11:02:06	23.710678	113.362103	
11	11:02:26	24.111088	111.3947	
12	11:02:45	24.914323	107.638689	
13	11:03:04	24.576205	109.189839	
14	11:03:23	24.852373	107.91973	
15	11:03:42	24.953101	107.463475	
16	11:04:02	25.495978	105.066547	
17	11:04:21	25.299245	105.923283	
18	11:04:40	26.616738	100.427422	PMT240
19	11:04:59	26.75664	99.875616	
20	11:05:18	26.979124	99.009872	
21	11:05:38	27.310666	97.745923	
22	11:05:57	26.830713	99.585781	
23	11:06:16	27.912251	95.529158	
24	11:06:35	28.048042	95.04194	
25	11:07:11	28.340949	94.006887	
26	11:07:31	28.683648	92.822717	
27	11:07:50	28.112576	94.812042	
28	11:08:09	28.968506	91.859736	
29	11:08:28	29.024604	91.672321	
30	11:08:48	28.626646	93.017718	
31	11:09:07	28.541154	93.31164	
32	11:09:26	29.144155	91.275325	
33	11:09:45	29.469447	90.211427	
34	11:10:05	29.265764	90.874823	
35	11:10:24	29.383432	90.490455	
36	11:10:43	29.422241	90.364359	
37	11:11:02	29.683618	89.523692	Set gas[mL/min]: 152 air, 228 N_2, 20 CO_2
38	11:11:22	29.498028	90.119071	
39	11:11:41	29.506788	90.0908	
40	11:12:00	30.002031	88.519369	
41	11:12:19	29.731593	89.370995	
42	11:12:38	30.327869	87.513458	
43	11:12:58	30.282944	87.650862	
44	11:13:17	30.656182	86.521534	
45	11:13:36	31.08365	85.261438	

46	11:13:55	31.130429	85.125643	
47	11:14:14	31.612081	83.750827	
48	11:14:33	31.918137	82.898786	
49	11:14:52	32.89746	80.278938	
50	11:15:11	32.909443	80.247846	
51	11:15:30	33.256373	79.357424	
52	11:15:49	33.226721	79.432802	
53	11:16:08	33.852472	77.870108	
54	11:16:27	33.387791	79.024961	
55	11:16:46	33.749697	78.122791	
56	11:17:05	34.05305	77.381358	
57	11:17:25	34.075597	77.326778	
58	11:17:44	33.613797	78.45929	
59	11:18:03	33.908535	77.732917	
60	11:18:22	33.944875	77.644231	Set gas[mL/min]: 134 air, 246 N_2, 20 CO_2
61	11:18:41	34.556623	76.1793	
62	11:19:00	34.338762	76.695021	
63	11:19:20	34.715184	75.808026	
64	11:19:39	34.438128	76.458993	
65	11:19:58	34.255307	76.894313	
66	11:20:17	34.270425	76.858139	
67	11:20:36	34.798803	75.613593	
68	11:20:55	34.951516	75.260899	
69	11:21:14	34.748601	75.730212	
70	11:21:34	35.129851	74.852916	
71	11:21:53	35.100427	74.919943	
72	11:22:12	35.504382	74.009426	
73	11:22:31	35.325625	74.409777	
74	11:22:50	35.830304	73.28976	
75	11:23:09	36.243613	72.395749	
76	11:23:29	36.272415	72.334208	
77	11:23:48	35.980037	72.963506	
78	11:24:07	36.657317	71.521072	
79	11:24:26	36.726757	71.376189	
80	11:24:45	36.629249	71.579789	
81	11:25:04	36.384978	72.094629	
82	11:25:24	36.940828	70.932969	
83	11:25:43	37.044149	70.720883	
84	11:26:02	37.192708	70.418004	
85	11:26:21	36.986191	70.839707	
86	11:26:40	37.639319	69.521855	
87	11:26:59	37.944187	68.922236	
88	11:27:19	38.151839	68.51931	
89	11:27:38	37.832181	69.141409	
90	11:27:57	37.582821	69.634044	
91	11:28:16	37.93305	68.943971	
92	11:28:35	37.913318	68.982511	
93	11:28:54	37.893927	69.020425	
94	11:29:13	37.568685	69.662168	

95	11:29:31	38.132149	68.557328	
96	11:29:51	38.083204	68.652003	
97	11:30:10	38.16082	68.501983	
98	11:30:29	38.141905	68.538487	
99	11:30:48	38.122976	68.575054	
100	11:31:07	38.244247	68.341409	
101	11:31:26	38.36268	68.114658	
102	11:31:45	38.403499	68.036831	
103	11:32:03	38.590927	67.681586	
104	11:32:22	38.545022	67.768275	
105	11:32:41	38.578845	67.704383	
106	11:33:00	38.740743	67.400102	
107	11:33:19	38.588262	67.686613	
108	11:33:38	38.450015	67.948344	
109	11:33:57	38.298291	68.237763	
110	11:34:16	38.433018	67.980652	
111	11:34:35	38.580009	67.702185	
112	11:35:42	37.937363	68.935553	Fiber on end channel
113	11:36:01	38.460993	67.927491	
114	11:36:20	39.151426	66.639527	
115	11:36:39	38.102676	68.614309	
116	11:36:58	38.493353	67.866093	
117	11:37:17	38.180785	68.463492	
118	11:37:36	37.805629	69.193555	
119	11:37:55	38.233236	68.362562	
120	11:38:14	38.737999	67.405238	
121	11:38:34	37.824735	69.156025	
122	11:38:53	38.088858	68.641054	
123	11:39:12	38.047875	68.720492	
124	11:39:31	38.433468	67.979798	
125	11:39:50	38.51168	67.831366	
126	11:40:09	38.527832	67.800789	
127	11:40:28	38.144751	68.532991	
128	11:40:47	38.538159	67.781252	
129	11:41:06	38.626403	67.614735	
130	11:41:25	38.290106	68.253442	
131	11:41:44	38.332907	68.17153	
132	11:42:03	38.400868	68.041843	
133	11:42:22	38.745643	67.390932	
134	11:42:41	38.682107	67.510011	
135	11:43:00	38.361687	68.116555	
136	11:43:19	38.393705	68.05549	
137	11:43:39	38.305366	68.224217	
138	11:43:58	38.647779	67.574512	
139	11:44:17	38.464438	67.92095	
140	11:44:36	38.331984	68.173295	
141	11:44:55	38.881652	67.137331	
142	11:45:14	38.652	67.566574	
143	11:45:33	38.322087	68.19222	

144	11:45:52	38.525706	67.804812	
145	11:46:11	39.035574	66.852462	
146	11:46:30	38.172093	68.480245	
147	11:46:49	38.448678	67.950884	
148	11:47:08	38.67392	67.525384	
149	11:47:27	38.552168	67.754765	
150	11:47:46	38.47113	67.908248	
151	11:48:05	38.545938	67.766542	
152	11:48:24	38.500563	67.852428	
153	11:48:44	38.361302	68.117289	
154	11:49:03	38.634213	67.600034	
155	11:49:22	38.792633	67.303113	
156	11:49:41	38.940275	67.028571	
157	11:50:00	38.666697	67.538952	
158	11:50:19	38.568635	67.723657	
159	11:50:38	38.039068	68.737585	
160	11:50:57	38.440122	67.967146	
161	11:51:16	38.752068	67.378912	Fiber on middle channel
162	11:52:18	40.664649	63.969669	
163	11:52:37	40.8844	63.598386	
164	11:52:56	41.062073	63.3011	
165	11:53:15	40.566026	64.137607	
166	11:53:34	41.019307	63.372422	
167	11:53:53	40.679085	63.945156	
168	11:54:12	41.130896	63.186635	
169	11:54:31	40.940263	63.504636	
170	11:54:50	40.628333	64.031414	
171	11:55:08	41.071023	63.286193	
172	11:55:27	40.814365	63.716279	
173	11:56:06	40.665529	63.968174	
174	11:56:24	41.033621	63.348534	
175	11:56:43	40.714976	63.884284	
176	11:57:02	40.80895	63.725412	
177	11:57:21	40.780398	63.773605	
178	11:57:40	40.067368	64.999393	
179	11:57:58	41.077564	63.275302	
180	11:58:17	41.097802	63.241629	
181	11:58:36	40.452046	64.332715	
182	11:58:55	40.419327	64.388926	
183	11:59:14	40.793578	63.75135	
184	11:59:33	41.18865	63.090874	
185	11:59:51	40.921419	63.536232	Start flow stop, continuous flash
186	12:00:18	40.889328	63.590105	
187	12:00:42	41.057722	63.30835	
188	12:00:52	40.959587	63.472267	
189	12:01:04	41.06806	63.291128	
190	12:01:14	40.952216	63.48461	
191	12:01:20	40.599611	64.080326	
192	12:01:30	40.824923	63.698481	

193	12:01:39	40.779505	63.775113	
194	12:01:48	40.852006	63.652866	
195	12:01:54	40.403684	64.415834	
196	12:01:59	40.627404	64.032995	
197	12:02:06	40.383041	64.451372	
198	12:02:11	40.387734	64.44329	
199	12:02:17	40.038669	65.049644	
200	12:02:23	39.9953	65.12572	
201	12:02:29	39.690912	65.664333	
202	12:02:36	39.605622	65.816739	
203	12:02:43	40.121247	64.905246	
204	12:02:50	39.655291	65.727904	
205	12:02:56	39.624755	65.782492	
206	12:03:02	38.976128	66.962215	
207	12:03:08	39.197209	66.555727	
208	12:03:15	38.934372	67.039506	
209	12:03:21	38.796542	67.295818	
210	12:03:29	38.2121	68.4032	End flow stop, intermittent flash
211	12:03:36	38.725919	67.427856	
212	12:05:51	38.025686	68.763573	
213	12:06:10	38.606918	67.651437	
214	12:06:30	39.722334	65.60835	
215	12:06:49	39.960089	65.187606	
216	12:07:07	39.678454	65.686554	
217	12:07:26	40.320856	64.558648	
218	12:07:45	39.857177	65.369109	
219	12:08:04	39.774593	65.515438	
220	12:08:23	40.272649	64.64204	
221	12:08:42	40.727962	63.862286	

F.6. System Validation: Cell Test

Measure oxygen on Micronit chip with HepaRG cell layer with coupled gas exchanger box. Laser settings: LP90, PP524. Medium at 45 mM PP.

Table F.13: Measurement data the HepaRG cell layer test at 35 μL/min medium flow. Laser settings: LP90, PP524. Medium at 45 mM PP.

MeasurementNr	Time [hh:mm:ss]	Lifetime [μs]	O2 [mmHg]	Notes
1	13:25:03	29.22176	91.019359	Fiber begin of channel, PMT320
2	13:25:22	29.381161	90.497845	Set gas[mL/min]: 134 air, 246 N_2, 20 CO_2
3	13:25:41	29.332405	90.656759	
4	13:26:01	29.459716	90.242914	
5	13:26:20	29.66151	89.594225	
6	13:26:39	30.038105	88.406928	
7	13:26:58	29.430972	90.336036	
8	13:27:18	29.290247	90.794593	
9	13:27:37	30.173635	87.986894	
10	13:27:56	30.122125	88.146088	
11	13:28:15	30.266157	87.702308	
12	13:28:35	30.399364	87.295628	
13	13:28:54	29.794893	89.170272	
14	13:29:13	29.948044	88.688147	
15	13:29:32	29.965392	88.633846	
16	13:29:52	30.025367	88.4466	
17	13:30:11	31.420471	84.292705	
18	13:30:30	31.197449	84.931801	
19	13:30:50	30.640975	86.567011	
20	13:31:09	30.885527	85.84113	
21	13:31:28	31.1735	85.000973	
22	13:31:47	31.282571	84.686798	
23	13:32:07	31.469075	84.154626	
24	13:32:26	31.069604	85.302294	
25	13:32:45	31.4649	84.16647	
26	13:33:04	31.665993	83.599542	
27	13:33:23	31.189705	84.954157	
28	13:33:43	31.775554	83.293684	
29	13:34:02	31.534836	83.968486	
30	13:34:21	30.931589	85.705694	
31	13:34:41	31.452149	84.202663	
32	13:35:00	31.139765	85.09859	
33	13:35:19	31.70503	83.490322	
34	13:35:39	31.949046	82.813644	
35	13:35:58	32.242861	82.012459	
36	13:36:17	32.867001	80.358069	
37	13:36:37	31.950322	82.810132	
38	13:36:56	32.394527	81.604579	
39	13:37:16	31.497707	84.073485	
40	13:37:35	31.932059	82.860415	
41	13:37:54	31.935219	82.85171	
42	13:38:14	32.8517	80.397874	

43	13:38:33	32.300738	81.856356
44	13:38:53	32.490728	81.347837
45	13:39:12	32.763853	80.627131
46	13:39:31	32.748136	80.66828
47	13:39:51	32.75182	80.658632
48	13:40:10	32.139455	82.292761
49	13:40:30	32.578675	81.114449
50	13:40:49	33.155953	79.613244
51	13:41:08	32.982184	80.059598
52	13:41:28	32.946215	80.152579
53	13:41:47	33.771659	78.068666
54	13:42:07	33.511138	78.715289
55	13:42:26	33.150029	79.628384
56	13:42:45	33.575172	78.555424
57	13:43:05	32.947392	80.149534
58	13:43:24	33.415236	78.955861
59	13:43:43	33.244278	79.388154
60	13:44:03	33.29857	79.250388
61	13:44:22	33.039871	79.910899
62	13:44:41	33.592998	78.51103
63	13:45:01	33.823394	77.941443
64	13:45:20	33.324209	79.185483
65	13:45:39	33.288434	79.276073
66	13:45:59	33.836537	77.909186
67	13:46:18	33.531727	78.66382
68	13:46:37	33.592342	78.512662
69	13:46:57	33.558761	78.596337
70	13:47:16	33.893857	77.768791
71	13:47:35	34.076143	77.325457
72	13:47:55	33.768014	78.077645
73	13:48:14	33.680543	78.293681
74	13:48:33	33.3357	79.156429
75	13:48:53	33.687885	78.275505
76	13:49:12	33.665986	78.329743
77	13:49:31	34.092733	77.285344
78	13:49:50	33.663779	78.335213
79	13:50:09	34.202092	77.021898
80	13:50:28	33.995522	77.520948
81	13:50:48	34.687324	75.873015
82	13:51:07	34.434258	76.46816
83	13:51:26	34.966174	75.22721
84	13:51:46	34.809981	75.587671
85	13:52:05	34.159557	77.124165
86	13:52:24	34.380111	76.596636
87	13:52:43	34.087832	77.297189
88	13:53:03	34.209418	77.004311
89	13:53:22	34.245609	76.917534
90	13:53:41	34.574336	76.137655
91	13:54:00	34.590265	76.100243

92	13:54:20	34.345448	76.679097	
93	13:54:39	34.459822	76.407641	Fiber on middle of channel
94	13:56:02	43.669535	59.216509	
95	13:56:21	43.051041	60.140618	
96	13:56:40	43.99768	58.736767	
97	13:56:59	46.237126	55.64455	
98	13:57:18	46.26289	55.610718	
99	13:57:37	45.730116	56.318106	
100	13:57:56	46.181054	55.718314	
101	13:58:15	46.139515	55.773074	
102	13:58:35	45.949712	56.024551	
103	13:58:54	45.002646	57.31105	
104	13:59:13	44.913739	57.434607	
105	13:59:32	44.682945	57.757646	
106	13:59:51	43.818384	58.998005	
107	14:00:11	44.444745	58.094568	
108	14:00:30	45.077661	57.207177	
109	14:00:49	45.012786	57.296989	
110	14:01:08	45.152742	57.10356	
111	14:01:27	44.503785	58.010722	Fiber on end of channel
112	14:02:31	57.196285	44.004133	
113	14:02:50	59.056596	42.457101	
114	14:03:09	57.227329	43.977491	
115	14:03:28	57.340296	43.880788	
116	14:03:47	57.005594	44.168417	
117	14:04:06	57.51597	43.731162	
118	14:04:25	56.867434	44.288132	
119	14:04:43	57.66811	43.602317	
120	14:05:03	58.604183	42.824288	
121	14:05:22	56.333998	44.755865	
122	14:05:40	57.057617	44.123488	
123	14:06:00	58.071098	43.264293	
124	14:06:18	57.489782	43.753409	
125	14:06:37	57.89652	43.41015	
126	14:06:56	58.302946	43.071938	
127	14:07:16	61.803558	40.343024	
128	14:07:35	61.9232	40.255209	
129	14:07:54	61.99351	40.203761	
130	14:08:13	62.640474	39.735779	Fiber end channel, upper left
131	14:09:02	47.207588	54.395656	
132	14:09:21	47.275169	54.310595	
133	14:09:40	47.642587	53.852366	
134	14:09:59	47.037861	54.61036	
135	14:10:18	46.73655	54.995361	
136	14:10:37	46.414689	55.412139	
137	14:10:56	46.732473	55.000604	
138	14:11:15	48.654507	52.62612	
139	14:11:35	50.166374	50.886206	
140	14:11:54	49.053517	52.156507	

141	14:12:13	49.45162	51.695513	Fiber end channel, upper right
142	14:12:59	52.338083	48.562821	
143	14:13:18	53.949653	46.959602	
144	14:13:37	50.772362	50.217902	
145	14:13:56	50.766224	50.224592	
146	14:14:16	52.158373	48.74774	
147	14:14:35	52.762821	48.13078	
148	14:14:54	52.169725	48.736021	
149	14:15:13	51.710629	49.214051	
150	14:15:32	53.123343	47.769479	
151	14:15:51	54.457242	46.474294	Fiber on middle of channel
152	14:17:19	46.670725	55.08013	
153	14:17:38	46.843988	54.857513	
154	14:17:57	45.772037	56.261848	
155	14:18:17	46.458432	55.355158	
156	14:18:36	46.348946	55.497983	
157	14:18:55	46.741872	54.988517	
158	14:19:14	48.002313	53.410528	
159	14:19:33	47.376689	54.183273	
160	14:19:52	46.072064	55.862206	
161	14:20:11	45.441901	56.707696	
162	14:20:31	45.073073	57.213521	
163	14:20:50	45.492918	56.638375	
164	14:21:09	45.617753	56.469406	
165	14:21:28	46.626589	55.137102	
166	14:21:47	48.450725	52.868944	
167	14:22:06	47.151663	54.46623	
168	14:22:25	46.929898	54.747741	
169	14:22:44	46.817466	54.891484	
170	14:23:04	45.998382	55.959869	Start flow stop, continuous flash
171	14:24:32	46.036508	55.909294	
172	14:24:38	47.094113	54.53903	
173	14:24:45	50.068779	50.995349	
174	14:24:50	53.960354	46.949278	
175	14:24:57	59.590397	42.031027	
176	14:25:02	65.02566	38.090906	
177	14:25:08	76.287106	31.714026	
178	14:25:14	93.238869	25.019548	
179	14:25:20	122.880894	17.75219	
180	14:25:25	154.361795	13.090183	End flow stop, intermittent flash
181	14:25:31	196.726048	9.17143	
182	14:26:06	146.81942	14.025018	
183	14:26:24	44.713119	57.715221	
184	14:26:44	46.751017	54.976762	
185	14:27:03	45.782912	56.247272	
186	14:27:22	46.077994	55.854359	
187	14:27:41	46.744361	54.985317	
188	14:28:01	46.212586	55.676811	
189	14:28:20	45.546817	56.565307	

190	14:28:39	47.052581	54.591678	
191	14:28:58	47.510206	54.01665	
192	14:29:17	46.988976	54.672487	
193	14:29:37	46.829501	54.876064	
194	14:29:56	47.367234	54.195108	
195	14:30:15	48.861269	52.381815	
196	14:30:34	47.729807	53.744626	
197	14:30:53	47.764585	53.701774	
198	14:31:12	46.774152	54.947044	
199	14:31:32	46.347534	55.499829	
200	14:31:51	45.815375	56.203798	
201	14:32:10	45.244501	56.977392	
202	14:32:29	45.105177	57.169164	
203	14:32:48	45.382631	56.788426	
204	14:33:07	46.053014	55.887426	
205	14:33:26	46.856907	54.840981	
206	14:33:45	47.300835	54.278354	
207	14:34:04	46.855909	54.842257	
208	14:34:24	46.74973	54.978416	
209	14:34:43	46.030868	55.916772	
210	14:35:02	46.14544	55.765257	
211	14:35:21	45.803699	56.219427	
212	14:35:40	45.097746	57.179426	
213	14:35:59	46.771693	54.950201	
214	14:36:19	45.306838	56.891971	
215	14:36:38	46.302977	55.558151	
216	14:36:57	46.602325	55.168469	
217	14:37:16	46.964661	54.703437	
218	14:37:36	47.586884	53.921382	
219	14:37:55	48.650695	52.630644	
220	14:38:14	47.407166	54.145157	
221	14:38:33	45.353976	56.827533	
222	14:38:52	46.458414	55.355181	
223	14:39:11	47.004054	54.653312	
224	14:39:31	47.512899	54.013299	
225	14:39:50	47.582616	53.926676	
226	14:40:09	47.329703	54.242133	
227	14:40:28	48.4081	52.919994	
228	14:40:48	48.118915	53.268727	
229	14:41:07	48.884187	52.354862	
230	14:41:26	47.230246	54.36711	
231	14:41:46	45.912718	56.073807	
232	14:42:05	46.103841	55.820182	
233	14:42:24	45.10549	57.168732	
234	14:42:43	45.249904	56.969979	
235	14:43:03	45.732235	56.31526	
236	14:43:22	45.500206	56.628486	
237	14:43:41	45.794146	56.232221	Start flow stop, continuous flash
238	14:44:32	47.218746	54.381594	

239	14:44:38	47.994306	53.42029	
240	14:44:44	50.166641	50.885908	
241	14:44:50	53.996052	46.914861	
242	14:44:56	58.974242	42.523521	
243	14:45:02	65.375861	37.859505	
244	14:45:07	73.558784	33.079741	
245	14:45:13	84.7662	28.030824	
246	14:45:19	100.58464	22.819365	
247	14:45:24	123.371022	17.661375	End flow stop, intermittent flash
248	14:45:48	248.208254	6.209812	
249	14:46:07	300.957567	4.226252	
250	14:46:25	47.616352	53.884851	
251	14:46:44	44.857616	57.512855	
252	14:47:03	45.387775	56.781411	
253	14:47:23	45.99183	55.968568	
254	14:47:42	45.803327	56.219925	
255	14:48:01	46.861618	54.834953	
256	14:48:20	45.942688	56.033898	
257	14:48:39	46.215657	55.672772	
258	14:48:58	46.257375	55.617957	
259	14:49:17	45.896204	56.095821	
260	14:49:36	46.356685	55.487865	
261	14:49:55	46.527358	55.265588	
262	14:50:15	45.252928	56.965831	
263	14:50:34	45.169947	57.079864	
264	14:50:53	46.409022	55.41953	
265	14:51:12	46.994628	54.665297	
266	14:51:31	46.744296	54.985401	
267	14:51:50	47.500496	54.028736	
268	14:52:09	47.274248	54.311753	
269	14:52:29	48.501518	52.808229	
270	14:52:48	48.546218	52.754902	
271	14:53:07	47.455817	54.084412	
272	14:53:26	47.518567	54.006247	
273	14:53:45	45.740127	56.304662	
274	14:54:04	45.829083	56.185459	
275	14:54:24	45.944674	56.031254	
276	14:54:43	48.735737	52.529893	
277	14:55:02	45.276067	56.934108	
278	14:55:21	45.159298	57.094529	
279	14:55:40	47.532161	53.98934	
280	14:55:59	46.629503	55.133337	
281	14:56:18	47.433276	54.11254	
282	14:56:37	47.219988	54.38003	
283	14:56:56	46.661317	55.092265	
284	14:57:15	46.987725	54.674079	
285	14:57:35	46.075513	55.857642	
286	14:57:54	45.949672	56.024604	
287	14:58:13	46.639135	55.120897	

288	14:58:32	46.976184	54.688766	
289	14:58:51	47.458815	54.080672	
290	14:59:11	46.872144	54.821493	
291	14:59:30	47.720681	53.75588	Start flow stop, continuous flash
292	15:00:00	48.289594	53.062397	
293	15:00:06	51.187126	49.769608	
294	15:00:12	55.241412	45.742077	
295	15:00:20	62.159948	40.082438	
296	15:00:26	68.736019	35.759077	
297	15:00:32	78.847207	30.518471	
298	15:00:38	87.379609	27.039707	
299	15:00:44	102.207438	22.375961	
300	15:00:49	126.166661	17.15686	End flow stop, intermittent flash
301	15:00:54	153.288149	13.21764	
302	15:01:19	277.006936	5.033247	
303	15:01:37	314.376073	3.82787	
304	15:01:56	48.311564	53.035944	
305	15:02:15	44.844559	57.531089	
306	15:02:34	45.415425	56.743733	
307	15:02:53	46.495589	55.306839	
308	15:03:12	46.666878	55.085091	
309	15:03:32	47.591679	53.915434	
310	15:03:51	47.777876	53.685415	
311	15:04:10	46.984701	54.677927	
312	15:04:29	50.662538	50.337834	
313	15:04:49	49.099504	52.102873	
314	15:05:08	47.821849	53.631354	
315	15:05:27	46.734579	54.997895	
316	15:05:46	46.314377	55.543218	
317	15:06:05	46.613812	55.153616	
318	15:06:24	46.195977	55.698666	
319	15:06:43	46.510762	55.28713	
320	15:07:03	45.786468	56.242507	
321	15:07:22	47.078359	54.558989	
322	15:07:41	47.366798	54.195654	
323	15:08:00	46.698151	55.044781	
324	15:08:19	46.682266	55.065251	
325	15:08:39	47.533963	53.987101	
326	15:08:58	47.712974	53.765388	
327	15:09:17	46.462425	55.349962	
328	15:09:36	47.797933	53.660744	
329	15:09:55	46.464617	55.347109	
330	15:10:14	46.464311	55.347508	
331	15:10:33	47.229831	54.367633	
332	15:10:53	47.841837	53.606813	
333	15:11:12	47.819545	53.634184	

Bibliography

[1] P. Gruber, M. P. Marques, N. Szita, and T. Mayr, "Integration and application of optical chemical sensors in microbioreactors," *Lab on a Chip*, vol. 17, no. 16, pp. 2693–2712, 2017.

[2] P. E. Oomen, M. D. Skolimowski, and E. Verpoorte, "Implementing oxygen control in chip-based cell and tissue culture systems," *Lab on a Chip*, vol. 16, no. 18, pp. 3394–3414, 2016.

[3] T. L. Place, F. E. Domann, and A. J. Case, "Limitations of oxygen delivery to cells in culture: An underappreciated problem in basic and translational research," *Free Radical Biology and Medicine*, vol. 113, no. October, pp. 311–322, 2017.

[4] F. A. Harms, W. J. Voorbeijtel, S. I. Bodmer, N. J. Raat, and E. G. Mik, "Cutaneous respirometry by dynamic measurement of mitochondrial oxygen tension for monitoring mitochondrial function in vivo," *Mitochondrion*, vol. 13, no. 5, pp. 507–514, 2013.

[5] K. Domansky, W. Inman, J. Serdy, A. Dash, M. H. Lim, and L. G. Griffith, "Perfused multiwell plate for 3D liver tissue engineering," *Lab on a Chip*, vol. 10, no. 1, pp. 51–58, 2010.

[6] M. Polinkovsky, E. Gutierrez, A. Levchenko, and A. Groisman, "Fine temporal control of the medium gas content and acidity and on-chip generation of series of oxygen concentrations for cell cultures," *Lab on a Chip*, vol. 9, no. 8, pp. 1073–1084, 2009.

[7] M. D. Brennan, M. L. Rexius-Hall, L. J. Elgass, and D. T. Eddington, "Oxygen control with microfluidics," *Lab on a Chip*, vol. 14, no. 22, pp. 4305–4318, 2014.

[8] D. Sticker, M. Rothbauer, J. Ehgartner, C. Steininger, O. Liske, R. Liska, W. Neuhaus, T. Mayr, T. Haraldsson, J. P. Kutter, and P. Ertl, "Oxygen Management at the Microscale: A Functional Biochip Material with Long-Lasting and Tunable Oxygen Scavenging Properties for Cell Culture Applications," *ACS Applied Materials and Interfaces*, vol. 11, no. 10, pp. 9730–9739, 2019.

[9] K. R. Rivera, M. A. Yokus, P. D. Erb, V. A. Pozdin, and M. Daniele, "Measuring and regulating oxygen levels in microphysiological systems: Design, material, and sensor considerations," *Analyst*, vol. 144, no. 10, pp. 3190–3215, 2019.

[10] S. M. Grist, J. C. Schmok, M. C. Andy Liu, L. Chrostowski, and K. C. Cheung, "Designing a microfluidic device with integrated ratiometric oxygen sensors for the long-term control and monitoring of chronic and cyclic hypoxia," *Sensors (Switzerland)*, vol. 15, no. 8, pp. 20030–20052, 2015.

[11] A. Ehrlich, D. Duche, G. Ouedraogo, and Y. Nahmias, "Challenges and Opportunities in the Design of Liver-on-Chip Microdevices," *Annual Review of Biomedical Engineering*, vol. 21, pp. 219–239, 2019.

[12] M. Busek, S. Grünzner, T. Steege, U. Klotzbach, and F. Sonntag, "Hypoxia-on-a-chip," *Current Directions in Biomedical Engineering*, vol. 2, no. 1, pp. 71–75, 2016.

[13] F. J. Norton, "Permeation of Gases through Solids," *Journal of Applied Physics*, vol. 28, no. 1, pp. 34–39, 1957.

[14] S. I. Bodmer, G. M. Balestra, F. A. Harms, T. Johannes, N. J. Raat, R. J. Stolker, and E. G. Mik, "Microvascular and mitochondrial PO 2 simultaneously measured by oxygen-dependent delayed luminescence," *Journal of Biophotonics*, vol. 5, no. 2, pp. 140–151, 2012.

[15] F. M. White, *Fluid Mechanics*. McGraw-Hill Education, 7th ed., 2011.

[16] J. F. Wong, C. A. Simmons, and E. W. Young, "Modeling and Measurement of Biomolecular Transport and Sensing in Microfluidic Cell Culture and Analysis Systems," *Modeling of Microscale Transport in Biological Processes*, pp. 41–75, 2017.

[17] A. Mills, *Basic Heat and Mass Transfer*. Pearson, 2nd ed., 2014.

[18] C. Poon, "Measuring the density and viscosity of culture media for optimized computational fluid dynamics analysis of in vitro devices," *bioRxiv Bioengineering*, no. i, 2020.

[19] C. C. Hu, T. C. Liu, K. R. Lee, R. C. Ruaan, and J. Y. Lai, "Zeolite-filled PMMA composite membranes: influence of coupling agent addition on gas separation properties," *Desalination*, vol. 193, no. 1-3, pp. 14–24, 2006.

[20] Granta Design, "CES EduPack," 2020.

[21] E. G. Mik, T. G. Van Leeuwen, N. J. Raat, and C. Ince, "Quantitative determination of localized tissue oxygen concentration in vivo by two-photon excitation phosphorescence lifetime measurements," *Journal of Applied Physiology*, vol. 97, no. 5, pp. 1962–1969, 2004.

[22] M. Sinaasappel and C. Ince, "Calibration of Pd-porphyrin phosphorescence for oxygen concentration measurements in vivo," *JAMA: The Journal of the American Medical Association*, vol. 184, no. 1, p. 47, 1996.

[23] F. Sonntag, S. Grünzner, F. Schmieder, M. Busek, U. Klotzbach, and V. Franke, "Multilayer based lab-on-a-chip-systems for substance testing," *Laser-based Micro- and Nanoprocessing IX*, vol. 9351, no. March 2015, p. 93510C, 2015.

[24] V. M. Lauschke, R. Z. Shafagh, D. F. Hendriks, and M. Ingelman-Sundberg, "3D Primary Hepatocyte Culture Systems for Analyses of Liver Diseases, Drug Metabolism, and Toxicity: Emerging Culture Paradigms and Applications," *Biotechnology Journal*, vol. 14, no. 7, pp. 1–12, 2019.

[25] B. Ungerböck, V. Charwat, P. Ertl, and T. Mayr, "Microfluidic oxygen imaging using integrated optical sensor layers and a color camera," *Lab on a Chip*, vol. 13, no. 8, pp. 1593–1601, 2013.

[26] Y. B. Kang, J. Eo, B. Bulutoglu, M. L. Yarmush, and O. B. Usta, "Progressive hypoxia-on-a-chip: An in vitro oxygen gradient model for capturing the effects of hypoxia on primary hepatocytes in health and disease," *Biotechnology and Bioengineering*, vol. 117, no. 3, pp. 763–775, 2020.

[27] K. Rennert, S. Steinborn, M. Gröger, B. Ungerböck, A. M. Jank, J. Ehgartner, S. Nietzsche, J. Dinger, M. Kiehntopf, H. Funke, F. T. Peters, A. Lupp, C. Gärtner, T. Mayr, M. Bauer, O. Huber, and A. S. Mosig, "A microfluidically perfused three dimensional human liver model," *Biomaterials*, vol. 71, pp. 119–131, 2015.

[28] R. H. Lam, M. C. Kim, and T. Thorsen, "Culturing aerobic and anaerobic bacteria and mammalian cells with a microfluidic differential oxygenator," *Analytical Chemistry*, vol. 81, no. 14, pp. 5918–5924, 2009.

[29] J. Winkelmann, *Diffusion of Nitrogen*, vol. 1. SpringerMaterials, 2007.